The Regulation of Mitochondrial Stress Responses in *Caenorhabditis elegans*

Christopher Bennett

A dissertation

submitted in partial fulfillment of the

requirements for the degree of

Doctor of Philosophy

University of Washington

2016

Reading Committee:

Matt R. Kaeberlein, Chair

Leo J. Pallanck

Philip G. Morgan

Program Authorized to Offer Degree:

Molecular and Cellular Biology

University of Washington

Abstract

The Regulation of Mitochondrial Stress Responses in *Caenorhabditis elegans*

Christopher Franklin Bennett

Chair of the Supervisory Committee:
Matt R. Kaeberlein
Department of Pathology, University of Washington

Abstract Organismal aging has been proposed to result, at least in part, from mitochondrial dysfunction and oxidative stress. Mitochondria play an important role in energy metabolism, molecular biosynthesis, apoptosis, and cellular signaling and are therefore complexly tied to cellular and organismal health. Paradoxically, there are numerous cases in *Caenorhabditis elegans,* in addition to other organisms, where inhibition of mitochondrial respiration is sufficient to extend lifespan. One proposed mechanism for this pro-longevity effect is the induction of the mitochondrial unfolded protein response (UPR^{mt}), which upregulates expression of mitochondrial-specific chaperones and proteases to re-establish protein homeostasis in the mitochondria. This thesis describes the use of *C. elegans* to understand the genetic regulation of the UPR^{mt} and importantly, the role of this response in stress resistance and aging. I first describe a genome-wide RNAi screen for negative regulators of the UPR^{mt} that takes advantage of a highly sensitive UPR^{mt} fluorescent reporter and RNAi feeding in *C. elegans*. I identify 95

inducers of the UPR^{mt} (RNAi gene knockdowns that increase reporter expression), which are enriched for mitochondrial genes that affect respiratory chain function. A subset of these positive hits differentially affect lifespan and for those that increase lifespan, do so independently of the UPR^{mt} transcription factor ATFS-1. I also find that constitutive activation of the UPR^{mt} is not sufficient for lifespan extension in *C. elegans*, and in fact, seems to harm animals. In the second part of this thesis, I follow-up on a specific gene, the cytosolic pentose phosphate pathway enzyme transaldolase, whose connection to mitochondrial proteostasis is not well understood. I find that transaldolase deficiency alters multiple parameters of mitochondrial function including respiration and mitochondrial dynamics, and promotes longevity through activation of redox-sensitive MAPK pathways and the autophagy regulator TFEB/HLH-30. I also discover that ETC RNAi extends lifespan through identical JNK MAPKs, implicating adaptive responses aside from the UPR^{mt} in longevity control from mitochondrial stress. Finally, I describe another genome-wide RNAi screen to identify positive regulators of UPR^{mt} signaling, to elucidate the complex network of regulatory factors that control this response. Further understanding of the mechanistic details of UPR^{mt} regulation will provide us with insights into the evolution of mitochondrial-nuclear communication and the growing list of human diseases associated with mitochondrial dysfunction.

TABLE OF CONTENTS

LIST OF FIGURES

LIST OF TABLES

LIST OF SUPPLEMENTAL FIGURES

LIST OF SUPPLEMENTAL TABLES

ACKNOWLEDGEMENTS

I would like to first thank the people that established my curiosity in science, for without you I would not be writing this thesis and pursuing a career in scientific research. I was undoubtedly influenced towards this career trajectory at an early age since both of my parents pursued medical-related degrees - both attained pharmacy degrees and my father went on to acquire a PhD in pharmacology. So, thank you mom and dad for fostering my fascination with science and nature, teaching me over the years, and most importantly supporting me through my various projects, hobbies, and interests that cumulatively put me on a path towards wanting to understand the biological world. I cannot thank you enough for the amount of opportunity and freedom you have given me.

Next, I would like to thank my first mentors in scientific research Thazha Prakash at Isis Pharmaceuticals, Adrian Krainer and Xavier Roca (former post-doc) at CSHL, and Nahum Sonenberg and Bruno Fonseca (former post-doc) at McGill University. These individuals introduced me to scientific research, working at the bench, and the realities of research – hard work, long hours, and slow progress – but also instilled in me the ambition for discovery that inspires me to this day. Of these people, I would like to especially thank Bruno Fonseca, since he invested a lot of time mentoring me, brought passion to his research, which motivated me to do the same, and encouraged me to apply to graduate school. He is an extremely talented and detail-oriented scientist and trained me to be incredibly proficient in scientific research, which coming into graduate school let me hit the ground running. For that, I am very grateful.

I must thank my thesis mentor Matt Kaeberlein for taking a chance on me, encouraging me to join his lab, and being so helpful over the years. Matt is an extremely knowledgeable and

driven scientist who fosters a lab atmosphere of collaboration and positivity that few can. He has been extremely supportive of my development as an independent scientist and has challenged me continuously throughout graduate school. His ambition and drive to discover, paired with his healthy skepticism that fosters robust scientific inquiry, has definitely influenced me. It has been a pleasure working in his laboratory over the years and there is no doubt in my mind that I made the right decision to join his lab.

My family and friends have all been essential to my success in graduate school. In Seattle, I have met many amazing people including my graduate school classmates and Kaeberlein lab members. This network of people has been there to ease the failures and celebrate the successes and I am very thankful to all of them. I will greatly miss the lab lunches, ski days, and nights hanging out with these individuals. I must also thank Erica Hildebrand for putting up with me for the entirety of graduate school and always being there for me. Lastly, I must thank childhood friends Jason Chung and Mazen Zawaideh. They are loyal, intelligent, and inspiring people that have motivated me through different points in my life and I am grateful for their friendship.

Chapter 1. INTRODUCTION TO THESIS

*** Parts of this chapter are modified from a review article that I published in Experimental Gerontology entitled "The mitochondrial unfolded protein response and increased longevity: Cause, consequence, or correlation?" [1]**

1.1 ABSTRACT

The discovery that inhibition of mitochondrial respiratory chain function leads to extended lifespan was made nearly 15 years ago [2, 3]. Since then, genetic studies in *C. elegans* have uncovered several factors that mediate this effect. However, the genuine role of these factors in mitochondrial longevity and their interconnectivity to other mitochondrial stress responses has not been extensively assessed. Here, I review mitochondrial quality control pathways and their regulatory mechanisms, with particular emphasis on the mitochondrial unfolded protein response (UPR^{mt}), which is implicated in lifespan extension from mitochondrial dysfunction. This introduction then covers the progression of the mitochondrial aging field and the redox-sensitive signaling pathways known to prolong lifespan.

1.2 INTRODUCTION TO THE POWERHOUSE OF THE CELL

Mitochondria are organelles that play diverse roles in cellular function including energy metabolism/ATP generation, amino acid and lipid metabolism, heme and iron–sulfur cluster biosynthesis, and regulation of intracellular calcium. In addition, mitochondria are appreciated for their roles in aging and disease due to their generation of reactive oxygen species (ROS) by the electron transport chain (ETC), mutations in their genome that accumulate with age, and regulation of cell death.

Mitochondria are composed of two lipid membranes, the mitochondrial outer membrane (MOM) and the mitochondrial inner membrane (MIM), along with two aqueous spaces termed the intermembrane space (IMS) and the matrix. The respiratory chain, composed of the ETC (Complex I-IV) and the mitochondrial ATP synthase (Complex V), lies within the MIM and functions by using energy derived from oxidation of macromolecules to pump protons across the MIM, creating a membrane potential ($\Delta\psi$). The proton gradient is coupled to ATP synthesis at the mitochondrial ATP synthase. The ETC is comprised of many tightly controlled redox reactions, where electrons derived from NADH and $FADH_2$ are transferred from donor molecules to more electronegative acceptor molecules, releasing energy that is coupled to proton transport across the MIM. The last redox reactions of the ETC occur at cytochrome c oxidase (Complex IV) and result in the conversion of O_2 to two molecules of H_2O. Despite the efficiency of the ETC, a small percentage of electrons leak from the ETC to O_2 to create the free-radical superoxide, the primary culprit behind oxidative stress.

1.5-2 billion years ago a symbiotic event between a α-proteobacterium and an ancient eukaryotic cell led to the generation of mitochondria [4]. This harmonious relationship led to mitochondria maintaining a small subset of their genomic information; only ~1% of mitochondrial proteins are encoded by the mitochondrial genome. For unknown reasons mitochondria lost the bulk of their genes; both gene transfer to the nuclear chromosomes or gene redundancy in the host cell may have driven this change. This necessitated the cytoplasmic synthesis and import of thousands of proteins into the mitochondria. This posed another problem: how to properly import, localize, and fold or assemble proteins. In addition, for components of the respiratory chain, this needs to occur in a coordinated manner since the multimeric protein complexes of the respiratory chain contain both nuclear- and mitochondrial-encoded proteins [5].

Efficient mitochondrial respiration thus requires a stoichiometric balance between nuclear- and mitochondrial-encoded respiratory chain subunits, and the proper machinery to translate, import, and assemble subunits at the MIM. Disruption to this intricate process causes mitochondrial proteotoxic stress and intriguingly, in some cases, is sufficient for lifespan extension in *C. elegans* [2, 3, 6-8].

1.3 Mitochondrial Proteostasis

1.3.1 *Mitochondrial protein import*

Mitochondria are incredibly complex organelles that exploit multiple mechanisms to regulate proteostasis. Despite the presence of 1,000+ proteins in the mitochondria [9], mitochondrial ribosomes only translate 12-13 proteins. The remaining proteins are nuclear-encoded and synthesized by cytoplasmic ribosomes. These proteins also function in multiple compartments and membranes within the mitochondria. Thus, mechanisms have evolved to properly import and sort proteins into correct mitochondrial subcompartments.

Once nuclear-encoded mitochondrial proteins are synthesized in the cytosol, they are transported to the mitochondria and threaded through translocases of the outer membrane (TOM) and inner membrane (TIM) [10]. In general, import of pre-cursor proteins is post-translational, requiring cytosolic chaperones to maintain them in an unfolded state to facilitate translocation. However, cytosolic ribosomes can associate with the mitochondria [11-13] and direct co-translational import of a subset of proteins such as inner membrane proteins [14-17]. Presumably this is because inner membrane proteins contain transmembrane domains, which can aggregate, cause cytosolic protein toxicity, and insert into inappropriate biological membranes [17].

There are two main types of import signals that target precursor proteins to mitochondrial subcompartments. The first class is amino terminus extensions, known as mitochondrion-targeting signals (MTS), which target precursors or preproteins to the mitochondrial matrix or the inner membrane if an additional hydrophobic sorting signal exists [18, 19]. The second class of import sequences, referred to as internal targeting signals, is contained within a polypeptide and remains within the mature protein [18, 19]. MTS are comprised of ~15-50 amino acids that are positively charged and form α-helices that first associate with the TOM complex and then the translocase of the inner membrane (TIM23) complex [18, 19]. Once imported, MTS are proteolytically removed by the mitochondrial processing peptidase (MPP).

The main entry point for proteins destined to the mitochondria is the TOM complex. It is comprised of multiple subunits including the β-barrel protein Tom40 that forms the central channel of the complex and the receptors Tom20 and Tom22 that bind to preproteins [19]. After import through the TOM complex, at least four main pathways are utilized to assemble each protein and target it to the correct compartment: 1) the presequence pathway that targets proteins to either the inner membrane or the matrix, 2) the carrier pathway that transports proteins with multiple transmembrane segments to the inner membrane, 3) the oxidative folding pathway of the intermembrane space, and 4) the transport pathways of the outer membrane such as the β-barrel pathway [18, 19]. The inner workings of all these import pathways are outside the focus of this thesis, but there are additional details to note. For the presequence pathway (discussed below), $\Delta\psi$ is extremely critical for the import of proteins. $\Delta\psi$ activates the TIM23 complex and causes an electrophoretic effect driving protein import into the matrix since the MTS of polypeptides is positively charged and the mitochondrial matrix is negatively charged compared to the IMS. The TIM23 complex interacts with the TOM complex to facilitate preprotein

transfer, the respiratory chain complexes, and the presequence translocase-associated motor (PAM). These latter two interactions occur in two distinct TIM23 complexes (**Figure 1.1**). $TIM23^{SORT}$ releases proteins with an internal targeting signal into the inner membrane and TIM23-PAM transports preproteins into the matrix [18, 19]. $TIM23^{SORT}$ contains the subunit Tim21, which associates with the TOM complex and complexes III and IV of the respiratory chain that pump protons across the MIM [20]. This interaction is intriguing as it may facilitate efficient coupling of proton transport to protein sorting into the inner membrane. TIM23-PAM includes the chaperone mtHsp70 and its five different co-chaperones that drive the preprotein translocation in an ATP-dependent manner [18, 19]. The mechanistic details are not well understood, but may include both the pulling of preproteins across the MIM and trapping of preproteins by mtHsp70 binding to prevent backsliding into the IMS. In later sections of this introduction, TIM23-PAM will be discussed further as its components are upregulated by the UPR^{mt} [21].

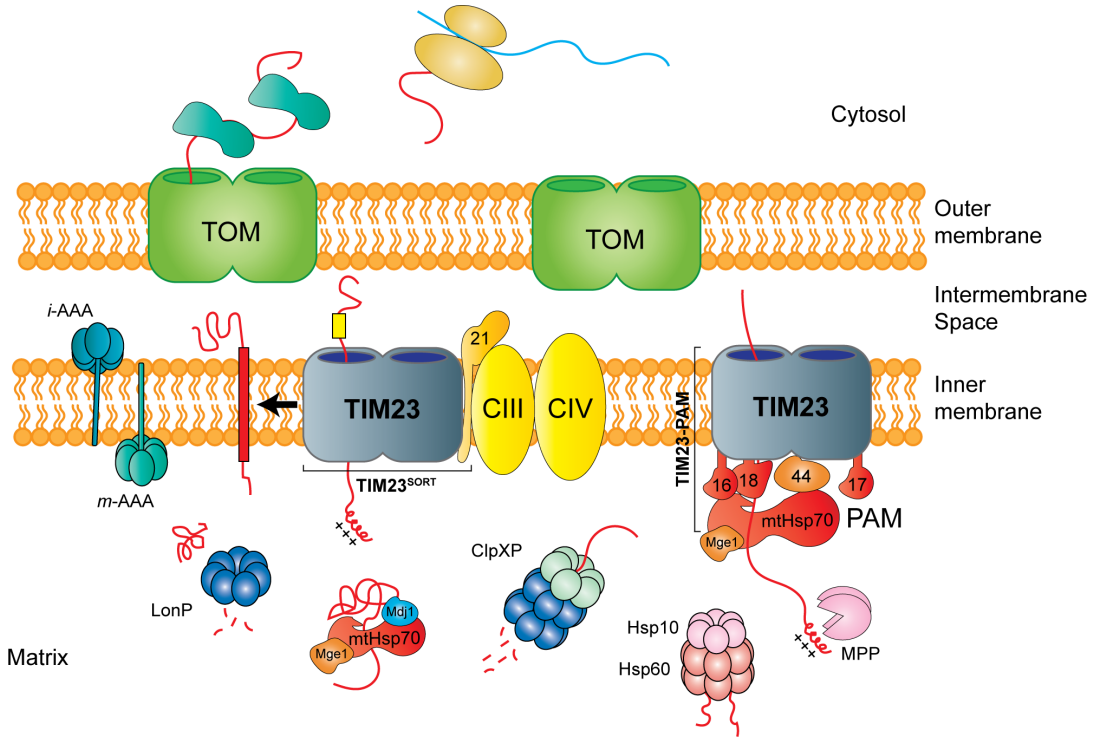

Figure 1.1. Model of mitochondrial protein import and proteostasis machinery

Nuclear-encoded proteins mitochondrial proteins are translated in the cytoplasm and imported through the TOM and TIM complexes to either the matrix (via TIM23-PAM) or inner membrane (via TIM23^{SORT}). Proteostasis in the mitochondria is maintained by the chaperones Hsp60/Hsp10 and mtHsp70, in addition to the major mitochondrial proteases ClpXP, LonP, *m*-AAA, and *i*-AAA.

1.3.2 *Mitochondrial protein folding, processing, and degradation*

The mitochondrial proteome is managed by mitochondrial chaperones that associate with newly imported proteins and mitochondrial proteases that process or degrade proteins [22]. These enzymatic systems are essential during mitochondrial biogenesis, when newly synthesized proteins are imported, folded, or assembled, and during mitochondrial dysfunction, when unfolded proteins accumulate. An appreciation of the proteostasis machinery is therefore critical for understanding adaptive responses such as the UPR^{mt} that modulate mitochondrial protein quality control. This section will delve into the different classes of chaperones and proteases of the mitochondria and furthermore, describe non-proteostasis functions of these enzymatic

machines.

The chaperones found in the mitochondria include members of the Hsp60, Hsp70, Hsp90, and Hsp100 families. mtHsp70 (*C. elegans* HSP-6) and Hsp60 (*C. elegans* HSP-60) are highly conserved and crucial for mitochondrial protein quality control. mtHsp70 is the core component of TIM23-PAM, which drives unfolded polypeptides across the inner membrane using ATP hydrolysis (**Figure 1.1**). This chaperone aids protein folding through its holdase function, which transiently binds partially or fully imported proteins. PAM is a highly complex machine composed of mtHsp70 and five co-chaperones that modulate its activity (**Figure 1.1**). Mge1 is a nucleotide exchange factor that promotes ADP release from mtHsp70, Tim44 is an adaptor between mtHsp70 and the TIM23 complex, PAM18 stimulates the ATPase activity of mtHsp70, PAM16 negatively regulates PAM18, and PAM17 is required for the organization of the PAM16-PAM18 complex with the TIM23 translocase [19, 23]. Interestingly, the role of mtHsp70 in protein folding extends past its function in the PAM. mtHsp70 also associates with proteins that are mitochondrial-encoded, translated in the mitochondrial matrix, and therefore not imported across the MIM [24]. In this form, mtHsp70 binds to Mge1 and Mdj1, a DnaJ chaperone, and is completely distinct from the membrane-bound form associated with the PAM (**Figure 1.1**) [25]. Mdj1 yeast mutants display respiratory defects and increased levels of misfolded and aggregated matrix proteins, including those imported into matrix [25, 26]. Therefore, the mtHsp70/Mdj1/Mge1 complex is proposed to fold both nuclear-encoded matrix proteins after complete import [27, 28] and mitochondrial-encoded proteins that are translated in the matrix [24].

Hsp60/Hsp10 is a mitochondrial chaperonin and is essential for protein folding in the mitochondrial matrix (**Figure 1.1**). In yeast, Hsp60 null mutants are inviable, while conditional

mutants exhibit increased aggregated protein levels in the matrix [29]. Hsp60 forms a homooligomer of 14 subunits resulting in a 'double-donut' chamber that is capable of encapsulating and folding proteins up to 50 kDa [25]. Initially, folding intermediates interact with the hydrophobic interior of the chamber. ATP-dependent conformational changes in the Hsp60 rings, which reduce hydrophobic interactions between the client protein and chamber interior, drive folding and release of the client protein [25]. Hsp10 forms the cap to the Hsp60 chamber and participates in the regulation of this reaction cycle [30-33]. Also, mtHsp70 coordinates protein folding of matrix proteins with Hsp60. Newly imported proteins are channeled from mtHsp70 to Hsp60, facilitating their folding and in the case of aggregation-prone proteins, preventing their accumulation [34-36]. mtHsp70 regulates Hsp60 function in other respects as well. TIM23-PAM imports Hsp60 monomers and mtHsp70 forms a mtHsp70:Hsp10 complex that promotes the maturation of heptameric Hsp60 rings [37]. Thus, the mitochondrial chaperone network is intimately tied together and suited to support folding of nuclear- and mitochondrial-encoded proteins.

Mitochondrial proteases exist in different subcompartments to process and turnover damaged proteins. Certain proteases also exert regulatory control of mitochondrial dynamics and biogenesis through proteolysis. There are several sub-types of mitochondrial proteases including processing proteases, ATP-dependent proteases, oligopeptidases, and others that are not functionally categorized [38]. Several processing proteases, in addition to MPP (mentioned above), exist to cleave polypeptides after MPP. For example, polypeptides destined to the IMS contain a bipartite sequence containing a MTS and a hydrophobic sorting signal that arrests translocation at the inner membrane. Once arrested, the membrane-bound inner membrane peptidase (IMP) or the rhomboid protease Pcp1 cleave the sorting signal, releasing the resulting

polypeptide into the IMS [39, 40]. Other processing steps can also occur for polypeptides localized to the mitochondrial matrix: octapeptide or a single amino acid residue removal by Oct1 or Icp55, respectively [38, 41-43]. These modifications are important for protein stability as many polypeptides contain unstable N-terminal residues post MPP cleavage [41-43].

The ATP-dependent proteases include the two matrix proteases ClpXP and PIM1/Lon, and the two inner membrane proteases *m*-AAA and *i*-AAA proteases, which face the matrix and IMS respectively (**Figure 1.1**). This class of proteases forms multimeric complexes and uses ATP hydrolysis to unfold proteins for transport into their proteolytic cavities. ClpXP is built of heteromeric subunits ClpP, which contains serine peptidase activity, and ClpX , which contains ATPase and chaperone activity and contributes substrate specificity [44, 45]. ClpP associates as two stacked heptameric rings, forming a central chamber with proteolytic activity, while ClpX assembles into two hexameric rings that axially align to each end of the ClpP tetradecamer [44, 45]. This interaction of ClpX with ClpP rings encourages the formation and catalytic activity of the ClpP tetradecamer [44]. Interestingly, ClpP is reported to signal the *C. elegans* UPR^{mt} and is also a target of the UPR^{mt} in multiple species (discussed in **Sections 1.3.4**, **1.3.5**) [46, 47], indicating its importance in mitochondrial protein quality control.

PIM1/Lon is another matrix protease that functions during stress and reacts with thermally denatured and oxidatively damaged proteins to prevent their accumulation (**Figure 1.1**) [48]. This protease associates into homo-oligomeric complexes comprised of heptameric rings [49] and recognizes large and exposed unfolded polypeptide stretches for degradation, but can also degrade folded substrates in vitro [50, 51]. Proteolysis by PIM1/Lon is assisted by Hsp70 chaperones that retain substrates in soluble conformations [52, 53]. Aside from degradation of unfolded proteins, PIM1/Lon also functions to regulate mitochondrial quality control pathways

through degradation of signaling factors. For example, the UPR^{mt} transcription factor ATFS-1 (discussed in **Section 1.3.5**) is degraded by Lon in *C. elegans* [21].

The *m*-AAA and *i*-AAA proteases regulate inner membrane proteostasis (**Figure 1.1**), which is a remarkable task considering the MIM is the protein-richest cellular membrane and harbors the respiratory chain. These proteases interact with solvent-exposed domains of membrane proteins and display degenerate substrate specificity [54]. Unassembled subunits of protein complexes or non-integral membrane proteins such a subunit 7 of ATP synthase are targets of AAA protease degradation [55]. However, these proteases also process certain substrates such as the mitochondrial ribosomal subunit MrpL32, allowing its assembly into ribosomal particles [56]. Despite having their active sites facing the matrix or the inner membrane space the *m*-AAA and *i*-AAA proteases are capable of degrading proteins with domains at both membrane surfaces [57]. As long as N- and C- terminal tails of ~20 amino acids extend from each side of the membrane, proteins can be extracted from the opposite side of the membrane (with respect to the active site of the protease) through a pulling type of mechanism and degraded [57]. The *m*-AAA protease, for example, dislocates Ccp1 from the inner membrane using an ATP-dependent reaction mechanism to enable further proteolytic processing by the Pcp1 protease [58]. A few regulatory factors of the AAA proteases are known. The mitochondrial prohibitins (PHB1 and PHB2) form heteromeric ring-like structures in the MIM and supercomplex with the *m*-AAA protease, negatively regulating its proteolytic activity [59]. How this occurs is not understood, but prohibitins may modulate substrate access of the *m*-AAA protease or the lipid microenvironment surrounding the protease [22].

Mitochondrial proteases perform regulatory functions in addition to their roles in protein quality control and processing. As mentioned, ClpXP positively and Lon negatively regulate

UPR^{mt} activation in *C. elegans*. The degradation of dysfunctional mitochondria through mitophagy is also negatively regulated through mitochondrial proteolysis. Under basal conditions, the serine/threonine-protein kinase PINK1 is imported into the mitochondria, cleaved by the MPP, and subsequently released from the mitochondria by the presenilins-associated rhomboid-like protein (PARL) protease. Under stress conditions, the import and proteolysis of PINK1 is inhibited causing its buildup on the mitochondrial outer membrane to promote mitophagy. Other mitochondrial proteases degrade PINK1 as well, adding further complexity to the proteolytic regulation of mitophagy [60]. Mitochondrial dynamics, the continuous fusion and fission of mitochondria, is also regulated by mitochondrial proteases. IM fusion is controlled by the dynamin-related GTPase Opa1, which exists in multiple isoforms generated by alternative splicing and proteolysis [61]. Two metalloproteases Oma1 and YmelL process Opa1 at S1 and S2 cleavage sites, respectively, leading to different ratios of long (L) and short (S) isoforms [61]. Appropriate ratios of these isoforms promote inner membrane fusion. In addition, proteolytic regulation of Opa1 allows IM fusion to be coupled to mitochondrial states: Yme1L (an ATP-dependent protease) cleavage at S2 reacts to increased mitochondrial respiration and promotes IM fusion, while Oma1 cleavage at S1 from CCCP treatment (mitochondrial uncoupler) or severe mitochondrial dysfunction causes loss of mitochondrial fusion [61].

In sum, mitochondrial function is regulated by multiple enzymatic complexes that ensure the proper localization, processing, and folding of mitochondrial proteins. The TOM and TIM import machinery targets proteins to correct mitochondrial subcompartments and maintains them in a linear conformation to facilitate import. Then, proteases process preproteins enabling their stabilization, while chaperones promote their folding to native state. All of these factors function in a coordinated manner to establish protein homeostasis in the mitochondria and are also

fundamental in the response to mitochondrial dysfunction.

1.3.3 *UPRs regulate compartmental protein folding*

The compartmentalization of the eukaryotic cell permitted spatial separation of different cellular processes and specialization of organellar function. However, this necessitated that protein folding be regulated in a compartment-specific fashion since it is energetically wasteful for protein folding stress in one organelle to cause activation of proteostatic mechanisms in another compartment. A miscued response such as this could cause alterations in protein function in an organelle that does not require high levels of chaperone or protease activity. Therefore, distinct UPRs exist in the cytosol, endoplasmic reticulum (ER), and mitochondria to handle each unique protein-folding environment.

The UPR transcriptionally upregulates compartment-specific chaperones and proteases to stabilize and degrade unfolded polypeptides. For instance, pharmacological treatments that disrupt protein folding in a particular compartment activate the corresponding UPR. Treatment of cells with arsenite, which disrupts cytoplasmic protein folding, specifically induces cytoplasmic chaperone expression; tunicamycin, a drug that inhibits N-linked glycosylation, specifically induces ER chaperone expression; ethidium bromide, which intercalates mtDNA, specifically induces mitochondrial chaperones Hsp60 and Hsp10 [62-66]. This is true of genetic interventions as well, e.g. RNAi knockdown of mitochondrial genes specifically activates the UPR^{mt} reporter in *C. elegans* [67].

In general, the level of chaperone occupancy is set by rate of protein synthesis, import, and folding environment within a compartment. Perturbations to any of these factors can offset the client load of chaperones, causing aberrant protein folding and disassembly of protein complexes. Sensing mechanisms thus operate to fine-tune the protein-folding environment if

chaperone protein-folding capacity is insufficient. One mechanism entails the chaperone-mediated sequestration of a signaling factor. When the protein burden increases, chaperones preferentially interact with unfolded proteins and release the signaling factor, leading to its activation. For example, cytosolic Hsp70 normally binds to the transcription factor HSF1 to repress its transcriptional activity, but releases it under heat-shock conditions [64, 68, 69]. The UPR^{mt} utilizes an alternative mechanism to respond to protein folding stress within the mitochondria. In *C. elegans*, the leucine zipper transcription factor ATFS-1 contains a MTS and is targeted to the mitochondria for degradation by the Lon protease under non-stress conditions, but a fraction is excluded from the mitochondria during stress [21]. This leads to ATFS-1 import into the nucleus to bind UPR^{mt} DNA elements to regulate chaperone, protease, TCA cycle, respiratory chain, and glycolytic genes important for recovery from mitochondrial dysfunction [21, 70].

1.3.4 *Identification and regulation of the mammalian UPR^{mt}*

The UPR^{mt} is a transcriptional response that upregulates mitochondrial chaperones and proteases during mitochondrial dysfunction. Pioneering studies by the Hoogenraad lab identified and characterized this response, specifically in mammalian cells. Deletion of mtDNA in rat hepatoma cells was found to activate the UPR^{mt}, defined by increased levels of mitochondrial chaperonins Hsp60 and Hsp10, but not cytosolic chaperones [62]. A follow-up study found that overexpression of a misfolded mutant of mitochondrial ornithine transcarbamylase (ΔOTC) is sufficient to induce the response, which also upregulates the mitochondrial protease ClpP and mtDnaJ chaperone (yeast Mdj1, previously discussed) [47].

In an effort to uncover the regulation of the UPR^{mt}, bioinformatic and biochemical approaches were employed in mammalian cells. Analysis of the Hsp60/Hsp10 bidirectional

promoter revealed a CEBP homology protein (CHOP) element [47]. Accordingly, the heterodimerization of CHOP and C/EBPβ and binding to the CHOP element were found to initiate UPR^{mt} gene expression [47]. JNK MAPK signaling was then shown to mediate the upregulation of CHOP and C/EBPβ through AP-1 (activator protein-1) promoter elements, implicating JNK MAPK signaling in the initial phase of the response [71]. Further bioinformatics led to the discovery of target genes containing both CHOP binding sites and flanking mitochondrial unfolded protein response elements (MUREs): mitochondrial proteases YME1L1 (*i*-AAA protease subunit) and MPPβ (MPP subunit), TIM17A (component of TIM23 complexes), Complex I subunit NDUFB2, and enzymes endonuclease G and thioredoxin 2 (**Table 1.1**) [72]. Similar to CHOP elements, MUREs are also required for UPR^{mt} gene expression [72] and present within additional UPR^{mt} target genes (**Table 1.1**) [73]; however, the factors that bind these elements are not known [72].

UPR^{mt} regulatory elements other than MUREs are also present in mammals. *C. elegans* studies identified the UPR^{mt} transcription factor ATFS-1, which prompted the search for a mammalian homolog, especially since putative ATFS-1 binding elements (known as UPR^{mt} promoter elements, not to be confused with MUREs) were found in genes induced by mitochondrial myopathy in mice [70, 74]. One candidate, mammalian ATF5, contains a weak mitochondrial targeting sequence, homology to the bZip domain of ATFS-1, and is transcriptionally induced in the context of mitochondrial diseases [74-76]. Accordingly, ATF5 complements ATFS-1 deficiency in worms, and induces expression of mitochondrial genes *HSP60*, *HSP10*, *mtHSP70*, and *LONP1* in mammalian cells [77]. Mitochondrial respiration and cellular recovery from mitochondrial insults (ΔOTC and ethidium bromide) are decreased in ATF5-depleted cells, indicating ATF5 is important for both general mitochondrial function and

proteostasis [77]. A related factor, ATF4, is also transcriptionally induced by the UPR^{mt} [73]. ATF4 is a known to signal a branch of the UPR^{ER} to increase CHOP transcription [78], but in the case of the UPR^{mt}, appears to be independent of the integrated stress response kinases GCN2, HRI, PERK and PKR associated with the UPR^{ER} [73]. Therefore, CHOP and ATF4 are regulated during mitochondrial stress in a fashion distinct from ER stress. Adding to recent complexity of the UPR^{mt} in mammals, ATF3, which also induces CHOP during ER stress [79], was found to be induced 1.5-4 fold during the UPR^{mt} [73]. However, it is currently unclear whether ATF3 signals or alters CHOP expression during the UPR^{mt}. These findings highlight the importance of the UPR^{mt} in mitochondrial proteostasis and suggest that in mammals, UPR^{mt} signaling evolved using identical factors to the UPR^{ER}, but gained specificity through unique regulatory mechanisms that are still unclear.

Table 1.1. UPR^{mt} target genes in mammals and *C. elegans*

This table lists UPR^{mt} target genes evidenced from mammals or *C. elegans* studies, along with the corresponding orthologs obtained from PPOD or BLASTP. * indicates the gene is a bonafide UPR^{mt} target in the corresponding model system. If a gene contains an * for both mammalian and *C. elegans* orthologs, it is a highly conserved UPR^{mt} target. Mammalian target genes were selected based off the presence of CHOP, MURE1, and MURE2 elements [72, 73], with exception of mtHsp70 and LONP, which were recently shown to be ATF5 targets [77]. *C. elegans* UPR^{mt} targets were drawn from publications by the Haynes lab [21, 70].

Mammalian Genes/Orthologs	***C. elegans* Genes/Orthologs**	**Functional Category**
HSPD1/CPN60/HSP60*	Y22D7AL.5 · *hsp-60**	Chaperone
HSPE1/CPN10/HSP10*	Y22D7AL.10	Chaperone
mtDnaJ/DNAJA3*	F22B7.5 · *dnj-10**	Chaperone
HSPA9/mtHsp70*	C37H5.8 · *hsp-6**	Chaperone
MPPb*	ZC410.2 · *mppb-1*	Protease
CLPP*	ZK970.2 · *clpp-1*	Protease
YME1L1*	M03C11.5 · *ymel-1**	Protease
LONP*	C34B2.6	Protease
TIMM17A*	E04A4.5 · *tim-17**	Protein Import
TIMM23B	F15D3.7 · *tim-23**	Protein Import
NDUFB2*	F44G4.2	Respiratory Chain
UQCRC1*	F56D2.1 · *ucr-1*	Respiratory Chain

NDUFA11*	N/A	Respiratory Chain
NDUFAF1	C50B8.3 · *nuaf-1**	Iron-Sulfur Biogenesis
NFU1	R10H10.1 · *lpd-8**	Iron-Sulfur Biogenesis
ECSIT*	Y17G9B.5*	Iron-Sulfur Biogenesis
DRP1	T12E12.4 · *drp-1**	Mitochondrial Dynamics
MFF	F55F8.6 · *mff-2**	Mitochondrial Dynamics
PDK3*	ZK370.5 · *pdhk-2**	Metabolism
ENO1L1	T21B10.2 · *enol-1**	Metabolism
LDHB	F13D12.2 · *ldh-1**	Metabolism
GAPDH	K10B3.8 · *gpd-2**	Metabolism
GPT2*	C32F10.8	Metabolism
IDI1*	K06H7.9 · *idi-1*	Metabolism
IREB2*	ZK455.1 · *aco-1*	Metabolism
GARS*	T10F2.1 · *grs-1**	Protein Synthesis
MRPL18*	D2007.4 · *mrpl-18*	Protein Synthesis
MRPL22*	Y39A1A.6 · *mrpl-22*	Protein Synthesis
MRPS31*	C32A3.2 · *mrps-31*	Protein Synthesis
NRF2	T19E7.2 · *skn-1**	Transcription Factor
TFB1M*	T03F1.7 · *tfbm-1*	Transcription Factor
SLC22A4*	F52F12.1 · *oct-1*	Transporter
ABCB10*	*haf-1*/*haf-2*/*haf-3**/*haf-4*/*haf-7*/*haf-8*/*haf-9*	Transporter
TRX2*	B0024.9 · *trx-2*	Antioxidant
ENDOG*	C41D11.8 · *cps-6*	Endonuclease
CARD12*	N/A	Other

1.3.5 *Genome-wide screens in C. elegans identify UPR^{mt} factors*

Initial studies in *C. elegans* using transgenically expressed GFP reporters of *hsp-6* and *hsp-60* sought to identify UPR^{mt} regulatory genes [46, 67, 80, 81]. At the time, CHOP and C/EBPβ were the only known signaling factors (with no obvious homologs in *C. elegans*), and ethidium bromide and misfolded ΔOTC were the only known inducers of the UPR^{mt} [47, 62]. Knowledge of the UPR^{mt} and mitochondrial proteostasis was in its infancy. A small RNAi screen of mitochondrial genes on chromosome I identified 32 RNAi clones that activate the UPR^{mt} [67]. Positive hits (RNAi clones that induce the UPR^{mt}) included genes involved in mitochondrial

transcription and translation, such as mitochondrial ribosomal proteins, tRNA synthetases, elongation factors, and a DNA helicase [67]. In addition, 24/30 mitochondrial RNAi clones that did not induce the UPR^{mt} were monomeric or homo-oligomeric [67], supporting the idea that stoichiometric imbalances between nuclear- and mitochondrial-encoded subunits activate the UPR^{mt} rather than depletion of mitochondrial proteins in general. Subsequent studies identified a few genes involved in the signaling of the UPR^{mt} by using a temperature-sensitive mutation (*zc32*) that conditionally activates the response at 25°C: mitochondrial ATP-dependent protease ClpXP, mitochondrial inner-membrane-localized ABC transporter HAF-1, basic leucine zipper protein ATFS-1, DNA binding protein homeobox domain protein DVE-1, and ubiquitin-like protein UBL-5 (**Figure 1.2**) [46, 80, 81]. Despite initial characterization of these genes, there has been limited follow-up on how these factors interact, how individually essential they are for the full UPR^{mt} response, and how they respond to unfolded proteins in the mitochondria. The exception to this is the transcription factor ATFS-1, which has been extensively characterized in recent years and is indispensable for the response.

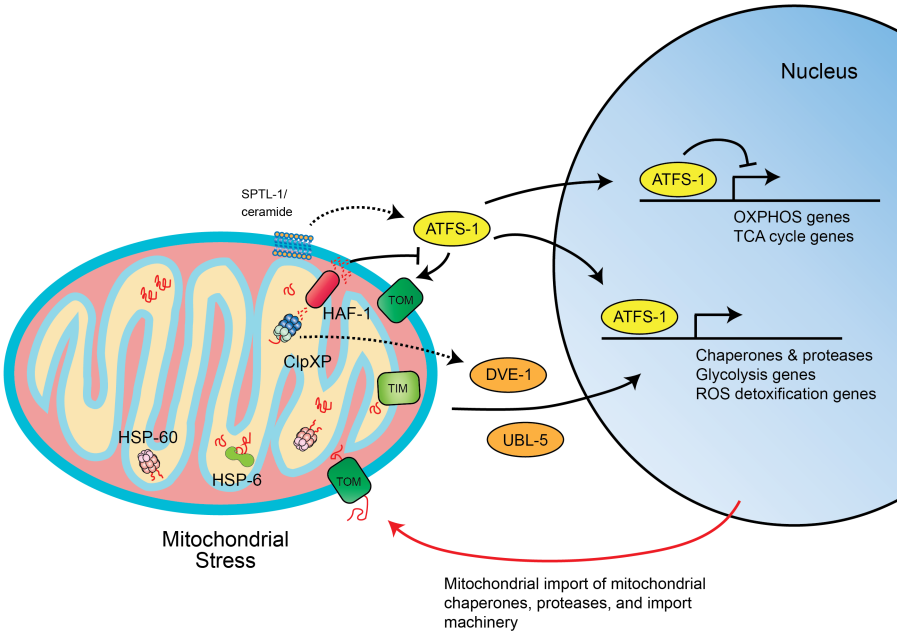

Figure 1.2. The UPR^{mt} signaling pathway in *C. elegans*

The UPR^{mt} responds to protein folding stress in the mitochondria and promotes nuclear translocation of the bZip transcription factor ATFS-1. During non-stress conditions, ATFS-1 is imported into the mitochondria via TOM and TIM and degraded by the Lon protease. Mitochondrial import of ATFS-1 is negatively regulated by HAF-1. During mitochondrial stress ATFS-1, DVE-1, and UBL-5 all traffic to the nucleus and upregulate expression of mitochondrial chaperones and proteases. In addition, ATFS-1 inhibits expression of respiratory chain (OXPHOS) and TCA cycle genes to promote mitochondrial recovery. The serine palmitoyltransferase SPTL-1 regulates sphingolipid biosynthesis and also regulates the UPR^{mt} upstream of ATFS-1 via an unknown mechanism that may involve ceramide at the mitochondrial outer membrane.

ATFS-1 stimulates mitochondrial-nuclear communication through organelle partitioning (**Figure 1.2**) [21]. A mitochondrial targeting sequence localizes ATFS-1 to the TOM and TIM import machinery for import into the mitochondrial matrix [21]. Once in the matrix, ATFS-1 is either degraded by the Lon protease, thereby negatively regulating UPR^{mt} signaling during non-stress conditions [21], or binds the mitochondrial DNA to reduce mitochondrial transcript levels during mitochondrial stress [70]. The major form of ATFS-1 that accumulates during mitochondrial stress is of high molecular weight, suggesting that its import into the mitochondria and processing by MPP is inhibited [21]. This occurs through at least two potential mechanisms: decreased import of mitochondrial proteins in general during mitochondrial stress (due to

reduced ATP generation, mitochondrial membrane potential, or chaperone availability) and negative regulation by the MIM-localized ABC transporter HAF-1 [21]. Supporting the latter mechanism, ATFS-1 accumulates in dysfunctional mitochondria in *haf-1(ok705)* deletion mutant animals, attenuating UPR^{mt} signaling [21]. However, HAF-1 is not required for UPR^{mt} signaling in cases of severe mitochondrial dysfunction that greatly diminish ATFS-1 import [21, 82]. Once in the nucleus, ATFS-1 upregulates genes for numerous processes including mitochondrial proteostasis, ROS detoxification (Nrf2/SKN-1), innate immunity, and glycolytic metabolism and downregulates TCA cycle and respiratory chain genes [21, 70]. By inducing expression of chaperones, proteases, and import machinery (*tim-17* and *tim-23*), while repressing expression of TCA cycle and respiratory chain genes, ATFS-1 reduces the protein burden on the folding and import machinery and promotes recovery from mitochondrial dysfunction.

In order to elucidate novel UPR^{mt} factors, multiple RNAi screens were performed over the last five years such as the project in this thesis (Chapter 2, Appendix A) and others [83, 84]. Runkel et al. [83] used the UPR^{mt}-inducer paraquat to identify 54 regulators of UPR^{mt} signaling. Their positive hits (RNAi clones that reduce *hsp-6p::gfp* expression) include vacuolar H+ ATPase subunits, proteasome subunits, cytosolic chaperonins, nuclear transport factors, pre-mRNA splicing proteins, and cytosolic protein synthesis genes (ribosomal subunits and translation factors) [83]. About half of these were specific for paraquat induction of the *hsp-6p::gfp* reporter, while the remaining hits also suppressed the *zc32* mutation induction of the *hsp-60p::gfp* reporter [83]. Thus, further characterization of these factors will be important to determine which are essential to UPR^{mt} signaling across conditions. The JNK MAPK KGB-1 was also found to negatively regulate the UPR^{mt} in some circumstances. KGB-1 regulates cellular surveillance-activated detoxification and defenses (cSADDs) that cause *C. elegans* to

avoid harmful RNAi treatments/bacterial lawns [85]. Runkel et al. [83] observed that the decrease in paraquat-induced *hsp-6p::gfp* expression from *elt-2(RNAi)* (a positive hit in their screen) is rescued by *kgb-1(um3)* mutation [83]. Thus, the authors conclude that for at least some positive hits, UPR^{mt} attenuation operates through the KGB-1 MAPK pathway. In a search for genes that regulate pro-longevity cytoprotective pathways, the Ruvkun lab also found several factors that signal the UPR^{mt} in the presence of the complex III inhibitor antimycin A [84]. In a follow-up study the authors used the *hsp-6p::gfp* reporter to re-screen positive hits in the context of the *isp-1(qm150)* mutation and *atp-2(RNAi)* [86]. A gene required for UPR^{mt} induction in all cases was *sptl-1*, a serine palmitoyltransferase that functions in sphingolipid biosynthesis [86]. Accordingly, supplementation with the sphingolipid ceramide rescues the *hsp-6p::gfp* induction defect caused by *sptl-1(RNAi)*. The mevalonate biosynthesis pathway also regulates the UPR^{mt} as *hmgs-1(RNAi)*, which targets HMG-CoA synthase, attenuates *hsp-6p::gfp* induction from mitochondrial stress. Therefore, sphingolipid and mevalonate biosynthesis pathways produce molecules that either directly signal or facilitate signaling of mitochondrial stress. In support of this notion, mitochondrial stress activates expression of components of these pathways and ceramide accumulation on the outer membrane precedes UPR^{mt} induction [86].

It should also be noted that recent studies in *C. elegans* implicate the UPR^{mt}/ATFS-1 in pathogen resistance and communication between organism and environment [86-88]. ATFS-1 increases expression of innate immunity genes such as those encoding secreted lysozyme and anti-microbial peptides, which regulate the resistance to and intestinal clearance of pathogenic bacteria [88]. Bacteria such as *Pseudomonas aeruginosa* also activate the UPR^{mt}, most likely through a combinatorial mechanism involving expression of pyocyanin, cyanide toxin genes, siderophores (iron-chelating compounds), and bacterial-derived ROS [87, 88]. Furthermore,

certain metabolic pathways such as mevalonate or sphingolipid biosynthesis (discussed above) are putative targets of microbial toxins and virulence factors that render *C. elegans* unresponsive to further mitochondrial insults [86]. Thus, the UPR^{mt} in *C. elegans*, and perhaps even in mammals, evolved to sense and anticipate insults from the environment that target mitochondria, in addition to regulating mitochondrial protein homeostasis.

1.3.6 *The UPR^{mt} promotes mitochondrial homeostasis via multiple mechanisms*

The UPR^{mt}, originally characterized by induction of mitochondrial chaperones and proteases, is appreciated for other gene regulatory and metabolic alterations as well. In *C. elegans*, extensive characterization of ATFS-1 by the Haynes lab led to insights into these other functions. As mentioned, ATFS-1 partitions between the cytosol, mitochondria, and nucleus and its nuclear localization activates UPR^{mt} gene expression [21, 70]. Once in the nucleus, ATFS-1 binds promoters of glycolysis, gluconeogenesis, ribosome, respiratory chain, TCA cycle, and autophagy genes, in addition to chaperones and proteases [70]. However, *atfs-1* deletion experiments revealed that ATFS-1 differentially regulates gene expression: no effect on ribosome or autophagy genes, positive regulation of glycolysis genes, and negative regulation of TCA cycle and respiratory chain genes [70]. The UPR^{mt} thereby promotes a metabolic program that shifts energy generation from mitochondrial respiration to glycolysis, presumably to encourage recovery from mitochondrial dysfunction [70]. ATFS-1 also localizes to the mitochondria, where it is degraded by the Lon protease, to attenuate UPR^{mt} signaling during non-stress conditions. However, a fraction of mitochondrial ATFS-1 regulates mitochondrial-encoded gene expression [70]. ATFS-1 binds the A-T rich segment of mtDNA that lacks protein or RNA coding genes and contains a UPR^{mt} promoter element [70]. As is the case for nuclear-encoded respiratory chain subunits, ATFS-1 limits the expression of mitochondrial-encoded subunits [70].

Whether this is through negative regulation of mitochondrial transcription or decreased mRNA turnover is not known. Similar to deletion of *atfs-1*, deletion of the MTS of *atfs-1* causes accumulation of mitochondrial transcripts, indicating mitochondrial ATFS-1, rather than nuclear ATFS-1, is required for negative regulation of mitochondrial-encoded respiratory chain subunits [70]. In addition, ATFS-1 fosters respiratory chain assembly through positive regulation of assembly factors including *nuaf-1* and Y17G9B.5 (NADH ubiquinone oxidoreductase assembly factors), and *lpd-8* (Fe-S cluster biogenesis component) [70].

Another branch of the UPR^{mt} discovered in *C. elegans* involves the eIF2α kinase GCN-2, which negatively regulates cytoplasmic protein synthesis [89]. It acts in a compensatory fashion to the ATFS-1/chaperone-induction branch of the UPR^{mt} such that inhibition of ATFS-1 causes increased GCN-2-mediated eIF2α phosphorylation and inhibition of GCN-2 causes increased ATFS-1-mediated chaperone induction [89]. The GCN-2 branch of the UPR^{mt} is downstream of ROS since ascorbate treatment prevents eIF2α phosphorylation and leads to increased *hsp-60* expression in the context of mitochondrial stress [89]. Thus, GCN-2 decreases cytosolic protein synthesis and reduces protein import into the mitochondria to facilitate recovery from mitochondrial stress.

Mitochondrial pre-RNA processing and protein synthesis are additional targets of the mammalian UPR^{mt}. The GTPP (matrix HSP90 inhibitor)-induced UPR^{mt} causes a reduction in mRNA and protein levels of MRPP3, the catalytic subunit of the RNA-free mitochondrial RNase P complex [73]. Mitochondrial RNA derived from mtDNA is polycistronic and contains tRNA genes that flank protein-coding and rRNA genes. RNase P cleaves pre-RNA 5' of tRNAs [90], while ELAC2 and PTCD1 cleaves 3' [91], releasing mt-mRNAs and mt-tRNAs. Upon UPR^{mt} induction MRPP3 levels decrease and a measurable increase in unprocessed $tRNA^{Lys}$ and

$tRNA^{Met}$ occurs [73]. In addition to decreased pre-RNA processing, protein levels of several mitochondrial ribosomal subunits are decreased from GTPP treatment and consequently mitochondrial protein synthesis is as well [73]. Thus, the mammalian UPR^{mt} re-establishes protein folding in the mitochondria by engaging multiple mechanisms including decreasing mitochondrial pre-RNA processing and mitochondrial protein synthesis to reduce respiratory chain formation.

1.3.7 *Conservation of UPR^{mt} signaling from worms to mammals*

The UPR^{mt} is highly conserved response to misfolded proteins in the mitochondria that induces specific chaperones and proteases. The discovery of ATF5 also confirms that an identical basic leucine zipper transcription factor regulates the response in both worms and mammals. However, differences do exist. The mammalian UPR^{mt} literature has not been cohesively tied together, so direct comparisons of the mammalian UPR^{mt} to the worm UPR^{mt} can be convoluted. For example, the interaction, if any, between CHOP and ATF5 is unclear (in addition to ATF3 and ATF4, which are also induced during the mammalian UPR^{mt} [73]), and a subset of UPR^{mt} targets are not universal to all studies in mammalian literature. Along this line, certain mammalian UPR^{mt} targets are not assayed for or perhaps, detected, in worms (**Table 1.1**). Thus, subtle differences in gene targets exist.

One main difference in UPR^{mt} regulation between worms and mammals is that a CHOP homolog does not exist in worms. In contrast, homologs for ATF3/4/5 exist in worms, but ATFS-1 is the only bZip transcription factor that increases mitochondrial chaperone expression [81]. This point does not completely preclude ATF homologs from impacting worm UPR^{mt} gene expression, as a subset of respiratory chain subunits are indirectly negatively regulated by ATFS-1, i.e. ATFS-1 negatively regulates their expression, but does not bind their promoters [70]. One

way this could occur is through formation of ATFS-1 inhibitory heterodimers with bZip transcription factors such as ATF homologs that normally function to increase respiratory chain gene expression.

It is also unclear if mitochondrial stress in mammalian cells causes GCN-2-mediated eIF2α phosphorylation and/or decreases in cytosolic protein synthesis. ATF5 expression (putative ATFS-1 homolog) is regulated by eIF2α phosphorylation in multiple cases [92], so it is feasible that GCN2 or another integrated stress response signaling kinase drives ATF5 expression during the mammalian UPR^{mt}. This is intriguing as ATF3/4/5 are all activated during the UPR^{mt} [73, 77] and UPR^{ER} [79, 93, 94], and in the latter case eIF2α kinases mediate this induction. Future studies will need to tease out the apparent differential regulation of eIF2α kinases and ATF proteins during mitochondrial and ER stress.

Other differences may exist between worms and mammals, but a lack of evidence does not prove a lack of conservation. For example, it has not been determined if the respiratory chain gene regulation that occurs during the *C. elegans* UPR^{mt} is conserved to mammals. Loss of *ATF5* (mammalian *atfs-1*) reduces basal respiration, overall respiratory capacity, and maximal respiration in mammalian cells, suggesting improper assembly or decreased levels of respiratory chain complexes [77]. Induction of UPR^{mt} by GTPP (matrix HSP90 inhibitor) in mammalian cells alters respiratory chain subunit expression at the mRNA and protein level; however, directional trends are not consistent across all subunits [73]. The GTPP-induced UPR^{mt} also decreases mitochondrial pre-RNA processing and mitochondrial translation. Whether this also occurs in worms is not known, but ATFS-1 negatively regulates gene expression of mitochondrial-encoded respiratory chain subunits [70]. Thus, different mechanisms may have evolved in mammals and worms to achieve the same outcome: decreased synthesis of

mitochondrial-encoded respiratory chain subunits.

1.4 Mitochondrial Stress Promotes Longevity

1.4.1 *Mitochondrial respiration is a longevity pathway*

The first two *C. elegans* genome-wide RNAi screens performed over a decade ago came to the identical conclusion that knockdown of mitochondrial ETC genes was sufficient to extend lifespan [2, 3]. Both studies found that knockdown of complex I, III, and IV subunits could extend lifespan of both wild-type and *daf-16* mutant animals, which are defective for insulin/IGF-1-like signaling (IIS) [2, 3]. A few non-ETC mitochondrial RNAi clones were found to be DAF-16 dependent, suggesting that certain types of mitochondrial dysfunction extend lifespan through IIS, while others do not [3]. Intriguingly, ETC RNAi could only extend lifespan if knockdown was initiated during development, rather than at the young adult stage despite comparable reductions in ATP, pumping rate, and mobility [2], suggesting some aspect of mitochondrial stress is sensed during development that confers longevity to adult animals. Despite lower ATP production, small body size, slow pumping rate, slow growth rate, and sterility [2], ETC RNAi animals are sometimes more resistant to certain types of stressors such as heat shock, hydrogen peroxide, or paraquat [3, 8]. In addition to ETC RNAi, a few mutations that perturb mitochondrial function and extend lifespan have also been identified. These include mutation of the gene encoding a coenzyme Q biosynthetic enzyme *clk-1*, the Rieske iron–sulfur protein gene *isp-1*, the mitochondrial complex I subunit (NUDFB4) gene *nuo-6,* and the thiamine pyrophosphokinase gene *tpk-1* [95-99]. These findings set the stage for the mitochondrial longevity field and spurred multiple discoveries establishing causal longevity factors and stress response pathways, in addition to conservation of this paradigm in yeast, flies, and mice [100-

105]. However, we still lack a mechanistic understanding of the regulatory factors that govern mitochondrial longevity and their interactions to each other. The current view is that cytoprotective adaptive responses triggered from mitochondrial dysfunction permit an organism to cope with altered respiratory chain function, metabolic changes, and increased ROS production. These adaptive responses will be discussed in detail in the following sections.

1.4.2 *HIF-1 regulates ROS-mediated lifespan extension*

One of the first proteins implicated in mitochondrial longevity is the hypoxia-inducible factor HIF-1, a transcription factor that promotes survival during hypoxia [106]. In a screen for RNAi clones that induce the HIF-1 reporter *nhr-57p::gfp*, a significant fraction of positive hits recovered targeted components of the ETC and ATP synthase [106]. Supporting this, mitochondrial gene mutations in *clk-1(qm30)* and *isp-1(qm150)* also induced the reporter, albeit to a lesser degree than respiratory chain RNAi [106]. This suggests that under normoxic conditions, inhibition of mitochondrial respiration causes activation of a hypoxic response. Further experiments established that HIF-1 is also required for both the longevity effects from mitochondrial mutations or respiratory chain RNAi clones. The lifespan extension of *clk-1* and *isp-1* mutants was completely abrogated by a *hif-1* loss of function mutation and *hif-1(RNAi)*; peculiarly, *hif-1(RNAi)* initiated from adulthood was sufficient to decrease lifespan, suggesting HIF-1 regulates lifespan during adulthood rather than the developmental window critical for respiratory chain RNAi longevity [106]. In contrast, *cco-1(RNAi)* or *cyc-1(RNAi)* longevity is only partially suppressed by *hif-1* mutation, suggesting that respiratory chain RNAi extends lifespan through an additional mechanism compared to *isp-1* and *clk-1* mutations [106]. Differentiating the physiological and pro-longevity responses, *hif-1* is not required for slow development and reduced brood size that accompanies mitochondrial stress [106]. In addition,

HIF-1 appears to be specific to mitochondrial longevity since it is not required for IIS-, DR-, or germline signaling-mediated lifespan extension [106], however, HIF-1 has been shown to regulate longevity from a specific DR regimen in *C. elegans* (there are several regimens) [107].

One model of HIF-1-mediated mitochondrial longevity is through production of ROS, which activates HIF-1 gene expression. Lee et al. [106] found that the free-radical generator paraquat at the low-dose of 0.25 mM was sufficient to activate *nhr-57p::gfp* and extend lifespan in a HIF-1-dependent fashion. Further genetic studies found that low-dose paraquat extends lifespan through a mechanism that partially overlaps with long-lived mitochondrial mutants *nuo-6(qm200)* and *isp-1(qm150)* [108], is completely independent of *hsf-1* and *jnk-1* [108], and partially dependent on *daf-16*, *aak-2*, and *hif-1* [106, 108, 109]. The mechanism of ROS-mediated HIF-1 activation is not completely understood, but probably involves modulation of the HIF-1 prolyl hydroxylase EGL-9. The classic model of HIF-1 regulation is that under normoxic conditions EGL-9 hydroxylates HIF-1, targeting it for proteasomal degradation by VHL-1 (von Hippel Lindau 1, E3 ubiquitin ligase), while under hypoxic conditions, EGL-9 activity is decreased leading to HIF-1 stabilization [110, 111]. H_2O_2 generated via mitochondrial stress is also proposed to inhibit EGL-9 through oxidation of Fe^{2+} to Fe^{3+} within its catalytic site, leading to its inactivation and subsequent HIF-1 stabilization [112]. Another mode of *C. elegans* HIF-1 regulation involves the AMP-activated protein kinase (AMPK) subunit AAK-2. HIF-1 activity in the presence of paraquat/ROS is negatively regulated by AAK-2, which lowers ROS levels and phosphorylates HIF-1 [109]. Simultaneous to this, HIF-1 amplifies ROS levels, stabilizes itself, and negatively feedbacks on AAK-2 through an unknown mechanism, completing a regulatory loop that appropriately responds to ROS [109].

HIF-1 is also sufficient to increase lifespan in *C. elegans* and is accomplished via different methods [107, 113-115]. Downregulation of *vhl-1* and *egl-9* and overexpression of *hif-1* all significantly increase lifespan in *C. elegans*, providing credence to HIF-1's role as a longevity factor. However, HIF-1's role in aging in others organisms is not so clear. ETC RNAi promotes lifespan extension in *D. melanogaster*, so a HIF-1 mechanism could be responsible for these effects [103]. In humans, VHL is a tumor suppressor and mutations in this gene cause an inherited form of cancer [116, 117]. Hyperactivation of HIF-1 is therefore not beneficial to mammals, but it is conceivable that mild HIF-1 activation could be. A promising workaround is to identify downstream components of HIF-1 signaling that are sufficient for longevity in *C. elegans* and determine conservation in mammals, thereby avoiding the harmful effects of general HIF-1 activation [118]. In sum, *C. elegans* HIF-1 studies provided the initial evidence that free-radicals derived from mitochondrial dysfunction can improve organismal health by activating pro-longevity redox sensitive signaling pathways.

1.4.3 *The mitohormesis model of longevity*

The current belief is that instead of being harmful, free radicals play an important role in cellular signaling which, under certain circumstances, is protective and even beneficial for longevity. As mentioned, low doses of the superoxide generating compound paraquat extend lifespan in *C. elegans* [106, 108, 109], in addition to deletion of the mitochondrial superoxide dismutase gene *sod-2*, which increases levels of oxidatively damaged proteins [119]. These and additional data in worms, along with complementary evidence in both yeast and flies, has led to the popularization of the "mitohormesis" model. This model suggests that reactive oxygen species produced by mitochondria result in an adaptive response that promotes cellular health and organismal longevity (reviewed in [120-122]). In particular, the mitohormesis model proposes

that the degree of mitochondrial dysfunction and reactive oxygen species production is important for the ultimate effect on longevity and healthspan. Specifically, low levels of potentially damaging reactive oxygen species activate beneficial cellular stress responses and signaling pathways, while higher levels are detrimental, resulting in frailty or premature death. Conditions suggested to promote longevity through reactive oxygen species include inhibition of glycolysis [123], impaired insulin-like signaling [124], and mutations in mitochondrial ETC components [108], among others. Despite the appeal of this model and some experimental support, there is limited direct evidence correlating the amount of oxidative stress with longevity. For example, there is increased oxidative damage in several of the mitochondrial mutants in *C. elegans*, but in some cases, such as in the complex I mutant *gas-1(fc21)* and complex III mutant *isp-1(qm150)*, similar levels of oxidative damage result in vastly different effects on lifespan [125].

One particular instance of mitohormesis originating from the Ristow lab refers to situations where mitochondrial respiration and concomitant ROS production are increased leading to adaptive signaling that improve antioxidant capacity. The genetic factors implicated in the lifespan benefits from such perturbations include the p38 MAPK PMK-1, the phase II detoxification response transcription factor Nrf2/SKN-1, and the AMP kinase subunit AAK-2 [123, 124]. It is important to point out that longevity from respiratory chain knockdown or mutations that reduce respiration, is independent of the SKN-1 pathway [126, 127]; however, AAK-2 has been shown to mediate *isp-1(qm150)* lifespan extension [128]. In contrast, treatments that promote a starvation-like state and increased mitochondrial respiration such as glycolysis inhibitors, *daf-2(RNAi)*, and metformin require AAK-2, PMK-1, or SKN-1 for lifespan extension [123, 124, 129]. Even low-dose Complex I inhibitors that decrease mitochondrial respiration, but increase superoxide production, require PMK-1 and SKN-1 to extend lifespan [130]. In the cell,

PMK-1 functions upstream of SKN-1, which promotes the expression of antioxidant and glutathione biosynthesis genes [131]. PMK-1 is responsive to oxidative stress and phosphorylates SKN-1, triggering its nuclear accumulation and activity [131]. Supporting its role in longevity, Nrf2/SKN-1 overexpression is sufficient to extend lifespan in *C. elegans* [127] and reducing expression of its negative regulator Keap1 in *D. melanogaster* enhances paraquat resistance and lifespan [132].

A recently discovered mitohormesis factor in *C. elegans* is the peroxiredoxin PRDX-2, a redox sensor upstream of p38/PMK-1 signaling [129]. Deletion of *prdx-2* rescues the increases in phospho-PMK-1 and lifespan extension caused by metformin treatment [129]. Peroxiredoxins directly act as H_2O_2 sensors and transducers due to their high reactivity towards H_2O_2 and their protein dithiol peroxidase activity resulting in disulfide bond formation in target proteins [133]. Redox sensitive proteins such as these, rather than direct effects of ROS on oxidation of unreactive cysteine residues in target proteins, are now being appreciated for their role in translating changes in cellular redox to downstream signaling networks. PRDX-2 is a 2-Cys peroxiredoxin [134] that forms an active homodimer when oxidized [135] and can interact with and activate substrates such as the MAP3K ASK1 (NSY-1 in *C. elegans*) [136]. The MAP3K ASK1 activates both the p38 and JNK family of MAPKs and responds to oxidative stress via homo-oligomerization and autophosphorylation of its activation loop [137]. These processes are fine-tuned by multiple redox sensors in the cell that positively (such as peroxiredoxin 1 in mammals or PRDX-2 in *C. elegans*) and negatively regulate ASK1 activity. The redox protein thioredoxin is a well-known negative regulator of ASK1 that binds to and inhibits its kinase activity under reducing conditions, but dissociates upon oxidation [138], permitting ASK1 to activate p38 and JNK MAPKs [139, 140]. In contrast, peroxiredoxin 1 catalyzes the oxidation of

ASK1 to a disulfide-linked oligomer increasing its activity [136]. Thus, the activity of a single kinase is regulated by multiple competing redox sensitive mechanisms. This allows for the proper activation of stress responses when the cell faces redox imbalances and inhibition once redox homeostasis is re-established.

Mitohormesis is gospel in the mitochondrial longevity field, but important details of this model are missing. Distinct mitochondrial perturbations can cause different downstream signaling responses, or at least, require different responses for lifespan extension. For instance, SKN-1 is not required for respiratory chain RNAi longevity [126, 127], but is important for longevity from many drug treatments that target the mitochondria. The exact reasons for this difference are not clear, but probably reflect the type of mitochondrial insult. One could expect that high levels of mitochondrial stress caused by a missing or mutated ETC subunit to cause a different stress response profile than drug inhibitors of the ETC (such as rotenone or metformin) that do not greatly impact ETC stability or assembly. Metformin, for instance, does not activate the *hsp-6p::gfp* reporter, while ETC RNAi does [129]. This notion is also supported by mammalian studies using cytoplasmic hybrid (cybrid) cells with increasing levels of the mtDNA $tRNA^{Leu(UUR)}$ 3243A>G mutation [141]. Depending on the level of mutant mtDNAs, cells display distinct cellular and mitochondrial phenotypes, and importantly, gene expression profiles [141]. In other words, the degree of mitochondrial dysfunction shapes the transcriptional network; interestingly, HSP60 and HSP10 are induced in a biphasic fashion, at low levels of mutant mtDNA (20-30%) and at the highest levels (90-100%) [141]. A similar analysis of the transcriptional response to various mitochondrial stressors in *C. elegans* would help clarify the genetic pathways underlying mitohormesis-mediated longevity and their interactions to each other. In addition, many of the studies purporting mitohormesis (Ristow model) observe

increases in mitochondrial respiration that accompany mitochondrial ROS production and lifespan extension [123, 124, 129]. Unfortunately, respiration measurements in these studies are biased by changes to animal size and biomass, which are commonly altered from mitochondrial or metabolic insults, since they normalize mitochondrial respiration to protein content. Thus, it is not clear if mitochondrial respiration is actually increased at the animal level from treatment with glycolysis inhibitors or metformin. In sum, the comprehensive identification of mitohormesis stress responses, the mapping of the genetic interactions between factors, and understanding the types of insults that promote stress signaling will be essential for us to grasp cellular adaption to mitochondrial dysfunction.

1.4.4 *The complex link between the UPR^{mt} and longevity*

The UPR^{mt} was first implicated in aging by Durieux et al. [142], who reported that lifespan extension from mutations in *isp-1* or *clk-1* could be suppressed by RNAi knockdown of *ubl-5*, *dve-1*, *hsp-6*, *hsp-60*, or *clpp-1*. Based on these and other observations, Durieux et al. [142] proposed that the UPR^{mt} is a "potent transducer of the ETC longevity pathway". Further support for this model was provided by a subsequent study reporting that *ubl-5(RNAi)* can attenuate lifespan extension from knockdown of *cco-1* or *mrps-5*, which encodes a mitochondrial ribosomal protein [143]. There are significant limitations in the experimental validation of the UPR^{mt}-longevity model, which are discussed below.

The mitochondrial prohibitins (PHB1 and PHB2) are a highly conserved protein pair that forms a ring-like structure in the mitochondrial inner membrane and influence mitochondrial respiration, mitochondrial fusion, and mitochondrial protein quality control [144-147]. Prohibitin deficiency induced by RNAi knockdown results in reduced lifespan in *C. elegans* and deletion of either prohibitin gene, PHB1 or PHB2, shortens replicative lifespan in the budding yeast

Saccharomyces cerevisiae [148-151]. A recent study showed that, in addition to shortening lifespan, prohibitin deficiency also causes enrichment of several UPR^{mt} components in mitochondria of yeast cells and increased expression of the *hsp-6p::gfp* and *hsp-60p::gfp* reporters in worms [152]. Both the reduction in lifespan and apparent induction of the UPR^{mt} were suppressed in each organism by reducing cytoplasmic translation, which was accomplished by dietary restriction or by inhibition of components of the mechanistic target of rapamycin (mTOR) pathway [152].

Thus, contrary to the model that the UPR^{mt} promotes longevity, in the case of prohibitin deficiency at least, induction of the UPR^{mt} is associated with reduced lifespan, and interventions that suppress this reduced lifespan also suppress the UPR^{mt}. One interpretation of these data is that the UPR^{mt} itself plays no beneficial role in enhancing longevity and may actually limit lifespan under some conditions. An alternative possibility is that in some cases the negative consequences of mitochondrial stress can offset any benefits from induction of the UPR^{mt} and result in a net shortening of lifespan, such as in the case of prohibitin deficiency. There are also other cases where mitochondrial dysfunction is associated with reduced lifespan in *C. elegans*. This includes mutation of the cytochrome b gene *mev-1* [153] or the NDUFS2 homolog *gas-1* [154]. Likewise, RNAi knockdown of some mitochondrial genes can shorten lifespan when knockdown exceeds a certain threshold [126]. For example RNAi knockdown of the mitochondrial ATPase subunit gene *atp-3* extends lifespan when it is diluted 1:10 but shortens lifespan when undiluted [126]. In general, for *atp-3(RNAi)* and other mitochondrial RNAi treatments, the level of knockdown correlates with *hsp-6p::gfp* induction [155]. However, the level of UPR^{mt} activation does not necessarily correlate with lifespan extension. In addition, the differential lifespan effects caused by distinct mitochondrial perturbations may be caused by the

specific deficiency rather than the level of UPR^{mt} activation. This may be one reason that the UPR^{mt} is not correlated with longevity, especially when mitochondrial dysfunction is elevated past a certain threshold.

As described above, the experimental evidence suggesting that the UPR^{mt} is necessary for lifespan extension arises from two initial studies reporting that RNAi knockdown of different UPR^{mt} factors can suppress lifespan extension in response to certain forms of mitochondrial dysfunction. One of these reports also argues that the degree of induction of the UPR^{mt} correlates with the magnitude of lifespan extension following RNAi knockdown of different mitochondrial ribosomal protein genes [143]. They show that GFP expression in animals expressing the *hsp-6p::gfp* reporter is highly correlated with the percent lifespan extension from mitochondrial ribosomal protein RNAi across 8 different RNAi clones that induce *hsp-6p::gfp* five to fifteen-fold. This is difficult to interpret, however, given that they also report in the same figure that knockdown of the UPR^{mt} factor *haf-1* prevents lifespan extension in *mrps-5(RNAi)* animals, even though the *hsp-6p::gfp* reporter is still induced about 15-fold. The observation that *haf-1(RNAi)* only modestly impairs induction of the *hsp-6p::gfp* reporter but does prevent lifespan extension following *mrps-5* knockdown [143] is particularly relevant, given that the other similar published experiments fail to show that the UPR^{mt} is attenuated or blocked upon knockdown of UPR^{mt} factors. For example, the studies reporting that *ubl-5(RNAi)* prevents lifespan extension in *isp-1(qm150)* or *clk-1(e2519)* animals did not also provide corresponding evidence that *ubl-5(RNAi)* prevented induction of the UPR^{mt} in those cases. These data are further complicated by the fact that any role for UBL-5 as a regulator of the UPR^{mt} may be non-specific, as the yeast ortholog of UBL-5 (Hub1) is localized to spliceosomes where it functions as a determinant of alternative pre-mRNA splicing [156]. A related weakness is the assumption that the *hsp-6p::gfp* reporter is a

faithful reporter of endogenous activation or repression of the UPR^{mt}. Several additional UPR^{mt} targets have been identified in mammalian cells [72, 73, 77] and, in a few cases, validated in *C. elegans* (**Table 1.1**) [21]. In addition, the UPR^{mt} transcription factor ATFS-1 has been shown to regulate numerous genes beyond *hsp-6* and other mitochondrial chaperones, including a large set of detoxification and metabolic genes (**Section 1.3.6**) [21]. Despite this wealth of information, the majority of studies linking the UPR^{mt} to aging in *C. elegans* have failed to quantify the expression of endogenous UPR^{mt} targets in the context of genetic experiments interpreted to support the UPR^{mt} longevity model.

These points of contention are still relevant in *C. elegans* UPR^{mt} papers published recently by the Dillin lab [157, 158]. The histone demethylases *jmjd-1.2* and *jmjd-3.1* were found to regulate UPR^{mt} induction from mitochondrial stress, linking chromatin rearrangements to this stress response; these factors are also sufficient for UPR^{mt} induction and lifespan extension [157]. Conspicuously, lifespan epistasis experiments with the long-lived *jmjd-1.2* or *jmjd-3.1* overexpression strains used *ubl-5(RNAi)* to suppress lifespan extension, without the corresponding reporter data demonstrating that *ubl-5(RNAi)* attenuates the UPR^{mt} in this context [157]. Instead, *hsp-6p::gfp* reporter experiments use *clpp-1(RNAi)* or *atfs-1(RNAi)* to suppress the UPR^{mt}, but oddly lack corresponding lifespan data [157].

Studies in flies and mammals correlate UPR^{mt} signaling with increased health and longevity. In *Drosophila*, mild mitochondrial stress through muscle-specific RNAi knockdown of NDUFS1/ND75, a subunit of complex I, improves muscle function with age and prolongs lifespan [105]. The longevity phenotype is, in part, proposed to result from increased UPR^{mt} signaling downstream of JNK MAPK signaling, which is sensitive to redox changes [105]. Accordingly, overexpression of antioxidant enzymes GTPx-1 or catalase prevents the hormetic

effects, the induction of JNK target gene *puckered* (*puc*), and the UPR^{mt} gene expression from ND75 RNAi [105]. Overexpression of the JNK target gene *D-Jun* is also sufficient for UPR^{mt} induction and required for lifespan extension from ND75 RNAi [105]. The authors thus conclude that the UPR^{mt} and redox signaling regulates mitohormesis longevity in flies. However, altering cellular redox can alter pathways other than the UPR^{mt}, and epistasis experiments with canonical UPR^{mt} factors were not performed. Along these lines, overexpression of mitochondrial chaperone TRAP1 in *Drosophila* improves healthspan, but not lifespan, in a manner dependent on homologs of *C. elegans* UPR^{mt} factors DVE-1 and CLPP-1 [159]. Regarding mammals, mice with a truncated version of the Complex IV assembly factor SURF1 are long-lived despite a 50%+ reduction in Complex IV activity [102, 160]. Surf1$^{(-/-)}$ mice exhibit increased markers of mitochondrial biogenesis such as PGC1α and tissue-specific activation of stress responses: UPR^{mt} signaling is elevated in skeletal muscles, while Nrf2 antioxidant signaling is elevated in cardiac tissue [160]. Primary dermal fibroblasts isolated from Surf1$^{(-/-)}$ mice also display elevated UPR^{mt} induction and are resistant to cell death from oxidative stressors paraquat or tert-Butyl hydroperoxide [161]. These studies are tempting to over interpret as UPR^{mt} signaling appears to be beneficial in both *Drosophila* and mammalian systems, but unfortunately the findings fail to go beyond correlation, and in the case of TRAP1 overexpression in flies, fail to detect a lifespan extension from UPR^{mt} signaling.

Recent studies of the ATFS-1 transcription factor in *C. elegans* suggest a potential path toward addressing the question of whether the UPR^{mt} plays a direct role in aging. As mentioned, ATFS-1 contains a mitochondrial targeting sequence that causes its import and degradation in the mitochondria under non-stress conditions and a nuclear localization sequence that facilitates its import to the nucleus during mitochondrial stress. Deletion or RNAi knockdown of *atfs-1*

prevents induction of the *hsp-60p::gfp* reporter in response to treatment with paraquat or RNAi knockdown of the mitochondrial metalloprotease gene *spg-7*, as well as induction of multiple endogenous UPR^{mt} genes, *dnj-10*, *tim-23*, *ymel-1*, *enol-1*, *ldh-1*, and *gpd-2,* in response to *spg-7(RNAi)* [21, 70]. Thus, ATFS-1 appears to be more specifically and directly required for induction of the UPR^{mt} than other factors such as HAF-1 and UBL-5. In Chapter 2, I analyze whether loss of function in *atfs-1* prevents lifespan extension in response to different forms of mitochondrial stress such as RNAi knockdown of ETC components and mutation of *isp-1*, to more robustly test the UPR^{mt} longevity model.

1.4.5 *Other factors implicated in mitochondrial longevity*

Over the past decade, multiple signaling factors and pathways have been implicated in mitochondrial longevity including HIF-1, p53/CEP-1, CEH-23, GCN-2, TAF- 4, AHA-1, CEH-18, JUN-1, NHR-27, NHR-49, PMK-3, the intrinsic apoptosis pathway, and the UPR^{mt} (covered in **Sections 1.3.4**, **1.3.5**, and **1.3.6**) [162, 163]. The UPR^{mt} initially gained considerable traction as the primary mechanism controlling mitochondrial longevity due to repeated publications by the Dillin and Auwerx labs. Its attractiveness as a model is reflected by its function in mitochondrial proteostasis, its robust association with multiple forms of mitochondrial stress, and its temporal overlaps with the longevity phenotype: the UPR^{mt} is only induced if RNAi is initiated before L3/4 stage [142]. Unfortunately, this model has been disproven, or at least complicated, in the literature [164] and by my own studies (Chapter 2). However, other factors may be more causal in mitochondrial longevity and the physiological responses to mitochondrial dysfunction, such as HIF-1, which regulates mitochondrial longevity in multiple contexts [106, 109], and other genetic pathways detailed in the following paragraphs.

Recently, the intrinsic apoptosis pathway comprised of CED-3/Casp9, CED-4/Apaf1, and

CED-9/Bcl2 was found to mediate longevity specifically from *isp-1* mutation, *nuo-6* mutation, or paraquat rather than respiratory chain RNAi [165]. Notably, the effect of these gene mutations on mitochondrial mutant longevity is independent of apoptosis as a mutation in the BH3-only protein EGL-1 blocks cell death but does not suppress the lifespan of *isp-1* or *nuo-6* mutants [165]. This pathway is not required for the lowered mitochondrial respiration or ATP phenotypes of *isp-1* and *nuo-6* mutants, but intriguingly required for some of the mitochondrial phenotypes including slow embryonic and postembryonic development, and reduced pumping, defecation, and thrashing rates [165]. Thus, activation of the apoptotic machinery through mitochondrial ROS regulates both the behavioral and longevity phenotypes of mitochondrial mutants. The interaction of this pathway with HIF-1 signaling will be of particular interest since both pathways are downstream of mitochondrial ROS and required for mitochondrial mutant longevity.

The p38 MAPK PMK-3 is a novel factor that regulates mitochondrial longevity and acts in a compensatory manner to the UPR^{mt} [162]. In a previous publication, the gene *tbb-6* was found to be upregulated by *spg-7(RNAi)* independent of *atfs-1* [21], suggesting the existence of a ATFS-1-independent signaling pathway. Munkácsy et al. [162] generated a *tbb-6p::gfp* reporter and discovered that this gene is upregulated by ETC RNAi and mutations. Activation of this reporter is independent of ATFS-1, DAF-16, and SKN-1 and other UPR^{mt} regulatory genes such as *hmgs-1*, *sptl-1*, or *ran-1*; however, the UPR^{mt} factor *cbp-3* (F40F12.7) that encodes a putative CREB-binding protein is necessary [162]. The MAPK cascade comprising DLK-1 (MAP3K), SEK-3 (MAP2K), and PMK-3 (MAPK) is also required for *tbb-6p::gfp* induction [162]. Accordingly, in cases where the *tbb-6* reporter is highly induced, PMK-3 is required for mitochondrial longevity. Complex I RNAi/mutation, for instance, weakly induces the reporter and does not require PMK-

3 for lifespan extension, while complex III, IV or V RNAi/mutation strongly activates the reporter and requires PMK-3 for lifespan extension [162].

Metabolic intermediates elevated from mitochondrial dysfunction may play a role in enzyme regulation and longevity as well. For instance, the excreted metabolome of long-lived mitochondrial mutants is concentrated in specific α-ketoacids and α-hydroxyacids resulting from inhibition of a-ketoacid dehydrogenases [166]. Similar α-ketoacids are known to inhibit prolyl hydroxylases such as EGL-9, which negatively regulates HIF-1 activity [167]. Another α-ketoacid, α-ketoglutarate, is proposed to extend lifespan in *C. elegans* through direct inhibition of the mitochondrial ATP synthase, which suppresses mTORC1-dependent signaling [168]. Mitochondrial stress pathways and metabolic networks thus impinge on each other to calibrate cellular responses to changing environmental or cellular conditions.

In summary, tremendous strides have been made over the last 15 years, discovering novel mitochondrial stress responses that control aging in multiple organisms. Due to the ease of genetic studies in *C. elegans*, the majority of these mechanisms have been elucidated in this model system. However, the underlying mechanisms governing these mitochondrial stress responses, their respective interactions, and their conservation with regards to lifespan control are still largely unknown. It is becoming clear that perhaps, some stress responses are required for all cases of mitohormesis-mediated longevity, while others are only engaged from distinct types of mitochondrial stress. In Chapter 3 of this thesis, I will explore additional genetic mechanisms underlying mitochondrial longevity, specifically in the context of pentose phosphate pathway (PPP) inhibition.

Chapter 2. ACTIVATION OF THE MITOCHONDRIAL UNFOLDED PROTEIN RESPONSE DOES NOT PREDICT LONGEVITY IN *CAENORHABDITIS ELEGANS*

*** Modified from an article of the same title from Nature Communications [82]**

Christopher F. Bennett[1], Helen Vander Wende[1], Marissa Simko[1], Shannon Klum[1], Sarah Barfield[1], Haeri Choi[1], Victor V. Pineda[1], Matt Kaeberlein[1]

[1]Department of Pathology, University of Washington, Seattle, WA, USA

[2]Molecular and Cellular Biology Program, University of Washington, Seattle, WA, USA

* Correspondence to: kaeber@uw.edu

2.1 ABSTRACT

Recent studies have propagated the model that the mitochondrial unfolded protein response (UPR^{mt}) is causal for lifespan extension from inhibition of the electron transport chain (ETC) in *C. elegans*. Here we report a genome-wide RNAi screen for negative regulators of the UPR^{mt}. Lifespan analysis of nineteen RNAi clones that induce the *hsp-6$_p$::gfp* reporter demonstrate differential effects on longevity. Deletion of *atfs-1*, which is required for induction of the UPR^{mt}, fails to prevent lifespan extension from knockdown of two genes identified in our screen or following knockdown of the ETC gene *cco-1*. RNAi knockdown of *atfs-1* also has no effect on lifespan extension caused by mutation of the ETC gene *isp-1*. Constitutive activation of the UPR^{mt} by gain of function mutations in *atfs-1* fails to extend lifespan. These observations identify several new factors that promote mitochondrial homeostasis and demonstrate that the UPR^{mt}, as currently defined, is neither necessary nor sufficient for lifespan extension.

2.2 INTRODUCTION

As the primary source of cellular energy and a major source of damage, mitochondria play an important role in modulating many age-related processes [169, 170]. Harman first proposed the free radical theory of aging, which posits that damage resulting from reactive oxygen species (ROS) produced as a by-product of mitochondria metabolism determines the rate of organismal aging [171]. Recent studies have demonstrated that the situation is more complex than originally proposed, however, with important pro-longevity signaling functions of ROS having been established in several species [122].

The effect of mitochondria on aging has been studied thoroughly in the nematode *Caenorhabditis elegans*, where RNAi knockdown of several mitochondrial electron transport chain (ETC) genes has been shown to extend lifespan [172, 173]. Knockdown of ETC genes must occur during a specific stage of development in order to promote longevity [2, 3, 126], suggesting that a signal or altered metabolic state is established following ETC disruption during development to modulate adult longevity. The requirement of developmental disruption of ETC function to enhance longevity is distinct from most other longevity interventions, such as reduced insulin/IGF-1-like signaling or dietary restriction (DR), which appear to act on aging primarily during adulthood [174, 175]. The effect of ETC knockdown on lifespan is also dose-responsive, such that too much inhibition of ETC function during development can shorten lifespan [126]. A few mutations that impair mitochondrial function have also been shown to extend lifespan in *C. elegans*, including alleles of the coenzyme Q biosynthetic gene *clk-1* [97, 99], the Rieske iron-sulfur protein gene *isp-1* [98], and thiamine pyrophosphokinase gene *tpk-1* [96, 166].

Several factors have been suggested to directly promote lifespan extension from ETC knockdown and mitochondrial inhibition in *C. elegans*. For example, inhibition of ETC function can lead to increased levels of ROS, which can induce lifespan extension [106, 108]. One effect of this ROS production is stabilization and activation of the hypoxia-inducible transcription factor HIF-1, which is also required for full lifespan extension in some mitochondrial mutants and RNAi knockdowns [106]. Stabilization of HIF-1 is sufficient to extend lifespan robustly through a mechanism that is also distinct from insulin/IGF-1-like signaling and DR [113-115, 176], providing a plausible explanation for lifespan extension in these cases. In addition to HIF-1, other factors have also been implicated in lifespan extension following inhibition of

mitochondrial function. These include AMP-activated protein kinase (AMPK) [128], the homeobox protein CEH-23 [177], the transcription factor TAF-4 [178], and the p53 homolog CEP-1 [179]. It remains unclear, however, whether any of these putative downstream mechanisms can account for a majority of the lifespan effects seen in the different long-lived models of mitochondrial inhibition.

Recently, induction of the mitochondrial unfolded protein response (UPR^{mt}) was proposed to directly mediate lifespan extension from ETC inhibition in a cell non-autonomous manner [142]. The UPR^{mt} is a stress response pathway first characterized in mammalian cells, whereby nuclear encoded mitochondrial chaperones are induced in response to misfolded proteins within the mitochondria or a stoichiometric imbalance of mitochondrial respiratory complexes [47, 62, 180]. The *C.elegans* UPR^{mt} appears similar to that of mammals [46, 67, 80, 81, 142], where induction of the UPR^{mt} results in transcriptional up-regulation of the mitochondrial chaperone genes *hsp-6* and *hsp-60*. RNAi knockdown of a subset of ETC components has been shown to induce the UPR^{mt} in *C. elegans* using GFP reporters for both *hsp-6* and *hsp-60* [67, 142]. In addition, the *C. elegans* UPR^{mt} can only be induced robustly when mitochondrial stress precedes the L3/L4 larval stage transition [142], a critical time period for mitochondrial biogenesis and longevity [126, 181]. This signaling pathway is not completely understood, but several factors are reported to be required for full induction of the response, including the HAF-1 peptide exporter [81], the CLPP-1 protease [46], a ubiquitin-like protein UBL-5 [80], and two transcription factors, DVE-1, and ATFS-1 (ZC376.7) [21, 46, 81, 83].

Durieux et al. [142] linked the UPR^{mt} to aging by showing that RNAi knockdown of UPR^{mt} components can suppress the lifespan extension from mutations in *isp-1* or *clk-1*. Most of these knockdowns shortened the lifespan of wild type animals, however, and also suppressed the

lifespan extension associated with non-mitochondrial factors such as *daf*-2 and *eat-2*, suggesting that the effects were non-specific. In one case, *ubl-5(RNAi)*, the suppression appeared to be specific for *isp-1* and *clk-1*, which was interpreted to indicate that induction of the UPR^{mt} plays a causal role in lifespan extension from ETC inhibition [142]. This model was further supported by experiments showing that *ubl-5(RNAi)* can also partially or completely prevent lifespan extension from knockdown of *cco-1*, which encodes cytochrome c oxidase subunit Vb/COX4, or *mrps-5*, which encodes a mitochondrial ribosomal protein [143].

Based on the report by Durieux et al. [142], we set out to identify additional genetic modifiers of lifespan by screening for RNAi clones that induce the UPR^{mt}. Here we report the identification and validation of 25 previously unreported negative regulators of the UPR^{mt}. Unexpectedly, several RNAi clones that induce the UPR^{mt} shorten lifespan, and among at least a subset of those that extend lifespan, induction of the UPR^{mt} is not required for lifespan extension. Constitutive activation of the UPR^{mt} in the absence of mitochondrial stress also fails to extend lifespan.

2.3 RESULTS

2.3.1 *A genomic screen for negative regulators of the UPR^{mt}*

We sought to identify RNAi clones that increase lifespan by screening for induction of fluorescence in animals expressing the *hsp-6$_p$::gfp* reporter following RNAi knockdown of individual genes (**Figure 2.1a**). We identified 95 putative inducers of the UPR^{mt} from the Vidal ORFeome RNAi library (11,511 clones) (**Supplemental Table 2.1**, **Supplemental Table 2.2**). Of these, 39 RNAi clones target subunits of the ETC and 22 target mitochondrial ribosomal subunits or translation factors (**Supplemental Table 2.2**). Of the 95 clones identified from this

screen, 29 have been previously reported to induce the UPR^{mt} [6, 21, 67, 84, 85, 143], and the remaining 66 are novel.

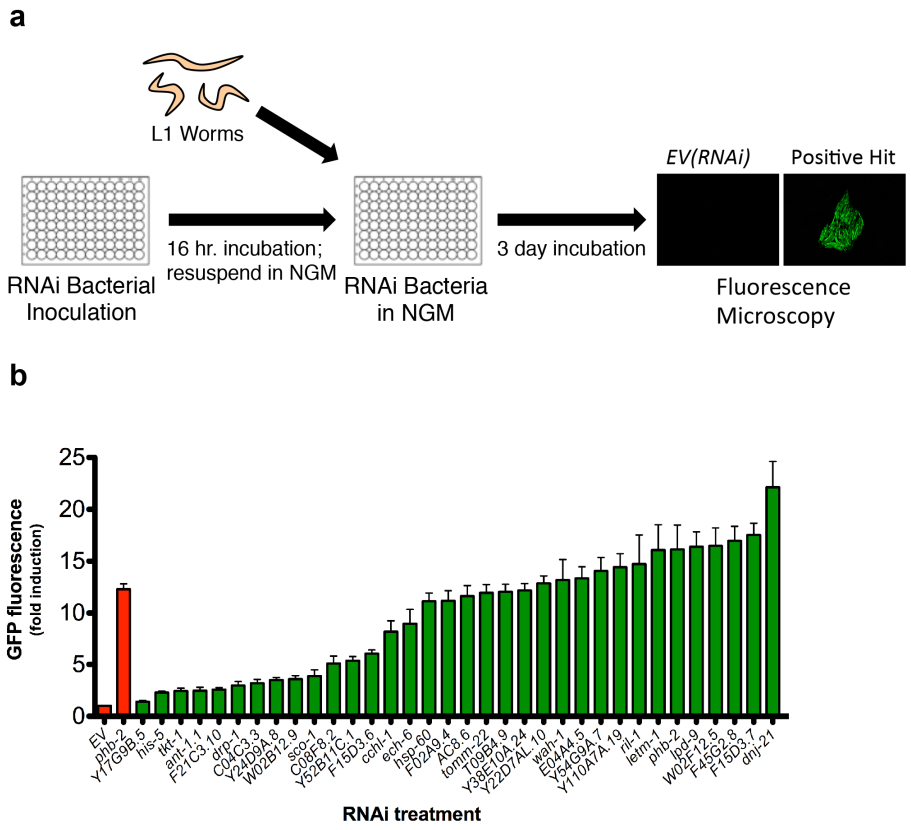

Figure 2.1. A genome-wide RNAi screen for negative regulators of the mitochondrial unfolded protein response.

(a) RNAi bacteria were grown overnight in 96-well plates, while *hsp-6p::gfp* animals were synchronized at L1 larval stage. The next day, RNAi bacteria was induced with IPTG, resuspended in liquid NGM and added to reporter animals in 96-well plates. Animals were allowed to develop for 3 days and GFP was measured by fluorescent microscopy. (b) *hsp-6p::gfp* induction was quantified for 34 RNAi clones corresponding to positive hits that were not annotated as functioning in the ETC or mitochondrial translation. Validation included sequencing each RNAi clone and GFP quantification of individual animals grown at 20°C. GFP fluorescence is the mean fluorescence relative to EV(RNAi) (N=3 independent experiments, error bars indicate s.e.m.). NGM, nematode growth media.

Since ETC components and mitochondrial ribosomal proteins are known to modulate both the UPR^{mt} and longevity [2, 3, 182], we chose to further characterize RNAi clones identified from our screen that have not been shown to play a direct role in these processes. After sequence-validation of these RNAi clones, we focused on 34 that reproducibly induced

expression of the *hsp-6$_p$::gfp* reporter relative to empty vector RNAi (**Figure 2.1b**). The targeted genes function in mitochondrial protein import, fat storage, sugar metabolism, and other aspects of mitochondrial biology such as mitochondrial fission, protein quality control, and ion transport (**Table 2.2, Supplemental Table 2.1**). Although several of the identified genes have not been shown to modulate mitochondrial function in *C. elegans*, some are homologous to known mitochondrial genes in other species or are expected to localize to the mitochondria based on predicted mitochondrial targeting sequences (**Supplemental Table 2.1**). About half (18/34) of the RNAi clones that induced expression of the *hsp-6$_p$::gfp* reporter also significantly induced expression of the mitochondrial *hsp-60$_p$::gfp* reporter, while none of the RNAi clones induced reporters of either the endoplasmic reticulum UPR (*hsp-4$_p$::gfp*) or the cytoplasmic heat shock response (*hsp-16.2$_p$::gfp*) to a detectable level, with the exception of *Y38E10A.24*(*RNAi*), which modestly increased fluorescence in the *hsp-4$_p$::gfp* strain (**Supplemental Table 2.3**).

Table 2.2. Effects of 19 UPR^{mt} regulators on lifespan.

RNAi knockdown of the shown genes significantly induced expression of the *hsp-6$_p$::gfp* reporter. The effect on mean lifespan from each RNAi clone is shown relative to empty vector (EV) treated animals. *p*-values are shown for a Wilcoxon Rank-Sum comparison to EV control. n is number of animals for a certain RNAi treatment compared to EV control.

		Effect on Mean Lifespan		
Condition	**Gene Function/Domain**	**(% EV)**	***p***	**n**
Y24D9A.8(RNAi)	Transaldolase	25.6	7.9E-42	316/284
letm-1(RNAi)	Ca2+-binding transmembrane protein, LETM1/MRS7	21.1	2.7E-39	318/320
Y110A7A.19(RNAi)	Pentatricopeptide repeat-containing protein 3	17.9	1.5E-34	360/267
F02A9.4(RNAi)	Methylcrotonoyl-Coenzyme A carboxylase 2, beta subunit	13.3	1.5E-16	302/266
wah-1(RNAi)	Programmed cell death 8, AIF homolog	12.7	7.1E-13	301/264
Y54G9A.7(RNAi)	Unknown	12.0	3.6E-13	266/279
lpd-9(RNAi)	Unknown	10.2	1.1E-11	226/293
W02F12.5(RNAi)	Dihydrolipoamide succinyltransferase (2-oxoglutarate dehydrogenase, E2 subunit)	8.2	7.0E-04	237/242
Y22D7AL.10(RNAi)	HSP10 homolog	5.5	4.8E-05	309/335
F15D3.6(RNAi)	UPS2/UPS3 homolog	4.8	1.6E-03	371/323

C04C3.3(RNAi)	Pyruvate dehydrogenase E1, beta subunit	-0.1	5.6E-01	302/279
ech-6(RNAi)	Enoyl-CoA hydratase	-1.1	9.4E-01	306/296
hsp-60(RNAi)	HSP60 homolog	-4.0	8.6E-02	187/282
F15D3.7(RNAi)	Translocase of inner mitochondrial membrane complex, subunit TIM23	-7.4	1.3E-07	217/260
E04A4.5(RNAi)	Translocase of inner mitochondrial membrane complex, subunit TIM17	-7.7	4.4E-07	199/260
F45G2.8(RNAi)	Translocase of inner mitochondrial membrane complex, subunit TIM16	-7.9	8.8E-05	291/279
dnj-21(RNAi)	Translocase of inner mitochondrial membrane complex, subunit TIM14	-10.5	4.5E-14	270/293
T09B4.9(RNAi)	Translocase of inner mitochondrial membrane complex, subunit TIM44	-11.1	2.4E-14	289/260
tomm-22(RNAi)	Translocase of outer mitochondrial membrane complex, subunit TOM22	-14.5	9.9E-28	327/335

2.3.2 *Relationship between the UPR^{mt} and longevity*

Based on the model that lifespan extension from ETC inhibition results from induction of the UPR^{mt}, we predicted that a majority of the clones identified from our screen would extend lifespan. Out of 19 RNAi clones tested, ten significantly increased lifespan ($p < 0.05$, Wilcoxon rank-sum, **Table 2.2**), of which seven increased lifespan by more than ten percent (**Figure 2.2a-g**). Six other RNAi clones significantly decreased mean lifespan (**Figure 2.3a-f**). No correlation between UPR^{mt} induction and lifespan was detected for knockdowns that significantly affected lifespan (**Figure 2.2h, Figure 2.3g, Figure 2.4a-c**). Notably, all of the clones that significantly reduced lifespan correspond to worm homologs of proteins important for transport of mitochondrial-localized proteins into the mitochondria. These included *tomm-22*, a component of the TOM complex which functions as a translocase in the outer mitochondrial membrane and *E04A4.5* (TIM17), *T09B4.9* (TIM44), *F45G2.8* (TIM16), *F15D3.7* (TIM23), and *dnj-21* (TIM14), which function in the TIM23 complex that transports proteins into the inner membrane and the matrix [18, 183]. The RNAi clones that significantly increased lifespan appear to correspond to functionally diverse proteins. These include LETM-1, a mitochondrial

transmembrane protein involved in potassium homeostasis that is associated with seizures in Wolf-Hirschhorn syndrome patients, LPD-9, a protein involved in fat storage, and *Y24D9A.8*, which is orthologous to human TALDO1 encoding transaldolase, an enzyme of the pentose phosphate pathway.

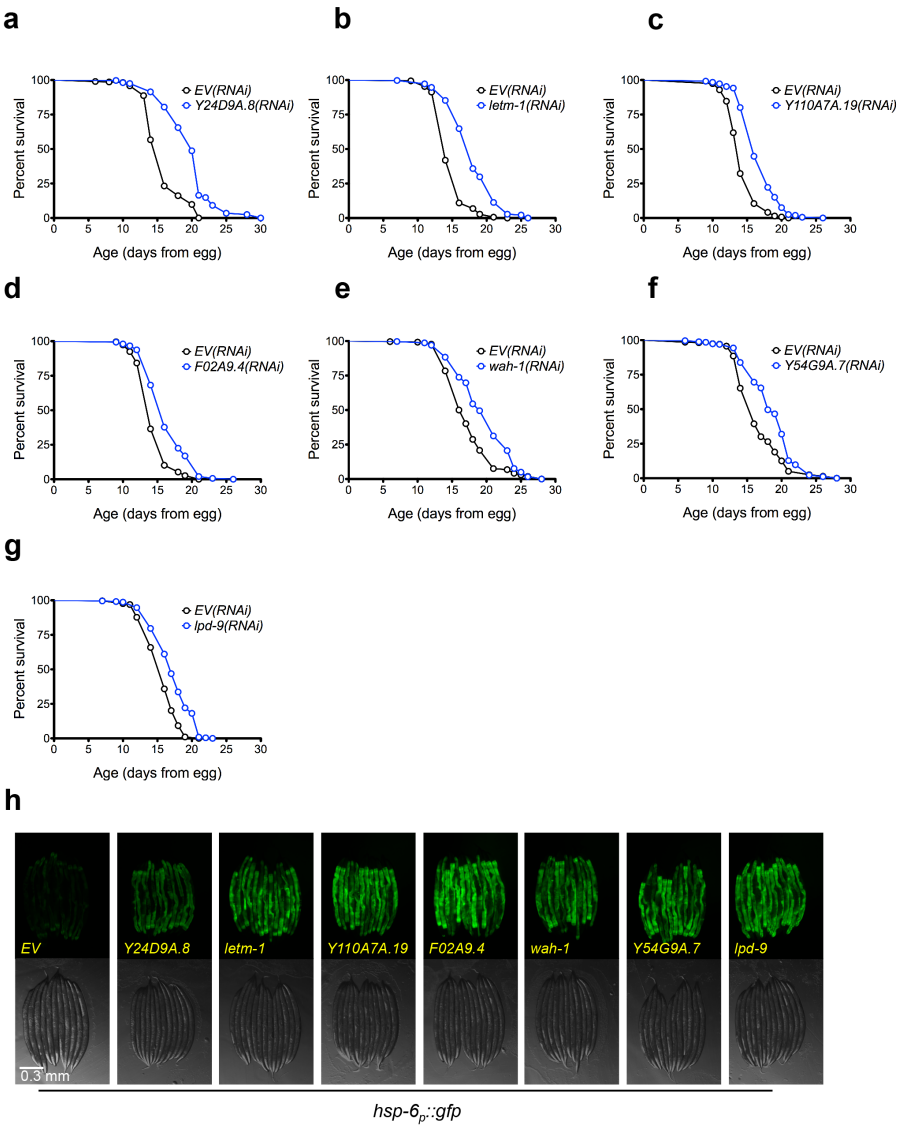

Figure 2.2. Several UPR^{mt} inducing RNAi clones extend lifespan.

(a) N2 fed *EV(RNAi)* (mean 15.8 ± .2 days, n = 284), N2 fed *Y24D9A.8(RNAi)* (mean 19.8 ± .2 days, n = 316, p < 0.0001). (b) N2 fed *EV(RNAi)* (mean 15.0 ± .1 days, n = 320), N2 fed *letm-1(RNAi)* (mean 18.1 ± .2 days, n = 318, p < 0.0001). (c) N2 fed *EV(RNAi)* (mean 14.3 ± .1 days, n = 267), N2 fed *Y110A7A.19(RNAi)* (mean 16.8 ± .1 days, n = 360, p < 0.0001). (d) N2 fed *EV(RNAi)* (mean 14.6 ± .1 days, n = 266), N2 fed *F02A9.4(RNAi)* (mean 16.6 ± .2 days, n = 302, p < 0.0001). (e) N2 fed *EV(RNAi)* (mean 17.4 ± .2 days, n = 264), N2 fed *wah-1(RNAi)* (mean 19.6 ± .2 days, n = 301, p < 0.0001). (f) N2 fed *EV(RNAi)* (mean 16.5 ± .2 days, n = 279), N2 fed *Y54G9A.7(RNAi)* (mean 18.5 ± .2 days, n = 266, p < 0.0001). (g) N2 fed *EV(RNAi)* (mean 15.7 ± .1 days, n = 293), N2 fed *lpd-9(RNAi)* (mean 17.3 ± .2 days, n = 226, p < 0.0001). (h) The *hsp-6$_p$::gfp* reporter is induced by knockdown of longevity conferring RNAi clones. *hsp-6$_p$::gfp* worms were placed onto RNAi bacteria from egg and GFP measurements were taken three days later. Scale bar, 0.3 mm. Lifespans experiments in this figure were performed at 25°C. N=3 independent experiments, with pooled data shown. Lifespans are indicated as mean +/- SEM and *p*-values were calculated using Wilcoxon rank-sum test. Data by individual experiment and statistical analysis provided in Supplementary Materials (**Supplemental Table 2.5**).

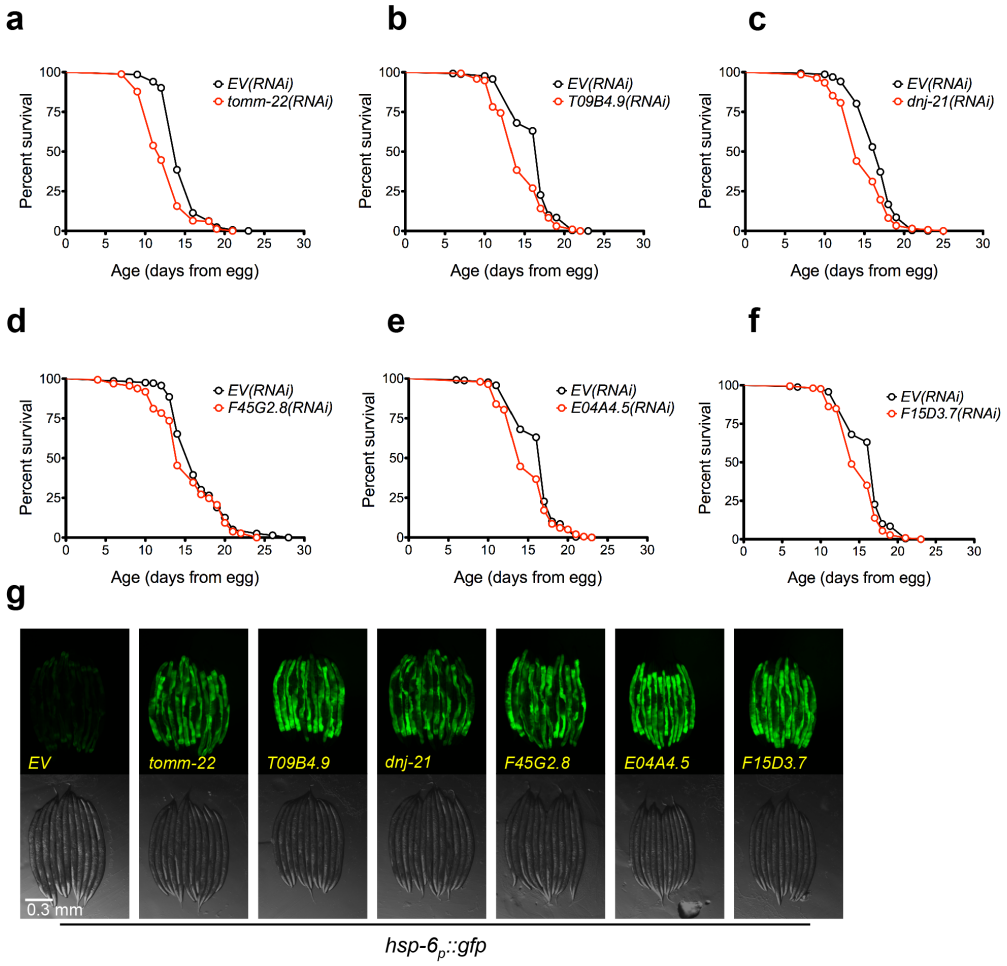

Figure 2.3. Several UPR^{mt} inducing RNAi clones shorten lifespan.

(a) N2 fed *EV(RNAi) (*mean 14.8 ± .1 days, n = 335), N2 fed *tomm-22(RNAi)* (mean 12.7 ± .2 days, n = 327, p < 0.0001). (b) N2 fed *EV(RNAi)* (mean 16.3 ± .2 days, n = 260), N2 fed *T09B4.9(RNAi)* (mean 14.5 ± .2 days, n = 289, p < 0.0001). (c) N2 fed *EV(RNAi)* (mean 16.7 ± .1 days, n = 293), N2 fed *dnj-21(RNAi)* (mean 14.9 ± .2 days, n = 270, p < 0.0001). (d) N2 fed *EV(RNAi)* (mean 16.5 ± .2 days, n = 279), N2 fed *F45G2.8(RNAi)* (mean 15.2 ± .2 days, n = 291, p < 0.0001). (e) N2 fed *EV(RNAi)* (mean 16.3 ± .2 days, n = 260), N2 fed *E04A4.5(RNAi)* (mean 15.1 ± .2 days, n = 199, p < 0.0001). (f) N2 fed *EV(RNAi)* (mean 16.3 ± .2 days, n = 260), N2 fed *F15D3.7(RNAi)* (mean 15.1 ± .2 days, n = 217, p < 0.0001). (g) The *hsp-6$_p$::gfp* reporter is induced by knockdown of RNAi clones that reduce lifespan. *hsp-6$_p$::gfp* worms were placed onto RNAi bacteria from egg and grown at 25°C. GFP measurements were taken three days later. Scale bar, 0.3 mm. Lifespan experiments in this figure were performed at 25°C. N=3 independent experiments, with pooled data shown. Lifespans are indicated as mean +/- SEM and *p*-values were calculated using Wilcoxon rank-sum test. Data by individual experiment and statistical analysis provided in Supplementary Materials (**Supplemental Table 2.5**).

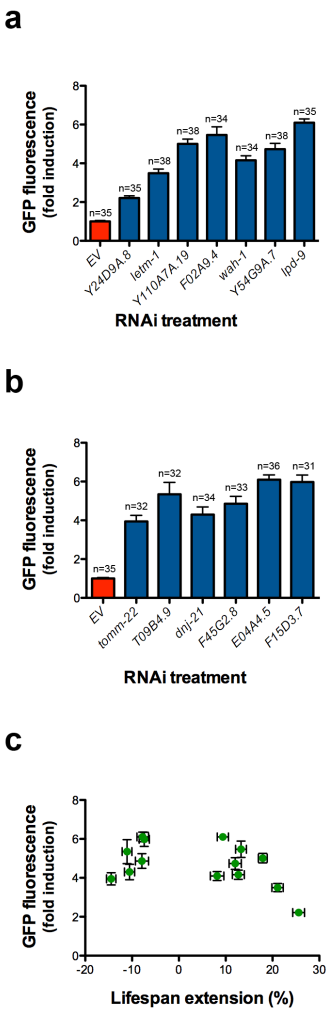

Figure 2.4. Induction of *hsp-6$_p$::gfp* is not correlated with lifespan extension.

hsp-6$_p$::gfp induction from three separate experiments performed at 25°C for (a) long-lived RNAi clones and (b) short-lived RNAi clones. GFP fluorescence is the average fluorescence of an individual worm relative to *EV(RNAi)* and error bars indicate SEM. (c) *hsp-6$_p$::gfp* induction is not significantly positively correlated with lifespan extension. The Pearson's correlation R^2 is 0.1912 and *p*-value is 0.12. Error bars indicate SEM for GFP fluorescence and % mean lifespan extension relative to *EV(RNAi)*.

2.3.3 *ATFS-1 is required for UPR^{mt} induction but not longevity*

We next set out to more directly characterize the role of the UPR^{mt} in lifespan extension from knockdown of two of the novel longevity clones identified from our screen: *letm-1* and *Y24D9A.8* (transaldolase). We first considered using the *haf-1(ok705)* mutant for epistasis experiments, but found that *haf-1* was not required for induction of the UPR^{mt} caused by RNAi knockdown of *cco-1* or by RNAi knockdown of the gene encoding the mitochondrial prohibitin *phb-2* (**Supplemental Figure 2.1**). Therefore, we utilized the *atfs-1(tm4525)* mutation, which has been shown to prevent induction of the UPR^{mt} following knockdown of mitochondrial AAA-protease *spg-7*, knockdown of mitochondrial import machinery, and ethidium bromide treatment [21]. In the absence of mitochondrial stress, ATFS-1 is imported into the mitochondria where it is degraded; when mitochondria are dysfunctional, import and degradation of ATFS-1 is impaired, and it relocalizes to the nucleus to induce expression of UPR^{mt} genes, including *hsp-6* and *hsp-60* [21]. Based on the model that the UPR^{mt} plays a causal role in lifespan extension, we reasoned that RNAi of either *letm-1* or *Y24D9A.8* (transaldolase) should have no effect on lifespan in the *atfs-1(tm4525)* background. Unexpectedly, deletion of *atfs-1* failed to significantly attenuate the lifespan extension from RNAi knockdown in either case (**Figure 2.5a,b**).

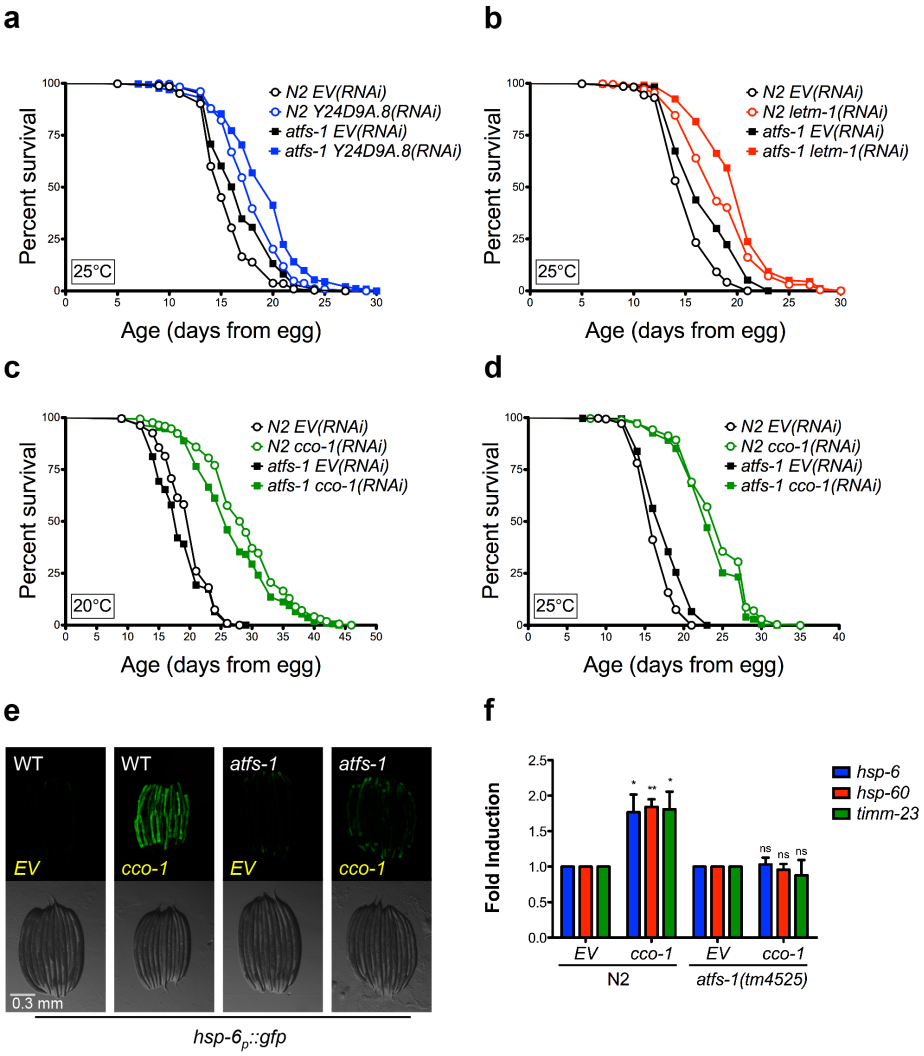

Figure 2.5. UPR^{mt} inducing RNAi clones do not require *atfs-1* for lifespan extension.

(a) *Y24D9A.8(RNAi)* lifespan extension is not dependent on *atfs-1*. N2 fed *EV(RNAi)* (mean 15.7 ± .1 days, n = 535), N2 fed *Y24D9A.8(RNAi)* (mean 18.1 ± .1 days, n = 456, p < 0.0001), *atfs-1(tm425)* fed *EV(RNAi)* (mean 17 ± .2 days, n = 417), *atfs-1(tm4525)* fed *Y24D9A.8(RNAi)* (19.2 ± .2 days, n = 334, p < 0.0001). (b) *letm-1(RNAi)* lifespan extension is not dependent on *atfs-1*. N2 fed *EV(RNAi)* (mean 15.5 ± .1, n = 460), N2 fed *letm-1(RNAi)* (mean 18.6 ± .2, n = 421, p < 0.0001), *atfs-1(tm425)* fed *EV(RNAi)* (mean 17 ± .2, n = 386), *atfs-1(tm4525)* fed *letm-1(RNAi)* (mean 20.1 ± .2, n = 358, p < 0.0001). (c) The long lifespan of *cco-1(RNAi)* is not dependent on *atfs-1* at 20°C. N2 fed *EV(RNAi)* (mean 19.9 ± .2, n = 215), N2 fed *cco-1(RNAi)* (mean 28.9 ± .5, n = 170, p < 0.0001), *atfs-1(tm425)* fed *EV(RNAi)* (mean 18.6 ± .3, n = 202), *atfs-1(tm4525)* fed *cco-1(RNAi)* (mean 26.9 ± .5, n = 170, p < 0.0001). (d) The long lifespan of *cco-1(RNAi)* is not dependent on *atfs-1* at 25°C. N2 fed *EV(RNAi)* (mean 16.6 ± .1, n = 279), N2 fed *cco-1(RNAi)* (mean 24.2 ± .3, n = 242, p < 0.0001), *atfs-1(tm425)* fed *EV(RNAi)* (mean 17.8 ± .2, n = 302), *atfs-1(tm4525)* fed *cco-1(RNAi)* (mean 23.5 ± .3, n = 202, p < 0.0001). (e) *hsp-6$_p$::gfp* induction by *cco-1(RNAi)* is attenuated in the *atfs-1(tm4525)* mutant. Scale bar, 0.3 mm. (f) Induction of UPR^{mt} targets *hsp-6*, *hsp-60*, and *timm-23* does not occur in the *atfs-1(tm4525)* mutant. N2 and *atfs-1(tm4525)* worms were grown on *cco-1(RNAi)* from egg at 20°C and harvested at L4. Gene expression was normalized to *EV(RNAi)*. (N=4, Error bars represent SEM, p* < 0.05, p** < 0.01), p > 0.05 is not significant (ns), student's t-test). Lifespan experiments in this figure represent pooled data, are indicated as mean +/- SEM, and *p*-values were calculated using Wilcoxon rank-sum test. Data by individual experiment and statistical analysis provided in Supplementary Materials (**Supplemental Table 2.6**).

In order to determine whether the lack of effect from *atfs-1* deletion on lifespan extension is specific to these newly identified UPR^{mt}-inducing clones, we asked whether knockdown of *cco-1*, which is already known to extend lifespan [2, 3, 126], was dependent on *atfs-1*. To rule out the possibility that high temperature (25°C) could influence the outcome by modulating expression of UPR^{mt} genes independently of the mitochondrial stress, we performed subsequent experiments at 20°C in addition to 25°C. Once again, deletion of *atfs-1* failed to significantly attenuate lifespan extension from *cco-1(RNAi)* at both temperatures (**Figure 2.5c,d**). The presence of the *atfs-1(tm4525)* allele was verified by PCR (**Supplemental Figure 2.2**), and deletion of *atfs-1* prevented induction of both *hsp-6$_p$::gfp* reporter, as well as three different endogenous UPR^{mt} genes, *hsp-6*, *hsp-60*, and *timm-23*, following *cco-1(RNAi)* (**Figure 2.5e,f**).

In order to further test the generality of our observations, we treated long-lived *isp-1(qm150)* mutant animals with *atfs-1(RNAi)*. As has been previously reported [21], we confirmed that *atfs-1(RNAi)* delayed the development of *isp-1* mutant animals (**Supplemental Figure 2.3**). Even when this delay is taken into account, mutation of *isp-1* significantly increased the lifespan of animals treated with *atfs-1(RNAi)* comparably to animals treated with empty vector RNAi (**Figure 2.6a**), despite the fact that *atfs-1(RNAi)* completely prevented induction of GFP in *isp-1(qm150)* animals expressing the *hsp-6$_p$::gfp* reporter (**Figure 2.6b**).

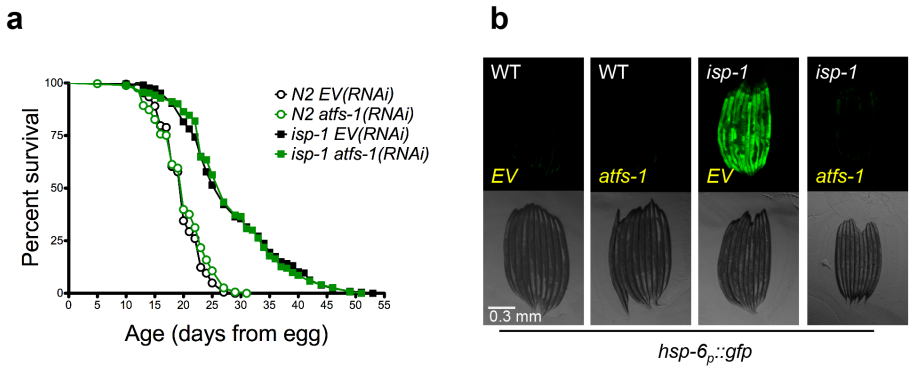

Figure 2.6. The UPR^{mt} is not required for *isp-1(qm150)* longevity.

(a) Knockdown of *atfs-1* does not attenuate the longevity of complex III mutant *isp-1(qm150)*. N2 fed *EV(RNAi)* (mean 19.7 ± .2, n = 365), N2 fed *atfs-1(RNAi)* (mean 20 ± .2 days, n = 346, p = 0.399), *isp1(qm150)* fed *EV(RNAi)* (mean 28.2 ± .6 days, n = 206), *isp-1(qm150)* fed *atfs-1(RNAi)* (mean 28.3 ± .5 days, n = 293, p = 0.612). (b) *hsp-6$_p$::gfp* induction by *isp-1(qm150)* mutation is attenuated by *atfs-1(RNAi)*. Scale bar, 0.3 mm. Lifespan experiments in this figure represent pooled data, are indicated as mean +/- SEM, and *p*-values were calculated using Wilcoxon rank-sum test. Data by individual experiment and statistical analysis provided in Supplementary Materials (**Supplemental Table 2.6**).

2.3.4 *Stabilization of ATFS-1 does not extend lifespan*

Recently, constitutively active alleles of ATFS-1 have been described which result in induction of the UPR^{mt} in the absence of exogenous mitochondrial stress [184]. To determine whether constitutive activation of the UPR^{mt} is sufficient to extend lifespan in the absence of ETC inhibition, we measured the lifespans of strains carrying either the *atfs-1(et17)* or *atfs-1(et18)* alleles. In both cases, lifespan was significantly reduced at 20°C, rather than extended (**Figure 2.7a,b**). Similar results were obtained at 25°C, although the reduction in lifespan was attenuated at the higher temperature (**Figure 2.7c,d).** The endogenous UPR^{mt} targets *hsp-6*, *hsp-60*, and *timm-23* were significantly induced in the *atfs-1(et17)* and *atfs-1(et18)* strains, relative to N2 (**Figure 2.7e**), demonstrating constitutive activation of the UPR^{mt} in these animals.

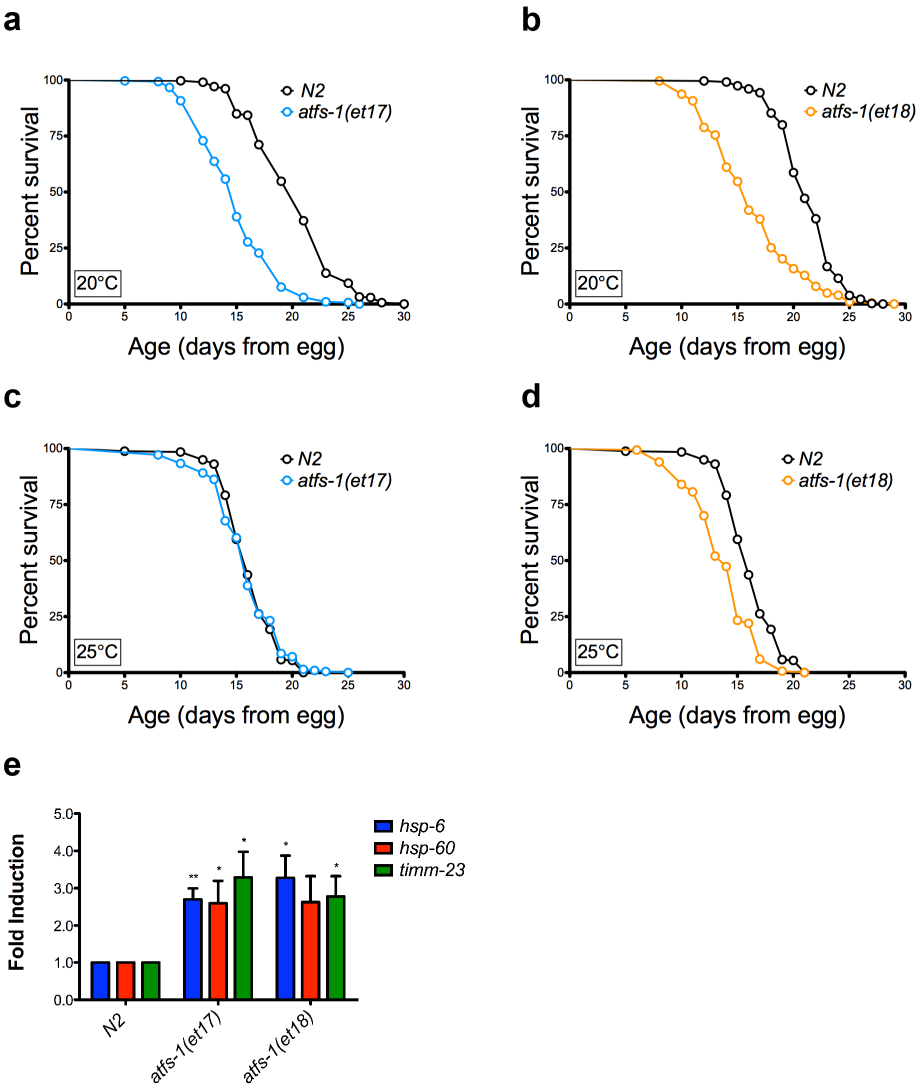

Figure 2.7. The UPR^{mt} is not sufficient for lifespan extension.

(a) Constitutive UPR^{mt} mutation *atfs-1(et17)* shortens lifespan at 20°C. N2 fed HT115 bacteria (mean 20.3 ± .2 days, n = 312), *atfs-1(et17)* fed HT115 bacteria (mean 15 ± .2, n = 303, p < 0.0001). (b) Constitutive UPR^{mt} mutation *atfs-1(et18)* shortens lifespan at 20°C. N2 fed HT115 bacteria (mean 21.3 ± .1, n = 418), *atfs-1(et18)* fed HT115 bacteria (mean 16.3 ± .3 days, n = 203, p < 0.0001). (c) *atfs-1(et17)* mutation does not affect lifespan at 25°C. N2 fed HT115 bacteria (mean = 16.2 ± .15 days), *atfs-1(et17)* fed HT115 bacteria (mean = 15.9 ± .21 days, p = 0.31). (d) *atfs-1(et18)* mutation shortens lifespan at 25°C. N2 fed HT115 bacteria (mean = 16.2 ± .15 days), *atfs-1(et18)* fed HT115 bacteria (mean = 13.8 ± .13 days, p < 0.0001). (e) Constitutive UPR^{mt} mutations *atfs-1(et17)* and *atfs-1(et18)* induce expression of *hsp-6*, *hsp-60*, and *timm-23*. Gene expression was normalized to N2 fed *EV(RNAi)*. (N=4, Error bars represent SEM, p* < 0.05, p** < 0.01, student's t-test). The gene expression data for *hsp-60* in the *atfs-1*(*et18) allele* is trending significant, with *p* = 0.05. Lifespan experiments in this figure represent pooled data, are indicated as mean +/- SEM, and *p*-values were calculated using Wilcoxon rank-sum test. Data by individual experiment and statistical analysis provided in Supplementary Materials (**Supplemental Table 2.6**).

2.4 DISCUSSION

The model that the UPR^{mt} plays a causal role in lifespan extension has become widely accepted, despite the correlative nature of the supporting data and the lack of evidence that induction of the UPR^{mt} is sufficient to increase lifespan. In this study, we identified 95 gene knockdowns that induce the UPR^{mt}, 66 of which are novel, and found that, at least for the subset tested here, there was no correlation between lifespan extension and the degree of UPR^{mt} induction. Furthermore, we found that the UPR^{mt} is neither necessary nor sufficient for lifespan extension by utilizing both null and gain of function mutations in the UPR^{mt} transcription factor ATFS-1.

As with prior studies of mitochondrial function in *C. elegans*, the studies described here are limited to mutations and RNAi knockdowns that only partially impair ETC function, since complete absence of ETC function is incompatible with life. Thus, we anticipate that additional genetic modifiers of the UPR^{mt}, which may have resulted in lethality or early larval arrest in our RNAi screen, remain to be identified. This is consistent with prior studies indicating that RNAi knockdown of some mitochondrial factors results in severe lifespan reduction or lethality when the RNAi is undiluted, but increase lifespan when the RNAi is diluted or initiated post-developmentally [126, 179, 182].

The best evidence that the UPR^{mt} directly promotes longevity comes from epistasis experiments reporting that knockdown of *ubl-5* or *haf-1*, which are required for full induction of the UPR^{mt}, prevents lifespan extension from *isp-1(qm150)* or RNAi knock-down of either *cco-1* or *mrps-5 [142, 143]*. One major caveat to these experiments, however, is that neither *ubl-5(RNAi)* nor *haf-1(RNAi)* actually prevented induction of the UPR^{mt} in these experiments. For example, in the study from Houtkooper et al. [143], double knock-down of *mrps-5* and *haf-1* still resulted in an approximately 15-fold induction of the *hsp-6$_p$::gfp* reporter relative to control

animals, suggesting that the UPR^{mt} is, at best, attenuated. Furthermore, no analysis of endogenous expression UPR^{mt} targets was reported in these studies. In addition, we found that *haf-1* is not required for induction of the UPR^{mt} caused by knockdown of two additional mitochondrial genes: *cco-1* and *phb-2*. In the case of *ubl*-5, which encodes an ubiquitin-like peptide homologous to the yeast splicing factor Hub1 [156], interpretation is further complicated by the fact that this protein likely has numerous functions beyond modulating the UPR^{mt}.

For these reasons, we felt that loss of *atfs-1*, which has no known function outside of the UPR^{mt}, might provide a useful alternative test of this model. In contrast to knockdown of either *haf-1* or *ubl-5*, we were able to demonstrate that deletion or RNAi knockdown of *atfs-1* largely or completely abolishes induction of both the *hsp-6$_p$::gfp* reporter and endogenous expression of three different UPR^{mt} components (*hsp-6*, *hsp-60*, and *timm-23*), while having minimal effect on lifespan extension from multiple forms of mitochondrial stress, including mutation of *isp-1*, RNAi knockdown of *cco-1*, and RNAi knock-down of two new aging genes identified in this study: *letm-1* and *Y24D9A.8*.

Our observations that longevity is reduced by constitutive activation of ATFS-1 or by a subset of RNAi clones related to mitochondrial protein import (*tomm-22*, *E04A4.5*, *T09B4.9*, *F45G2.8*, *F15D3.7*, and *dnj-21*), further argue against a direct causal link between the UPR^{mt} and longevity, and demonstrate that activation of the UPR^{mt} is not sufficient to enhance longevity. This is also consistent with prior reports showing that knockdown of the gene encoding the mitochondrial prohibitin *phb-2* induces the UPR^{mt} in both yeast and worms while simultaneously shortening lifespan in both organisms [148, 152]. In the case of prohibitin deficiency, the lifespan defects can be suppressed by a reduction in cytoplasmic translation in yeast or by deletion of the S6 kinase homolog *rsks-1* in worms, which both attenuate the UPR^{mt}. It will be of

interest to determine whether loss of *rsks-1* or deletion of *atfs-1* can prevent lifespan shortening in response to knockdown of mitochondrial protein import machinery.

Although we reach a different conclusion with respect to the role of the UPR^{mt} in longevity than has been previously suggested, the data presented in this study are generally consistent with the prior data from Durieux et al. [142] and Houtkooper et al. [143]. Our data also do not address the "mitokine" mechanism proposed by Durieux et al. [142], whereby a neuronal signal is transmitted to distal cells to induce the UPR^{mt} in a cell non-autonomous manner. By utilizing both RNAi and mutant alleles of *atfs-1*, however, we are able to exclude the possibility that the presence (or absence) of neuronal UPR^{mt} signaling (knockdown by RNAi feeding is generally less efficient in neurons) could yield different outcomes with respect to lifespan.

It is also important to consider that the UPR^{mt} is still relatively poorly characterized and imprecisely defined. Nearly every study of the UPR^{mt} in *C. elegans* has utilized either the *hsp-6$_p$::gfp* reporter or the *hsp-60$_p$::gfp* reporter, with analysis of endogenous expression of *hsp-6*, *hsp-60*, or other UPR^{mt} targets rarely performed. Our data indicate that some RNAi clones that robustly induce expression of *hsp-6$_p$::gfp* do not strongly induce expression of *hsp-60$_p$::gfp* (**Supplemental Table 2.3**). Whether this represents a biologically relevant difference in regulation of *hsp-6* and *hsp-60* or simply reflects differential sensitivities of the two reporters will require further study, but it does point out the possibility that there may be substantial differences in regulation of individual UPR^{mt} targets, depending on the type of mitochondrial stress and the resulting signals from the mitochondria to the nucleus. For this reason, we chose to directly quantify mRNA levels for three mitoUPR-regulated genes, in addition to utilizing these GFP reporter strains. In each case, similar changes in expression were observed. Our data therefore dissociate the mitoUPR, as commonly defined in the field, from longevity; however, it

remains possible that additional, as yet unknown, UPR^{mt} targets that are regulated independently of ATFS-1 could influence lifespan directly. Thus, although we do not completely rule out a causal role for the UPR^{mt} in aging, our data strongly suggest that if the UPR^{mt} does play any direct longevity-promoting role it is subtle, variable, and highly context-dependent. Indeed, our interpretation of the entire body of data is that a stronger case can be made that the UPR^{mt} generally suppresses longevity, and that inhibition of ETC function increases lifespan *in spite of*, rather than *because of*, the UPR^{mt}.

Our observation that the lifespan-extending RNAi clones which also induce the UPR^{mt} appear to encompass a range of mitochondrial and cytoplasmic functions suggests that the mechanisms by which mitochondrial perturbations modulate aging in *C. elegans* may extend beyond reduced ETC function or inhibition of mitochondrial translation. The fact that each of these RNAi clones also induces the UPR^{mt} indicates that they are likely perturbing mitochondrial homeostasis, or at least inducing a signal of mitochondrial stress. It will be important to understand how each of these factors is influencing mitochondrial function, particularly in those cases where there is no obvious link to mitochondria, such as transaldolase deficiency. In this regard, it is interesting to note that altered expression of pentose phosphate pathway enzymes has been associated with lifespan extension from calorie restriction in rhesus monkeys [185], and transaldolase deficiency in mice causes loss of mitochondrial membrane potential and morphology in spermatozoa [186].

In addition to the UPR^{mt}, several cellular pathways and factors have been proposed to mediate enhanced longevity following mitochondrial stress in *C. elegans*. As with prior studies on the UPR^{mt}, however, each of these factors (e.g. HIF-1, CEH-23, AMP kinase, p53/cep-1, TAF-4) have only been tested relative to one or a few long-lived mutants or RNAi clones. For

now, it remains an open question as to whether a single mechanism will ultimately explain all of the various mitochondrial longevity interventions, or if multiple overlapping but distinct mechanisms contribute. Given the central role of mitochondrial function in metabolism, nutrient response, and energetics, it is perhaps not surprising that the role of mitochondria in aging is complex and challenging to understand solely through genetic analyses.

2.5 CONCLUSION

Taken together with prior studies, the observations reported here demonstrate that the relationship between the UPR^{mt} and aging is significantly more complex than currently appreciated. At best, induction of the UPR^{mt} is only weakly correlated with longevity, since many RNAi clones that induce the UPR^{mt} either have no effect on lifespan or reduce lifespan, and induction of the UPR^{mt} in the absence of mitochondrial stress fails to increase lifespan. Of the additional factors previously implicated in mitochondrial longevity, it remains unclear whether any represent a unifying mechanism. Despite the mechanistic uncertainties, however, the identification here of several novel RNAi clones that induce the UPR^{mt}, at least eight of which also extend lifespan, further emphasizes the central importance of this pathway and suggests that this will be a fertile area for future research and insights into the fundamental mechanisms of mitochondrial quality control and aging.

2.6 METHODS

Strains

NQ887 *(isp-1(qm150))*, QC117 (*atfs-1(et17)*), QC118 (*atfs-1(et18)*), SJ4100 (zcIs13[*hsp-6$_p$::gfp*]), SJ4058 (zcIs9[*hsp-60$_p$::gfp*]), CL2070 (dvIs[*hsp-16.2$_p$::gfp*]), and SJ4005 (zcIs4[*hsp-*

4$_p$::gfp]) were obtained from the Caenorhabditis Genetics Center (Minneapolis, MN). The *atfs-1(tm4525)* was obtained from the National BioResource Project (Tokyo, Japan) and backcrossed to our lab N2 strain twice.

RNAi Screen and Fluorescence Microscopy

All fluorescence microscopy was performed using a Zeiss SteREO Lumar.V12 microscope (Thornwood, NY, USA). The RNAi screen was performed using the Vidal RNAi library [187] and *hsp-6$_p$::gfp* worms. RNAi bacteria were inoculated into LB^{Amp} media and GFP reporter worms were hypochlorite treated and hatched in M9 overnight. The next day, RNAi bacteria were induced with 4mM IPTG for 1 hour, pelleted, and resuspended in liquid NGM supplemented with ampicillin and IPTG. RNAi bacteria were then added to 96-well plates with ~30 L1 reporter worms per well. After 3 days, GFP fluorescence was assessed manually by scoring photos as weak induction, strong induction, or no induction.

For validation of RNAi clones and quantification of different GFP reporter expression, GFP fluorescence of individual worms was quantified using IMAGEJ (Rasband, 1997–2012). Relative fluorescence to empty-vector was calculated and fluorescence data was pooled across three independent experiments. A Student's t-test was used to calculate significance with a Bonferonni correction to account for multiple comparisons. Synchronized eggs were grown on RNAi bacteria at 20°C, unless otherwise stated. After 3 days, worms were assayed for GFP expression by fluorescence microscopy. For the *hsp-16.2$_p$::gfp* and *hsp-4$_p$::gfp* reporters, expression was induced by treatment with 4+ hour 30°C heat shock and tunicamycin respectively. At least two independent experiments, with approximately 10 animals per condition per experiment, performed on different days from different RNAi cultures, was obtained for each reporter with similar results.

Lifespan Analyses

Lifespans were performed as described previously [188]. Synchronized eggs obtained by treating adult animals with hypochlorite were grown on NGM plates containing 4 mM IPTG, 25 μg ml^{-1} carbenicillin and seeded with HT115(DE3) RNAi bacteria. At larval stage 4, worms were transferred to plates with 50 μM FUDR to prevent hatching of progeny. Lifespans were performed at 25°C for the lifespan screen and at 20°C and 25°C in other experiments as described in the text and figures. Cohorts were examined every 1–3 days using tactile stimulation to verify viability of animals. Animals lost due to foraging were not included in the analysis. All lifespan analyses were replicated using independent cohorts on different dates with replicate statistics provided in Supplementary Tables (**Supplemental Table 2.5Supplemental Table 2.6**). *P*-values were calculated using the Wilcoxon rank-sum test. GraphPad Prism was used for Pearson's correlation statistics of *hsp-6*$_p$*::gfp* induction versus lifespan.

qRT-PCR

RNA was isolated from L4 worms using a TRIzol (Life Technologies) chloroform extraction and cDNA was prepared according to the SuperScript III First Strand Synthesis protocol (Life Technologies). qRT-PCR was used to measure the expression levels of *hsp-6*, *hsp-60*, *timm-23* (primers in Supplementary Table 4) and normalization controls *pmp-3* and *cdc-42* (TaqMan® Gene Expression Assays, Life Technologies). The relative standard curve method was used to calculate gene expression.

2.7 ACKNOWLEDGEMENTS

This work was supported by NIH Grant R01AG039390 to MK. CFB was supported by NIH training grants T32GM07270 and T32ES007032.

2.8 SUPPLEMENTAL FIGURES AND TABLES

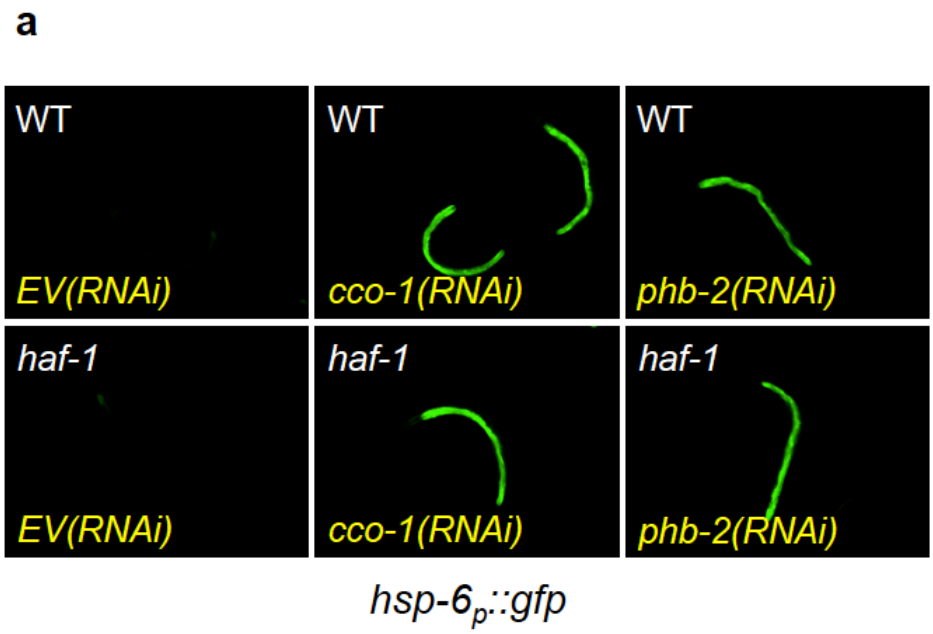

Supplemental Figure 2.1. HAF-1 is not required for UPR^{mt} induction caused by *cco-1* and *phb-2* RNAi.

(a) *hsp-6$_p$::gfp* induction was measured 3 days from hatch at 20°C in wild-type and *haf-1(ok705)* animals.

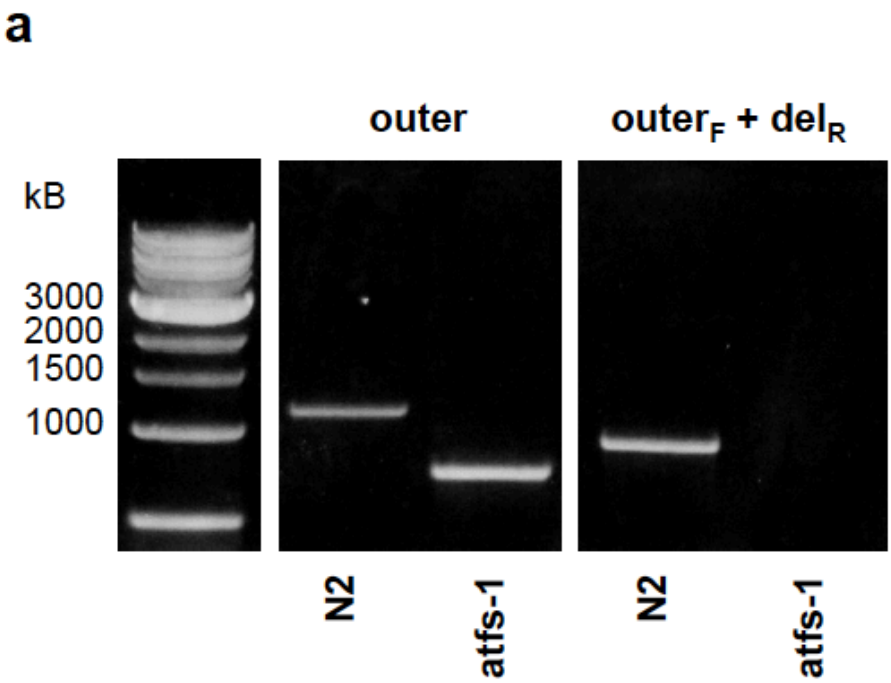

Supplemental Figure 2.2. Genotyping of *atfs-1(tm4525)* mutant.

(a) Outer primers, which bind outside the deletion, give a WT band of ~1200 bp and a *tm4525* band of ~800. The del$_R$ primer is inside the *tm4525* deletion. The outer$_F$ and del$_R$ give a WT band of ~1000 bp and no *tm4525* band.

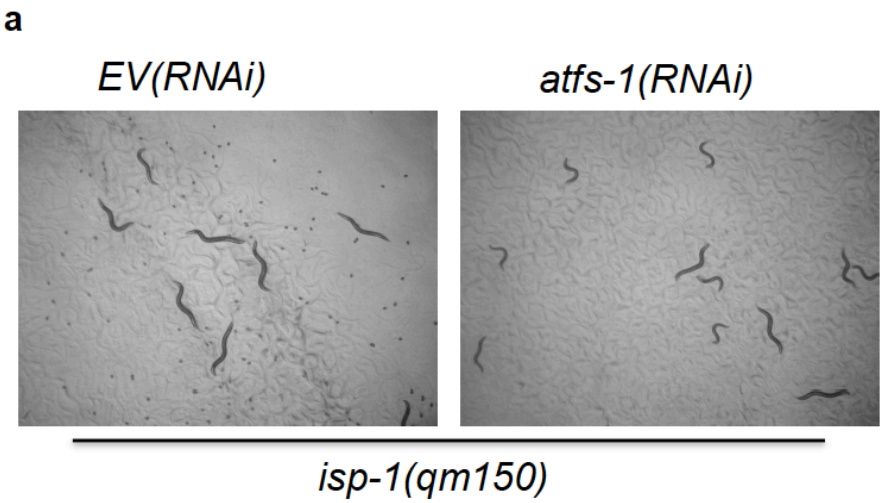

Supplemental Figure 2.3. The developmental rate of *isp-1(qm150)* is delayed by *atfs-1(RNAi)*.

(a) *isp-1(qm150)* were grown from egg on *EV(RNAi)* and *atfs-1(RNAi)* for 6 days.

Supplemental Table 2.1. Validated RNAi Inducers of the UPR^{mt}.

RNAi knockdown of the following 34 genes significantly induced the *hsp-6$_p$::gfp* reporter. The eukaryotic orthologous groups (KOGs) annotation and PPOD derived human and yeast orthologs for each gene are shown. Annotation for mitochondrial targeting is based off of Go Term "Mitochondrion" annotation (A), orthology to a known mitochondrial gene by PPOD (B), MitoProt II probability estimation >0.8 (C), or presence in a published *C. elegans* mitochondrial proteome data set by Li, J., et al., Proteomics, 2009 [1] (D). Reported effects on longevity are shown as WBRNAi experiments or Chen, D., et al., Aging Cell, 2007 [2] (E). Reported effects on the UPR^{mt} are based on the work of Yoneda, T., et al., Journal of Cell Science, 2004 [3] (F), Nargund, A., et al., Science, 2012 [4] (G), Melo, J., et al., Cell, 2012 [5] (H), and Shore, D., et al., PLoS Genet, 2012 [6] (I).

Gene Name	NCBI KOG Annotation	PPOD (Human | Yeast Ortholog)	Mito. Targeted	Extended Lifespan	Reported UPR^{mt} inducer
E04A4.5	Mitochondrial import inner membrane translocase, subunit TIM17	TIM17A/TIM17 B | TIM17	A, B, D		
F15D3.7	Mitochondrial import inner membrane translocase, subunit TIM23	TIMM23B | TIM23	A, B, D		G, H
T09B4.9	Mitochondrial import inner membrane translocase, subunit TIM44	TIM44 | TIM44	A, B, C, D		F
W02F12.5	Dihydrolipoamide succinyltransferase (2-oxoglutarate dehydrogenase, E2 subunit)	DLTS | KGD2	B, C, D		H
dnj-21	Molecular chaperone (DnaJ superfamily)	TIM14;DNAJC15; DNAJC19 | TIM14/PAM18	A, B, D		F
lpd-9			C, D		
phb-2		PHB2 | PHB2	A, B, D		F
C04C3.3	Pyruvate dehydrogenase E1, beta subunit	PDHB | PDB1	A, B, C, D		
wah-1	Programmed cell death 8 (apoptosis-inducing factor)	AIFM1 |	A, B, C, D		
F45G2.8	Uncharacterized conserved protein	PAM16 | PAM16	A, B, D		
Y54G9A.7			C, D		
ech-6	Enoyl-CoA hydratase	ECHS1 |	A, B, C, D		
Y110A7A.19	Uncharacterized conserved protein	PTCD3 |	B, C, D		
sco-1	Putative cytochrome C oxidase assembly protein	SCO1 | SCO1; SCO2	B, D	E	
cchl-1	Holocytochrome c synthase/heme-lyase	CCHL | CYC3	A, B, D	WBRNAi 00063981	I
ril-1			D	WBRNAi 00063960	I
tomm-22	Translocase of outer mitochondrial membrane complex, subunit TOM22	TOM22 |	B, D		
Y22D7AL.10	Mitochondrial chaperonin	HSPE1 | HSP10	B, C, D		

Y17G9B.5	Intermediate in Toll signal transduction pathway (ECSIT)	ECSIT |	B, C, D		
his-5	Histone H4	Histone H4 | HHF2	C		
letm-1	Ca2+-binding transmembrane protein LETM1/MRS7	LETM1 | MDM38	B, C		
C08F8.2	Mitochondrial RNA helicase SUV3, DEAD-box superfamily	SUPV3L1 | SUV3	A, B, C		
F02A9.4	3-Methylcrotonyl-CoA carboxylase	MCCC2 |	A, B, C		
hsp-60	Mitochondrial chaperonin, Cpn60/Hsp60p	HSPD1 | HSP60	A, B, C		F, H
Y38E10A.24					
tkt-1	Transketolase	TKTL1; TKTL2 | TKL1; TKL2		WBRNAi 00078549	H
ant-1.1	Mitochondrial ADP/ATP carrier proteins	ANT1; ANT2; ANT3 | AAC1; AAC2; AAC3	A, B	WBRNAi 00078570	
drp-1	Vacuolar sorting protein VPS1, dynamin, and related proteins	DRP1 | DNM1	A, B		
Y52B11C.1					
F15D3.6	Predicted member of the intramitochondrial sorting protein family	SLMO2 | UPS2; UPS3	B		
Y24D9A.8	Transaldolase	TALDO1 | TAL1			
W02B12.9	Mitochondrial carrier protein MRS3/4	MFRN | MRS3; MRS4	A, B		
AC8.6					
F21C3.10					

Supplemental Table 2.2. Non-Validated RNAi Inducers of the UPR^{mt}.

This table represents 61 positive inducers of *hsp-6$_p$::gfp* identified in our screen that target components of the electron transport chain or mitochondrial translation machinery. Since similar hits have been reported to induce the UPR^{mt}, we focused our validation elsewhere, but this list is expected to represent genuine inducers of the UPR^{mt} and in some cases, have been validated by other groups. Putative Mitochondrial Function is based off KOG annotation, PPOD orthology analysis, or blastP homology analysis. Mitochondrial targeting is based of inclusion in the C. elegans mitochondrial proteome data set by Li, J., et al., Proteomics, 2009 [1]. Reported effects on longevity or UPR^{mt} induction are shown as WBRNAi experiments or Houtkooper, R., et al., Nature, 2013 [7] (A), Lee, S.S., et al., Nature Gen, 2003 [8] (B), Chen, D., et al., Aging Cell, 2007 [2] (C), Yoneda, T., et al., Journal of Cell Science, 2004 [3] (D), Hamilton, B., et al., Genes Dev, 2005 [9] (E), Melo, J., et al., Cell, 2012 [5] (F), and Shore, D., et al., PLoS Genet, 2012 [6] (G).

Gene Name	NCBI KOG Annotation	Putative Mito. Function	Mito. Targeted	Extended Lifespan	Reported UPR^{mt} inducer
F44G4.2	Unnamed protein	Complex I	✔		
B0491.5		Complex I	✔	C	
nuo-1	NADH:ubiquinone oxidoreductase, NDUFV1/51kDa subunit	Complex I	✔	WBRNAi00066177	G
nduf-2.2	NADH:ubiquinone oxidoreductase, NDUFS2/49 kDa subunit	Complex I	✔	WBRNAi00078565	
ZK809.3	NADH:ubiquinone oxidoreductase, NDUFB6/B17 subunit	Complex I	✔	WBRNAi00078577	
F31D4.9		Complex I			
gas-1	NADH:ubiquinone oxidoreductase, NDUFS2/49 kDa subunit	Complex I	✔		
nduf-7	NADH-ubiquinone oxidoreductase, NUFS7/PSST/20 kDa subunit	Complex I	✔		
C16A3.5	NADH:ubiquinone oxidoreductase, NDUFB9/B22 subunit	Complex I	✔		
nduf-5	NADH:ubiquinone oxidoreductase, NDUFS5/15kDa	Complex I	✔		
D2030.4	NADH:ubiquinone oxidoreductase, NDUFB7/B18 subunit	Complex I	✔	WBRNAi00065275	D, E, G
F59C6.5	NADH-ubiquinone oxidoreductase, subunit NDUFB10/PDSW	Complex I	✔	WBRNAi00066189	D, G
T20H4.5	NADH:ubiquinone oxidoreductase, NDUFS8/23 kDa subunit	Complex I	✔	WBRNAi00065279	E, G
nduf-6	NADH:ubiquinone oxidoreductase, NDUFS6/13 kDa subunit	Complex I	✔		D
Y51H1A.3	NADH:ubiquinone oxidoreductase, NDUFB8/ASHI subunit	Complex I			
F42G8.10	Uncharacterized conserved	Complex I			

	protein				
nuo-4	NADH:ubiquinone oxidoreductase, NDUFA10/42kDa subunit	Complex I		WBRNAi00065278	E, G
ucr-1	Mitochondrial processing peptidase, beta subunit, and related enzymes (insulinase superfamily)	Complex III	✔	WBRNAi00078564	
T02H6.11	Ubiquinol cytochrome c reductase, subunit QCR7	Complex III	✔	B	
F45H10.2	Ubiquinol cytochrome c reductase, subunit QCR8	Complex III	✔		
R07E4.3	Ubiquinol cytochrome c reductase, subunit QCR8	Complex III	✔		
F29B9.11		Complex IV	✔		
cco-2	Cytochrome c oxidase, subunit Va/COX6	Complex IV	✔	WBRNAi00063991	G
F29C4.2	Unnamed protein	Complex IV	✔	WBRNAi00078571	
cco-1	Cytochrome c oxidase, subunit Vb/COX4	Complex IV	✔	WBRNAi00063967	D, E, F
F26E4.6	Cytochrome c oxidase, subunit VIIc/COX8	Complex IV	✔	WBRNAi00065276	D, E, G
atp-2	F0F1-type ATP synthase, beta subunit	Complex V	✔	WBRNAi00066144	F, G
atp-4	Mitochondrial F1F0-ATP synthase, subunit Cf6 (coupling factor 6)	Complex V	✔	WBRNAi00063979	G
R53.4	Mitochondrial F1F0-ATP synthase, subunit f	Complex V	✔	C	
F32D1.2	Mitochondrial F1F0-ATP synthase, subunit epsilon/ATP15	Complex V	✔		
F58F12.1	Mitochondrial F1F0-ATP synthase, subunit delta/ATP16	Complex V	✔		
H28O16.1	F0F1-type ATP synthase, alpha subunit	Complex V		WBRNAi00066165	D, F, G
atp-3	Mitochondrial F1F0-ATP synthase, subunit OSCP/ATP5	Complex V		WBRNAi00063970	G
R04F11.2	Mitochondrial F1F0-ATP synthase, subunit e	Complex V	✔		
asg-2	Mitochondrial F1F0-ATP synthase, subunit g/ATP20	Complex V	✔	WBRNAi00065274	E, G
asg-1	Mitochondrial F1F0-ATP synthase, subunit g/ATP20	Complex V	✔		D
T26E3.7	F0F1-type ATP synthase, alpha subunit	Complex V			
Y82E9BR.3	Mitochondrial F1F0-ATP synthase, subunit c/ATP9/proteolipid	Complex V			
cyc-2.1	Cytochrome c	Cytochrome C	✔	WBRNAi00078573	
F33D4.5	50S ribosomal protein L1	Mitochondrial Translation	✔	WBRNAi00078562	A
C30C11.1	Mitochondrial ribosomal protein L32	Mitochondrial Translation	✔		

F09G8.3	Mitochondrial/chloroplast ribosomal protein S9	Mitochondrial Translation	✔	WBRNAi00078568	
F59A3.3	Mitochondrial/chloroplast ribosomal protein L24	Mitochondrial Translation	✔	C	
K01C8.6	Mitochondrial ribosomal protein L10	Mitochondrial Translation	✔	C	
tag-264	Mitochondrial 28S ribosomal protein S30	Mitochondrial Translation	✔	C	D, A
tufm-1	Mitochondrial translation elongation factor Tu	Mitochondrial Translation	✔	WBRNAi00078595	
T04A8.11		Mitochondrial Translation	✔		
dap-3	Mitochondrial ribosome small subunit component, mediator of apoptosis DAP3	Mitochondrial Translation	✔		
F45E12.5	Mitochondrial ribosomal protein L14	Mitochondrial Translation			
mrpl-37		Mitochondrial Translation	✔	A	A
mrps-5	Ribosomal protein S5	Mitochondrial Translation	✔	A	A
F56B3.8	Mitochondrial/chloroplast ribosomal protein L2	Mitochondrial Translation	✔	A	A
sars-2	Seryl-tRNA synthetase	Mitochondrial Translation	✔		
T13H5.5	Mitochondrial ribosomal protein S18b	Mitochondrial Translation	✔		
T23B12.2	Mitochondrial/chloroplast ribosomal protein L4	Mitochondrial Translation	✔		
T23B12.3	Mitochondrial/chloroplast ribosomal protein S2	Mitochondrial Translation	✔		
W04B5.4	Mitochondrial ribosomal protein L30	Mitochondrial Translation	✔		
Y39A1A.6	Mitochondrial/chloroplast ribosomal protein L22	Mitochondrial Translation	✔		
Y39B6A.39	Mitochondrial ribosomal protein S28	Mitochondrial Translation	✔		
Y48C3A.10	Mitochondrial/chloroplast ribosomal protein L20	Mitochondrial Translation	✔		
Y34D9A.1	Phosphatidylethanolamine binding protein	Mitochondrial Translation	✔		

Supplemental Table 2.3. Effects of 34 Validated RNAi inducers of the UPR^{mt} on other stress response reporters.

RNAi knockdown of the shown genes significantly induced expression of the *hsp-6$_p$::gfp* reporter. The effect on mean GFP fluorescence from each RNAi clone is shown relative to empty vector (EV) treated animals (± SEM, N=3). Worms were grown at 20°C and imaged 3 days from hatching. Gene knockdowns that significantly increased (student's t-test with Bonferroni correction) each reporter are highlighted in gray.

RNAi/cond.	*hsp-6$_p$::gfp*	*hsp-60$_p$::gfp*	*hsp-4$_p$::gfp*	*hsp-16.2$_p$::gfp*
EV	1 ± 0.02	1 ± 0.02	1 ± 0.04	1 ± 0.03
phb-2	12.29 ± 0.52	1.88 ± 0.07	1.23 ± 0.05	0.82 ± 0.07
EV + Heat Shock	#N/A	#N/A	#N/A	7.13 ± 0.46
EV + Tunicamycin	#N/A	#N/A	7.15 ± 0.63	#N/A
Y17G9B.5	1.4 ± 0.11	1.07 ± 0.05	0.92 ± 0.05	0.84 ± 0.04
his-5	2.27 ± 0.14	0.96 ± 0.03	1.18 ± 0.07	0.09 ± 0.01
tkt-1	2.42 ± 0.28	0.76 ± 0.02	0.98 ± 0.05	0.57 ± 0.02
ant-1.1	2.46 ± 0.33	0.86 ± 0.03	0.72 ± 0.04	0.83 ± 0.03
F21C3.10	2.56 ± 0.2	1.02 ± 0.05	1.09 ± 0.06	0.94 ± 0.06
drp-1	2.96 ± 0.39	0.92 ± 0.04	0.78 ± 0.03	1.02 ± 0.06
C04C3.3	3.19 ± 0.35	1.07 ± 0.05	1.19 ± 0.06	0.87 ± 0.04
Y24D9A.8	3.49 ± 0.25	0.75 ± 0.04	0.91 ± 0.08	0.55 ± 0.02
W02B12.9	3.58 ± 0.34	1.01 ± 0.03	1.16 ± 0.12	0.81 ± 0.05
sco-1	3.87 ± 0.59	1.16 ± 0.04	0.84 ± 0.09	0.92 ± 0.05
C08F8.2	5.08 ± 0.72	1.06 ± 0.05	0.9 ± 0.03	0.87 ± 0.05
Y52B11C.1	5.35 ± 0.39	1.35 ± 0.05	0.95 ± 0.06	1.1 ± 0.05
F15D3.6	6.03 ± 0.35	1.36 ± 0.07	0.82 ± 0.03	0.86 ± 0.05
cchl-1	8.2 ± 1.04	1.42 ± 0.04	0.84 ± 0.04	1.01 ± 0.04
ech-6	8.97 ± 1.37	1.45 ± 0.06	0.93 ± 0.04	0.93 ± 0.04
hsp-60	11.14 ± 0.78	1.01 ± 0.03	1.09 ± 0.04	0.59 ± 0.03
F02A9.4	11.17 ± 0.96	1.33 ± 0.06	0.87 ± 0.07	0.79 ± 0.03
AC8.6	11.62 ± 1	1.28 ± 0.06	0.76 ± 0.04	1 ± 0.04
tomm-22	11.93 ± 0.81	1.14 ± 0.05	1.19 ± 0.11	0.65 ± 0.04
T09B4.9	12.04 ± 0.73	1.65 ± 0.14	1.02 ± 0.04	0.7 ± 0.03
Y38E10A.24	12.16 ± 0.67	1.07 ± 0.05	1.44 ± 0.08	0.72 ± 0.02
Y22D7AL.10	12.85 ± 0.71	0.93 ± 0.03	0.76 ± 0.06	0.84 ± 0.04
wah-1	13.17 ± 1.99	1.36 ± 0.04	1.14 ± 0.04	0.93 ± 0.06
E04A4.5	13.33 ± 1.12	1.4 ± 0.11	0.97 ± 0.09	0.64 ± 0.02
Y54G9A.7	14.04 ± 1.31	1.28 ± 0.05	1.14 ± 0.08	0.92 ± 0.06
Y110A7A.19	14.41 ± 1.3	1.45 ± 0.08	0.84 ± 0.05	0.77 ± 0.03
ril-1	14.71 ± 2.81	1.05 ± 0.06	0.59 ± 0.04	0.35 ± 0.02
letm-1	16.06 ± 2.44	1.22 ± 0.05	0.83 ± 0.03	0.73 ± 0.03
phb-2	16.11 ± 2.36	1.99 ± 0.11	1.2 ± 0.06	0.55 ± 0.03
lpd-9	16.37 ± 1.45	1.46 ± 0.07	1.15 ± 0.08	0.97 ± 0.05
W02F12.5	16.47 ± 1.73	1.15 ± 0.06	1.1 ± 0.07	0.73 ± 0.03
F45G2.8	16.95 ± 1.4	1.37 ± 0.05	1.07 ± 0.09	0.81 ± 0.04
F15D3.7	17.52 ± 1.13	1.67 ± 0.08	0.93 ± 0.06	0.61 ± 0.04
dnj-21	22.12 ± 2.48	1.93 ± 0.1	1.19 ± 0.08	0.87 ± 0.04

Supplemental Table 2.4. Primers used for qRT-PCR.

qRT-PCR was used to measure expression of mitoUPR targets.

Primer	Sequence
hsp-6_F	TCGTGAACGTTTCAGCCAGA
hsp-6_R	CTCAGCGGCATTCTTTTCGG
hsp-60_F	GGGGAAGCCCAAAGATCACA
hsp-60_R	TCCAGCCTCCTCATTAGCCT
timm-23_F	CTCCGATCGATCTCAGTGCC
timm-23_R	ATAGGGTGTCATTTGCCGGG

Supplemental Table 2.5. Effects of 19 UPR^{mt} regulators on lifespan.

RNAi knockdown of the shown genes significantly induced expression of the *hsp-6p::gfp* reporter. A total of three blinded experimental replicates were performed for each RNAi. p-values are shown for a Wilcoxon Rank-Sum comparison to EV control.

Experiment	RNAi	Mean (±SEM)	Mean (%EV)	Median	N	*p*-value
1	*EV*	17.6 ± 0.3		18	81	
1	*E04A4.5*	15.6 ± 0.3	-11.5	16	67	1.90E-05
2	*EV*	16.1 ± 0.3		17	75	
2	*E04A4.5*	16.1 ± 0.5	0.1	17	39	9.20E-01
3	*EV*	15.5 ± 0.2		15.5	104	
3	*E04A4.5*	14.2 ± 0.2	-8	14	93	3.90E-04
Total	*EV*	16.3 ± 0.2		17	260	
Total	*E04A4.5*	15 ± 0.2	-7.7	14	199	4.40E-07
1	*EV*	17.6 ± 0.3		18	81	
1	*F15D3.7*	15.7 ± 0.3	-10.5	16	81	9.30E-06
2	*EV*	16.1 ± 0.3		17	75	
2	*F15D3.7*	16.1 ± 0.3	-0.1	17	56	8.10E-01
3	*EV*	15.5 ± 0.2		15.5	104	
3	*F15D3.7*	13.8 ± 0.2	-10.9	14	80	7.50E-07
Total	*EV*	16.3 ± 0.2		17	260	
Total	*F15D3.7*	15.1 ± 0.2	-7.4	14	217	1.30E-07
1	*EV*	17.6 ± 0.3		18	81	
1	*T09B4.9*	15.3 ± 0.2	-13.2	16	99	3.10E-08
2	*EV*	16.1 ± 0.3		17	75	
2	*T09B4.9*	15.7 ± 0.4	-2.6	17	77	3.00E-01
3	*EV*	15.5 ± 0.2		15.5	104	
3	*T09B4.9*	13 ± 0.2	-15.7	14	113	2.70E-12
Total	*EV*	16.3 ± 0.2		17	260	
Total	*T09B4.9*	14.5 ± 0.2	-11.1	14	289	2.40E-14
1	*EV*	13.8 ± 0.4		12	54	
1	*W02F12.5*	15.7 ± 0.4	13.5	16	59	2.30E-03
2	*EV*	16.1 ± 0.3		17	75	
2	*W02F12.5*	19.5 ± 0.5	21.2	19	66	1.20E-08
3	*EV*	16.3 ± 0.1		16	113	
3	*W02F12.5*	16.1 ± 0.2	-1	16	112	4.30E-01
Total	*EV*	15.7 ± 0.2		16	242	
Total	*W02F12.5*	17 ± 0.2	8.2	16	237	7.00E-04

1	*EV*	17.6 ± 0.3		18	81	
1	*dnj-21*	15.6 ± 0.4	-11.3	16	59	8.10E-04
2	*EV*	16.4 ± 0.3		17	99	
2	*dnj-21*	15.6 ± 0.3	-4.9	17	100	2.50E-02
3	*EV*	16.3 ± 0.1		16	113	
3	*dnj-21*	14 ± 0.2	-14.2	14	111	7.80E-17
Total	*EV*	16.7 ± 0.1		17	293	
Total	*dnj-21*	14.9 ± 0.2	-10.5	14	270	4.50E-14
1	*EV*	16.4 ± 0.3		17	99	
1	*lpd-9*	18.2 ± 0.2	11	19	83	8.30E-06
2	*EV*	16.3 ± 0.1		16	113	
2	*lpd-9*	17.5 ± 0.3	7.8	18	82	1.90E-04
3	*EV*	14 ± 0.2		14	81	
3	*lpd-9*	15.7 ± 0.3	12.2	16	61	3.20E-04
Total	*EV*	15.7 ± 0.1		16	293	
Total	*lpd-9*	17.3 ± 0.2	10.2	17	226	1.10E-11
1	*EV*	16.2 ± 0.2		16	74	
1	*C04C3.3*	14.5 ± 0.2	-10.6	14	81	1.10E-07
2	*EV*	16.4 ± 0.3		17	99	
2	*C04C3.3*	17.2 ± 0.2	5.1	17	89	8.80E-02
3	*EV*	17.2 ± 0.3		16	106	
3	*C04C3.3*	17.6 ± 0.3	2.1	16	132	3.10E-01
Total	*EV*	16.6 ± 0.2		16	279	
Total	*C04C3.3*	16.6 ± 0.2	-0.1	16	302	5.60E-01
1	*EV*	16.2 ± 0.2		16	74	
1	*wah-1*	18.4 ± 0.4	13.5	18	88	1.30E-05
2	*EV*	18.8 ± 0.4		19	84	
2	*wah-1*	21 ± 0.4	11.5	21	107	1.20E-04
3	*EV*	17.2 ± 0.3		16	106	
3	*wah-1*	19.4 ± 0.4	12.5	18	106	1.70E-06
Total	*EV*	17.4 ± 0.2		16.5	264	
Total	*wah-1*	19.6 ± 0.2	12.7	19	301	7.10E-13
1	*EV*	15.4 ± 0.3		16	109	
1	*hsp-60*	16.8 ± 0.4	9.2	16	78	1.60E-03
2	*EV*	18.8 ± 0.4		19	84	
2	*hsp-60*	17.3 ± 0.8	-7.9	19	30	3.60E-01

3	*EV*	16.2 ± 0.3		16	89	
3	*hsp-60*	14.7 ± 0.3	-9.4	14	79	1.20E-03
Total	*EV*	16.7 ± 0.2		16	282	
Total	*hsp-60*	16 ± 0.3	-4	16	187	8.60E-02
1	*EV*	15.4 ± 0.3		16	109	
1	*F45G2.8*	16.6 ± 0.4	7.8	16	87	2.10E-02
2	*EV*	18.8 ± 0.4		19	84	
2	*F45G2.8*	15.7 ± 0.5	-16.4	17	94	1.10E-05
3	*EV*	15.8 ± 0.3		15	86	
3	*F45G2.8*	13.7 ± 0.3	-12.9	14	110	6.20E-07
Total	*EV*	16.5 ± 0.2		16	279	
Total	*F45G2.8*	15.2 ± 0.2	-7.9	14	291	8.80E-05
1	*EV*	15.4 ± 0.3		16	109	
1	*Y54G9A.7*	17.8 ± 0.4	15.6	20	86	2.40E-06
2	*EV*	18.8 ± 0.4		19	84	
2	*Y54G9A.7*	20.4 ± 0.5	8.8	21	67	3.00E-03
3	*EV*	15.8 ± 0.3		15	86	
3	*Y54G9A.7*	17.9 ± 0.2	13.7	18	113	4.80E-09
Total	*EV*	16.5 ± 0.2		16	279	
Total	*Y54G9A.7*	18.5 ± 0.2	12	18	266	3.60E-13
1	*EV*	15.4 ± 0.3		16	109	
1	*Y24D9A.8*	18.8 ± 0.4	22.3	20	83	4.80E-12
2	*EV*	16.2 ± 0.3		16	89	
2	*Y24D9A.8*	19.8 ± 0.4	22.4	21	103	5.00E-11
3	*EV*	15.8 ± 0.3		15	86	
3	*Y24D9A.8*	20.4 ± 0.3	29.2	21	130	3.10E-20
Total	*EV*	15.8 ± 0.2		16	284	
Total	*Y24D9A.8*	19.8 ± 0.2	25.6	20	316	7.90E-42
1	*EV*	17.6 ± 0.4		16	95	
1	*ech-6*	17.7 ± 0.5	0.7	19	79	8.70E-01
2	*EV*	16.2 ± 0.3		16	89	
2	*ech-6*	14.7 ± 0.3	-8.9	16	112	1.40E-02
3	*EV*	14.2 ± 0.2		13	112	
3	*ech-6*	15.3 ± 0.2	7.6	16	115	3.70E-04
Total	*EV*	15.9 ± 0.2		16	296	
Total	*ech-6*	15.7 ± 0.2	-1.1	16	306	9.40E-01

1	*EV*	17.6 ± 0.4		16	95	
1	*F15D3.6*	19.5 ± 0.4	11.3	21	99	2.60E-04
2	*EV*	14.3 ± 0.2		14	116	
2	*F15D3.6*	14.7 ± 0.1	2.9	14	132	6.60E-02
3	*EV*	14.2 ± 0.2		13	112	
3	*F15D3.6*	14.6 ± 0.2	2.8	14	140	1.90E-02
Total	*EV*	15.2 ± 0.2		14	323	
Total	*F15D3.6*	16 ± 0.2	4.8	16	371	1.60E-03
1	*EV*	13.8 ± 0.4		12	54	
1	*Y110A7A.19*	16.9 ± 0.4	22.2	16	99	2.40E-07
2	*EV*	14.6 ± 0.2		14	101	
2	*Y110A7A.19*	16.3 ± 0.2	11.2	16	112	1.80E-08
3	*EV*	14.2 ± 0.2		13	112	
3	*Y110A7A.19*	17.2 ± 0.2	21.5	18	149	1.30E-22
Total	*EV*	14.3 ± 0.1		14	267	
Total	*Y110A7A.19*	16.8 ± 0.1	17.9	16	360	1.50E-34
1	*EV*	13.8 ± 0.4		12	54	
1	*F02A9.4*	16.2 ± 0.4	16.9	16	73	1.40E-04
2	*EV*	14.6 ± 0.2		14	101	
2	*F02A9.4*	15.9 ± 0.2	8.6	16	116	1.20E-04
3	*EV*	15 ± 0.2		14	111	
3	*F02A9.4*	17.5 ± 0.2	16.8	16	113	6.80E-13
Total	*EV*	14.6 ± 0.1		14	266	
Total	*F02A9.4*	16.6 ± 0.2	13.3	16	302	1.50E-16
1	*EV*	15.2 ± 0.2		14	108	
1	*letm-1*	18.1 ± 0.5	18.6	19	78	3.30E-06
2	*EV*	14.6 ± 0.2		14	101	
2	*letm-1*	17.2 ± 0.3	17.2	18	104	6.00E-13
3	*EV*	15 ± 0.2		14	111	
3	*letm-1*	18.9 ± 0.2	25.9	18	136	2.50E-25
Total	*EV*	15 ± 0.1		14	320	
Total	*letm-1*	18.1 ± 0.2	21.1	18	318	2.70E-39
1	*EV*	15.2 ± 0.2		14	108	
1	*tomm-22*	14.8 ± 0.3	-2.6	14	94	1.10E-01
2	*EV*	14.3 ± 0.2		14	116	
2	*tomm-22*	11.5 ± 0.2	-19.7	11	129	9.90E-18
3	*EV*	15 ± 0.2		14	111	

3	*tomm-22*	12.2 ± 0.2	-18.5	11	104	7.50E-16
Total	*EV*	14.8 ± 0.1		14	335	
Total	*tomm-22*	12.7 ± 0.1	-14.5	12	327	9.90E-28
1	*EV*	15.2 ± 0.2		14	108	
1	*Y22D7AL.10*	16.6 ± 0.4	8.9	16	79	3.90E-02
2	*EV*	14.3 ± 0.2		14	116	
2	*Y22D7AL.10*	15.4 ± 0.2	7.4	16	117	2.00E-05
3	*EV*	15 ± 0.2		14	111	
3	*Y22D7AL.10*	15.3 ± 0.2	2	14	113	2.30E-01
Total	*EV*	14.8 ± 0.1		14	335	
Total	*Y22D7AL.10*	15.7 ± 0.1	5.5	16	309	4.80E-05

Supplemental Table 2.6. Effects of UPR^{mt} attenuation and constitutive activation on lifespan.

The following strains were used in these experiments: N2, *atfs-1(tm4525)*, *atfs-1(et17)*, *atfs-1(et18)*, and *isp-1(qm150)*. p-values are shown for condition comparison* or genotype comparison** and calculated using Wilcoxon Rank-Sum test.

Exp.	Genotype + RNAi	T	Mean (±SEM)	Mean (%)*	Mean (%)**	Median	N	*p*-value*	*p*-value**
1	*N2 EV*	25°C	17.2 ± 0.3			17	131		
1	*N2 Y24D9A.8*	25°C	19.5 ± 0.3	13.9		20	106	4.70 E-09	
1	*atfs-1 EV*	25°C	19.2 ± 0.4		11.7	20	95		1.10 E-05
1	*atfs-1 Y24D9A.8*	25°C	20.5 ± 0.5	6.9	4.8	20	64	1.20 E-02	2.20 E-02
2	*N2 EV*	25°C	16.8 ± 0.2			17	126		
2	*N2 Y24D9A.8*	25°C	18.5 ± 0.3	9.7		20	124	1.40 E-05	
2	*atfs-1 EV*	25°C	17.5 ± 0.2		3.9	17	135		4.10 E-02
2	*atfs-1 Y24D9A.8*	25°C	19.5 ± 0.4	11.3	5.4	20	81	5.90 E-06	3.00 E-02
3	*N2 EV*	25°C	14.8 ± 0.1			14	152		
3	*N2 Y24D9A.8*	25°C	17.3 ± 0.2	17.2		18	113	1.10 E-16	
3	*atfs-1 EV*	25°C	15 ± 0.2		1.3	14	88		6.70 E-01
3	*atfs-1 Y24D9A.8*	25°C	18.1 ± 0.4	20.7	4.4	18	100	2.30 E-12	2.20 E-02
4	*N2 EV*	25°C	14.1 ± 0.2			14	126		
4	*N2 Y24D9A.8*	25°C	17 ± 0.3	20.3		16	113	3.20 E-16	
4	*atfs-1 EV*	25°C	16 ± 0.3		13.2	14	99		7.90 E-05
4	*atfs-1 Y24D9A.8*	25°C	19.2 ± 0.5	20.3	13.2	21	89	7.40 E-09	1.10 E-05
Total	*N2 EV*	25°C	15.7 ± 0.1			15	535		
Total	*N2 Y24D9A.8*	25°C	18.1 ± 0.1	15.3		18	456	1.60 E-64	
Total	*atfs-1 EV*	25°C	17 ± 0.2		8.4	17	417		3.00 E-21
Total	*atfs-1 Y24D9A.8*	25°C	19.2 ± 0.2	13	6.2	20	334	1.40 E-19	1.50 E-07
1	*N2 EV*	25°C	14.8 ± 0.1			14	152		
1	*N2 letm-1*	25°C	17.8 ± 0.2	20.4		18	131	4.10 E-21	
1	*atfs-1 EV*	25°C	15 ± 0.2		1.3	14	88		6.70 E-01

1	*atfs-1 letm-1*	25°C	19 ± 0.3	26.8	6.7	18	103	4.00 E-19	1.30 E-03
2	*N2 EV*	25°C	14.1 ± 0.2			14	126		
2	*N2 letm-1*	25°C	17.9 ± 0.3	27		18	126	9.20 E-23	
2	*atfs-1 EV*	25°C	16 ± 0.3		13.2	14	99		7.90 E-05
2	*atfs-1 letm-1*	25°C	19.9 ± 0.4	24.5	11	21	87	4.20 E-12	5.60 E-05
3	*N2 EV*	25°C	16.2 ± 0.3			16	63		
3	*N2 letm-1*	25°C	18 ± 0.5	10.8		19	78	5.90 E-03	
3	*atfs-1 EV*	25°C	17.4 ± 0.3		7.2	16	83		1.30 E-02
3	*atfs-1 letm-1*	25°C	19.8 ± 0.3	13.6	9.9	20	78	1.90 E-07	1.60 E-02
4	*N2 EV*	25°C	17.4 ± 0.2			18	119		
4	*N2 letm-1*	25°C	21.5 ± 0.4	23.6		21	86	2.70 E-14	
4	*atfs-1 EV*	25°C	19.1 ± 0.3		10.1	18	116		3.00 E-07
4	*atfs-1 letm-1*	25°C	21.9 ± 0.4	14.5	2	21	90	5.70 E-08	7.00 E-01
Total	*N2 EV*	25°C	15.5 ± 0.1			16	460		
Total	*N2 letm-1*	25°C	18.6 ± 0.2	20.4		18	421	7.80 E-40	
Total	*atfs-1 EV*	25°C	17 ± 0.2		10	16	386		9.50 E-12
Total	*atfs-1 letm-1*	25°C	20.1 ± 0.2	18.3	8	21	358	1.80 E-31	9.60 E-09
1	*N2 EV*	25°C	16.2 ± 0.3			16	63		
1	*N2 cco-1*	25°C	22.3 ± 0.6	37.4		23	67	3.90 E-13	
1	*atfs-1 EV*	25°C	17.4 ± 0.3		7.2	16	83		1.30 E-02
1	*atfs-1 cco-1*	25°C	21.9 ± 0.5	25.7	-1.9	23	74	1.40 E-11	4.20 E-01
2	*N2 EV*	25°C	17.4 ± 0.2			18	119		
2	*N2 cco-1*	25°C	26 ± 0.4	49.5		28	77	4.30 E-28	
2	*atfs-1 EV*	25°C	19.1 ± 0.3		10.1	18	116		3.00 E-07
2	*atfs-1 cco-1*	25°C	24.9 ± 0.4	30.4	-3.9	25	53	9.80 E-18	8.20 E-02
3	*N2 EV*	25°C	15.9 ± 0.2			16	97		
3	*N2 cco-1*	25°C	24.2 ± 0.3	51.9		25	98	9.90 E-31	
3	*atfs-1 EV*	25°C	16.5 ± 0.2		3.6	16	103		1.20 E-01
3	*atfs-1 cco-1*	25°C	24.1 ± 0.4	45.9	-0.5	25	75	1.10 E-25	8.20 E-01

Total	*N2 EV*	25°C	16.6 ± 0.1			16	279		
Total	*N2 cco-1*	25°C	24.2 ± 0.3	45.9		25	242	1.20 E-66	
Total	*atfs-1 EV*	25°C	17.8 ± 0.2		6.9	18	302		1.70 E-06
Total	*atfs-1 cco-1*	25°C	23.5 ± 0.3	32.3	-3	23	202	1.70 E-47	4.90 E-02
1	*N2 EV*	20°C	19.9 ± 0.4			21	107		
1	*N2 cco-1*	20°C	29.8 ± 0.9	50		29	65	3.70 E-17	
1	*atfs-1 EV*	20°C	19.7 ± 0.5		-1	19	95		6.50 E-01
1	*atfs-1 cco-1*	20°C	27.1 ± 0.9	37.4	-9.3	26	70	1.20 E-10	3.70 E-02
2	*N2 EV*	20°C	19.8 ± 0.3			21	108		
2	*N2 cco-1*	20°C	28.3 ± 0.6	42.7		28	105	1.10 E-22	
2	*atfs-1 EV*	20°C	17.5 ± 0.3		-11.5	18	107		1.80 E-06
2	*atfs-1 cco-1*	20°C	26.8 ± 0.6	52.8	-5.3	26	100	2.30 E-25	5.10 E-02
Total	*N2 EV*	20°C	19.9 ± 0.2			21	215		
Total	*N2 cco-1*	20°C	28.9 ± 0.5	45.5		28.5	170	1.20 E-38	
Total	*atfs-1 EV*	20°C	18.6 ± 0.3		-6.6	18	202		3.70 E-04
Total	*atfs-1 cco-1*	20°C	26.9 ± 0.5	45	-6.8	26	170	5.70 E-33	4.70 E-03
1	*N2 EV*	20°C	22.6 ± 0.3			23	114		
1	*atfs-1(et17) EV*	20°C	16.3 ± 0.3	-28		16	121	2.40 E-28	
2	*N2 EV*	20°C	18.9 ± 0.3			17	106		
2	*atfs-1(et17) EV*	20°C	14.4 ± 0.3	-23.7		15	110	2.10 E-18	
3	*N2 EV*	20°C	19.1 ± 0.3			19	92		
3	*atfs-1(et17) EV*	20°C	13.9 ± 0.4	-27		13	72	9.90 E-15	
Total	*N2 EV*	20°C	20.3 ± 0.2			21	312		
Total	*atfs-1(et17) EV*	20°C	15 ± 0.2	-25.9		15	303	1.30 E-49	
1	*N2 EV*	25°C	16.8 ± 0.2			17	153		
1	*atfs-1(et17) EV*	25°C	17.7 ± 0.2	5.6		17	94	1.00 E-02	
2	*N2 EV*	25°C	15.3 ± 0.2			16	106		
2	*atfs-1(et17) EV*	25°C	14.5 ± 0.2	-5.5		14	117	2.70 E-02	
Total	*N2 EV*	25°C	16.2 ± 0.2			16	259		

Total	*atfs-1(et17) EV*	25°C	15.9 ± 0.2	-1.6		16	211	3.10 E-01	
1	*N2 EV*	20°C	21.3 ± 0.2			20	139		
1	*atfs-1(et18) EV*	20°C	16 ± 0.4	-24.8		16	66	5.00 E-20	
2	*N2 EV*	20°C	21.4 ± 0.2			21	146		
2	*atfs-1(et18) EV*	20°C	17.4 ± 0.6	-18.7		17	61	5.20 E-10	
3	*N2 EV*	20°C	21.1 ± 0.2			22	133		
3	*atfs-1(et18) EV*	20°C	15.6 ± 0.4	-26.3		14	76	2.50 E-17	
Total	*N2 EV*	20°C	21.3 ± 0.1			21	418		
Total	*atfs-1(et18) EV*	20°C	16.3 ± 0.3	-23.6		16	203	1.20 E-44	
1	*N2 EV*	25°C	16.8 ± 0.2			17	153		
1	*atfs-1(et18) EV*	25°C	15.1 ± 0.2	-10		15	101	1.00 E-08	
2	*N2 EV*	25°C	15.3 ± 0.2			16	106		
2	*atfs-1(et18) EV*	25°C	11.1 ± 0.3	-27.7		12	49	6.20 E-17	
Total	*N2 EV*	25°C	16.2 ± 0.2			16	259		
Total	*atfs-1(et18) EV*	25°C	13.8 ± 0.2	-14.8		14	150	7.00 E-16	
1	*N2 EV*	20°C	20.1 ± 0.4			21	102		
1	*N2 atfs-1*	20°C	17.4 ± 0.5	-13.5		15	86	1.50 E-04	
1	*isp-1 EV*	20°C	30.4 ± 1.2		51.3	31	50		9.50 E-12
1	*isp-1 atfs-1*	20°C	26.1 ± 0.7	-14.2	50	25	109	4.30 E-03	3.00 E-14
2	*N2 EV*	20°C	20.4 ± 0.3			20	88		
2	*N2 atfs-1*	20°C	20.6 ± 0.4	1.2		20	83	4.30 E-01	
2	*isp-1 EV*	20°C	24 ± 0.7		18	23	40		2.30 E-07
2	*isp-1 atfs-1*	20°C	24 ± 0.5	-0.2	16.4	23	61	9.00 E-01	2.30 E-06
3	*N2 EV*	20°C	19.2 ± 0.2			18	175		
3	*N2 atfs-1*	20°C	21 ± 0.3	9		20	177	3.00 E-05	
3	*isp-1 EV*	20°C	28.7 ± 0.8		49.4	27	116		2.90 E-23
3	*isp-1 atfs-1*	20°C	32.3 ± 0.8	12.5	54.2	33	123	9.70 E-04	3.20 E-29
Total	*N2 EV*	20°C	19.7 ± 0.2			20	365		
Total	*N2 atfs-1*	20°C	20 ± 0.2	1.2		20	346	4.00 E-01	

Total	*isp-1 EV*	20°C	28.2 ± 0.6		43	27	206		1.30 E-38
Total	*isp-1 atfs-1*	20°C	28.3 ± 0.5	0.1	41.4	27	293	6.10 E-01	3.70 E-43

SUPPLEMENTAL REFERENCES

1) Li, J., Cai, T., Wu, P., Cui, Z., Chen, X., Hou, J., Xie, Z., Xue, P., Shi, L., Liu, P., et al. (2009). Proteomic analysis of mitochondria from Caenorhabditis elegans. Proteomics *9*, 4539-4553.

2) Chen, D., Pan, K.Z., Palter, J.E., and Kapahi, P. (2007). Longevity determined by developmental arrest genes in Caenorhabditis elegans. Aging Cell *6*, 525-533.

3) Yoneda, T. et al. Compartment-specific perturbation of protein handling activates genes encoding mitochondrial chaperones. J Cell Sci 117, 4055-4066, doi:10.1242/jcs.01275 (2004).

4) Nargund, A. M., Pellegrino, M. W., Fiorese, C. J., Baker, B. M. & Haynes, C. M. Mitochondrial import efficiency of ATFS-1 regulates mitochondrial UPR activation. Science 337, 587-590, doi:10.1126/science.1223560 (2012).

5) Melo, J.A., and Ruvkun, G. Inactivation of Conserved C. elegans Genes Engages Pathogen- and Xenobiotic-Associated Defenses. Cell 149, 452–466 (2012).

6) Shore, D.E., Carr, C.E., and Ruvkun, G. Induction of Cytoprotective Pathways Is Central to the Extension of Lifespan Conferred by Multiple Longevity Pathways. PLoS Genet 8, e1002792 (2012).

7) Houtkooper, R. H. et al. Mitonuclear protein imbalance as a conserved longevity mechanism. Nature 497, 451-457, doi:10.1038/nature12188 (2013).

8) Lee, S. S. et al. A systematic RNAi screen identifies a critical role for mitochondria in C. elegans longevity. Nat Genet 33, 40-48, doi:10.1038/ng1056 (2003).

9) Hamilton, B. et al. A systematic RNAi screen for longevity genes in C. elegans. Genes Dev 19, 1544-1555 (2005).

Chapter 3. TRANSALDOLASE INHIBITION IMPAIRS MITOCHONDRIAL RESPIRATION AND INDUCES A STARVATION-LIKE LONGEVITY RESPONSE IN *C. ELEGANS*

*** Modified from an unpublished manuscript of the same title**

Christopher F. Bennett[1,2], Jane Kwon[1], Christine Chen[1], Kathlyn Acosta[1], Helen Vander Wende[1], Marissa Simko[1], Victor Pineda[1], Ryan Rossner[1,3], Brian M. Wasko[1], Haeri Choi[1], Shiwen Chen[1], Shirley Park[1], Gholamali Jafari[1], Bryan Sands[4], Carissa Perez Olsen[4], Alex Mendenhall[1], Philip G. Morgan[5,6], Matt Kaeberlein[1,2,3]

[1] Department of Pathology, University of Washington, Seattle, WA, USA

[2] Molecular and Cellular Biology Program, University of Washington, Seattle, WA, USA

[3] Molecular Medicine and Mechanisms of Disease Program, University of Washington, Seattle, WA, USA

[4] Division of Basic Sciences, Fred Hutchinson Cancer Research Center, Seattle, WA, USA

[5] Center for Integrated Brain Research, Seattle Children's Research Institute, Seattle, WA, USA

[6] Department of Anesthesiology, University of Washington School of Medicine, Seattle, WA, USA

* Correspondence to: kaeber@uw.edu

3.1 ABSTRACT

Mitochondrial dysfunction can increase oxidative stress and extend lifespan in *Caenorhabditis elegans*. Homeostatic mechanisms exist to cope with disruptions to mitochondrial function that promote cellular health and organismal longevity. Previously, we determined that decreased expression of the cytosolic pentose phosphate pathway (PPP) enzyme transaldolase activates the mitochondrial unfolded protein response (UPR^{mt}) and extends lifespan. Here we report that transaldolase (*tald-1*) deficiency impairs mitochondrial function *in vivo*, as evidenced by altered mitochondrial morphology, decreased respiration, and increased cellular H_2O_2 levels. Lifespan extension from knockdown of *tald-1* is associated with an oxidative stress response involving p38 and c-Jun N-terminal kinase (JNK) MAPKs and a starvation-like response regulated by the transcription factor EB (TFEB) homolog HLH-30. The latter response promotes autophagy and increases expression of the flavin-containing monooxygenase 2 (*fmo-2*). We conclude that cytosolic redox established through the PPP is a key regulator of mitochondrial function and defines a new mechanism for mitochondrial regulation of longevity.

3.2 INTRODUCTION

Mitochondria are the primary sites of aerobic metabolism and energy production in the cell. The mitochondrial free radical theory of aging posits that reactive oxygen species (ROS) produced by mitochondria during oxidative metabolism cause damage to macromolecules which, over time, leads to the accumulation of cellular, tissue, and organismal declines, and ultimately death [189, 190]. In general, mitochondrial dysfunction is detrimental, and has been causally implicated in several age-related diseases, as well as severe, early-onset mitochondrial disorders. Paradoxically, however, inhibition of mitochondrial function has, in some cases, been associated

with increased longevity in laboratory organisms from yeast to mammals [191]. This is particularly evident in *C. elegans*, where inhibition of mitochondrial respiration by mutation or knockdown of numerous electron transport chain (ETC) components usually increases lifespan [2, 3]. Mild oxidative stress can also increase lifespan [191], perhaps by inducing adaptive responses that compensate for these insults and provide cytoprotective effects to improve cellular stress resistance [122].

The mechanistic basis for lifespan extension in response to mitochondrial inhibition and mild oxidative stress in *C. elegans* is an active area of investigation. One mitochondrial stress pathway that has been associated with worm longevity in this context is the mitochondrial unfolded protein response (UPR^{mt}) [142, 143, 192]. The UPR^{mt} is a coordinated response to mitochondrial stress resulting in upregulation of mitochondrial chaperones, import machinery, and proteases, while negatively regulating expression of nuclear- and mitochondrial-encoded ETC components [21, 67, 70]. Activation of the UPR^{mt} is regulated by the ATFS-1 transcription factor, which translocates to the nucleus in response to mitochondrial stress and directly activates transcription of several UPR^{mt} target genes [21, 81]. Whether the UPR^{mt} plays a direct role in determining longevity remains unclear. Lifespan extension by ETC inhibition or treatment with the ROS-generating compound paraquat is correlated with induction of the UPR^{mt} [6, 67, 142]; however, deletion or RNAi knockdown of *atfs-1* blocks induction of several UPR^{mt} target genes but does not prevent or attenuate lifespan extension following inhibition of the ETC [82, 164]. Similarly, constitutive active alleles of *atfs-1* cause activation of the UPR^{mt} but do not extend lifespan [82, 164, 184].

There is experimental evidence supporting a role for several factors other than the UPR^{mt} in lifespan extension downstream of mitochondrial inhibition in *C. elegans*, including the hypoxic

response transcription factor HIF-1, CEP-1/p53, the CEH-23 transcription factor, components of the intrinsic apoptotic pathway, and the p38 MAPK PMK-3 [106, 162, 165, 177, 179]. A majority of these studies have been performed using mutants with defective ETC function, such as the Rieske iron-sulfur protein gene *isp-1(qm150)* allele and the ubiquinone biosynthetic gene *clk-1(qm30)* allele. With the possible exception of *pmk-3*, none of these factors is able to account for the full lifespan extension following RNAi knockdown of ETC genes such as the cytochrome c oxidase gene *cco-1*. This is consistent with a model proposed by the Hekimi lab that RNAi inhibition of ETC function promotes worm longevity by a mechanism distinct from mutations that impair ETC function [95].

Uncovering the genetic pathways and molecular mechanisms by which mitochondria influence aging and disease is critical both for developing better models of biological aging, as well as for identifying interventions to promote health and longevity. As mentioned above, low levels of oxidative stress can be beneficial to cellular health, but high levels can cause irreparable damage. This biphasic or non-linear relationship between mitochondrial ROS and survival is commonly referred to as mitohormesis, and posits that ROS act as signaling molecules to induce adaptive mechanisms [122]. This has been observed in *C. elegans*, where different levels of RNAi knockdown of a single mitochondrial gene can cause differential effects on lifespan and other physiological markers [126, 155]. The beneficial hormetic effects associated with elevated ROS are due to the contribution of multiple protective responses that are still being discovered. Therefore, we sought to identify and determine the interconnectivity of novel longevity pathways distinct from the UPR^{mt} that are engaged by oxidative and mitochondrial stress.

Although the UPR^{mt} does not appear to directly mediate lifespan extension, we reasoned that the partial correlation between activation of the UPR^{mt} and longevity could be used to identify

novel factors and mechanisms of action within the mitochondrial longevity network. To identify such factors, we performed a genome-wide RNAi screen for *C. elegans* genes that negatively regulate the UPR^{mt} by looking for RNAi clones that activated the UPR^{mt} reporter *hsp-6p::gfp* [82]. Some, but not all, of these genes also negatively affected lifespan such that RNAi knockdown increased longevity. One such gene is *tald-1*, which encodes the pentose phosphate pathway (PPP) enzyme transaldolase. The PPP pathway is a cytosolic metabolic pathway that functions to produce NADPH, ribose-5-phosphate, and interconvert 3-7 carbon sugars. The observation that *tald-1(RNAi)* induced the UPR^{mt} reporter and increased lifespan intrigued us, as transaldolase is not a mitochondrial protein and has not been previously implicated in longevity control in any organism. Here we report that transaldolase deficiency indeed alters mitochondrial function, as evidenced by changes in mitochondrial morphology and direct measurement of mitochondrial respiration. The lifespan extension from *tald-1(RNAi)* is independent of the UPR^{mt}, and instead involves activation of an oxidative stress response mediated by the p38 MAPK PMK-1 and JNK MAPKs JNK-1 and KGB-1, and a concomitant starvation-like response that signals through the transcription factor EB (TFEB) homolog HLH-30. Furthermore, we find that activation of the starvation-like response transcriptionally activates HLH-30-dependent autophagy markers, increases autophagic flux, and increases expression of the longevity-promoting flavin-containing monooxygenase 2 (*fmo-2*).

3.3 RESULTS

3.3.1 *The pentose phosphate pathway modulates mitochondrial proteostasis and lifespan in C. elegans.*

From an unbiased genome-wide RNAi screen for negative regulators of the mitochondrial unfolded protein response (UPR^{mt}), we found that knockdown of either of the pentose phosphate

pathway (PPP) enzymes transaldolase (*tald-1*) or transketolase (*tkt-1*) activates the UPR^{mt} reporter *hsp-6p::gfp* in *C. elegans* [82]. These enzymes function in the non-oxidative branch of the PPP, generating ribose-5-P for nucleotide synthesis and interconverting three, four, five, six, and seven carbon sugars (**Figure 3.1A**). To determine if *tald-1* and *tkt-1* deficiencies specifically cause mitochondrial stress independent of the PPP, we tested if knockdown of other PPP enzymes not detected in the initial RNAi screen could also induce the *hsp-6p::gfp* reporter. RNAi knockdown of T25B9.9, which encodes the oxidative PPP enzyme 6-phosphogluconate dehydrogenase (6PGD), also caused a significant increase in *hsp-6p::gfp* expression (+89%), albeit less robustly than *tald-1(RNAi)* (+187%) (**Figure 3.1B,C**). Therefore, inhibition of the PPP at multiple enzymatic steps is sufficient to increase expression of a mitochondrial stress reporter. Next, we asked if inhibition of these enzymatic steps increases lifespan similar to other RNAi clones that activate the *hsp-6p::gfp* reporter. We found that knockdown of *tald-1*, *tkt-1,* and T25B9.9/6PGD all increased lifespan (**Figure 3.1D**). Since *tald-1(RNAi)* resulted in the strongest phenotypes among PPP enzymes tested, we chose to focus our studies on understanding the mechanisms by which *tald-1* knockdown induces mitochondrial stress and enhances longevity.

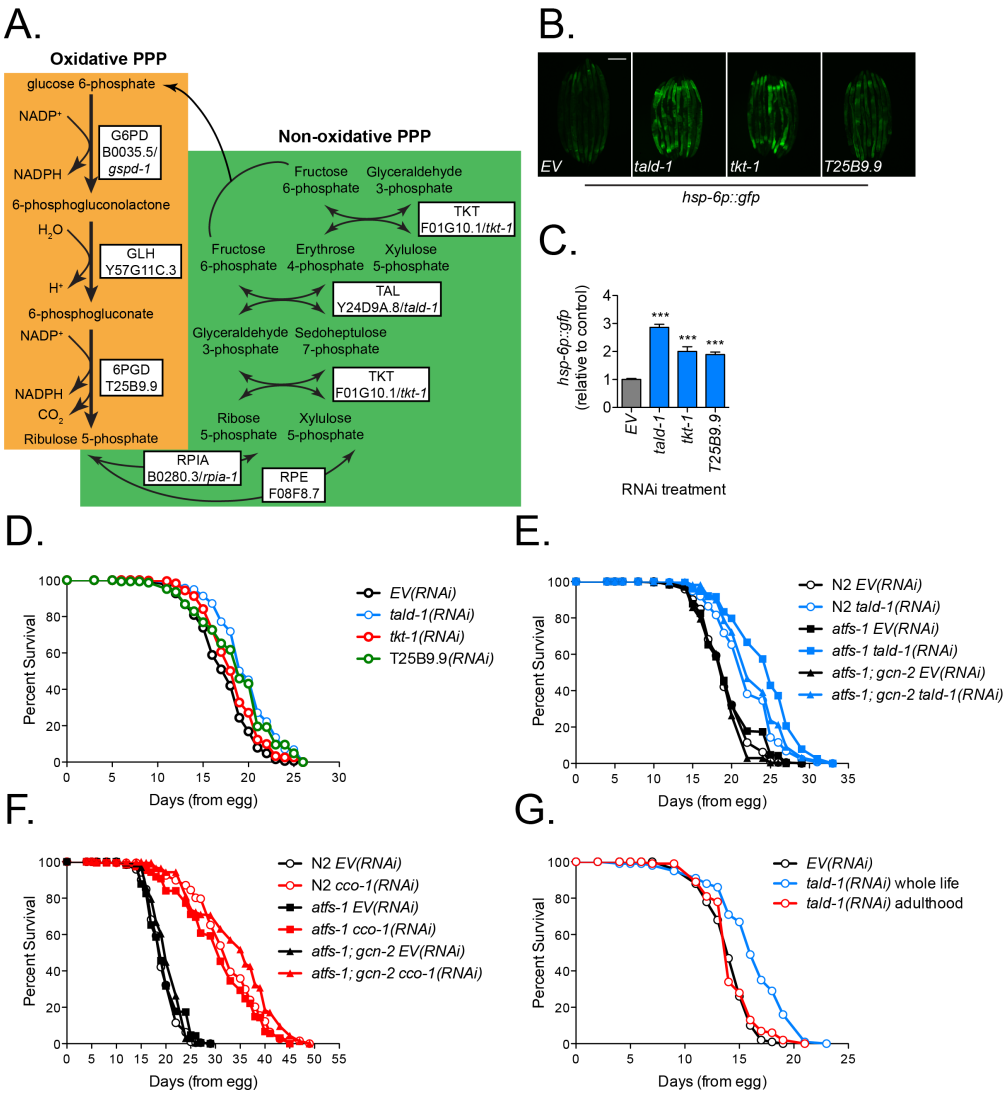

Figure 3.1. Inhibition of the pentose phosphate pathway activates the UPR^{mt} and extends lifespan.

(A) Diagram of both the oxidative and non-oxidative branches of the PPP. The oxidative branch produces NADPH, while the non-oxidative branch produces ribose-5-P and interconverts sugar carbon backbones. The white boxes contain enzyme names with the human gene listed above the *C. elegans* homolog. **(B)** PPP gene knockdown increases *hsp-6p::gfp* reporter expression. **(C)** Mean relative fluorescence of *hsp-6p::gfp* animals grown on PPP RNAi. Fluorescence is calculated relative to *EV(RNAi)* controls (N = 4 independent experiments, pooled individual worm values, error bars indicate s.e.m., student's t-test with Bonferroni's correction). **(D)** RNAi knockdown of PPP genes extends *C. elegans* lifespan. N2 fed *EV(RNAi)* (mean 17.4±0.1 days, n=455), N2 fed *tald-1(RNAi)* (mean 19.9±0.2 days, n=391), N2 fed *tkt-1(RNAi)* (mean 18.4±0.1 days, n=461), N2 fed T25B9.9*(RNAi)* (mean 18.8±0.2 days, n=311). Lifespans were performed at 25°C, with pooled data from four independent experiments shown. **(E)** RNAi knockdown of *tald-1* extends lifespan independently of the UPR^{mt}. N2 fed *EV(RNAi)* (mean 19.3±0.2 days, n=192), N2 fed *tald-1(RNAi)* (mean 22.1±0.2 days, n=251), *atfs-1(tm4525)* fed *EV(RNAi)* (mean 19.6±0.2 days, n=230), *atfs-1(tm4525)* fed *tald-1(RNAi)* (mean 24.5±0.3 days, n=228), *atfs-1(tm4525);gcn-2(ok871)* fed *EV(RNAi)* (mean 18.9±0.2 days, n=205), *atfs-1(tm4525);gcn-2(ok871)* fed *tald-1(RNAi)* (mean 23.1±0.3 days, n=220). Lifespans were performed at 20°C, with pooled data from two independent experiments shown. **(F)** RNAi knockdown of *cco-1* extends lifespan independently of the UPR^{mt}. N2 fed *EV(RNAi)* (mean 19.3±0.2 days, n=192), N2 fed *cco-1(RNAi)* (mean 32.3±0.5 days, n=187), *atfs-1(tm4525)* fed *EV(RNAi)* (mean 19.6±0.2 days, n=230), *atfs-*

1(tm4525) fed *cco-1(RNAi)* (mean 29±0.6 days, n=194), *atfs-1(tm4525);gcn-2(ok871)* fed *EV(RNAi)* (mean 18.9±0.2 days, n=205), *atfs-1(tm4525);gcn-2(ok871)* fed *cco-1(RNAi)* (mean 32.6±0.5 days, n=228). Lifespans were performed at 20°C, with pooled data from two independent experiments shown. **(G)** RNAi knockdown of *tald-1* extends lifespan only when knockdown occurs during development. N2 fed *EV(RNAi)* (mean 14.2±0.1 days, n=361), N2 fed *tald-1(RNAi)* from hatching (mean 16.4±0.2 days, n=468), N2 fed *tald-1(RNAi)* from L4 (mean 14.4±0.1 days, n=330). Lifespans were performed at 25°C, with pooled data from three independent experiments shown. Lifespans in this figure are indicated as mean±s.e.m. and statistical analysis is provided in **Supplemental Table 3.1**. In this figure, statistics are displayed as: * $p<0.05$, ** $p<0.01$, *** $p<0.001$.

The ATFS-1 transcription factor and the GCN-2 kinase, respectively, mediate the transcriptional and translational changes in response to mitochondrial stress that comprise the UPR^{mt} [21, 89]. Loss of either ATFS-1 or GCN-2 does not prevent the lifespan extension from mitochondrial inhibition [82, 164]. These factors act in a compensatory fashion, however, and GCN-2 may be able to establish mitochondrial protein homeostasis in the absence of ATFS-1 or vice versa. Therefore, to convincingly assess whether the UPR^{mt} regulates longevity from ETC or PPP inhibition, we examined if simultaneous loss of both *atfs-1* and *gcn-2* could prevent lifespan extension from RNAi knockdown of either *tald-1* or the Complex IV subunit cytochrome c oxidase 1 gene, *cco-1*. Both RNAi clones significantly increased the lifespan of *atfs-1(tm4525); gcn-2(ok871)* animals comparable to their effects in wild-type nematodes (**Figure 3.1E,F**). Thus, we conclude that neither ATFS-1 nor GCN-2 are required for lifespan extension from mitochondrial RNAi treatment, further supporting the model that mitochondrial stress or ETC inhibition affect lifespan independently of the UPR^{mt}.

We next examined the temporal and genetic requirements for *tald-1(RNAi)* lifespan extension in the context of previously described *C. elegans* longevity pathways. Like RNAi knockdown of ETC genes [2, 126], *tald-1(RNAi)* only extended lifespan when knockdown occurred during development (feeding beginning at L1), and adult-specific knockdown (feeding beginning at ~L4/young adult) had no effect on longevity (**Figure 3.1G**). Knockdown of *tald-1* also extended lifespan in animals carrying mutations of the FOXO-transcription factor *daf-16*,

the AMP-activated protein kinase *aak-2*, and the germline-signaling factor *glp-1* (**Supplemental Figure 3.1A-C**), consistent with the reported effects of mitochondrial RNAi treatments [2, 3, 7, 143, 193]. Interestingly, *tald-1(RNAi)* resulted in a larger lifespan extension in animals lacking the hypoxic response transcription factor HIF-1 (**Supplemental Figure 3.1D**), while loss of *hif-1* attenuated the lifespan extension from *cco-1(RNAi)* (**Supplemental Figure 3.1E**), as has been previously reported [106]. These data are consistent with a model that inhibition of the PPP extends lifespan by a mechanism that is overlapping but partially distinct from ETC inhibition.

3.3.2 *Transaldolase deficiency impairs mitochondrial respiration and increases oxidative stress in vivo.*

Based on our findings that developmental knockdown of *tald-1* induced the UPR^{mt}, we asked whether other parameters of mitochondrial function are affected by *tald-1(RNAi)*. First, we decided to use confocal microscopy to characterize any changes to intestinal mitochondrial morphology and content, since this tissue is particularly responsive to mitochondrial stress, as measured by the *hsp-6p::gfp* reporter. Using a mitochondrial-targeted GFP reporter whose expression is restricted to the intestine via the *ges-1* promoter, we observed that *tald-1(RNAi)* caused a disruption to normal mitochondrial morphology in intestinal cells (**Figure 3.2A,B**). Mitochondria in these animals became thin and smaller in size, reflecting a potential change in mitochondrial dynamics. A similar change in morphology occurred following *cco-1(RNAi)* (**Figure 3.2B**). Interestingly, despite the smaller size of mitochondria following *tald-1(RNAi)* and *cco-1(RNAi)*, there was increased GFP area per cell compared to controls (**Figure 3.2C**). This could indicate increased mitochondrial content; however, we did not observe any change in whole worm mitochondrial DNA abundance in these animals (**Supplemental Figure 3.2**).

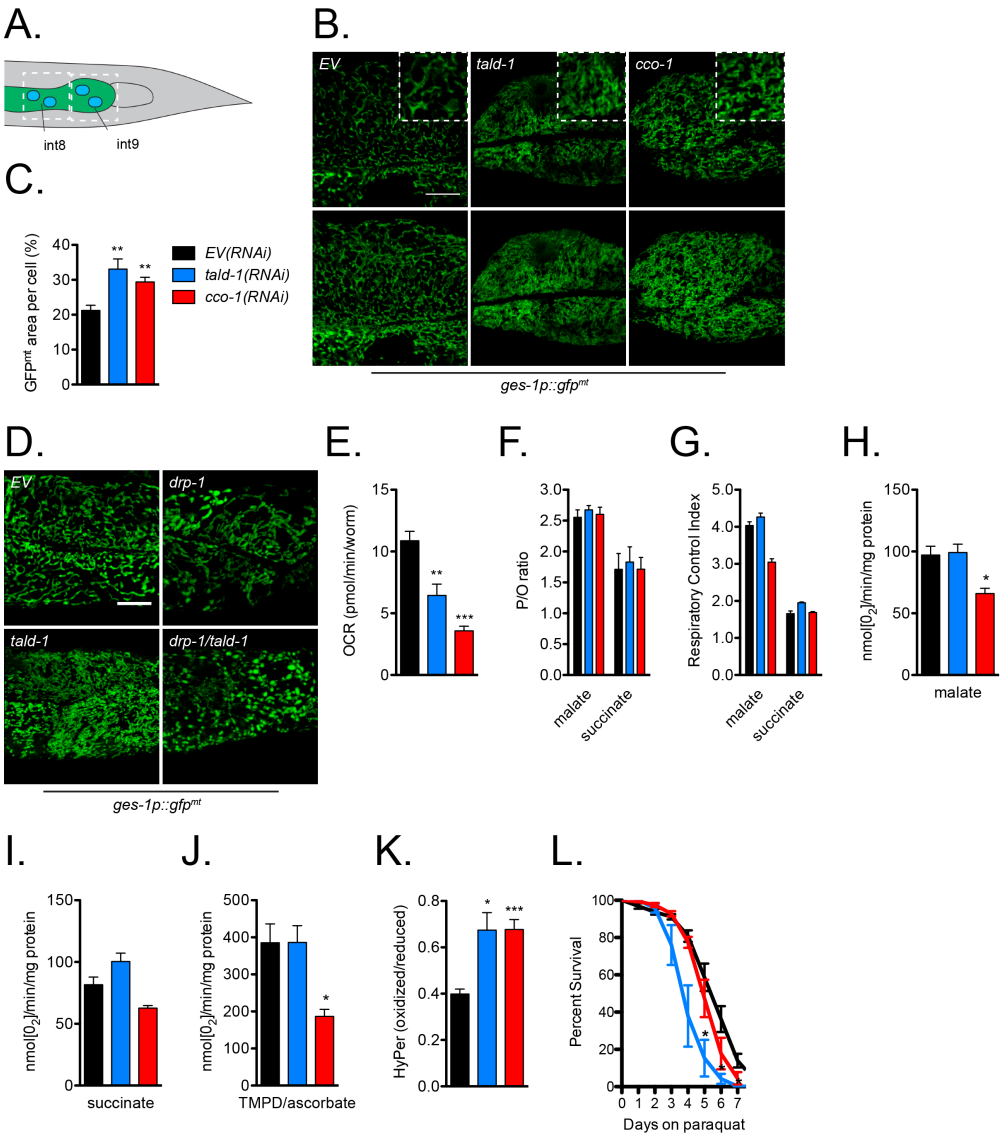

Figure 3.2. Transaldolase deficiency alters mitochondrial morphology, decreases *in vivo* mitochondrial respiration, and causes oxidative stress.

(A) Diagram depicting the posterior intestinal cells that were visualized for mitochondrial morphology. **(B)** Intestinal mitochondrial morphology is altered by *tald-1(RNAi)* and *cco-1(RNAi)*. The top panel represents a single 0.34 µm slice imaged using confocal microscopy, with a magnified area displayed in a white dotted box to highlight morphology differences. The bottom panel consists of a max intensity projection of five z-slices to emphasize mitochondrial content in these cells. Scale bar, 10 µm. **(C)** Quantification of percent mitochondrial area per cell. (N = 2 independent experiments, error bars indicate s.e.m., student's t-test with Bonferroni's correction). **(D)** Mitochondrial morphology changes from *tald-1(RNAi)* are regulated by DRP-1. RNAi treatments include *EV(RNAi)*, *tald-1(RNAi)* [50:50 with *EV(RNAi)*], *drp-1(RNAi)* [50:50 with *EV(RNAi)*], and *tald-1(RNAi)* [50:50 with *drp-1(RNAi)*]. Scale bar, 10 µm. **(E)** Oxygen consumption rate decreases with *tald-1(RNAi)* and *cco-1(RNAi)*. OCR was measured using the Seahorse XF Analyzer and normalized to animal number (N = 6 independent experiments, error bars indicate s.e.m., student's t-test with Bonferroni's correction). **(F)** P/O ratio (the ATP produced per oxygen atom reduced), (G) respiratory control index (State 3:State 4 rates), (H) malate-driven respiration (Complex I-IV), **(I)** succinate-driven respiration (Complex II-IV), **(J)** and TMPD/ascorbate-driven respiration (Complex IV) were measured using the OXPHOS assay on isolated mitochondria from RNAi treated animals. Respiratory rates were

measured as rate of disappearance of oxygen (nmol[O_2]) per minute per mg protein (N = 4 independent experiments, error bars indicate s.e.m., student's t-test with Bonferroni's correction). **(K)** H_2O_2 levels increase from RNAi knockdown of *tald-1* or *cco-1* (N = 7 independent experiments, error bars indicate s.e.m., student's t-test with Bonferroni's correction). **(L)** RNAi knockdown of *tald-1* causes sensitivity to paraquat. Percent survival of N2 worms grown on RNAi bacteria and 10 mM paraquat was measured over seven days. Survival analyses were performed at 25°C (N = 6 independent experiments, error bars indicate s.e.m., student's t-test with Bonferroni's correction). In this figure, statistics are displayed as: * $p<0.05$**,** ** $p<0.01$, *** $p<0.001$. Also, in this figure, color coating of bars and lines reflect the legend in (C).

To better understand the effect of *tald-1(RNAi)* on mitochondrial morphology, we examined its interaction with factors known to regulate mitochondrial fusion and fission. As expected, knockdown of the fission factor dynamin-related GTPase *drp-1* (*DRP1*/*DNM1* homolog) caused intestinal mitochondria to swell and aggregate, while knockdown of the inner membrane fusion GTPase *eat-3* (*OPA1*/*MGM1* homolog) caused mitochondria to fragment and lack normal tubular structure (**Supplemental Figure 3.3A**). Outer membrane fusion GTPase *fzo-1* (*MFN1*/*FZO1* homolog) knockdown also caused mitochondria to fragment, but morphology was remarkably similar to *tald-1(RNAi)* mitochondria, suggesting a mild pro-fission phenotype (**Supplemental Figure 3.3A**). Accordingly, *drp-1(RNAi)* prevented the shift in mitochondrial morphology following *tald-1* knockdown (**Figure 3.2D**), indicating that the core fission machinery is required for this response. In contrast, *fzo-1* and the mitophagy components *pdr-1* (*PARK2* homolog) and *pink-1* (*PINK1* homolog) were not required for this phenotype (**Supplemental Figure 3.3B,C**).

Since mitochondrial stress and mitochondrial fragmentation are associated with decreased mitochondrial function, we sought to directly measure metabolic activity in whole animals. The Seahorse XF24 Analyzer allows measurements of basal and real time changes in O_2 consumption in *C. elegans* [194]. We found that knockdown of *tald-1* caused an approximately 41% reduction in oxygen consumption, while knockdown of *cco-1* caused a 67% reduction (**Figure 3.2E**). The reduction in oxygen consumption could not be fully explained by changes to worm length or

density (**Supplemental Figure 3.4A,B**), arguing that *tald-1(RNAi)* decreases basal mitochondrial respiration in whole animals.

To determine whether *tald-1(RNAi)* causes decreased mitochondrial respiration by altering ETC function or stability, mitochondria were isolated from animals and oxygen consumption of intact mitochondria was measured using malate, succinate, and TMPD/ascorbate as electron donors to drive complex I-, complex II-, and complex IV-dependent respirations, respectively. The mitochondria isolated in all trials retained normal coupling (P/O ratios) and a normal respiratory control index (State 3:State 4), indicating purification of healthy mitochondria (**Figure 3.2F,G**). As expected with Complex IV RNAi [195], *cco-1(RNAi)* decreased Complex I- and Complex IV-dependent respiration (**Figure 3.2H-J**). In contrast to *cco-1(RNAi)*, *tald-1(RNAi)* did not cause a change in any rates measured (**Figure 3.2H-J**). Therefore, *tald-1(RNAi)* decreases whole animal respiration without altering maximal ETC capacity, potentially by decreasing reducing equivalents to the ETC *in vivo*.

Mitochondrial dysfunction has been proposed to extend lifespan in *C. elegans* through increased production of ROS and altered redox signaling [106, 108, 123, 129]. To specifically observe *in vivo* changes in redox environment, we utilized a transgenic strain expressing the ratiometric H_2O_2-specific biosensor HyPer, which is comprised of the regulatory domain of the bacterial transcription factor OxyR (OxyR-RD) fused to circularly permuted yellow fluorescent protein [196]. The OxyR-RD of HyPer is selectively oxidized by H_2O_2, generating a disulphide bridge that consequently alters the fluorescent properties of cpYFP. RNAi knockdown of either *tald-1* or *cco-1* significantly increased the oxidation of HyPer, indicating elevated cytoplasmic H_2O_2 levels in these animals (**Figure 3.2K**). In accordance with higher endogenous levels of oxidative stress, *tald-1(RNAi)* animals were sensitive to 10mM paraquat treatment, which leads

to the production of mitochondrial superoxide (**Figure 3.2L**). Thus, the presence of a functional PPP is required for normal resistance to exogenous oxidative stress.

3.3.3 *MAPKs mediate lifespan extension from transaldolase deficiency.*

Transaldolase deficiency in mammals causes a shift towards a more oxidative cellular redox status and compensatory activation of JNK MAPK signaling [186, 197, 198], prompting us to explore whether a similar response occurs in nematodes to regulate stress resistance and longevity. Remarkably, deletion of either *jnk-1* or *kgb-1*, which encode *C. elegans* JNK MAPKs, fully prevented the lifespan extension from *tald-1(RNAi)* and significantly attenuated the lifespan extension from *cco-1(RNAi)* (**Figure 3.3A-D**). This effect was specific to mitochondrial longevity, since *daf-2(RNAi)* robustly extended the lifespan of *jnk-1(gk7)* and *kgb-1(um3)* animals (**Supplemental Figure 3.5A,B**). Although deletion of either *jnk-1* or *kgb-1* prevented lifespan extension in response to either *tald-1(RNAi)* or *cco-1(RNAi)*, these mutations did not prevent the effects on mitochondrial respiration or UPR^{mt} induction (**Supplemental Figure 3.5C-E**).

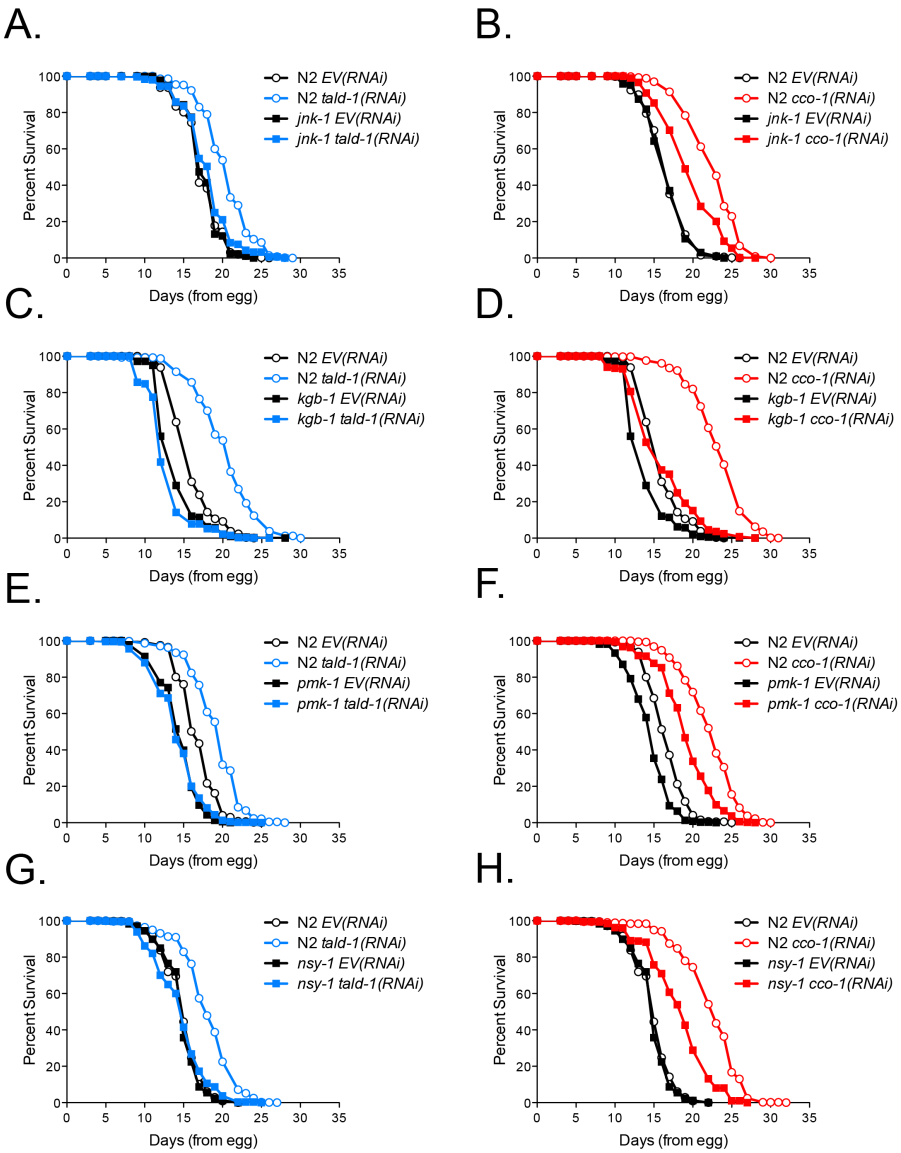

Figure 3.3. Lifespan extension from *tald-1(RNAi)* or *cco-1(RNAi)* requires stress-activated MAPKs.

(A) RNAi knockdown of *tald-1* extends lifespan through the JNK MAPK JNK-1. N2 fed *EV(RNAi)* (mean 17.2±0.1 days, n=506), N2 fed *tald-1(RNAi)* (mean 20.4±0.1 days, n=500), *jnk-1(gk7)* fed *EV(RNAi)* (mean 17±0.1 days, n=582), *jnk-1(gk7)* fed *tald-1(RNAi)* (mean 18.1±0.1 days, n=488). Lifespans were performed at 25°C, with pooled data from five independent experiments shown. **(B)** RNAi knockdown of *cco-1* extends lifespan partially through the JNK MAPK JNK-1. N2 fed *EV(RNAi)* (mean 16.9±0.1 days, n=494), N2 fed *cco-1(RNAi)* (mean 22.7±0.2 days, n=431), *jnk-1(gk7)* fed *EV(RNAi)* (mean 16.1±0.1 days, n=594), *jnk-1(gk7)* fed *cco-1(RNAi)* (mean 19.9±0.2 days, n=408). Lifespans were performed at 25°C, with pooled data from four independent experiments shown. **(C)** RNAi knockdown of *tald-1* extends lifespan through the JNK MAPK KGB-1. N2 fed *EV(RNAi)* (mean 15±0.1 days, n=630), N2 fed *tald-1(RNAi)* (mean 18.7±0.1 days, n=657), *kgb-1(um3)* fed *EV(RNAi)* (mean 13.1±0.1 days, n=580), *kgb-1* fed *tald-1(RNAi)* (mean 11.9±0.1 days, n=600). Lifespans were performed at 25°C, with pooled data from four independent experiments shown. **(D)** RNAi knockdown of *cco-1* extends lifespan partially through the JNK MAPK KGB-1. N2 fed *EV(RNAi)* (mean 15±0.1 days, n=630), N2 fed *cco-1(RNAi)* (mean 23.2±0.2 days, n=511), *kgb-1(um3)* fed *EV(RNAi)* (mean 13.1±0.1 days, n=580), *kgb-1* fed *cco-1(RNAi)* (mean 15.8±0.2 days, n=501). Lifespans were performed at 25°C, with pooled data from four independent experiments shown. **(E)** RNAi

knockdown of *tald-1* extends lifespan through the p38 MAPK PMK-1. N2 fed *EV(RNAi)* (mean 16.8±0.1 days, n=494), N2 fed *tald-1(RNAi)* (mean 19.3±0.1 days, n=460), *pmk-1(km25)* fed *EV(RNAi)* (mean 14.3±0.1 days, n=514), *pmk-1(km25)* fed *tald-1(RNAi)* (mean 14±0.1 days, n=525). Lifespans were performed at 25°C, with pooled data from four independent experiments shown. **(F)** RNAi knockdown of *cco-1* does not require the p38 MAPK PMK-1 for lifespan extension. N2 fed *EV(RNAi)* (mean 16±0.1 days, n=575), N2 fed *cco-1(RNAi)* (mean 22.3±0.2 days, n=448), *pmk-1(km25)* fed *EV(RNAi)* (mean 13.8±0.1 days, n=609), *pmk-1(km25)* fed *cco-1(RNAi)* (mean 18.7±0.1 days, n=535). Lifespans were performed at 25°C, with pooled data from four independent experiments shown. **(G)** RNAi knockdown of *tald-1* extends lifespan through the MAP3K NSY-1. N2 fed *EV(RNAi)* (mean 14.6±0.1 days, n=542), N2 fed *tald-1(RNAi)* (mean 17.2±0.1 days, n=599), *nsy-1(ag3)* fed *EV(RNAi)* (mean 14.9±0.1 days, n=473), *nsy-1(ag3)* fed *tald-1(RNAi)* (mean 14.4±0.1 days, n=508). Lifespans were performed at 25°C, with pooled data from four independent experiments shown. **(H)** RNAi knockdown of *cco-1* extends lifespan partially through the MAP3K NSY-1. N2 fed *EV(RNAi)* (mean 14.6±0.1 days, n=542), N2 fed *cco-1(RNAi)* (mean 22.5±0.2 days, n=454), *nsy-1(ag3)* fed *EV(RNAi)* (mean 14.9±0.1 days, n=473), *nsy-1(ag3)* fed *cco-1(RNAi)* (mean 18.5±0.2 days, n=458). Lifespans were performed at 25°C, with pooled data from four independent experiments shown. Lifespans in this figure are indicated as mean±s.e.m. and statistical analysis is provided in **Supplemental Table 3.1**.

The p38 MAPK PMK-1 has been implicated in mitohormesis-induced lifespan extension in response to reduced insulin/IGF-1-like signaling, metformin treatment, or glycolysis inhibition [123, 124, 129]. Interestingly, PMK-1 was also required for lifespan extension from *tald-1(RNAi),* but not from *cco-1(RNAi)* (**Figure 3.3E,F**). Therefore, despite some similar mitochondrial phenotypes and interactions with MAPK signaling, PPP inhibition and mitochondrial ETC RNAi longevity require both overlapping and distinct pathways. In addition, as previously reported [124], we also found that PMK-1 regulates *daf-2(RNAi)* lifespan extension (**Supplemental Figure 3.5F**) and is not specific to PPP inhibition.

The MAP3K ASK1 is a well-established factor upstream of p38 and JNK MAPKs that responds to oxidative stress via interactions with redox proteins [139, 140, 199]. In *C. elegans*, the ASK1 homolog NSY-1 was found to act upstream of PMK-1, JNK-1, and KGB-1 in various contexts [200-205]. Accordingly, we found that loss of NSY-1 attenuated the lifespan extension from *tald-1(RNAi)* or *cco-1(RNAi)*, suggesting this factor responds to oxidative stress in both of these instances to promote longevity (**Figure 3.3G,H**). In agreement with NSY-1 regulating PMK-1 activity, we found that NSY-1 attenuated the lifespan extension from *daf-2(RNAi)* (**Supplemental Figure 3.5G**). Therefore, NSY-1 is an essential MAP3K for the activation of

multiple longevity mechanisms, highlighting the importance of redox sensing in *C. elegans* longevity.

3.3.4 *Loss of transaldolase alters lipid metabolism and initiates a fasting-like response.*

In addition to reducing *in vivo* respiration rates, we noted that *tald-1(RNAi)* and *cco-1(RNAi)* also caused dramatic reductions in intestinal fat levels, as assessed by Oil Red O (ORO) staining (**Figure 3.4A,B**). Such a response could reflect decreased lipid synthesis, increased fatty acid oxidation (associated with starvation), or decreased fatty acid absorption. Because *C. elegans* acquire the majority of lipid species from their bacterial diet and not from *de novo* fatty acid synthesis, with the exception of monomethyl branched-chain fatty acids [206], we focused on determining whether there were changes in expression of metabolic genes regulated by starvation including lipases, β-oxidation, monounsaturated fatty acid synthesis, and glyoxylate pathway genes [207].

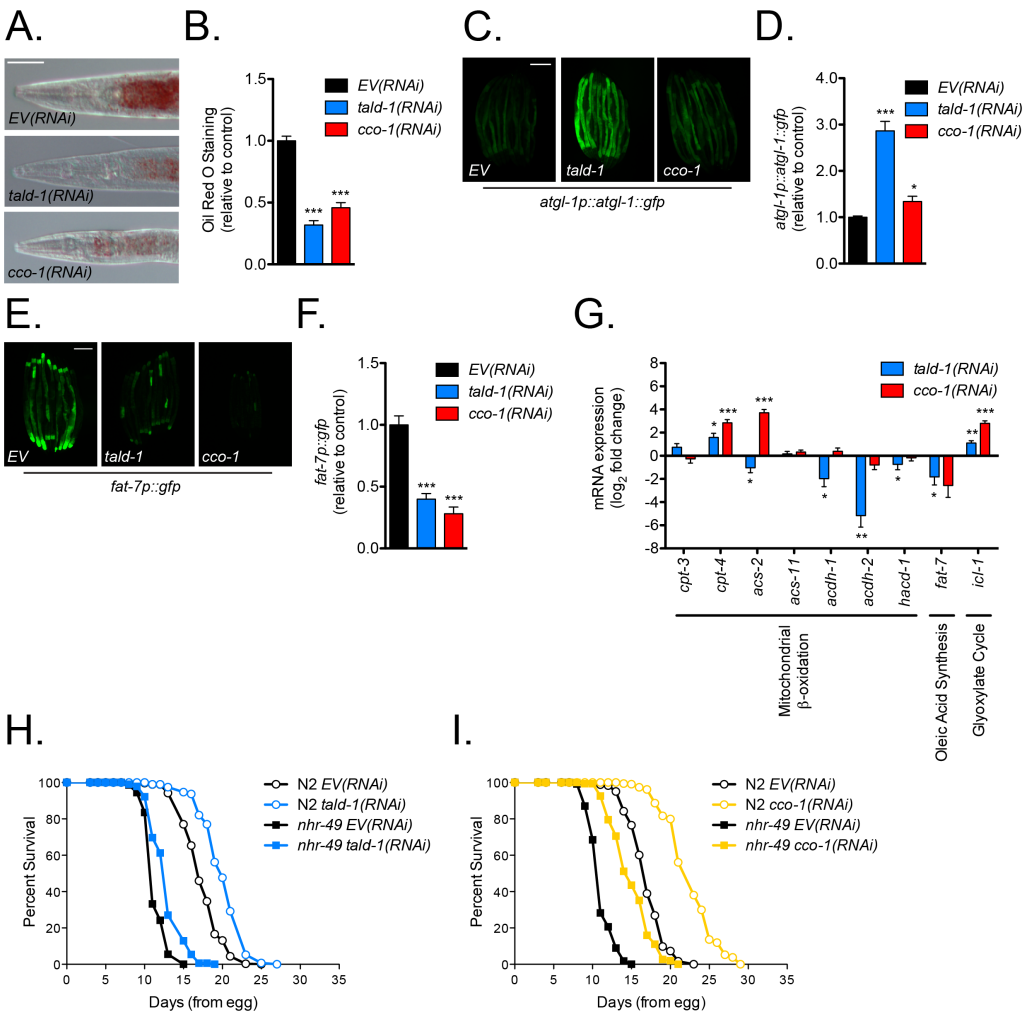

Figure 3.4. Transaldolase deficiency causes a starvation-like response that decreases animal fat content and rewires lipid metabolism gene expression.

(A) Intestinal fat staining decreases from RNAi knockdown of *tald-1* or *cco-1*. Oil Red O (ORO) staining was performed on day 3 from hatching animals propagated at 20°C. Scale bar, 50 µm. **(B)** Quantification of ORO staining within anterior intestine (N = 2 independent experiments, pooled individual worm values, error bars indicate s.e.m., student's t-test with Bonferroni's correction). **(C)** RNAi knockdown of *tald-1* causes an increase in adipose triglyceride lipase ATGL-1 protein levels. Scale bar, 200 µm. **(D)** Mean relative fluorescence of ATGL-1::GFP signal in animals grown on *tald-1(RNAi)* or *cco-1(RNAi)*. Fluorescence is calculated relative to *EV(RNAi)* controls (N = 4 independent experiments, pooled individual worm values, error bars indicate s.e.m., student's t-test with Bonferroni's correction). **(E)** RNAi knockdown of *tald-1* or *cco-1* causes a decrease in stearoyl-CoA desaturase *fat-7p::gfp* reporter expression. Scale bar, 200 µm. **(F)** Mean relative fluorescence of *fat-7p::gfp* reporter animals grown on *tald-1(RNAi)* or *cco-1(RNAi)*. Fluorescence is calculated relative to *EV(RNAi)* controls (N = 3 independent experiments, pooled individual worm values, error bars indicate s.e.m., student's t-test with Bonferroni's correction). **(G)** Gene expression of starvation-responsive lipid metabolism genes is altered in *tald-1(RNAi)* animals. Log2 fold change calculated to emphasize the increases and decreases in gene expression levels from RNAi treatments (N = 6-8 independent experiments, error bars indicate s.e.m., paired student's t-tests with Bonferroni's correction). **(H)** RNAi knockdown of *tald-1* does not require NHR-49 for lifespan extension. N2 fed *EV(RNAi)* (mean 17.5±0.1 days, n=366), N2 fed *tald-1(RNAi)* (mean 20.1±0.1 days, n=397), *nhr-49(nr2041)* fed *EV(RNAi)* (mean 11.5±0.1 days, n=310), *nhr-49(nr2041)* fed *tald-1(RNAi)* (mean 12.9±0.1 days, n=333). Lifespans were performed at 25°C, with pooled data from three independent experiments shown. **(I)** RNAi knockdown of *cco-1*

does not require NHR-49 for lifespan extension. N2 fed *EV(RNAi)* (mean 17±0.1 days, n=532), N2 fed *cco-1(RNAi)* (mean 22.6±0.2 days, n=344), *nhr-49(nr2041)* fed *EV(RNAi)* (mean 11.1±0.1 days, n=495), *nhr-49(nr2041)* fed *cco-1(RNAi)* (mean 15±0.1 days, n=489). Lifespans were performed at 25°C, with pooled data from four independent experiments shown. Lifespans in this figure are indicated as mean±s.e.m. and statistical analysis is provided in **Supplemental Table 3.1**. In this figure, statistics are displayed as: * $p<0.05$**,** ** $p<0.01$, *** $p<0.001$.

First, we examined if decreased ORO staining might reflect degradation of cytoplasmic lipid droplets. The adipose triglyceride lipase ATGL-1 is an important lipase that is stabilized and localized to lipid droplets during fasting to mediate lipolysis [208]. Using the *atgl-1p::atgl-1::gfp* translational reporter, we found that *tald-1(RNAi)* dramatically increased ATGL-1::GFP levels, suggesting enhanced breakdown of lipid droplets in these animals (**Figure 3.4C,D**). The stearoyl-CoA desaturase *fat-7* controls the relative abundance of saturated and mono-unsaturated fatty acids by converting stearic acid (18:0) to oleic acid (18:1). Expression of *fat-7* is positively regulated by NHR-49 in fed conditions but is repressed during starvation, independent of NHR-49, to preserve saturated fatty acid levels [207, 209]. Using the *fat-7p::gfp* reporter we found that *fat-7* expression was dramatically repressed in *tald-1(RNAi)* or *cco-1(RNAi)* animals (**Figure 3.4E,F**). This observation was also confirmed by qRT-PCR (**Figure 3.4G**). In a similar fashion, other metabolic genes known to be regulated by starvation [200, 207], such as genes involved in β-oxidation and the glyoxylate pathway, also change in *tald-1(RNAi)* animals and *cco-1(RNAi)* animals (**Figure 3.4G**). For example, we observed increased expression of carnitine palmitoyltransferases following *tald-1(RNAi)* or *cco-1(RNAi)*, suggesting increased import of long-chain fatty acids into the mitochondria (**Figure 3.4G**). In addition, we observed increased expression of the bifunctional glyoxylate gene *icl-1* with *tald-1(RNAi)* or *cco-1(RNAi)*, indicating increased metabolism of fatty acids to promote gluconeogenesis and generation of succinate without concomitant NAD^+ consumption and carbon loss (**Figure 3.4G**).

To explore if the starvation-like metabolic response underlies the pro-longevity effects of

tald-1(RNAi) or *cco-1(RNAi)*, we performed epistasis analyses with starvation responsive transcription factors NHR-49 and HLH-30. NHR-49 is a master regulator of gene expression changes that enable the mobilization of fat for energy metabolism, and HLH-30 regulates autophagy, fat storage, and has been previously implicated in lifespan extension downstream of dietary restriction and insulin/IGF-1-like signaling [210-212]. Interestingly, NHR-49 is not required for the lifespan effect of either *tald-1(RNAi)* or *cco-1(RNAi)* (**Figure 3.4H,I**). This agrees with a previous study that found reduced complex I, III, and IV activity caused NHR-49 dependent gene expression changes and increased lifespan independent of NHR-49 [213]. In contrast, *tald-1(RNAi)* caused nuclear localization of HLH-30 similar to starvation (**Figure 3.5A,B**), and also required HLH-30 for lifespan extension (**Figure 3.5C**). Importantly, *tald-1(RNAi)* did not affect food consumption, as measured by pharyngeal pumping rate (**Supplemental Figure 3.6A**). In contrast to *tald-1, cco-1(RNAi*) did not induce HLH-30 nuclear localization and the lifespan extension in this case was independent of HLH-30 (**Figure 3.5A-B,D**). Thus, transaldolase deficiency induces a starvation-like response and requires the autophagy regulator TFEB/HLH-30 for lifespan extension.

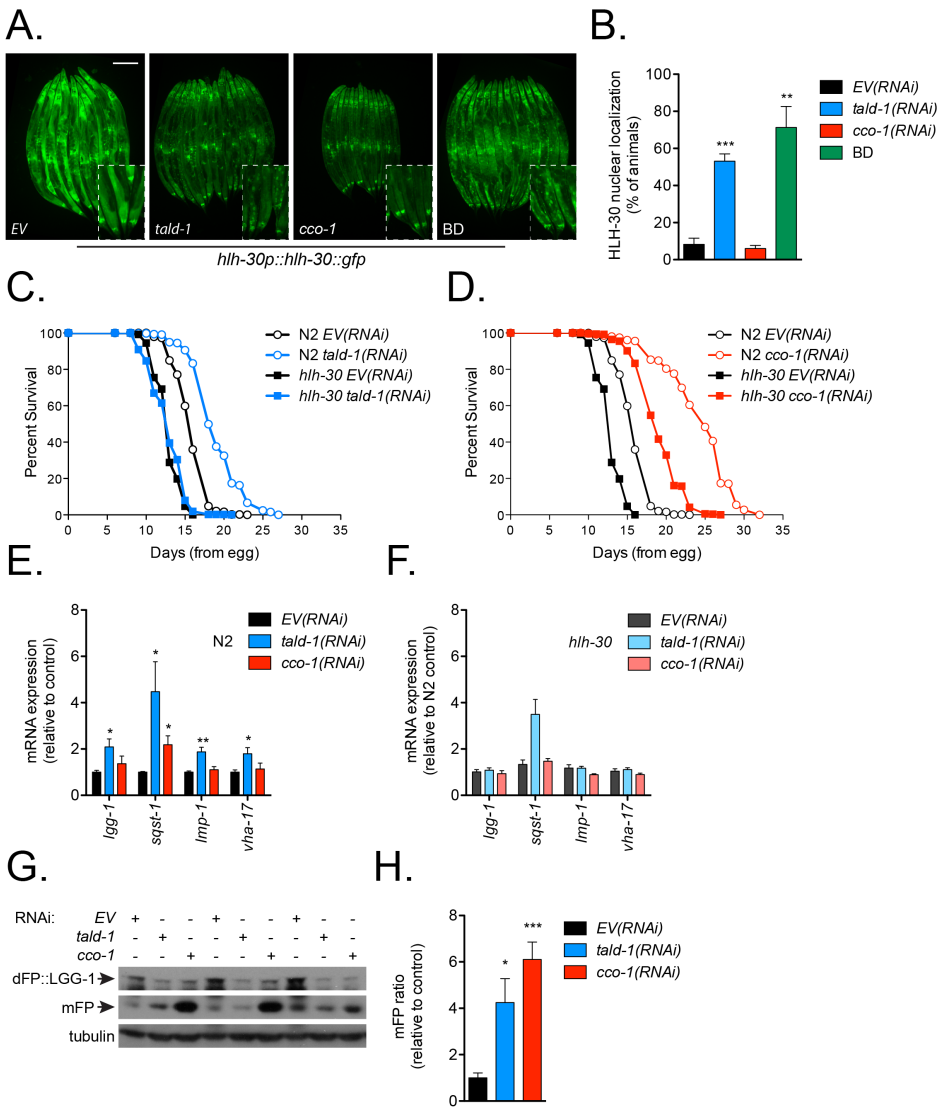

Figure 3.5. HLH-30 mediates the lifespan extension and autophagy gene expression from *tald-1(RNAi).*

(A) RNAi knockdown of *tald-1* increases nuclear localization of HLH-30 similarly to starvation. BD animals were starved for 8 hours on FUDR plates prior to imaging. Scale bar, 200 µm. **(B)** Percent of animals displaying HLH-30 nuclear localization. (N = 8 independent experiments, error bars indicate s.e.m., student's t-test with Bonferroni's correction). **(C)** HLH-30 is required for the lifespan extension from *tald-1(RNAi)*. N2 fed *EV(RNAi)* (mean 16±0.1 days, n=476), N2 fed *tald-1(RNAi)* (mean 19.2±0.1 days, n=455), *hlh-30(tm1978)* fed *EV(RNAi)* (mean 12.9±0.1 days, n=510), *hlh-30(tm1978)* fed *tald-1(RNAi)* (mean 12.9±0.1 days, n=514). Lifespans were performed at 25°C, with pooled data from four independent experiments shown. **(D)** HLH-30 is not required for the lifespan extension from *cco-1(RNAi)*. N2 fed *EV(RNAi)* (mean 16±0.1 days, n=476), N2 fed *cco-1(RNAi)* (mean 24.3±0.2 days, n=362), *hlh-30(tm1978)* fed *EV(RNAi)* (mean 12.9±0.1 days, n=510), *hlh-30(tm1978)* fed *cco-1(RNAi)* (mean 19.2±0.1 days, n=533). Lifespans were performed at 25°C, with pooled data from four independent experiments shown. **(E)** Gene expression of autophagy genes is upregulated in *tald-1(RNAi)* animals (N = 6 biological replicates, error bars indicate s.e.m., student's t-test with Bonferroni's correction). **(F)** HLH-30 is required for the upregulation of autophagy genes by *tald-1(RNAi)*. qRT-PCR was performed on RNA isolated from *hlh-30(tm1978)* animals (N = 3 biological replicates, error bars indicate s.e.m., student's t-test with Bonferroni's correction). **(G)** Autophagic flux increases from RNAi knockdown of *tald-1* or *cco-1*. Western blot analysis was performed on protein lysates from

eft-3p::dFP::lgg-1 animals using an anti-GFP antibody to detect full-length dFP-LGG-1 and monomeric FP. An anti-α-tubulin antibody was used as a loading control. Three biological replicates for each RNAi treatment are presented. **(H)** Quantification of the dFP::LGG-1 ratiometric reporter. The intensity of monomeric FP to full-length dFP::LGG-1 was measured to determine autophagic flux (N = 5 independent experiments, error bars indicate s.e.m., student's t-test with Bonferroni's correction). Lifespans in this figure are indicated as mean±s.e.m. and statistical analysis is provided in **Supplemental Table 3.1**. In this figure, statistics are displayed as: * $p<0.05$**,** ** $p<0.01$, *** $p<0.001$.

3.3.5 *HLH-30 activates autophagy and flavin-containing monooxygenase 2 in response to transaldolase deficiency*

One major function of TFEB/HLH-30 is to promote autophagy [210, 211, 214], and this activity of HLH-30 is necessary for lifespan extension in response to dietary restriction and reduced insulin/IGF-1-like signaling [210]. Consistent with our observation that *tald-1(RNAi)* induces nuclear localization of HLH-30, we found that components of the autophagy pathway [210] were upregulated in a HLH-30-dependent fashion, including *lgg-1* (*LC3* homolog), *sqst-1* (p62/*SQSTM1* homolog), *lmp-1* (*LAMP1* homolog), and lysosomal subunit *vha-17* (**Figure 3.5E,F**). In addition, autophagic flux is increased by *tald-1(RNAi)* (**Figure 3.5G,H**), as measured by a recently described LGG-1 reporter of lysosomal protease activity [215].

Another important target of HLH-30 recently implicated in longevity control is the flavin-containing monooxygenase FMO-2. FMO-2 is induced by both hypoxic signaling and starvation, and its induction by starvation is dependent on HLH-30 [118]. Utilizing an *fmo-2p::mCherry* transcriptional reporter, we found that *tald-1(RNAi)* also robustly induced *fmo-2* expression, although not to the same extent as complete removal of the bacterial food source (bacterial deprivation, BD) (**Figure 3.6A-C**). Unexpectedly, whereas, *tald-1(RNAi)* or starvation causes intestinal *fmo-2* expression, *cco-1(RNAi)* causes *fmo-2* expression in the pharynx and cells proximal to the anterior bulb (**Supplemental Figure 3.7A**). The increased expression of *fmo-2* indicated by the reporter was confirmed by qRT-PCR (**Figure 3.6D**).

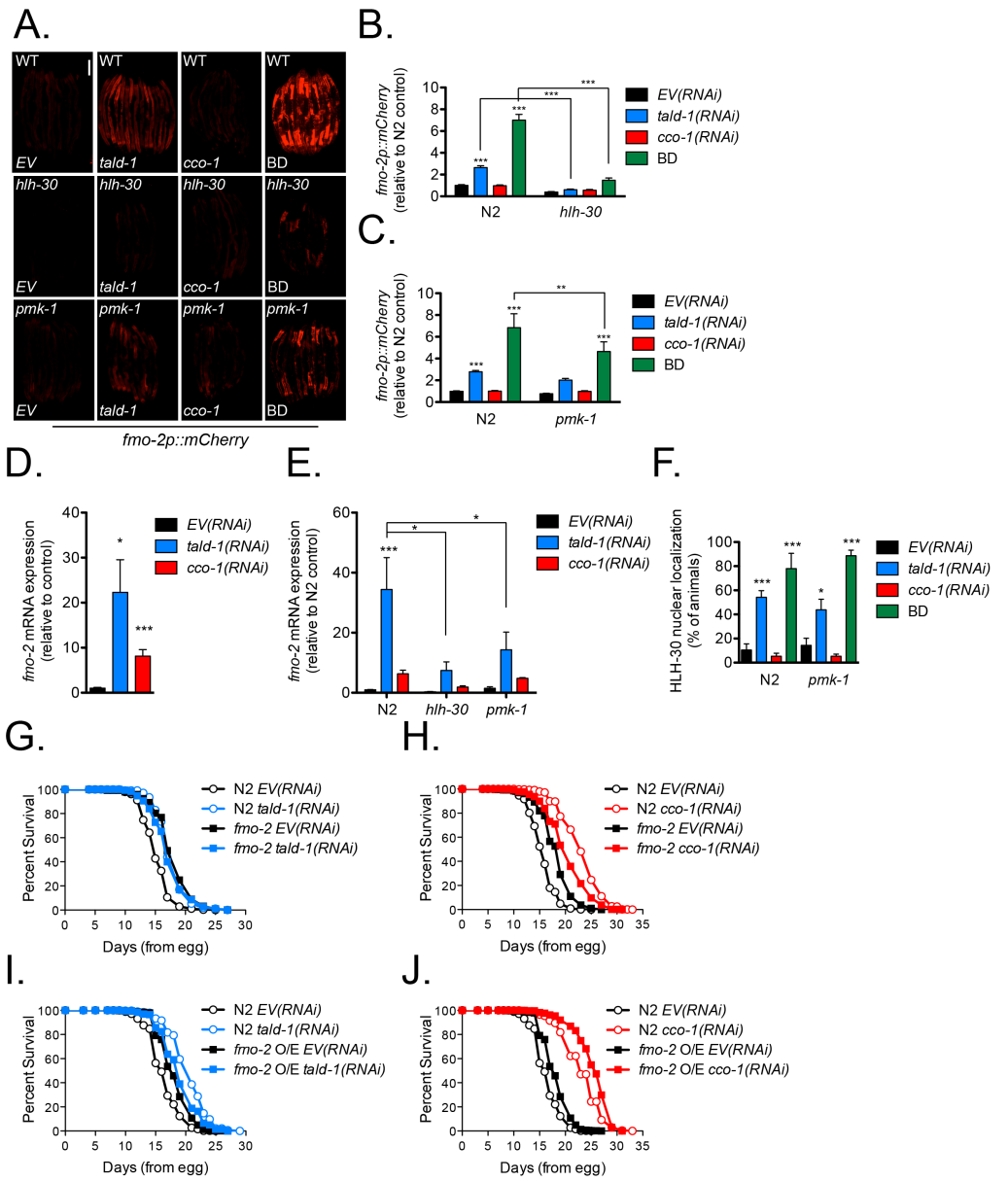

Figure 3.6. The flavin-containing monooxygenase FMO-2 is upregulated in a HLH-30 and PMK-1 dependent fashion and regulates the lifespan extension from *tald-1(RNAi)*.

(A) *fmo-2p::mCherry* reporter expression is increased by *tald-1(RNAi)* or BD in a HLH-30 and PMK-1 dependent fashion. BD animals were starved for 24 hours on FUDR plates prior to imaging. Scale bar, 200 µm. **(B)** Mean relative fluorescence of *fmo-2p::mCherry* reporter animals in the context of the *hlh-30(tm1978)* mutation. Fluorescence is calculated relative to N2 *EV(RNAi)* controls (N = 3 independent experiments, pooled individual worm values, error bars indicate s.e.m., ANOVA with Bonferroni's post-hoc). **(C)** Mean relative fluorescence of *fmo-2p::mCherry* reporter animals in the context of the *pmk-1(km25)* mutation. Fluorescence is calculated relative to N2 *EV(RNAi)* controls (N = 5 independent experiments, pooled individual worm values, error bars indicate s.e.m., ANOVA with Bonferroni's post-hoc). **(D)** Gene expression of *fmo-2* is upregulated by *tald-1(RNAi)* or *cco-1(RNAi)* (N = 11 biological replicates, error bars indicate s.e.m., student's t-test with Bonferroni's correction). **(E)** Gene expression of *fmo-2* is upregulated by *tald-1(RNAi)* in a HLH-30 and PMK-1 dependent fashion (N = 3-6 biological replicates, error bars indicate s.e.m., ANOVA with Bonferroni's post-hoc). **(F)** Percent of animals displaying HLH-30 nuclear localization. BD animals were starved for 8 hours on FUDR plates prior to imaging (N = 5 independent

experiments, error bars indicate s.e.m., ANOVA with Bonferroni's post-hoc). **(G)** FMO-2 is required for the lifespan extension from *tald-1(RNAi)*. N2 fed *EV(RNAi)* (mean 15.3±0.1 days, n=341), N2 fed *tald-1(RNAi)* (mean 17.8±0.1 days, n=353), *fmo-2(ok2147)* fed *EV(RNAi)* (mean 18±0.2 days, n=314), *fmo-2(ok2147)* fed *tald-1(RNAi)* (mean 17.4±0.2 days, n=382). Lifespans were performed at 25°C, with pooled data from three independent experiments shown. **(H)** FMO-2 is partially required for the lifespan extension from *cco-1(RNAi)*. N2 fed *EV(RNAi)* (mean 15.7±0.1 days, n=562), N2 fed *cco-1(RNAi)* (mean 23.3±0.2 days, n=616), *fmo-2(ok2147)* fed *EV(RNAi)* (mean 18.3±0.1 days, n=474), *fmo-2(ok2147)* fed *cco-1(RNAi)* (mean 20.5±0.2 days, n=473). Lifespans were performed at 25°C, with pooled data from five independent experiments shown. **(I)** Lifespan extension from *fmo-2* overexpression is not additive with *tald-1(RNAi)*. N2 fed *EV(RNAi)* (mean 16.5±0.1 days, n=453), N2 fed *tald-1(RNAi)* (mean 20.6±0.1 days, n=421), *eft-3p::fmo-2* fed *EV(RNAi)* (mean 18.2±0.1 days, n=439), *eft-3p::fmo-2* fed *tald-1(RNAi)* (mean 19.1±0.1 days, n=435). Lifespans were performed at 25°C, with pooled data from three independent experiments shown. **(J)** Lifespan extension from *fmo-2* overexpression is additive with *cco-1(RNAi)*. N2 fed *EV(RNAi)* (mean 16.5±0.1 days, n=453), N2 fed *cco-1(RNAi)* (mean 23.3±0.2 days, n=259), *eft-3p::fmo-2* fed *EV(RNAi)* (mean 18.2±0.1 days, n=439), *eft-3p::fmo-2* fed *cco-1(RNAi)* (mean 25.5±0.2 days, n=352). Lifespans were performed at 25°C, with pooled data from three independent experiments shown. Lifespans in this figure are indicated as mean±s.e.m. and statistical analysis is provided in **Supplemental Table 3.1**. In this figure, statistics are displayed as: * $p<0.05$, ** $p<0.01$, *** $p<0.001$.

Since the regulation of *fmo-2* is not well understood, we decided to test if HLH-30 is an essential regulatory factor of *fmo-2* in multiple contexts. In support of this, we found that HLH-30 mediates *fmo-2* expression from both BD and *tald-1(RNAi)* (**Figure 3.6A,B**). This observation was supported by qRT-PCR (**Figure 3.6E**). Thus, we decided to use the *fmo-2* transcriptional reporter as a proxy for HLH-30 activity to determine genetic relationships between HLH-30 and the MAPKs that mediate *tald-1(RNAi)* lifespan extension. JNK-1 and KGB-1 were not required for *fmo-2p::mCherry* induction from *tald-1(RNAi)* or BD (**Supplemental Figure 3.7B**), arguing that these MAPKs are not upstream of HLH-30. However, the p38 MAPK PMK-1 was required for induction of *fmo-2p::mCherry* from BD and there was a similar trend for *tald-1(RNAi)* (**Figure 3.6A,C**). Supporting this, *fmo-2* induction by *tald-1(RNAi)* was attenuated in *pmk-1(km25)* animals by qRT-PCR (**Figure 3.6E**). Since loss of function in *hlh-30* and *pmk-1* cause similar effects with respect to *fmo-2* expression and lifespan epistasis with *tald-1(RNAi)* and *cco-1(RNAi)*, we tested if PMK-1 is upstream of HLH-30. Surprisingly, we found that *pmk-1(km25)* mutation did not alter HLH-30 nuclear localization from *tald-1(RNAi)* or BD (**Figure 3.6F**). Therefore, the simplest model is that PMK-1 functions

in parallel with HLH-30 to activate *fmo-2* expression.

To determine if FMO-2 activation contributes to the lifespan extension from transaldolase deficiency, we treated *fmo-2(ok2147)* mutants with *tald-1(RNAi)*. We found that *tald-1(RNAi)* did not extend the lifespan of *fmo-2(ok2147)* animals (**Figure 3.6G**). In addition, *cco-1(RNAi)* longevity partially required *fmo-2* (**Figure 3.6H**). In neither case did deletion of *fmo-2* affect induction of the UPR^{mt} reporter (**Supplemental Figure 3.7C**). Consistent with the model that FMO-2 acts downstream of *tald-1(RNAi)* to promote longevity, *tald-1(RNAi)* did not further extend the lifespan of long-lived *eft-3p::fmo-2* animals ubiquitously overexpressing *fmo-2* (**Figure 3.6I**).

3.4 DISCUSSION

In this study, we found that the inhibition of the PPP enzyme transaldolase impairs mitochondrial respiration, induces a starvation-like metabolic response, and activates MAPK signaling pathways that together promote longevity in *C. elegans*. These observations define unexpected new connections between the cytosolic PPP, mitochondrial metabolism, and aging. Although our interest in transaldolase stemmed from the observation that *tald-1(RNAi)* induces the UPR^{mt}, activation of this mitochondrial stress response does not appear to be involved in mediating the longevity phenotype. Instead, lifespan extension from *tald-1(RNAi)* likely involves at least two outputs previously associated with longevity: induction of autophagy and activation of the flavin-containing monooxygenase 2 (**Figure 3.7**).

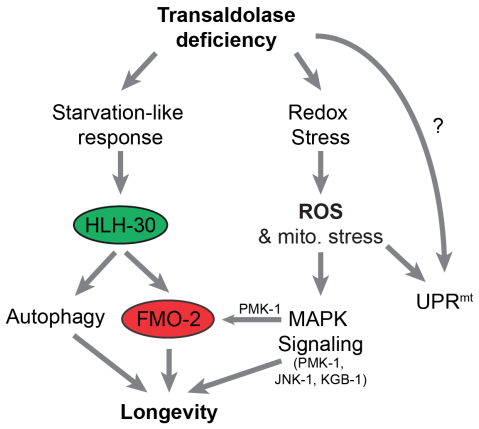

Figure 3.7. Model of transaldolase deficiency mediated longevity.

Reduced activity of the pentose phosphate pathway enzyme transaldolase has several consequences, including inhibition of mitochondrial respiration, induction of a mitochondrial stress response, alterations in redox homeostasis, and activation of a starvation-like metabolic response. Lifespan extension in response to transaldolase deficiency appears to be mediated by both MAPK signaling and HLH-30 mediated induction of autophagy and activation of FMO-2.

The relationship between PPP activity and mitochondrial function is particularly intriguing. Our studies indicate that inhibition of the PPP is sufficient to reduce respiration rates *in vivo* and remodel the mitochondrial network by activating mitochondrial fission, but importantly, this is accomplished without apparent functional changes to the ETC itself, as evidenced by the normal *in vitro* activity of purified mitochondria. This mechanistically differentiates *tald-1(RNAi)* from the well-characterized long-lived ETC-deficient animals such as *cco-1(RNAi)* and *isp-1(qm150)*, which directly impair ETC structure and function [195, 216]. Our findings also support mammalian literature where mitochondrial function is altered by transaldolase deficiency. For example, lymphoblasts isolated from transaldolase deficient patients exhibit decreased mitochondrial membrane potential, increased mitochondrial mass, and increased H_2O_2 levels, while transaldolase deficient mice are infertile due to mitochondrial defects in spermatozoa [186, 197]. Although the UPR^{mt} is apparently not involved in mediating the lifespan effects, its activation clearly indicates mitochondrial stress *in vivo* in the *tald-1(RNAi)* animals. One

potential source of this mitochondrial stress could be increased levels of ROS, as indicated by the HyPer reporter and the enhanced sensitivity of *tald-1(RNAi)* animals to paraquat.

These findings highlight the importance of the PPP not only as a key pathway involved in central carbon metabolism, but also as a signaling hub. This close monitoring of PPP activity is logical, as it lies at the intersection of nucleotide metabolism, fatty acid/sterol synthesis, redox regulation, and glycolysis. In this light, the starvation like-response to *tald-1(RNAi)* is of particular interest, since it suggests that decreased PPP flux is monitored by the cell and results in diminished growth signaling. We speculate this occurs at least partially through decreased mTORC1 signaling, as we observed increased autophagic flux and activation of HLH-30, which is negatively regulated by mTORC1 [211, 217-220]. Furthermore, this starvation-like response caused a metabolic shift that depleted intestinal fat stores and rewired lipid metabolism to downregulate the *stearoyl-CoA desaturase* (Δ-9-*desaturase, SCD*) *fat-7*, upregulate mitochondrial fatty acid import genes, and the glyoxylate gene *icl-1,* among others. A reduction in *fat-7* expression limits monounsaturated fatty acid synthesis, which maintains saturated fatty acid levels, but could also alter cellular and membrane lipid composition, including that of the mitochondria [221]. Alternatively, decreased *fat-7* levels may indicate one arm of a concerted effort to breakdown fats through gene expression changes, as *fat-7* negatively regulates ß-oxidation [209, 222]. We suspect this gene expression program promotes the mobilization and breakdown of fatty acids for both energy metabolism and gluconeogenesis through the mitochondrial glyoxylate pathway [223].

In this study, we implicated stress-activated MAPKs as one class of sensors that respond to reduced PPP activity and appear to be independent of HLH-30 activity. NADPH produced by the PPP not only maintains a reduced cytosolic redox environment, but also affects antioxidant

systems such as thioredoxin, glutaredoxin, and peroxiredoxin that respond to oxidative stress via thiol-based chemistry to initiate downstream signaling events. For example, activity of the MAP3K ASK1/NSY-1 is fine-tuned via thiol-disulphide exchange reactions mediated by these redox proteins [136, 138, 224-226]. Thus, a shift to a more oxidative cytosolic redox is coupled to activation of ASK1/NSY-1 and downstream p38 and JNK MAPK signaling. Accordingly, in a context dependent fashion, *C. elegans* p38 and JNK MAPKs regulate stress resistance from various oxidative insults and longevity from dietary restriction interventions such as intermittent fasting and metformin treatment [129, 200]. Our data further confirms that elevated cytosolic H_2O_2 correlates with MAPK mediated lifespan extension in novel and distinct contexts: RNAi knockdown of a PPP enzyme and an ETC Complex IV subunit. Interestingly, the MAP3K NSY-1 was required for the full lifespan extension from both interventions, but differences existed for downstream MAPK requirements. For example, *tald-1(RNAi)* required both the p38 MAPK PMK-1 and the JNK MAPKs JNK-1 and KGB-1 for lifespan extension, while *cco-1(RNAi)* only required the JNK MAPK branch. Furthermore, our discovery of an unreported role for the JNK MAPK pathway in mediating ETC RNAi longevity is intriguing, as no other genes outside *hif-1* and the p38 MAPK *pmk-3* have been reported to mediate these effects in *C. elegans* [106].

The simplest model for enhanced longevity downstream of *tald-1(RNAi)* is through activation of HLH-30, which has been previously shown to promote longevity downstream of dietary restriction, mTOR signaling, and insulin/IGF-1-like signaling [210]. Prior studies have focused primarily on activation of autophagy and lipophagy by HLH-30 [210, 211], but we recently reported that FMO-2 is another important pro-longevity HLH-30 target that is activated by both dietary restriction and the hypoxic response [118]. The exact role of FMO enzymes outside xenobiotic metabolism is not well understood, but they are induced by various redox

stressors and are important for resistance to reductive stress, which affects endoplasmic reticulum protein homeostasis [118, 227, 228]. Hence, one function of FMOs may be to counterbalance GSH-mediated redox buffering to promote an oxidative redox environment through O_2- and NADPH-dependent oxidation of biological thiols [227-229].

One intriguing twist to this simple model is that, unlike either dietary restriction [230, 231] or activation of the hypoxic response [114], *tald-1(RNAi)* must occur during development in order to promote longevity. This is similar to the mitochondrial longevity mutants, which have previously been thought to be largely mechanistically distinct from these other longevity pathways. HIF-1 is known to be activated in some long-lived mitochondrial mutants in response to ROS and to mediate part of their lifespan extension [106]; however, HIF-1 is not required for lifespan extension from *tald-1(RNAi)*. Thus, our data suggest that the PPP mediates a complex interaction between several portions of the overall longevity network in worms that have previously been studied as genetically distinct "pathways". These interactions will be of interest for future studies of longevity and aging in *C. elegans*.

Given the highly conserved nature of the PPP and its interactions with cellular metabolism, redox balance, and stress resistance, it is interesting to consider the extent to which the observations reported here will translate to mammals. As previously mentioned, there is good reason to believe that transaldolase deficiency can similarly impact mitochondrial function, metabolism, and oxidative stress resistance in mammals. To the best of our knowledge, there are no reports of PPP or transaldolase inhibition extending lifespan in a mammal; however, the downstream effectors of *tald-1(RNAi)* in worms are likely to play a conserved role in aging, as numerous studies have implicated autophagy in mammalian aging [232] and FMO-2 orthologs

are among the most consistently induced enzymes in numerous long-lived mouse models [233, 234].

In summary, we uncovered a novel role of the PPP not only as a central metabolic pathway, but also as a signaling hub that connects the UPR^{mt}, p38 and JNK MAPK signaling, and a starvation response mediated by HLH-30 and FMO-2 to promote cellular homeostasis and organismal longevity.

3.5 MATERIALS AND METHODS

Strains

RB967 (*gcn-2(ok871)*), ZG31 (*hif-1(ia4)*), CF1038 (*daf-16(mu86)*), CB4037 (*glp-1(e2141)*), VC8 (*jnk-1(gk7)*), KB3 (*kgb-1(um3)*), KU25 (*pmk-1(km25)*), VC1668 (*fmo-2(ok2147*)), STE68 (*nhr-49(nr2041)*), VC1024 (*pdr-1(gk448)*), SJ4100 (zcIs13[*hsp-6*$_p$::*gfp*]), SJ4143 (zcIs17[*ges-1p::gfp*^{mt}]), BX113 (waEx15 [*fat-7p::gfp* + *lin-15*(+)]), MAH235 (sqIs19 [*hlh-30p::hlh-30::gfp* + *rol-6(su1006)*]), KAE9 (*eft-3p::fmo-2* + *h2b::gfp* + Cbr-*unc-119*(+)), and VS20 (hjIs67 [*atgl-1p::atgl-1::gfp* + *mec-7::rfp*]) were obtained from the Caenorhabditis Genetics Center (Minneapolis, MN). The *atfs-1(tm4525)* and *hlh-30(tm1978)* strains were obtained from the National BioResource Project (Tokyo, Japan).

The *fmo-2p::mCherry* reporter strain, a transcriptional reporter, was created by microinjecting RBW6699 worms with a solution of 50ng/µL of the BSP190 construct containing 2076 bp of genomic sequence preceding the ATG of the *fmo-2* coding sequence followed by the mCherry coding sequence and the unc-54 3' UTR. A single copy insertion was generated at the chromosome II *ttTi5605* locus using the Mos1 mediated Single Copy transgene Insertion (MosSCI) protocol [235].

Fluorescence and Confocal Microscopy

Fluorescence microscopy was performed using Zeiss SteREO Lumar.V12 and Nikon Eclipse E600 microscopes. Worms were immobilized using sodium azide, mounted onto 3% agarose pads, and imaged within a few minutes for reporter experiments. Levamisole was avoided for imaging *hlh-30p::hlh-30::gfp* animals, since it caused rapid HLH-30 nuclear localization. For reporter assays worms were developed on RNAi bacteria at 20°C and imaged on day 1 of adulthood, except for *fmo-2* reporter experiments, where day 2 adults were imaged. At least three independent experiments with approximately 10 animals per condition per experiment were performed for each reporter with similar results. Statistical analysis for quantification of reporters was performed using student's t-test with Bonferroni's correction or ANOVA with Bonferroni's post-hoc, * $p<0.05$**,** ** $p<0.01$, *** $p<0.001$.

Confocal microscopy was performed using the Zeiss 510 META Confocal. For imaging intestinal mitochondrial morphology, animals were immobilized using levamisole and mounted on 10% agarose pads to prevent movement during image acquisition. Mitochondria were imaged with a 100X oil objective and Z-stacks of the posterior intestinal cells were taken at 0.34 μm increments. Gain settings for each image were maximized without over-saturation to emphasize mitochondrial content regardless of GFP expression, import, and folding levels. For imaging processing, Z-stacks were deconvoluted using the Iterative Deconvolve 3D plugin in Fiji and 5 image slices were projected using max intensity projection. Mitochondrial content was analyzed by thresholding the 5 image slice projections of different animals for each condition and quantifying the % area of signal within cell boundaries. For quantification, multiple animals for each condition in at least 2 independent experiments were analyzed.

Lifespan Analyses

Synchronized eggs or L1 larvae were grown on NGM plates containing 4 mM IPTG, 25 μg/ml carbenicillin and seeded with RNAi bacteria. At the L4/young adult stage, worms were transferred to plates with 50 μM FUDR to prevent hatching of progeny. When necessary, worms were transferred to new plates with fresh bacteria. Lifespans were performed at 25°C for the majority of experiments, unless otherwise noted in the text and figures. Cohorts were examined every 1–3 days using tactile stimulation to verify viability of animals. Animals that displayed vulval rupture were included in analysis, since it is an age-related phenotype [176, 236]. Animals lost due to foraging or bagging were not included in the analysis. All lifespan analyses were replicated using independent cohorts on different dates with replicate statistics provided in **Supplemental Table 3.1**. *p*-values were calculated using the Wilcoxon rank-sum test.

Seahorse Bioscience Respiration Assay

To measure *in vivo* oxygen consumption in *C. elegans*, we utilized the Seahorse X24 Bioanalyzer (Seahorse Biosciences) as previously described [194]. Worms were grown on concentrated RNAi bacteria (0.15 g/ml) for 3 days at 20°C starting from the L1 stage, washed from plates, and rinsed from bacteria with M9 buffer 4+ times, before being placed in Seahorse XF24 Cell Culture Microplates for analysis. Basal respiration for each condition was analyzed using the average respiration of 5 well replicates over the course of one hour. Respiration for each genotype was measured in at least 4 independent experiments.

Mitochondrial Isolation and Clark Electrode Assays

To measure activity of the ETC, mitochondria were isolated from *C. elegans* treated with RNAi bacteria as previously described [154, 237]. To ensure sufficient material for mitochondrial isolations, worm populations were grown for three generations at 20°C. Initially, animals were grown on concentrated RNAi bacteria for two generations and then transferred into 4-6 250 ml

liquid cultures. Liquid cultures were propagated for 4-5 days depending on condition and monitored for developmental progression of animals and bacterial density (maintained at ~2 x 10^{10} cells/ml) to avoid starvation. Animals treated with *cco-1(RNAi)* were grown for two generations on *EV(RNAi)* bacteria and then transferred to liquid cultures containing *cco-1(RNAi)*, due to developmental and fecundity issues associated with multiple generations of *cco-1(RNAi)*. Respiration of isolated mitochondria was measured in 4 independent experiments for each condition.

H_2O_2 Assay

Measurement of *in vivo* H_2O_2 levels was performed using the transgenic HyPer reporter as previously described [196]. Worms were grown on concentrated RNAi bacteria for 4 days starting from L1 (due to growth delay of this strain), washed from plates, and rinsed from bacteria with M9 buffer. At least 3 replicates of 1,000 worms for each condition were pipetted into a black flat bottom 96-well plate. N2 animals grown on *EV(RNAi)* were used as a background control. Fluorescence measurements were made using a BioTek Synergy H1M plate reader.

Fat Staining

Oil Red O staining and analysis was performed as previously described [238]. To quantify fat staining for each condition photos were converted to RGB color, a pseudo flat field correction was applied, images were separated into their respective RGB channels, and fat staining was thresholded in the green channel consistently across all images for a particular experiment. Fat content for each worm was quantified using the integrated density (limited to thresholded signal) of a 40 pixel diameter circle placed below the pharynx (i.e. over the anterior intestinal cells). Two independent experiments were obtained for quantification.

qRT–PCR

RNA was isolated from young adult worms using a TRIzol (Life Technologies) chloroform extraction and cDNA was prepared using iScript™ Reverse Transcription Supermix for qRT-PCR (Bio-Rad). qRT-PCR was used to measure the expression levels of target genes (iTaq™ Universal SYBR® Green Supermix, Bio-Rad) and normalization controls *pmp-3* and *cdc-42* (TaqMan® Gene Expression Assays, Life Technologies). The relative standard curve method was used to calculate gene expression. Primers of target genes are listed in **Supplemental Table 3.2**.

Western blotting

Protein was isolated from adult day 1 worms by flash freezing worm pellets in liquid nitrogen followed by extraction in lysis buffer [20 mM HEPES, pH 7.4, 150 mM NaCl, 1 mM EDTA, 1 mM EGTA, 1% (v/v) Triton X-100, and 1x Pierce™ Protease Inhibitor Mini Tablets, EDTA Free (88666, ThermoFisher Scientific)]. Proteins of interest were detected by immunoblot using anti-GFP (sc-9996; Santa Cruz Biotechnology) and anti-alpha-tubulin (Clone: DM1A, MS-581-P0, Neomarkers) antibodies both at a 1:1000 dilution in 5% BSA TBST.

3.6 ACKNOWLEDGEMENTS

We thank members of the Kaeberlein, Morgan, and Sedensky labs for helpful comments regarding experiments and manuscript preparation, especially Dr. Ernst-Bernhard Kayser and Dr. Beatrice Predoi for their expertise and assistance with mitochondrial preparations and OXPHOS measurements. We would like to also thank the W.M. Keck Center for Advanced Studies in Neural Signaling for imaging assistance and the National Bioresource Project and the *C. elegans* Genetics Center for *C. elegans* strains. This work was supported by the National Institutes of

Health grant R01AG038518 to M.K. and training grants T32GM07270 and T32ES007032 to C.F.B. Additional support was provided by the University of Washington Nathan Shock Center of Excellence in the Basic Biology of Aging (NIH grant P30AG013280).

3.7 SUPPLEMENTAL FIGURES AND TABLES

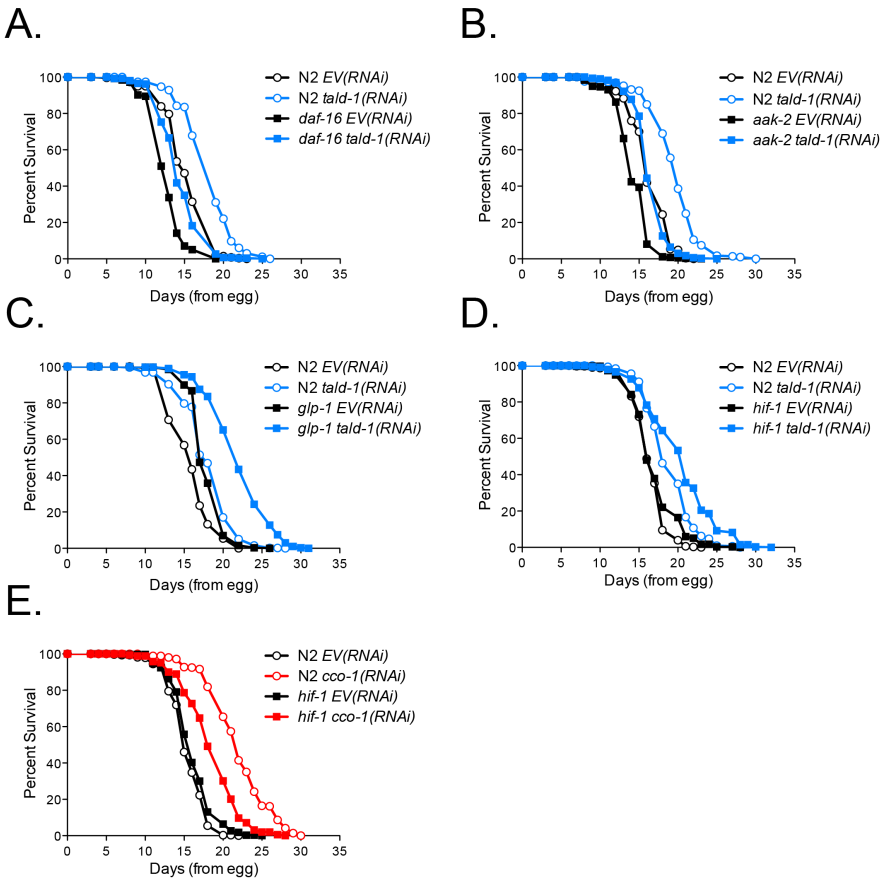

Supplemental Figure 3.1. RNAi knockdown of *tald-1(RNAi)* extends lifespan independent of *daf-16*, *aak-2*, *glp-1*, and *hif-1*.

(A) N2 fed *EV(RNAi)* (mean 15.4±0.2 days, n=261), N2 fed *tald-1(RNAi)* (mean 18.2±0.2 days, n=267), *daf-16(mu86)* fed *EV(RNAi)* (mean 12.9±0.1 days, n=255), *daf-16(mu86)* fed *tald-1(RNAi)* (mean 14.6±0.1 days, n=263). Lifespans were performed at 25°C, with pooled data from three independent experiments shown. **(B)** N2 fed *EV(RNAi)* (mean 16.3±0.2 days, n=283), N2 fed *tald-1(RNAi)* (mean 19.6±0.2 days, n=293), *aak-2(ok524)* fed *EV(RNAi)* (mean 14.3±0.1 days, n=358), *aak-2(ok524)* fed *tald-1(RNAi)* (mean 16.7±0.1 days, n=293). Lifespans were performed at 25°C, with pooled data from three independent experiments shown. **(C)** N2 fed *EV(RNAi)* (mean 16±0.1 days, n=331), N2 fed *tald-1(RNAi)* (mean 18.2±0.2 days, n=433), *glp-1(e2141)* fed *EV(RNAi)* (mean 18.1±0.1 days, n=385), *glp-1(e2141)* fed *tald-1(RNAi)* (mean 22.3±0.1 days, n=359). Lifespans were performed at 25°C, with pooled data from three independent experiments shown. **(D)** N2 fed *EV(RNAi)* (mean 16.5±0.1 days, n=303), N2 fed *tald-1(RNAi)* (mean 18.9±0.2 days, n=317), *hif-1(ia4)* fed *EV(RNAi)* (mean 17.1±0.2 days, n=335), *hif-1(ia4)* fed *tald-1(RNAi)* (mean 20.4±0.2 days, n=328). Lifespans were performed at 25°C, with pooled data from three independent experiments shown. **(E)** N2 fed *EV(RNAi)* (mean 15.5±0.1 days, n=328), N2 fed *cco-1(RNAi)* (mean 22±0.2 days, n=359), *hif-1(ia4)* fed *EV(RNAi)* (mean 16.2±0.1 days, n=330), *hif-1(ia4)* fed *cco-1(RNAi)* (mean 18.6±0.2 days, n=352). Lifespans were performed at 25°C, with pooled data from three independent experiments shown. Lifespans in this figure are indicated as mean±s.e.m. and statistical analysis is provided in **Supplemental Table 3.1**.

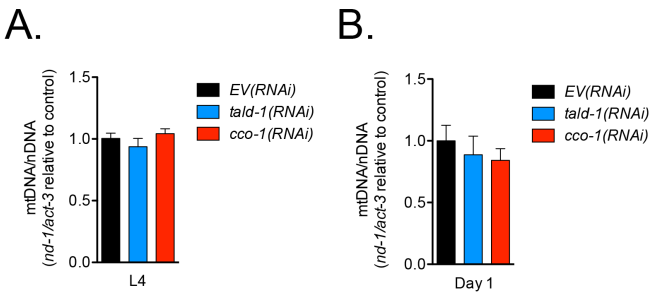

Supplemental Figure 3.2. Transaldolase deficiency does not alter whole-animal mtDNA content.

(A) mtDNA content (*nd-1/act-3* DNA) in L4 *tald-1(RNAi)* or *cco-1(RNAi)* animals does not change (n = 15 animals, error bars indicate s.e.m., student's t-test with Bonferroni's correction). **(B)** mtDNA content (*nd-1/act-3* DNA) in adult day 1 *tald-1(RNAi)* or *cco-1(RNAi)* animals does not change (n = 16 animals, error bars indicate s.e.m., student's t-test with Bonferroni's correction).

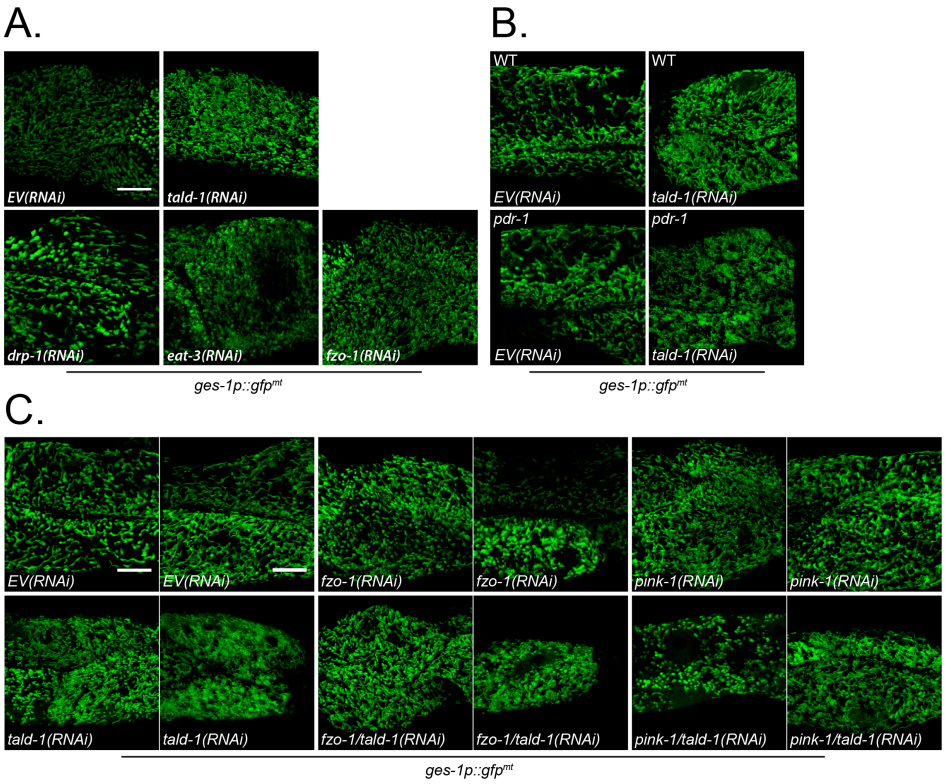

Supplemental Figure 3.3. Transaldolase deficiency causes a mitochondrial morphology shift independent of *pdr-1*, *pink-1*, and *fzo-1*.

(A) RNAi knockdown of mitochondrial fusion and fission factors alters intestinal mitochondrial morphology. *ges-1p::gfp*^{mt} reporter animals were imaged and max intensity projections of five z-slices are presented. RNAi knockdown of *tald-1* alters mitochondrial morphology independent of **(B)** *pdr-1*, **(C)** *fzo-1*, and *pink-1*. For (B), *pdr-1(gk448)* mutants were used. *ges-1p::gfp*^{mt} reporter animals were imaged and max intensity projections of five z-slices are presented. Scale bar, 10 μm.

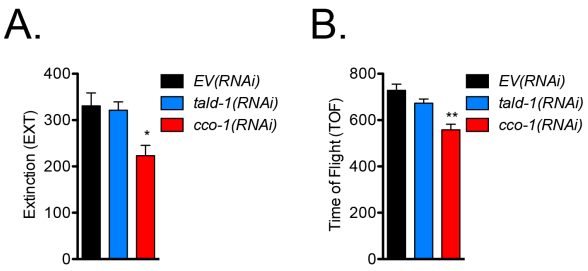

Supplemental Figure 3.4. Length and density of *tald-1(RNAi)* and *cco-1(RNAi)* animals.

RNAi knockdown of *cco-1*, but not *tald-1* reduces the **(A)** extinction coefficient and **(B)** time of flight of *C. elegans*. N2 animals were grown on RNAi bacteria for 3 days from hatching, washed off plates, and analyzed using the COPAS BIOSORT. In this figure, statistics are displayed as: * $p<0.05$**,** ** $p<0.01$, *** $p<0.001$.

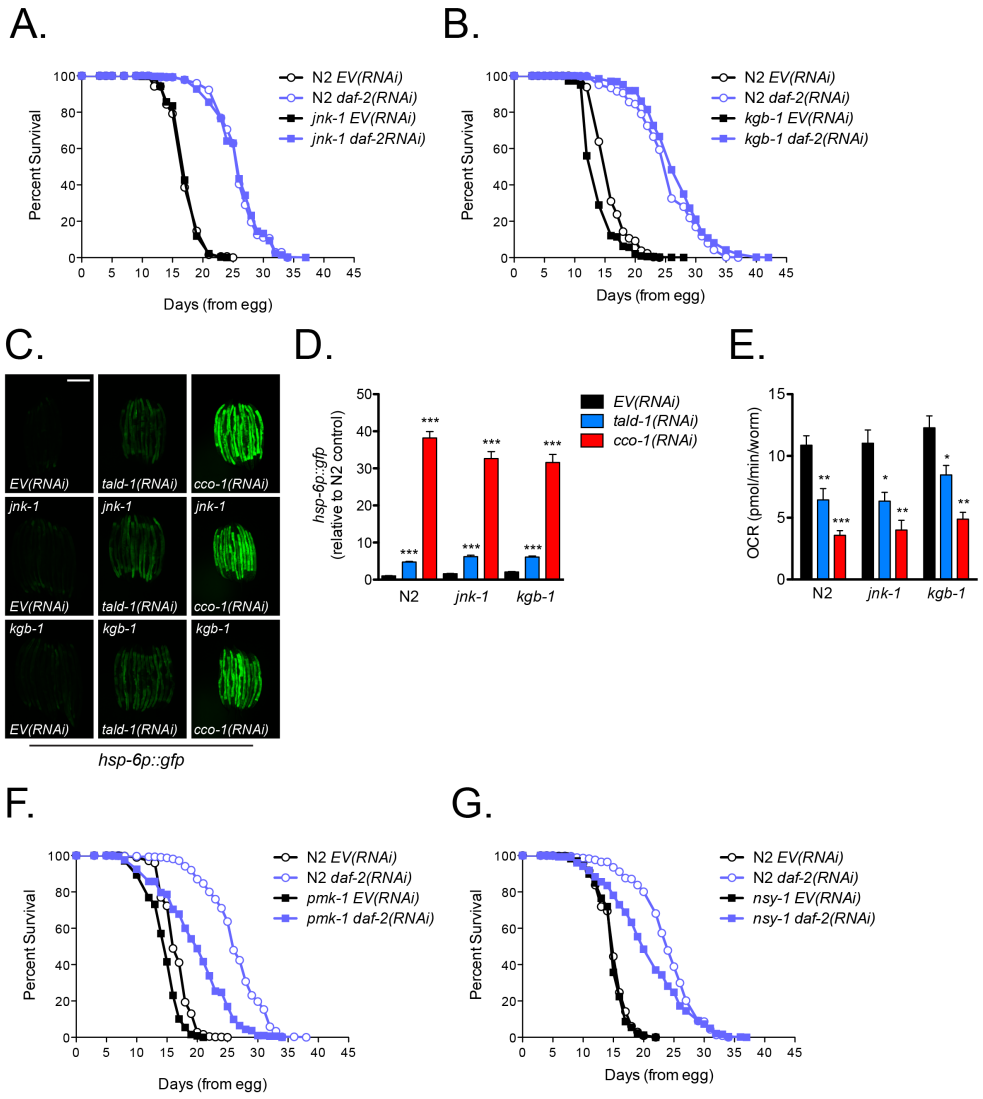

Supplemental Figure 3.5. JNK MAPKs do not alter mitochondrial dysfunction from *tald-1(RNAi)* or *cco-1(RNAi)* and are not required for *daf-2(RNAi)* longevity; NSY-1/PMK-1 is required for *daf-2(RNAi)* longevity.

(A) JNK-1 is not required for *daf-2(RNAi)* lifespan extension. N2 fed *EV(RNAi)* (mean 17.4±0.1 days, n=313), N2 fed *daf-2 (RNAi)* (mean 26.1±0.2 days, n=272), *jnk-1(gk7)* fed *EV(RNAi)* (mean 17.6±0.1 days, n=363), *jnk-1(gk7)* fed *daf-2(RNAi)* (mean 26±0.2 days, n=332). Lifespans were performed at 25°C, with pooled data from three independent experiments shown. **(B)** KGB-1 is not required for *daf-2(RNAi)* lifespan extension. N2 fed *EV(RNAi)* (mean 15±0.1 days, n=630), N2 fed *daf-2 (RNAi)* (mean 23.4±0.2 days, n=633), *kgb-1(um3)* fed *EV(RNAi)* (mean 13.1±0.1 days, n=580), *kgb-1(um3)* fed *daf-2(RNAi)* (mean 25.5±0.2 days, n=563). Lifespans were performed at 25°C, with pooled data from four independent experiments shown. **(C)** *hsp-6p::gfp* reporter induction in *tald-1(RNAi)* or *cco-1(RNAi)* animals is not prevented from *jnk-1(gk7) and kgb-1(um3)* mutations. Scale bar, 200 µm. **(D)** Mean relative fluorescence of *hsp-6p::gfp* reporter animals. Fluorescence is calculated relative to N2 *EV(RNAi)* controls (N = 2 independent experiments, pooled individual worm values, error bars indicate s.e.m., student's t-test with Bonferroni's correction). **(E)** Oxygen consumption rate decreases independent of JNK-1 and KGB-1 from *tald-1(RNAi)* or *cco-1(RNAi)*. OCR was measured using the Seahorse XF Analyzer and normalized to animal number (N = 6 independent experiments for N2 animals, N = 4 independent experiments for *jnk-1(gk7)* and *kgb-1(um3)* animals, error bars indicate s.e.m., student's t-test with Bonferroni's correction). **(F)** PMK-1 is partially required for

daf-2(RNAi) lifespan extension. N2 fed *EV(RNAi)* (mean 16.7±0.1 days, n=423), N2 fed *daf-2 (RNAi)* (mean 26.3±0.3 days, n=325), *pmk-1(km25)* fed *EV(RNAi)* (mean 14.6±0.1 days, n=385), *pmk-1(km25)* fed *daf-2(RNAi)* (mean 19.8±0.3 days, n=295). Lifespans were performed at 25°C, with pooled data from three independent experiments shown. **(G)** NSY-1 is partially required for *daf-2(RNAi)* lifespan extension. N2 fed *EV(RNAi)* (mean 14.6±0.1 days, n=542), N2 fed *daf-2 (RNAi)* (mean 23.1±0.2 days, n=544), *nsy-1(ag3)* fed *EV(RNAi)* (mean 14.9±0.1 days, n=473), *nsy-1(ag3)* fed *daf-2(RNAi)* (mean 20.7±0.3 days, n=480). Lifespans were performed at 25°C, with pooled data from four independent experiments shown. Lifespans in this figure are indicated as mean±s.e.m. and statistical analysis is provided in **Supplemental Table 3.1**. In this figure, statistics are displayed as: * $p<0.05$**,** ** $p<0.01$, *** $p<0.001$.

A.

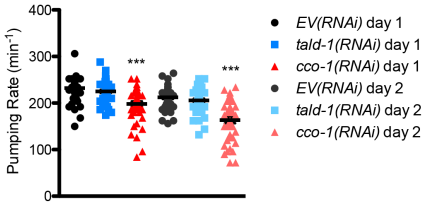

Supplemental Figure 3.6. RNAi knockdown of *cco-1*, but not *tald-1* reduces pharyngeal pumping rate in young animals.

(A) Pumping rate per minute was measured for individual animals, with each dot representing an individual (N=3 independent experiments, error bars indicate s.e.m., student's t-test with Bonferroni's correction). In this figure, statistics are displayed as: * $p<0.05$**,** ** $p<0.01$, *** $p<0.001$.

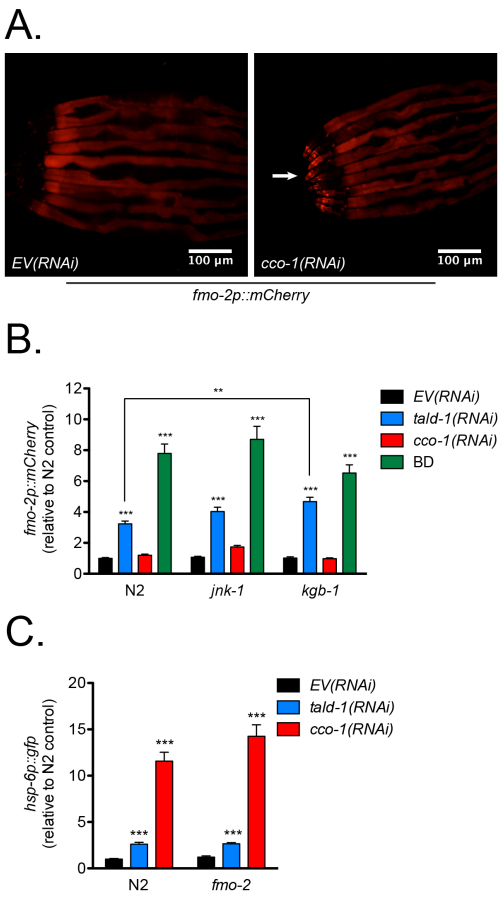

Supplemental Figure 3.7. JNK-1 and KGB-1 are not required for *fmo-2* reporter induction and FMO-2 is not required for *hsp-6* reporter induction.

(A) RNAi knockdown of *cco-1* increases *fmo-2p::mCherry* reporter induction in cells proximal to the anterior bulb. *fmo-2p::mCherry* reporter animals were grown on RNAi bacteria from hatching and imaged 4 days later using fluorescent microscopy. **(B)** Mean relative fluorescence of *fmo-2p::mCherry* reporter animals in the context of *jnk-1(gk7)* and *kgb-1(um3)* mutations. Fluorescence is calculated relative to N2 *EV(RNAi)* controls (N = 3 independent experiments, pooled individual worm values, error bars indicate s.e.m., ANOVA with Bonferroni's post-hoc). **(C)** Mean relative fluorescence of *hsp-6p::gfp* reporter animals in the context of the *fmo-2(ok2147)* mutation. Fluorescence is calculated relative to N2 *EV(RNAi)* controls (N = 3 independent experiments, pooled individual worm values, error bars indicate s.e.m., student's t-test with Bonferroni's correction). In this figure, statistics are displayed as: * $p<0.05$**,** ** $p<0.01$, *** $p<0.001$.

Supplemental Table 3.1. Lifespan data and statistical analyses.

This table is attached to the thesis as Supplemental File 1. *P*-values are shown for condition comparison* or genotype to N2 comparison** and calculated using Wilcoxon Rank-Sum test.

Supplemental Table 3.2. qRT-PCR primer list

Sequence Name	Gene Name	Forward sequence	Reverse sequence
Y48G9A.10	*cpt-3*	GTTGGCGAAAATCGTCTCCG	AGGAAGAATTTCCGGCGGTT
K11D12.4	*cpt-4*	CGCACCTCCACAGCTATCTT	TGAATGCTTCGTCCCTCGTT
F28F8.2	*acs-2*	TGTGAAGGGTGGTGAGAACG	GCGCAGATGTTCTCTCCGTA
F41C3.3	*acs-11*	TCCGATCCTTCGAAGCTCCT	GAGCAGCTGTATCGGTCGTT
C55B7.4	*acdh-1*	GGAATCCGAGCTTCATCCACT	ATCGAAACAACCCTGAGCCA
C17C3.12	*acdh-2*	TTGATCCGGCGATTGCATTG	CAACTTCCGAAAGTGCGAAGG
R09B5.6	*hacd-1*	CAATGGCGATTGAGGCTGTG	CGAATAGTGCCGGGTTCTGA
F10D2.9	*fat-7*	CGCAGCCATTGGACTTTACG	GCTCCAGCTGTGATACCGAA
C05E4.9	*icl-1*	GAAATCCTTTCGCTCACCGC	GGAAGCGAAGAGCATCTGGT
C32D5.9	*lgg-1*	ACCATGACCACAATGGGACAA	TTCGTCACTGTAGGCGATGT
T12G3.1	*sqst-1*	AGAACTGTTCCCATCGGCTG	GTAGGGCTGTTGGACGAAGG
C03B1.12	*lmp-1*	CAACGGAGTCCGCAACAATC	CGTAACGGGCAGATTGTCCT
F49C12.13	*vha-17*	CCGCCTTCTGGGCTATCATT	TGAAGGAACACCATGATCCAGA
K08C7.5	*fmo-2*	TTTCTGGCACCGTTCCAAGT	TGTTCCCAGTGGCTACTTCC
MTCE.11	*nd-1/nduo-1*	AGCGTCATTTATTGGGAAGAA	AAGCTTGTGCTAATCCCATAA
T04C12.4	*act-3*	TGCGACATTGATATCCGTAAGG	GGTGGTTCTCCGGAAAGAA

Chapter 4. PERSPECTIVES AND CONCLUSIONS

The aging field has grown tremendously over the past two decades spurring novel discoveries at unprecedented rates. This has led to a greater understanding of the genetic pathways that influence longevity and an increased appreciation for mitochondria. These organelles are increasingly linked to numerous ailments from cancer to neurodegenerative disease, and their dysfunction is correlated with the aging process. Mitochondrial homeostasis is essential for cellular health since mitochondria regulate energy metabolism and biosynthesis of various metabolites including iron-sulfur clusters, phospholipids, nucleotides, and even acetyl groups for chromatin dynamics. Perhaps just as notable is their impact on various signaling pathways that control stress resistance, cell growth, cell survival, and apoptosis. Due to this and the beneficial effects of low-levels of mitochondrial stress on longevity, the aging field has been focused on examining mitochondrial-signaling networks.

In this thesis, I uncovered additional regulatory mechanisms of the UPR^{mt} through two genome-wide RNAi screens (Chapter 2, Appendix A). I established that the UPR^{mt} is activated by multiple mitochondrial insults, several that are pro-longevity, but surprisingly, is not required or sufficient for lifespan extension in *C. elegans*. Furthermore, I find that inhibition of the pentose phosphate pathway, by RNAi knockdown of the enzyme transaldolase, causes induction of the UPR^{mt}, decreases mitochondrial respiration, and increases lifespan through non-UPR^{mt} dependent mechanisms involving the JNK MAPK and TFEB/HLH-30 pathways. Some of the current questions in the mitochondrial and aging fields are 1) how is the UPR^{mt} regulated and 2) if not the UPR^{mt}, what genetic pathways control mitochondrial longevity in *C. elegans* and other organisms? In this section I will speculate on how findings in this thesis address these fundamental questions.

4.1 THE UPR^{MT} IS ACTIVATED BY DISTINCT PERTURBATIONS

The types of mitochondrial insults that cause UPR^{mt} induction are distinct from other mitochondrial quality control pathways. Mitochondrial uncouplers that are often used to induce mitophagy, for example, do not activate the UPR^{mt} in worms [67]. Similarly, in mammalian cells decreased membrane potential is not required for UPR^{mt} induction even though many treatments (i.e. respiratory chain inhibitors) which activate the response also lower membrane potential [77]. The role of mitochondrial ROS in UPR^{mt} induction is also not unambiguous. The free-radical generator paraquat activates the UPR^{mt} in a manner dependent on ROS (the antioxidant N-acetyl cysteine blunts this effect) [83]. Mitochondrial ROS is therefore sufficient for UPR^{mt} induction. However, antioxidant treatment does not prevent UPR^{mt} chaperone induction from *clk-1* or *isp-1* mutations in worms, but instead exacerbates it due to inhibition of GCN-2 [89]. Thus, the UPR^{mt} is intertwined with functional parameters of mitochondria such as membrane potential and ROS production, but its signaling is not dependent on these parameters.

The UPR^{mt} responds to a distinct type of folding stress within the mitochondria that results from a buildup of unassembled hetero-oligomeric complex subunits or mismatched stoichiometry. Supporting this, knockdown of mitochondrial genes that assemble into hetero-oligomeric complexes activates the UPR^{mt}, whereas knockdown of genes that form homo-oligomeric complexes does not [67]. The genome-wide RNAi screen discussed in Chapter 2 also favors this model. I identify numerous negative regulators of the UPR^{mt} including subunits of the ETC and proteins involved in mitochondrial translation that function to synthesize mitochondrial-encoded ETC subunits. This screen also uncovers multiple factors that either assemble into hetero-oligomeric complexes or impact the stability of the ETC. One class of positive hits was metabolic enzymes that function in hetero-oligomeric complexes such as a

subunit of pyruvate dehydrogenase (C04C3.3), a subunit of 2-oxoglutarate dehydrogenase (W02F12.5), an enoyl-CoA hydratase (*ech-6*) that forms the trifunctional β-oxidation protein complex, and a subunit in the 3-methylcrotonyl-CoA carboxylase, a biotin-requiring enzyme that functions in branched-chain amino acid degradation. Another class of hits were factors that directly influence ETC subunit synthesis, assembly, or stability such as the SUV3 helicase (C08F8.2) that facilitates processing of polycistronic mitochondrial transcripts, the pentatricopeptide repeat domain protein 3 (PTCD3/Y110A7A.19) that associates with the small subunit of the mitochondrial ribosome, the holocytochrome c synthase (*cchl-1*) that attaches heme to cytochrome c, a cytochrome c oxidase assembly protein (*sco-1*), and the apoptosis-inducing factor (*wah-1*) and evolutionarily-conserved signaling intermediate in toll pathway (ECSIT/Y17G9B.5) that both regulate Complex I levels. Understanding how these factors, and others – there was a subset of hits that lack clear homology - affect ETC function will be of interest to the mitochondrial field.

Findings from my screen (Chapter 2) and from Yoneda et al. [67] reinforce the model that the UPR^{mt} is induced by specific genetic perturbations that target mitochondrial proteins that are either 1) subunits of the ETC, 2) assembly factors of the ETC, 3) components of the mitochondrial translation machinery, 4) components of hetero-oligomeric protein complexes, or 5) proteins that regulate mitochondrial RNA processing, stability, or translation. Conceivably, targeting any of these factors or processes should affect ETC formation and increase the unfolded protein load within the mitochondria. Furthermore, the buildup of unstable polypeptides appears to be the initial event that triggers the UPR^{mt} since ROS and lowered membrane potential are not required for the response. Certain proteins such as CLPP-1 (required for UPR^{mt} induction in worms) that interact with unfolded polypeptides are candidate sensor

molecules that relay information regarding the protein-folding environment in the mitochondria to the rest of the cell. Further characterization of these sensor mechanisms will be of particular importance since it will help clarify how mitochondria sense protein-folding stress and also could provide an avenue for therapeutic targeting of mitochondrial responses.

4.2 THE UPR^{MT} DOES NOT REGULATE LONGEVITY IN *C. ELEGANS*

The view in the aging field for years has been that the UPR^{mt} is causal for longevity downstream of mitochondrial dysfunction. Recent publications continue to propagate this model without strong experimental evidence. The UPR^{mt} is a conserved response that is critical for the maintenance of mitochondrial function in the face of proteotoxic stress. However, this does not warrant its role in mitochondrial longevity. Robust genetic evidence is necessary to convincingly argue this. In this section, I will discuss the current evidence for UPR^{mt} longevity and summarize my findings that contradict this model.

The initial publication by Durieux et al. [142] demonstrated that knockdown of the UPR^{mt} factor *ubl-5* reduces the long lifespan of *isp-1(qm150)* worms. However, it was not shown whether *ubl-5(RNAi)* attenuates UPR^{mt} induction in *isp-1(qm150)* worms, complicating interpretation. In fact, I observe that *ubl-5(RNAi)* fails to affect *hsp-6p::gfp* reporter induction in *isp-1(qm150)* worms, indicating that their experimental approach is flawed. In another publication Houtkooper et al. [143] find that *ubl-5(RNAi)* or *haf-1(RNAi)* partially suppress the lifespan extension and *hsp-6p::gfp* induction from *mrps-5(RNAi)* or *cco-1(RNAi)*. However, this result is slightly convoluted since a 10-fold+ induction of the *hsp-6p::gfp* reporter occurs in the context of *ubl-5(RNAi)* or *haf-1(RNAi)*, suggesting these RNAi clones may limit lifespan independent of UPR^{mt} induction. Notably both of these studies hinge on *ubl-5* or *haf-1* being

critical for UPR^{mt} induction, which is not the case [21, 82]. In a similar approach, my experiments employ *atfs-1*, a canonical UPR^{mt} gene that is essential for the response in *C. elegans*. I find that loss of function in *atfs-1* does not prevent the lifespan extension from ETC RNAi or mutation, despite abrogating induction of the *hsp-6p::gfp* reporter and other UPR^{mt} target genes. I also find that constitutive active alleles of *atfs-1* that cause UPR^{mt} induction fail to extend lifespan. These results complicate the UPR^{mt} longevity model, but important points and criticisms can be applied to my work as well. Firstly, I utilize the *atfs-1(tm4525)* mutant to perform the majority of lifespan epistasis analysis. This allele causes a frame shift in *atfs-1* and is frequently used since it prevents UPR^{mt} induction and does not produce ATFS-1 protein [21]. However, *atfs-1(tm4525)* worms appear phenotypically wild-type, whereas the *atfs-1(tm4919)* and *atfs-1(gk3094)* deletion alleles are slow growing. The reasons for this are unclear, but one possibility is the *atfs-1(tm4525)* allele does not prevent expression of short isoforms of *atfs-1* (*atfs-1d.1*, *atfs-1d.2*) that lack a mitochondrial targeting sequence but still contain a basic leucine zipper domain. In contrast, the larger *atfs-1(gk3094)* mutation affects the 5' UTR of *atfs-1* d isoforms and perhaps their expression. Regardless, in my hands *cco-1(RNAi)* extends the lifespan of both *atfs-1(tm4919)* and *atfs-1(gk3094)* mutants. This also agrees with Ren et al. [164] who published that the *atfs-1(gk3094)* allele does not affect mitochondrial longevity. Double RNAi experiments recently published by the Dillin lab also acknowledge that *atfs-1* is not fully required for mitochondrial longevity [158]. Furthermore, I find that *atfs-1(RNAi)*, which should target all isoforms of *atfs-1* (RNAi clone expresses complete *atfs-1* ORF), fully blocks UPR^{mt} induction in *isp-1(qm150)* animals, but does not prevent lifespan extension. Thus, multiple points of evidence firmly establish that ATFS-1-mediated chaperone induction is not required for mitochondrial longevity. Secondly, I use *atfs-1* constitutive active alleles to demonstrate that the

UPR^{mt} is not sufficient for lifespan extension. One could argue that preventing ATFS-1 localization to the mitochondria (through point mutations in the MTS) causes mitochondrial defects that mask the positive effects of chaperone induction. Accordingly, loss of the mitochondrial ATFS-1 does decrease levels of assembled ETC complexes and mitochondrial respiration in the context of mitochondrial stress [70]. To address this criticism one could express the constitutive nuclear *atfs-1* allele in the background of wild-type *atfs-1*, but this too may cause excessive negative regulation of nuclear-encoded ETC subunits that could lead to stoichiometric imbalances and mitochondrial dysfunction.

In conclusion, this thesis and work by others [164] determine that ATFS-1 is not required or sufficient for mitochondrial longevity, uncoupling mitochondrial chaperone induction from lifespan extension. To date, this is the cleanest attempt to address whether the UPR^{mt} is important for longevity in *C. elegans*. Other studies arguing UPR^{mt} longevity do not use proper genetic tools to test the model, complicating interpretation. In addition, the discovery of non-UPR^{mt} mechanisms that regulate mitochondrial longevity such as HIF-1 [106] and the MAPK pathways described in Chapter 3 and by Munkácsy et al. [162] are intriguing and confirm that the UPR^{mt} is not the be-all end-all in mitochondrial longevity.

4.3 Genetic Pathways That Function Independently of the UPR^{MT} Regulate Mitochondrial Longevity

One major question facing the aging field is "how does mitochondrial inhibition extend lifespan?" The UPR^{mt} was one of the first attractive mechanisms since the temporal requirements necessary for UPR^{mt} induction are identical to that of longevity: mitochondrial stress must occur during development [142]. Unfortunately the UPR^{mt} model of longevity is complicated by the

recent finding that ATFS-1 is not required for lifespan extension following mitochondrial stress [82, 164]. The aging field is currently shifting thinking towards other genetic mechanisms (discussed in **Section 1.4**). For example, HIF-1 is a factor that is required for all mitochondrial longevity interventions [106]. The p38 MAPK PMK-3 also acts in a compensatory manner to the UPR^{mt} and regulates longevity from mitochondrial stress in multiple contexts [162]. This response possibly clarifies the association between the UPR^{mt} and longevity that has plagued the literature.

In this thesis, I uncover additional pathways that regulate mitochondrial longevity through the study of the PPP gene transaldolase, a negative regulator of the UPR^{mt} (Chapter 3). Transaldolase deficiency in mice causes hypersensitivity to oxidative stress and consequent JNK MAPK activation. I find that *tald-1(RNAi)* in *C. elegans* elevates cytosolic H_2O_2 and extends lifespan through JNK MAPKs JNK-1 and KGB-1. In a similar fashion, *cco-1(RNAi)* animals also require these JNK MAPKs for long-life, implicating JNK MAPKs in mitochondrial longevity for the first time. This is especially intriguing since *tald-1(RNAi)* and *cco-1(RNAi)* are distinct cellular perturbations and presumably elicit specific cellular responses, despite both causing mitochondrial stress. JNK-1 and KGB-1 appear to function independently of known mitochondrial stress pathways since they are not required for activation of the UPR^{mt} (however, KGB-1 is proposed to negatively regulate the UPR^{mt}) nor the PMK-3 pathway [162]. The regulation of *C. elegans* JNK MAPKs from mitochondrial stress is largely unknown, as are the downstream targets, complicating the study of this pathway. However, the putative upstream MAP3K, NSY-1, is required for both *tald-1(RNAi)* and *cco-1(RNAi)* lifespan extension. This is fascinating as ASK1/NSY-1 activity is fine-tuned by the redox environment in the cytoplasm. A shift towards a more oxidative redox environment stimulates ASK1/NSY-1 to phosphorylate

downstream components of both the p38 and JNK MAPKs. If other MAP3Ks affect JNK-1 and KGB-1 activity during oxidative stress, and which MAP2Ks do, is not known and an important area of future research.

Other genetic experiments in the context of *tald-1(RNAi)* led to my discovery that the TFEB homolog HLH-30 is important for lifespan extension. HLH-30 regulates expression of autophagy genes in addition to the flavin-containing monooxygenase *fmo-2*, which is activated by multiple stressors such as starvation or hypoxia [118]. Interestingly, I find that HLH-30 specifically regulates the lifespan extension from *tald-1(RNAi)* and not *cco-1(RNAi)*. Expression of *fmo-2* is induced in the intestine by *tald-1(RNAi)* (this overlaps with HLH-30 nuclear localization in this tissue); however, *cco-1(RNAi)* specifically activates *fmo-2* expression in cells proximal to the anterior bulb. Thus, intestinal induction of FMO-2 appears to be critical for longevity. From a small-scale screen for *fmo-2* regulators, I find that the p38 MAPK PMK-1 is also required for *tald-1(RNAi)*-mediated *fmo-2* induction and lifespan extension. PMK-1 appears to do this independently of HLH-30 since *pmk-1* deletion does not affect HLH-30 nuclear localization. Thus, multiple longevity pathways appear to impinge on FMO-2. The identification of FMO-2's endogenous substrates and mechanism of longevity control will be important area of future research. In conclusion, I find that JNK MAPKs, PMK-1, HLH-30, and FMO-2 are longevity factors downstream of transaldolase deficiency and mitochondrial stress.

Chapter 5. FUTURE DIRECTIONS

5.1 CHARACTERIZATION OF UPR^{MT} REGULATORY FACTORS AND THEIR ROLES IN LONGEVITY

In Appendix A, I identify 44 novel UPR^{mt} factors that regulate UPR^{mt} induction in the context of a Complex III mutation. Other labs recently identified a large list of UPR^{mt} signaling factors as well, but with limited follow-up. To fully understand UPR^{mt} regulation there needs to be a serious effort to characterize these hits. Positive hits from these screens fall into at least three categories: 1) signaling factors of the UPR^{mt} (such as a transcription factors or sensor molecules), 2) modulators of mitochondrial stress (such as ribosomal proteins), 3) or non-specific hits that affect fluorescent reporter splicing, transcription, or translation in general. Placing putative UPR^{mt} regulators in these categories will establish those that are signaling factors from those that modulate mitochondrial stress. I would predict that genes in the first category will not influence lifespan (similar to *atfs-1*), but those in the second could. One approach is to test specificity of positive hits to mitochondrial function by assaying mitochondrial morphology or respiration in the context of mitochondrial stress. Another approach is to analyze effects of hits on *isp-1* or *clk-1* mutant development; knockdown of factors important for mitochondrial health should delay the development or fecundity of mitochondrial mutants. Also, it will be important to know whether positive hits impact other stress responses or are specific to the UPR^{mt}. Either finding is interesting since cross talk between stress responses is a relatively unexplored area of research and could yield information more pertinent to longevity. Lastly, clarifying the epistatic relationships between positive hits and canonical signaling factors such as ATFS-1, DVE-1, or CLPP-1 will help generate a complete picture of the UPR^{mt} signaling cascade.

5.2 IDENTIFICATION OF TARGETS DOWNSTREAM OF JNK MAPKS

In Chapter 3 I define the role of JNK MAPKs in regulation of mitochondrial longevity in two different contexts: *tald-1(RNAi)* and *cco-1(RNAi)*. A logical area of further investigation is the determination of factors that lie downstream of JNK MAPKs to regulate lifespan. JNK MAPKs phosphorylate a range of substrates in mammalian cells, modulating their activity in positive or negative manners [239]. One class of substrates is transcription factors of the Jun family, which heterodimerize with other bZip transcription factors such as Fos and ATF2 family members generating activator protein 1 (AP-1) [239]. AP-1 controls various cellular processes including cell growth, differentiation, and apoptosis, and in *C. elegans*, controls longevity from intermittent fasting [200]. Preliminary data (**Figure A. 3**) suggests that JUN-1 is required for *tald-1(RNAi)* but not *cco-1(RNAi)* lifespan extension, obscuring any clear model. It is possible that different JNK MAPK substrates are required for either *tald-1(RNAi)* or *cco-1(RNAi)* lifespan extension. Screening additional AP-1 factors for lifespan effects could be helpful to elucidate mechanisms downstream of JNK-1 and KGB-1. Other possible JNK targets (non AP-1 proteins) associated with longevity in *C. elegans* include p53/*cep-1*, HSF1/*hsf-1*, the apoptotic machinery on the mitochondria, and HIF1/*hif-1*, which is positively regulated by JNK MAPKs in mammalian cells [240]. Genetic studies such as these could yield answers to what lies downstream of JNK-1 and KGB-1 in the context of mitochondrial stress, but unbiased approaches may be more productive. Proteomics methods, for example, that measure the abundance of phosphorylated and total proteins (since JNK MAPKs can modulate activity of E3 ligases and thus the levels of numerous proteins) could directly elucidate JNK MAPK targets in *C. elegans*. Defining a mitochondrial stress specific phospho-proteome map would also help

reveal the signaling pathways (MAPK dependent and independent) that are engaged during mitochondrial dysfunction.

APPENDIX A

Identification of positive regulators of the UPR^{mt} in *C. elegans*

Numerous screens have been performed over the years to elucidate signaling factors that regulate the UPR^{mt} in *C. elegans* [46, 81, 83, 84, 86]. This has extended our understanding of UPR^{mt} regulation in worms and also in some cases, mammalian cells. The Ron/Haynes lab identified the first list of canonical UPR^{mt} factors. Using the temperature-sensitive mutation (*zc32*), which conditionally activates the response at 25°C, they identified the mitochondrial protease ClpXP, mitochondrial ABC transporter HAF-1, basic leucine zipper protein ATFS-1, homeobox domain protein DVE-1, and ubiquitin-like protein UBL-5 [46, 80, 81]. Similar RNAi screens were performed by Runkel et al. [83] and Shore et al. [84] using paraquat and antimycin A, respectively, identifying dozens of other factors. However, whether the majority of these factors directly sense and relay information about mitochondrial protein-folding stress is not clear. It is possible that a number of hits non-specifically regulate multi-copy array reporter expression or perhaps attenuate the effects of the mitochondrial insults in these screens, thereby reducing UPR^{mt} signaling. In other words, any mechanistic details underlying these factors' role in UPR^{mt} signaling have not been explored.

To further define the UPR^{mt} pathway, I performed a genome-wide RNAi screen using the long-lived Complex III mutant *isp-1(qm150)* in the *hsp-6p::gfp* reporter background. I chose this strategy since it is specific to a mitochondrial ETC mutation rather than uncharacterized mutations (*zc32*) or exogenous agents that undoubtedly alter bacterial metabolism. Furthermore, since the screen is performed in a long-lived mutant, identified factors could potentially regulate mitochondrial longevity. It is worth noting that when the screen began, a limited number of

UPR^{mt} factors were known (*ubl-5*, *dve-1*, *clpp-1*, *haf-1*, and *atfs-1*). Initially, I identified a total of 145 putative gene knockdowns within the Vidal ORFeome RNAi library (11,511 clones) that attenuated *hsp-6p::gfp* reporter expression in *isp-1(qm150)* animals. To confirm the reproducibility of these observations, RNAi clones were sequence-validated and re-tested across three independent experiments on solid agar plates. If a positive hit was significant in 3/3 experiments, it was considered a validated hit. If a positive hit was significant in 2/3 experiments, it was re-tested and considered genuine if it was significant 3/4 times. In all, 50 hits, 44 which are novel, were confirmed to be bona fide regulators of *hsp-6p::gfp* expression (**Table A. 1, Figure A. 1**). These gene targets function in various cellular processes including cell cycle regulation, pre-mRNA splicing, protein translation, nuclear protein import/export, and vesicle transport (**Table A. 1**).

Table A. 1. 50 positive hits from *isp-1(qm150); hsp-6p::gfp* screen

Information for RNAi hits that attenuated *isp-1(qm150); hsp-6p::gfp* expression including gene name, KOG info, and self-annotated functional category.

Gene	KOG Info	Functional Group
cdk-9	[KOG0669] Cyclin T-dependent kinase CDK9	Cell cycle
cul-1	[KOG2166] Cullins	Cell cycle
mat-1	[KOG1126] DNA-binding cell division cycle control protein	Cell cycle
mag-1	[KOG3392] Exon-exon junction complex, Magoh component	EJC complex; nonsense-mediated decay
rnp-4	[KOG0130] RNA-binding protein RBM8/Tsunagi (RRM superfamily)	EJC complex; nonsense-mediated decay
F32H2.6	[KOG1202] Animal-type fatty acid synthase and related proteins	Fatty acid metabolism
cel-1	[KOG2386] mRNA capping enzyme, guanylyltransferase (alpha) subunit	mRNA capping
F54C8.4	[KOG2386] mRNA capping enzyme, guanylyltransferase (alpha) subunit	mRNA capping
C23G10.8	[LSE1050] Unnamed protein; Serine/arginine repetitive matrix protein 5	mRNA splicing
mfap-1	[KOG1425] Microfibrillar-associated protein MFAP1	mRNA splicing
C30B5.4	[KOG0126] Predicted RNA-binding protein (RRM superfamily)	mRNA splicing; hnRNP; RNA binding protein

T08G11.4	[KOG2730] Methylase	mRNA splicing; methylase of snRNAs & snoRNAs
D1054.14	[KOG2889] Predicted PRP38-like splicing factor	mRNA splicing; miscellaneous splicing factor
icln-1	[KOG3238] Chloride ion current inducer protein	mRNA splicing; negative regulator of snRNP biogenesis; putative ion channel
R08D7.1	[KOG2654] Uncharacterized conserved protein	mRNA splicing; nuclear pre-mRNA retention
dnj-22	[KOG0691] Molecular chaperone (DnaJ superfamily)	mRNA splicing; RNA binding protein; chaperone
R11A8.2	[KOG4315] G-patch nucleic acid binding protein	mRNA splicing; RNA binding protein; MOS2 homolog
rnp-6	[KOG0124] Polypyrimidine tract-binding protein PUF60 (RRM superfamily)	mRNA splicing; RNA binding proteins
sna-2		mRNA splicing; snRNP-binding protein
stip-1		mRNA splicing; spliceosome disassembly
xpo-2	[KOG1992] Nuclear export receptor CSE1/CAS (importin beta superfamily)	Nuclear protein import/export
imb-3	[KOG2171] Karyopherin (importin) beta 3	Nuclear protein import/export
C53H9.2		Protein translation; 60S ribosomal subunit biogenesis
F55B12.4	[KOG2159] tRNA nucleotidyltransferase/poly(A) polymerase	Protein translation; CCA tRNA nucleotidyltransferase 1, mitochondrial
eef-1A.2	[KOG0052] Translation elongation factor EF-1 alpha/Tu	Protein translation; elongation factor
C37C3.2	[KOG2767] Translation initiation factor 5 (eIF-5)	Protein translation; initiation factor
rpl-43	[KOG0402] 60S ribosomal protein L37	Protein translation; ribosomal protein
rps-29	[KOG3506] 40S ribosomal protein S29	Protein translation; ribosomal protein
rps-14	[KOG0407] 40S ribosomal protein S14	Protein translation; ribosomal protein
rps-6	[KOG1646] 40S ribosomal protein S6	Protein translation; ribosomal protein
rps-12	[KOG3406] 40S ribosomal protein S12	Protein translation; ribosomal protein
rps-7	[KOG3320] 40S ribosomal protein S7	Protein translation; ribosomal protein
pars-1	[KOG4163] Prolyl-tRNA synthetase	Protein translation; tRNA synthetase
fars-1	[KOG2784] Phenylalanyl-tRNA synthetase, beta subunit	Protein translation; tRNA synthetase
nrd-1	[KOG0132] RNA polymerase II C-terminal domain-binding protein RA4, contains RPR and RRM domains	Transcription
rpb-5	[KOG3218] RNA polymerase, 25-kDa subunit (common to polymerases I, II and III)	Transcription
spt-5	[KOG1999] RNA polymerase II transcription elongation factor DSIF/SUPT5H/SPT5	Transcription
cir-1	[KOG3794] CBF1-interacting corepressor CIR and related proteins	Transcription; Chromatin modifier
egl-18	[KOG1601] GATA-4/5/6 transcription factors	Transcription; GATA transcription factor
nhr-19	[KOG3575] Hormone receptors	Transcription; Hormone receptor
gei-11	[KOG0049] Transcription factor, Myb superfamily	Transcription; snRNA transcription
snrp-200	Activating signal cointegrator 1 complex subunit 3	Transcription; Transcriptional coactivator

F37C4.4		Unknown
T04D3.1	[LSE0192] Uncharacterized coiled-coil containing protein	Unknown
F01F1.1	[KOG1861] Leucine permease transcriptional regulator	Unknown; LENG8 homolog
Y57G11C.31	[LSE0512] Uncharacterized protein	Unknown; Putative Nucleotide-diphospho-sugar transferase
B0336.3	[KOG2135] Proteins containing the RNA recognition motif	Unknown; RNA binding protein
apg-1	[KOG1062] Vesicle coat complex AP-1, gamma subunit	Vesicle transport
npp-20	[KOG1332] Vesicle coat complex COPII, subunit SEC13	Vesicle transport
sec-24.1	[KOG1984] Vesicle coat complex COPII, subunit SFB3	Vesicle transport

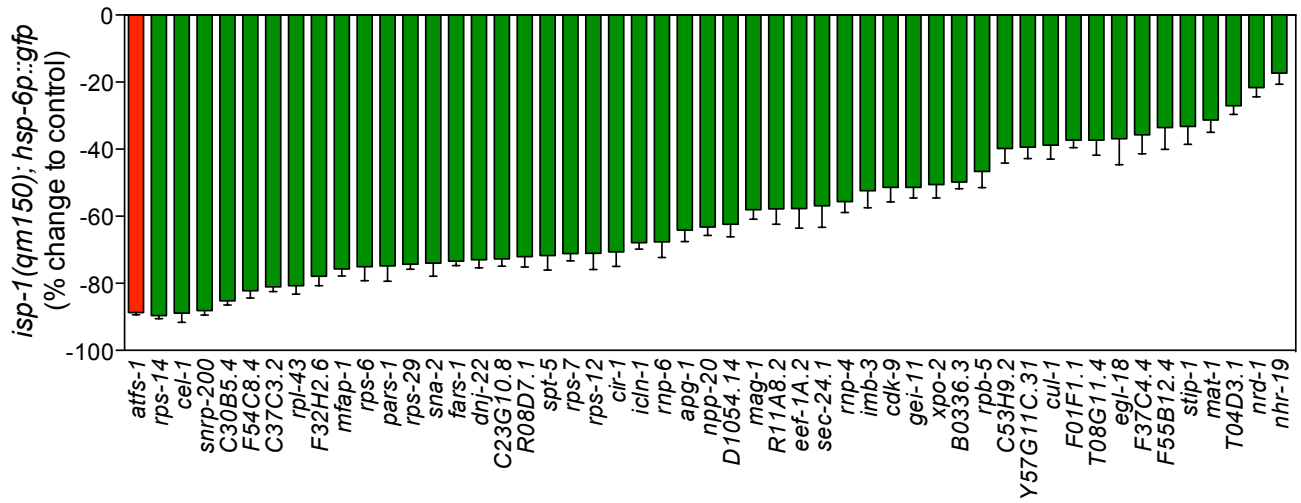

Figure A. 1. RNAi hits that reduce *hsp-6p::gfp* induction in *isp-1(qm150)* animals

hsp-6p::gfp induction was quantified for the 50 RNAi clones hits. Validation included sequencing each RNAi clone and GFP quantification of individual animals grown at 20°C. GFP fluorescence is the % change in mean fluorescence compared to *EV(RNAi)* (N=3-4 independent experiments for each RNAi clone, error bars indicate s.e.m. of pooled worm data).

Surprisingly, I did not detect any of the canonical UPR^{mt} factors as hits such as *atfs-1*, despite using *atfs-1(RNAi)* as a control. Thus, it is safe to assume that multiple false negatives occurred in this screen. This is probably due to the inherent initial screening of fluorescent images that was biased towards RNAi treatments that do not greatly affect growth. Reporter

animals express *hsp-6p::gfp* at the highest levels towards L4/adulthood. Treatments that greatly slow development can appear dim compared to *EV(RNAi)* controls and in this screen were noted (for future reference), but excluded from subsequent validation. Also, slight variability in experimental setup over time could have lead to different thresholds of detection and scoring for a particular experiment, leading to additional false negatives.

In all, this screen was successful and uncovered many novel inducers of the UPR^{mt}. Many of the positive hits also fall into functional categories reported by Runkel et al. [83]. Particular categories of interest include vesicle transport (ER-golgi, plasma membrane), nuclear factors such as *cir-1* or *egl-18*, and RNA binding proteins such as the chaperone *dnj-22*, which is predicted to be mitochondrial [241], or R11A8.2/MOS2 homolog, which is important in the innate immune response of Arabidopsis thaliana [242]. Understanding how these genes control *hsp-6p::gfp* induction and whether they affect expression of other UPR^{mt} targets will be of particular significance. Determining whether they affect *hsp-6p::gfp* expression from multiple forms of mitochondrial stress will also be important.

APPENDIX B

Lifespan epistasis with MAPK pathway factors

In screening for mutants that regulate *tald-1(RNAi)* or *cco-1(RNAi)* longevity, there were cases where a gene mutant did not prevent lifespan extension or did for only one treatment. In this appendix, I report on these factors. The other JNK MAPK in *C. elegans* (aside from JNK-1 and KGB-1) KGB-2 does not prevent lifespan extension from *tald-1(RNAi)* or *cco-1(RNAi)* (tested via *kgb-2(gk361)* mutation) (**Figure A. 2**). There appears to be a small attenuation of lifespan in this background, but more experimental replicates are needed to convincingly argue this. In a search for factors downstream of JNK MAPKs, I tested the effects of *jun-1(gk577)* on lifespan extension from *tald-1(RNAi)* or *cco-1(RNAi)*. Interestingly, JUN-1 is required for *tald-1(RNAi)* but not *cco-1(RNAi)* lifespan extension, complicating interpretation (both treatments require upstream JNK MAPKs) (**Figure A. 3**). The peroxiredoxin PRDX-2 has been implicated in metformin lifespan extension proposed to act through NSY-1/PMK-1 signaling [129]. However, in the case of *tald-1(RNAi)* or *cco-1(RNAi)*, PRDX-2 is not required for lifespan extension (tested via *prdx-2(gk169)* mutation) (**Figure A. 4**). Thus, NSY-1-mediated longevity possibly occurs through other redox sensors such as other peroxiredoxins, thioredoxins, or glutaredoxins.

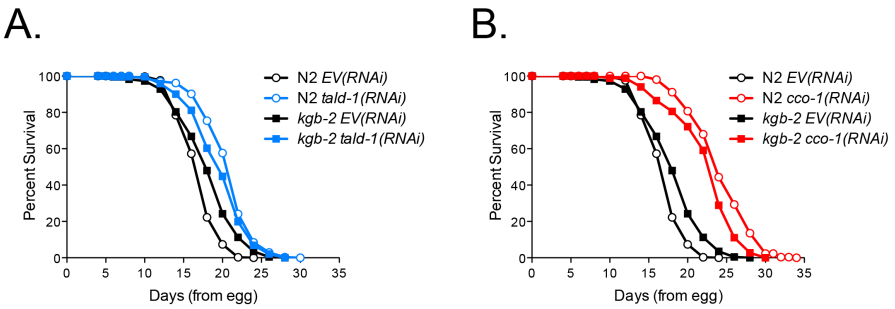

Figure A. 2. KGB-2 is not required for *tald-1(RNAi)* or *cco-1(RNAi)* lifespan extension.

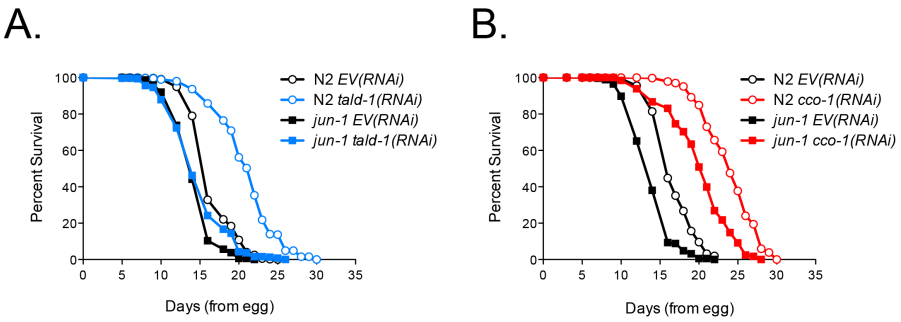

Figure A. 3. JUN-1 is required for *tald-1(RNAi)*, but not *cco-1(RNAi)* lifespan extension.

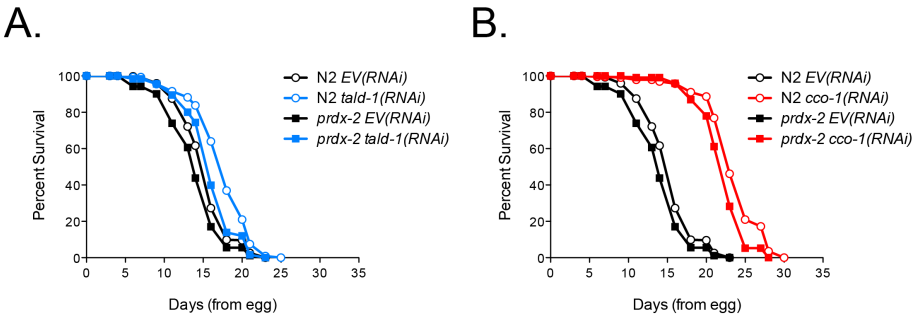

Figure A. 4. PRDX-2 is not required for *tald-1(RNAi)* or *cco-1(RNAi)* lifespan extension.

BIBLIOGRAPHY

1. Bennett CF, Kaeberlein M. The mitochondrial unfolded protein response and increased longevity: cause, consequence, or correlation? Exp Gerontol. 2014;56:142-6. doi: 10.1016/j.exger.2014.02.002. PubMed PMID: 24518875; PubMed Central PMCID: PMCPMC4048780.

2. Dillin A, Hsu AL, Arantes-Oliveira N, Lehrer-Graiwer J, Hsin H, Fraser AG, et al. Rates of behavior and aging specified by mitochondrial function during development. Science. 2002;298(5602):2398-401. doi: 1077780 [pii] 10.1126/science.1077780. PubMed PMID: 12471266.

3. Lee SS, Lee RY, Fraser AG, Kamath RS, Ahringer J, Ruvkun G. A systematic RNAi screen identifies a critical role for mitochondria in C. elegans longevity. Nat Genet. 2003;33(1):40-8. doi: ng1056 [pii] 10.1038/ng1056. PubMed PMID: 12447374.

4. Dolezal P, Likic V, Tachezy J, Lithgow T. Evolution of the molecular machines for protein import into mitochondria. Science. 2006;313(5785):314-8. doi: 10.1126/science.1127895. PubMed PMID: 16857931.

5. Bratic I, Hench J, Trifunovic A. Caenorhabditis elegans as a model system for mtDNA replication defects. Methods. 2010;51(4):437-43. doi: S1046-2023(10)00102-7 [pii] 10.1016/j.ymeth.2010.03.003. PubMed PMID: 20230897.

6. Hamilton B, Dong Y, Shindo M, Liu W, Odell I, Ruvkun G, et al. A systematic RNAi screen for longevity genes in C. elegans. Genes Dev. 2005;19(13):1544-55. doi: 19/13/1544 [pii] 10.1101/gad.1308205. PubMed PMID: 15998808; PubMed Central PMCID: PMCPMC1172061.

7. Hansen M, Hsu AL, Dillin A, Kenyon C. New genes tied to endocrine, metabolic, and dietary regulation of lifespan from a Caenorhabditis elegans genomic RNAi screen. PLoS Genet. 2005;1(1):119-28. doi: 10.1371/journal.pgen.0010017. PubMed PMID: 16103914; PubMed Central PMCID: PMCPMC1183531.

8. Kim Y, Sun H. Functional genomic approach to identify novel genes involved in the regulation of oxidative stress resistance and animal lifespan. Aging Cell. 2007;6(4):489-503. doi: ACE302 [pii]
10.1111/j.1474-9726.2007.00302.x. PubMed PMID: 17608836.

9. Calvo SE, Clauser KR, Mootha VK. MitoCarta2.0: an updated inventory of mammalian mitochondrial proteins. Nucleic Acids Res. 2016;44(D1):D1251-7. doi: 10.1093/nar/gkv1003. PubMed PMID: 26450961; PubMed Central PMCID: PMCPMC4702768.

10. Chacinska A, Koehler CM, Milenkovic D, Lithgow T, Pfanner N. Importing mitochondrial proteins: machineries and mechanisms. Cell. 2009;138(4):628-44. doi: S0092-8674(09)00967-2 [pii]
10.1016/j.cell.2009.08.005. PubMed PMID: 19703392.

11. Kellems RE, Allison VF, Butow RA. Cytoplasmic type 80S ribosomes associated with yeast mitochondria. IV. Attachment of ribosomes to the outer membrane of isolated mitochondria. J Cell Biol. 1975;65(1):1-14. PubMed PMID: 1092698; PubMed Central PMCID: PMCPMC2111154.

12. George R, Walsh P, Beddoe T, Lithgow T. The nascent polypeptide-associated complex (NAC) promotes interaction of ribosomes with the mitochondrial surface in vivo. FEBS Lett. 2002;516(1-3):213-6. PubMed PMID: 11959135.

13. MacKenzie JA, Payne RM. Ribosomes specifically bind to mammalian mitochondria via protease-sensitive proteins on the outer membrane. J Biol Chem. 2004;279(11):9803-10. doi: 10.1074/jbc.M307167200. PubMed PMID: 14668341.

14. Margeot A, Blugeon C, Sylvestre J, Vialette S, Jacq C, Corral-Debrinski M. In Saccharomyces cerevisiae, ATP2 mRNA sorting to the vicinity of mitochondria is essential for respiratory function. EMBO J. 2002;21(24):6893-904. PubMed PMID: 12486010; PubMed Central PMCID: PMCPMC139110.

15. Corral-Debrinski M, Blugeon C, Jacq C. In yeast, the 3' untranslated region or the presequence of ATM1 is required for the exclusive localization of its mRNA to the vicinity of mitochondria. Mol Cell Biol. 2000;20(21):7881-92. PubMed PMID: 11027259; PubMed Central PMCID: PMCPMC86399.

16. Marc P, Margeot A, Devaux F, Blugeon C, Corral-Debrinski M, Jacq C. Genome-wide analysis of mRNAs targeted to yeast mitochondria. EMBO Rep. 2002;3(2):159-64. doi: 10.1093/embo-reports/kvf025. PubMed PMID: 11818335; PubMed Central PMCID: PMCPMC1083966.

17. Williams CC, Jan CH, Weissman JS. Targeting and plasticity of mitochondrial proteins revealed by proximity-specific ribosome profiling. Science. 2014;346(6210):748-51. doi: 10.1126/science.1257522. PubMed PMID: 25378625; PubMed Central PMCID: PMCPMC4263316.

18. Neupert W, Herrmann JM. Translocation of proteins into mitochondria. Annu Rev Biochem. 2007;76:723-49. doi: 10.1146/annurev.biochem.76.052705.163409. PubMed PMID: 17263664.

19. Schmidt O, Pfanner N, Meisinger C. Mitochondrial protein import: from proteomics to functional mechanisms. Nat Rev Mol Cell Biol. 2010;11(9):655-67. doi: nrm2959 [pii] 10.1038/nrm2959. PubMed PMID: 20729931.

20. van der Laan M, Wiedemann N, Mick DU, Guiard B, Rehling P, Pfanner N. A role for Tim21 in membrane-potential-dependent preprotein sorting in mitochondria. Curr Biol. 2006;16(22):2271-6. doi: 10.1016/j.cub.2006.10.025. PubMed PMID: 17113393.

21. Nargund AM, Pellegrino MW, Fiorese CJ, Baker BM, Haynes CM. Mitochondrial import efficiency of ATFS-1 regulates mitochondrial UPR activation. Science. 2012;337(6094):587-90. doi: science.1223560 [pii] 10.1126/science.1223560. PubMed PMID: 22700657.

22. Tatsuta T. Protein quality control in mitochondria. J Biochem. 2009;146(4):455-61. doi: mvp122 [pii] 10.1093/jb/mvp122. PubMed PMID: 19666648.

23. van der Laan M, Chacinska A, Lind M, Perschil I, Sickmann A, Meyer HE, et al. Pam17 is required for architecture and translocation activity of the mitochondrial protein import motor. Mol Cell Biol. 2005;25(17):7449-58. doi: 10.1128/MCB.25.17.7449-7458.2005. PubMed PMID: 16107694; PubMed Central PMCID: PMCPMC1190294.

24. Herrmann JM, Stuart RA, Craig EA, Neupert W. Mitochondrial heat shock protein 70, a molecular chaperone for proteins encoded by mitochondrial DNA. J Cell Biol. 1994;127(4):893-902. PubMed PMID: 7962074; PubMed Central PMCID: PMCPMC2200046.

25. Voos W, Röttgers K. Molecular chaperones as essential mediators of mitochondrial biogenesis. Biochim Biophys Acta. 2002;1592(1):51-62. doi: S0167488902002641 [pii]. PubMed PMID: 12191768.

26. Prip-Buus C, Westerman B, Schmitt M, Langer T, Neupert W, Schwarz E. Role of the mitochondrial DnaJ homologue, Mdj1p, in the prevention of heat-induced protein aggregation. FEBS Lett. 1996;380(1-2):142-6. PubMed PMID: 8603724.

27. Horst M, Oppliger W, Rospert S, Schönfeld HJ, Schatz G, Azem A. Sequential action of two hsp70 complexes during protein import into mitochondria. EMBO J. 1997;16(8):1842-9. doi: 10.1093/emboj/16.8.1842. PubMed PMID: 9155010; PubMed Central PMCID: PMCPMC1169787.

28. Rowley N, Prip-Buus C, Westermann B, Brown C, Schwarz E, Barrell B, et al. Mdj1p, a novel chaperone of the DnaJ family, is involved in mitochondrial biogenesis and protein folding. Cell. 1994;77(2):249-59. PubMed PMID: 8168133.

29. Cheng MY, Hartl FU, Martin J, Pollock RA, Kalousek F, Neupert W, et al. Mitochondrial heat-shock protein hsp60 is essential for assembly of proteins imported into yeast mitochondria. Nature. 1989;337(6208):620-5. doi: 10.1038/337620a0. PubMed PMID: 2645524.

30. Lubben TH, Gatenby AA, Donaldson GK, Lorimer GH, Viitanen PV. Identification of a groES-like chaperonin in mitochondria that facilitates protein folding. Proc Natl Acad Sci U S A. 1990;87(19):7683-7. PubMed PMID: 1977163; PubMed Central PMCID: PMCPMC54812.

31. Rospert S, Junne T, Glick BS, Schatz G. Cloning and disruption of the gene encoding yeast mitochondrial chaperonin 10, the homolog of E. coli groES. FEBS Lett. 1993;335(3):358-60. PubMed PMID: 7903252.

32. Fenton WA, Weissman JS, Horwich AL. Putting a lid on protein folding: structure and function of the co-chaperonin, GroES. Chem Biol. 1996;3(3):157-61. PubMed PMID: 8807841.

33. Martin J, Mayhew M, Langer T, Hartl FU. The reaction cycle of GroEL and GroES in chaperonin-assisted protein folding. Nature. 1993;366(6452):228-33. doi: 10.1038/366228a0. PubMed PMID: 7901770.

34. Ostermann J, Horwich AL, Neupert W, Hartl FU. Protein folding in mitochondria requires complex formation with hsp60 and ATP hydrolysis. Nature. 1989;341(6238):125-30. doi: 10.1038/341125a0. PubMed PMID: 2528694.

35. Heyrovská N, Frydman J, Höhfeld J, Hartl FU. Directionality of polypeptide transfer in the mitochondrial pathway of chaperone-mediated protein folding. Biol Chem. 1998;379(3):301-9. PubMed PMID: 9563826.

36. Manning-Krieg UC, Scherer PE, Schatz G. Sequential action of mitochondrial chaperones in protein import into the matrix. EMBO J. 1991;10(11):3273-80. PubMed PMID: 1915294; PubMed Central PMCID: PMCPMC453052.

37. Böttinger L, Oeljeklaus S, Guiard B, Rospert S, Warscheid B, Becker T. Mitochondrial heat shock protein (Hsp) 70 and Hsp10 cooperate in the formation of Hsp60 complexes. J Biol Chem. 2015;290(18):11611-22. doi: 10.1074/jbc.M115.642017. PubMed PMID: 25792736; PubMed Central PMCID: PMCPMC4416864.

38. Koppen M, Langer T. Protein degradation within mitochondria: versatile activities of AAA proteases and other peptidases. Crit Rev Biochem Mol Biol. 2007;42(3):221-42. doi: 10.1080/10409230701380452. PubMed PMID: 17562452.

39. Gakh O, Cavadini P, Isaya G. Mitochondrial processing peptidases. Biochim Biophys Acta. 2002;1592(1):63-77. PubMed PMID: 12191769.

40. Esser K, Tursun B, Ingenhoven M, Michaelis G, Pratje E. A novel two-step mechanism for removal of a mitochondrial signal sequence involves the mAAA complex and the putative rhomboid protease Pcp1. J Mol Biol. 2002;323(5):835-43. PubMed PMID: 12417197.

41. Naamati A, Regev-Rudzki N, Galperin S, Lill R, Pines O. Dual targeting of Nfs1 and discovery of its novel processing enzyme, Icp55. J Biol Chem. 2009;284(44):30200-8. doi: 10.1074/jbc.M109.034694. PubMed PMID: 19720832; PubMed Central PMCID: PMCPMC2781575.

42. Vögtle FN, Wortelkamp S, Zahedi RP, Becker D, Leidhold C, Gevaert K, et al. Global analysis of the mitochondrial N-proteome identifies a processing peptidase critical for protein stability. Cell. 2009;139(2):428-39. doi: 10.1016/j.cell.2009.07.045. PubMed PMID: 19837041.

43. Vögtle FN, Prinz C, Kellermann J, Lottspeich F, Pfanner N, Meisinger C. Mitochondrial protein turnover: role of the precursor intermediate peptidase Oct1 in protein stabilization. Mol Biol Cell. 2011;22(13):2135-43. doi: 10.1091/mbc.E11-02-0169. PubMed PMID: 21525245; PubMed Central PMCID: PMCPMC3128517.

44. Kang SG, Dimitrova MN, Ortega J, Ginsburg A, Maurizi MR. Human mitochondrial ClpP is a stable heptamer that assembles into a tetradecamer in the presence of ClpX. J Biol Chem. 2005;280(42):35424-32. doi: 10.1074/jbc.M507240200. PubMed PMID: 16115876.

45. Kang SG, Ortega J, Singh SK, Wang N, Huang NN, Steven AC, et al. Functional proteolytic complexes of the human mitochondrial ATP-dependent protease, hClpXP. J Biol Chem. 2002;277(23):21095-102. doi: 10.1074/jbc.M201642200. PubMed PMID: 11923310.

46. Haynes CM, Petrova K, Benedetti C, Yang Y, Ron D. ClpP mediates activation of a mitochondrial unfolded protein response in C. elegans. Dev Cell. 2007;13(4):467-80. doi: S1534-5807(07)00277-8 [pii]

10.1016/j.devcel.2007.07.016. PubMed PMID: 17925224.

47. Zhao Q, Wang J, Levichkin IV, Stasinopoulos S, Ryan MT, Hoogenraad NJ. A mitochondrial specific stress response in mammalian cells. EMBO J. 2002;21(17):4411-9. PubMed PMID: 12198143; PubMed Central PMCID: PMCPMC126185.

48. Bota DA, Davies KJ. Lon protease preferentially degrades oxidized mitochondrial aconitase by an ATP-stimulated mechanism. Nat Cell Biol. 2002;4(9):674-80. doi: 10.1038/ncb836. PubMed PMID: 12198491.

49. Stahlberg H, Kutejová E, Suda K, Wolpensinger B, Lustig A, Schatz G, et al. Mitochondrial Lon of Saccharomyces cerevisiae is a ring-shaped protease with seven flexible subunits. Proc Natl Acad Sci U S A. 1999;96(12):6787-90. PubMed PMID: 10359790; PubMed Central PMCID: PMCPMC21993.

50. Ondrovicová G, Liu T, Singh K, Tian B, Li H, Gakh O, et al. Cleavage site selection within a folded substrate by the ATP-dependent lon protease. J Biol Chem. 2005;280(26):25103-10. doi: 10.1074/jbc.M502796200. PubMed PMID: 15870080.

51. von Janowsky B, Knapp K, Major T, Krayl M, Guiard B, Voos W. Structural properties of substrate proteins determine their proteolysis by the mitochondrial AAA+ protease Pim1. Biol Chem. 2005;386(12):1307-17. doi: 10.1515/BC.2005.149. PubMed PMID: 16336126.

52. Wagner I, Arlt H, van Dyck L, Langer T, Neupert W. Molecular chaperones cooperate with PIM1 protease in the degradation of misfolded proteins in mitochondria. EMBO J. 1994;13(21):5135-45. PubMed PMID: 7957078; PubMed Central PMCID: PMCPMC395461.

53. Savel'ev AS, Novikova LA, Kovaleva IE, Luzikov VN, Neupert W, Langer T. ATP-dependent proteolysis in mitochondria. m-AAA protease and PIM1 protease exert overlapping

substrate specificities and cooperate with the mtHsp70 system. J Biol Chem. 1998;273(32):20596-602. PubMed PMID: 9685417.

54. Leonhard K, Stiegler A, Neupert W, Langer T. Chaperone-like activity of the AAA domain of the yeast Yme1 AAA protease. Nature. 1999;398(6725):348-51. doi: 10.1038/18704. PubMed PMID: 10192337.

55. Korbel D, Wurth S, Käser M, Langer T. Membrane protein turnover by the m-AAA protease in mitochondria depends on the transmembrane domains of its subunits. EMBO Rep. 2004;5(7):698-703. doi: 10.1038/sj.embor.7400186. PubMed PMID: 15205678; PubMed Central PMCID: PMCPMC1299097.

56. Nolden M, Ehses S, Koppen M, Bernacchia A, Rugarli EI, Langer T. The m-AAA protease defective in hereditary spastic paraplegia controls ribosome assembly in mitochondria. Cell. 2005;123(2):277-89. doi: 10.1016/j.cell.2005.08.003. PubMed PMID: 16239145.

57. Leonhard K, Guiard B, Pellecchia G, Tzagoloff A, Neupert W, Langer T. Membrane protein degradation by AAA proteases in mitochondria: extraction of substrates from either membrane surface. Mol Cell. 2000;5(4):629-38. PubMed PMID: 10882099.

58. Tatsuta T, Augustin S, Nolden M, Friedrichs B, Langer T. m-AAA protease-driven membrane dislocation allows intramembrane cleavage by rhomboid in mitochondria. EMBO J. 2007;26(2):325-35. doi: 10.1038/sj.emboj.7601514. PubMed PMID: 17245427; PubMed Central PMCID: PMCPMC1783466.

59. Steglich G, Neupert W, Langer T. Prohibitins regulate membrane protein degradation by the m-AAA protease in mitochondria. Mol Cell Biol. 1999;19(5):3435-42. PubMed PMID: 10207067; PubMed Central PMCID: PMCPMC84136.

60. Greene AW, Grenier K, Aguileta MA, Muise S, Farazifard R, Haque ME, et al. Mitochondrial processing peptidase regulates PINK1 processing, import and Parkin recruitment. EMBO Rep. 2012;13(4):378-85. doi: 10.1038/embor.2012.14. PubMed PMID: 22354088; PubMed Central PMCID: PMCPMC3321149.

61. Mishra P, Carelli V, Manfredi G, Chan DC. Proteolytic cleavage of Opa1 stimulates mitochondrial inner membrane fusion and couples fusion to oxidative phosphorylation. Cell Metab. 2014;19(4):630-41. doi: 10.1016/j.cmet.2014.03.011. PubMed PMID: 24703695; PubMed Central PMCID: PMCPMC4018240.

62. Martinus RD, Garth GP, Webster TL, Cartwright P, Naylor DJ, Høj PB, et al. Selective induction of mitochondrial chaperones in response to loss of the mitochondrial genome. Eur J Biochem. 1996;240(1):98-103. PubMed PMID: 8797841.

63. Liu RY, Corry PM, Lee YJ. Regulation of chemical stress-induced hsp70 gene expression in murine L929 cells. J Cell Sci. 1994;107 (Pt 8):2209-14. PubMed PMID: 7983179.

64. Mosser DD, Duchaine J, Massie B. The DNA-binding activity of the human heat shock transcription factor is regulated in vivo by hsp70. Mol Cell Biol. 1993;13(9):5427-38. PubMed PMID: 8355691; PubMed Central PMCID: PMCPMC360250.

65. Rose MD, Misra LM, Vogel JP. KAR2, a karyogamy gene, is the yeast homolog of the mammalian BiP/GRP78 gene. Cell. 1989;57(7):1211-21. doi: 0092-8674(89)90058-5 [pii]. PubMed PMID: 2661018.

66. Kozutsumi Y, Segal M, Normington K, Gething MJ, Sambrook J. The presence of malfolded proteins in the endoplasmic reticulum signals the induction of glucose-regulated proteins. Nature. 1988;332(6163):462-4. doi: 10.1038/332462a0. PubMed PMID: 3352747.

67. Yoneda T, Benedetti C, Urano F, Clark SG, Harding HP, Ron D. Compartment-specific perturbation of protein handling activates genes encoding mitochondrial chaperones. J Cell Sci. 2004;117(Pt 18):4055-66. doi: jcs.01275 [pii]
10.1242/jcs.01275. PubMed PMID: 15280428.

68. Perisic O, Xiao H, Lis JT. Stable binding of Drosophila heat shock factor to head-to-head and tail-to-tail repeats of a conserved 5 bp recognition unit. Cell. 1989;59(5):797-806. doi: 0092-8674(89)90603-X [pii]. PubMed PMID: 2590940.

69. Shi Y, Mosser DD, Morimoto RI. Molecular chaperones as HSF1-specific transcriptional repressors. Genes Dev. 1998;12(5):654-66. PubMed PMID: 9499401; PubMed Central PMCID: PMCPMC316571.

70. Nargund AM, Fiorese CJ, Pellegrino MW, Deng P, Haynes CM. Mitochondrial and nuclear accumulation of the transcription factor ATFS-1 promotes OXPHOS recovery during the UPR(mt). Mol Cell. 2015;58(1):123-33. doi: 10.1016/j.molcel.2015.02.008. PubMed PMID: 25773600; PubMed Central PMCID: PMCPMC4385436.

71. Horibe T, Hoogenraad NJ. The chop gene contains an element for the positive regulation of the mitochondrial unfolded protein response. PLoS One. 2007;2(9):e835. doi: 10.1371/journal.pone.0000835. PubMed PMID: 17848986; PubMed Central PMCID: PMCPMC1950685.

72. Aldridge JE, Horibe T, Hoogenraad NJ. Discovery of genes activated by the mitochondrial unfolded protein response (mtUPR) and cognate promoter elements. PLoS One. 2007;2(9):e874. doi: 10.1371/journal.pone.0000874. PubMed PMID: 17849004; PubMed Central PMCID: PMCPMC1964532.

73. Münch C, Harper JW. Mitochondrial unfolded protein response controls matrix pre-RNA processing and translation. Nature. 2016;534(7609):710-3. doi: 10.1038/nature18302. PubMed PMID: 27350246; PubMed Central PMCID: PMCPMC4939261.

74. Tyynismaa H, Carroll CJ, Raimundo N, Ahola-Erkkilä S, Wenz T, Ruhanen H, et al. Mitochondrial myopathy induces a starvation-like response. Hum Mol Genet. 2010;19(20):3948-58. doi: 10.1093/hmg/ddq310. PubMed PMID: 20656789.

75. Mancini C, Roncaglia P, Brussino A, Stevanin G, Lo Buono N, Krmac H, et al. Genome-wide expression profiling and functional characterization of SCA28 lymphoblastoid cell lines reveal impairment in cell growth and activation of apoptotic pathways. BMC Med Genomics. 2013;6:22. doi: 10.1186/1755-8794-6-22. PubMed PMID: 23777634; PubMed Central PMCID: PMCPMC3689607.

76. Dogan SA, Pujol C, Maiti P, Kukat A, Wang S, Hermans S, et al. Tissue-specific loss of DARS2 activates stress responses independently of respiratory chain deficiency in the heart. Cell Metab. 2014;19(3):458-69. doi: 10.1016/j.cmet.2014.02.004. PubMed PMID: 24606902.

77. Fiorese CJ, Schulz AM, Lin YF, Rosin N, Pellegrino MW, Haynes CM. The Transcription Factor ATF5 Mediates a Mammalian Mitochondrial UPR. Curr Biol. 2016;26(15):2037-43. doi: 10.1016/j.cub.2016.06.002. PubMed PMID: 27426517; PubMed Central PMCID: PMCPMC4980197.

78. Walter P, Ron D. The unfolded protein response: from stress pathway to homeostatic regulation. Science. 2011;334(6059):1081-6. doi: 10.1126/science.1209038. PubMed PMID: 22116877.

79. Jiang HY, Wek SA, McGrath BC, Lu D, Hai T, Harding HP, et al. Activating transcription factor 3 is integral to the eukaryotic initiation factor 2 kinase stress response. Mol

Cell Biol. 2004;24(3):1365-77. PubMed PMID: 14729979; PubMed Central PMCID: PMCPMC321431.

80. Benedetti C, Haynes CM, Yang Y, Harding HP, Ron D. Ubiquitin-like protein 5 positively regulates chaperone gene expression in the mitochondrial unfolded protein response. Genetics. 2006;174(1):229-39. doi: genetics.106.061580 [pii] 10.1534/genetics.106.061580. PubMed PMID: 16816413; PubMed Central PMCID: PMCPMC1569816.

81. Haynes CM, Yang Y, Blais SP, Neubert TA, Ron D. The matrix peptide exporter HAF-1 signals a mitochondrial UPR by activating the transcription factor ZC376.7 in C. elegans. Mol Cell. 2010;37(4):529-40. doi: S1097-2765(10)00044-4 [pii] 10.1016/j.molcel.2010.01.015. PubMed PMID: 20188671; PubMed Central PMCID: PMCPMC2846537.

82. Bennett CF, Vander Wende H, Simko M, Klum S, Barfield S, Choi H, et al. Activation of the mitochondrial unfolded protein response does not predict longevity in Caenorhabditis elegans. Nat Commun. 2014;5:3483. doi: 10.1038/ncomms4483. PubMed PMID: 24662282; PubMed Central PMCID: PMCPMC3984390.

83. Runkel ED, Liu S, Baumeister R, Schulze E. Surveillance-activated defenses block the ROS-induced mitochondrial unfolded protein response. PLoS Genet. 2013;9(3):e1003346. doi: 10.1371/journal.pgen.1003346. PubMed PMID: 23516373; PubMed Central PMCID: PMCPMC3597513.

84. Shore DE, Carr CE, Ruvkun G. Induction of cytoprotective pathways is central to the extension of lifespan conferred by multiple longevity pathways. PLoS Genet.

2012;8(7):e1002792. doi: 10.1371/journal.pgen.1002792. PubMed PMID: 22829775; PubMed Central PMCID: PMCPMC3400582.

85. Melo JA, Ruvkun G. Inactivation of conserved C. elegans genes engages pathogen- and xenobiotic-associated defenses. Cell. 2012;149(2):452-66. doi: 10.1016/j.cell.2012.02.050. PubMed PMID: 22500807; PubMed Central PMCID: PMCPMC3613046.

86. Liu Y, Samuel BS, Breen PC, Ruvkun G. Caenorhabditis elegans pathways that surveil and defend mitochondria. Nature. 2014;508(7496):406-10. doi: 10.1038/nature13204. PubMed PMID: 24695221; PubMed Central PMCID: PMCPMC4102179.

87. Govindan JA, Jayamani E, Zhang X, Mylonakis E, Ruvkun G. Dialogue between E. coli free radical pathways and the mitochondria of C. elegans. Proc Natl Acad Sci U S A. 2015;112(40):12456-61. doi: 10.1073/pnas.1517448112. PubMed PMID: 26392561; PubMed Central PMCID: PMCPMC4603447.

88. Pellegrino MW, Nargund AM, Kirienko NV, Gillis R, Fiorese CJ, Haynes CM. Mitochondrial UPR-regulated innate immunity provides resistance to pathogen infection. Nature. 2014;516(7531):414-7. doi: 10.1038/nature13818. PubMed PMID: 25274306; PubMed Central PMCID: PMCPMC4270954.

89. Baker BM, Nargund AM, Sun T, Haynes CM. Protective coupling of mitochondrial function and protein synthesis via the eIF2α kinase GCN-2. PLoS Genet. 2012;8(6):e1002760. doi: PGENETICS-D-11-02269 [pii]
10.1371/journal.pgen.1002760. PubMed PMID: 22719267; PubMed Central PMCID: PMCPMC3375257.

90. Holzmann J, Frank P, Löffler E, Bennett KL, Gerner C, Rossmanith W. RNase P without RNA: identification and functional reconstitution of the human mitochondrial tRNA processing enzyme. Cell. 2008;135(3):462-74. doi: 10.1016/j.cell.2008.09.013. PubMed PMID: 18984158.

91. Sanchez MI, Mercer TR, Davies SM, Shearwood AM, Nygård KK, Richman TR, et al. RNA processing in human mitochondria. Cell Cycle. 2011;10(17):2904-16. doi: 10.4161/cc.10.17.17060. PubMed PMID: 21857155.

92. Zhou D, Palam LR, Jiang L, Narasimhan J, Staschke KA, Wek RC. Phosphorylation of eIF2 directs ATF5 translational control in response to diverse stress conditions. J Biol Chem. 2008;283(11):7064-73. doi: 10.1074/jbc.M708530200. PubMed PMID: 18195013.

93. Blais JD, Filipenko V, Bi M, Harding HP, Ron D, Koumenis C, et al. Activating transcription factor 4 is translationally regulated by hypoxic stress. Mol Cell Biol. 2004;24(17):7469-82. doi: 10.1128/MCB.24.17.7469-7482.2004. PubMed PMID: 15314157; PubMed Central PMCID: PMCPMC506979.

94. Teske BF, Fusakio ME, Zhou D, Shan J, McClintick JN, Kilberg MS, et al. CHOP induces activating transcription factor 5 (ATF5) to trigger apoptosis in response to perturbations in protein homeostasis. Mol Biol Cell. 2013;24(15):2477-90. doi: 10.1091/mbc.E13-01-0067. PubMed PMID: 23761072; PubMed Central PMCID: PMCPMC3727939.

95. Yang W, Hekimi S. Two modes of mitochondrial dysfunction lead independently to lifespan extension in Caenorhabditis elegans. Aging Cell. 2010;9(3):433-47. doi: 10.1111/j.1474-9726.2010.00571.x. PubMed PMID: 20346072.

96. de Jong L, Meng Y, Dent J, Hekimi S. Thiamine pyrophosphate biosynthesis and transport in the nematode Caenorhabditis elegans. Genetics. 2004;168(2):845-54. doi:

10.1534/genetics.104.028605. PubMed PMID: 15514058; PubMed Central PMCID: PMCPMC1448845.

97. Felkai S, Ewbank JJ, Lemieux J, Labbé JC, Brown GG, Hekimi S. CLK-1 controls respiration, behavior and aging in the nematode Caenorhabditis elegans. EMBO J. 1999;18(7):1783-92. doi: 10.1093/emboj/18.7.1783. PubMed PMID: 10202142; PubMed Central PMCID: PMCPMC1171264.

98. Feng J, Bussière F, Hekimi S. Mitochondrial electron transport is a key determinant of life span in Caenorhabditis elegans. Dev Cell. 2001;1(5):633-44. doi: S1534-5807(01)00071-5 [pii]. PubMed PMID: 11709184.

99. Lakowski B, Hekimi S. Determination of life-span in Caenorhabditis elegans by four clock genes. Science. 1996;272(5264):1010-3. PubMed PMID: 8638122.

100. Kirchman PA, Kim S, Lai CY, Jazwinski SM. Interorganelle signaling is a determinant of longevity in Saccharomyces cerevisiae. Genetics. 1999;152(1):179-90. PubMed PMID: 10224252; PubMed Central PMCID: PMCPMC1460582.

101. Liu X, Jiang N, Hughes B, Bigras E, Shoubridge E, Hekimi S. Evolutionary conservation of the clk-1-dependent mechanism of longevity: loss of mclk1 increases cellular fitness and lifespan in mice. Genes Dev. 2005;19(20):2424-34. doi: gad.1352905 [pii] 10.1101/gad.1352905. PubMed PMID: 16195414; PubMed Central PMCID: PMCPMC1257397.

102. Dell'agnello C, Leo S, Agostino A, Szabadkai G, Tiveron C, Zulian A, et al. Increased longevity and refractoriness to Ca(2+)-dependent neurodegeneration in Surf1 knockout mice. Hum Mol Genet. 2007;16(4):431-44. doi: ddl477 [pii] 10.1093/hmg/ddl477. PubMed PMID: 17210671.

103. Copeland JM, Cho J, Lo T, Hur JH, Bahadorani S, Arabyan T, et al. Extension of Drosophila life span by RNAi of the mitochondrial respiratory chain. Curr Biol. 2009;19(19):1591-8. doi: S0960-9822(09)01586-3 [pii] 10.1016/j.cub.2009.08.016. PubMed PMID: 19747824.

104. Lapointe J, Stepanyan Z, Bigras E, Hekimi S. Reversal of the mitochondrial phenotype and slow development of oxidative biomarkers of aging in long-lived Mclk1+/- mice. J Biol Chem. 2009;284(30):20364-74. doi: M109.006569 [pii] 10.1074/jbc.M109.006569. PubMed PMID: 19478076; PubMed Central PMCID: PMCPMC2740461.

105. Owusu-Ansah E, Song W, Perrimon N. Muscle mitohormesis promotes longevity via systemic repression of insulin signaling. Cell. 2013;155(3):699-712. doi: 10.1016/j.cell.2013.09.021. PubMed PMID: 24243023; PubMed Central PMCID: PMCPMC3856681.

106. Lee SJ, Hwang AB, Kenyon C. Inhibition of respiration extends C. elegans life span via reactive oxygen species that increase HIF-1 activity. Curr Biol. 2010;20(23):2131-6. doi: S0960-9822(10)01374-6 [pii] 10.1016/j.cub.2010.10.057. PubMed PMID: 21093262; PubMed Central PMCID: PMCPMC3058811.

107. Chen D, Thomas EL, Kapahi P. HIF-1 modulates dietary restriction-mediated lifespan extension via IRE-1 in Caenorhabditis elegans. PLoS Genet. 2009;5(5):e1000486. doi: 10.1371/journal.pgen.1000486. PubMed PMID: 19461873; PubMed Central PMCID: PMCPMC2676694.

108. Yang W, Hekimi S. A mitochondrial superoxide signal triggers increased longevity in Caenorhabditis elegans. PLoS Biol. 2010;8(12):e1000556. doi: 10.1371/journal.pbio.1000556. PubMed PMID: 21151885; PubMed Central PMCID: PMCPMC2998438.

109. Hwang AB, Ryu EA, Artan M, Chang HW, Kabir MH, Nam HJ, et al. Feedback regulation via AMPK and HIF-1 mediates ROS-dependent longevity in Caenorhabditis elegans. Proc Natl Acad Sci U S A. 2014;111(42):E4458-67. doi: 10.1073/pnas.1411199111. PubMed PMID: 25288734; PubMed Central PMCID: PMCPMC4210294.

110. Epstein AC, Gleadle JM, McNeill LA, Hewitson KS, O'Rourke J, Mole DR, et al. C. elegans EGL-9 and mammalian homologs define a family of dioxygenases that regulate HIF by prolyl hydroxylation. Cell. 2001;107(1):43-54. doi: S0092-8674(01)00507-4 [pii]. PubMed PMID: 11595184.

111. Bishop T, Lau KW, Epstein AC, Kim SK, Jiang M, O'Rourke D, et al. Genetic analysis of pathways regulated by the von Hippel-Lindau tumor suppressor in Caenorhabditis elegans. PLoS Biol. 2004;2(10):e289. doi: 10.1371/journal.pbio.0020289. PubMed PMID: 15361934; PubMed Central PMCID: PMCPMC515368.

112. Marinho HS, Real C, Cyrne L, Soares H, Antunes F. Hydrogen peroxide sensing, signaling and regulation of transcription factors. Redox Biol. 2014;2:535-62. doi: 10.1016/j.redox.2014.02.006. PubMed PMID: 24634836; PubMed Central PMCID: PMCPMC3953959.

113. Zhang Y, Shao Z, Zhai Z, Shen C, Powell-Coffman JA. The HIF-1 hypoxia-inducible factor modulates lifespan in C. elegans. PLoS One. 2009;4(7):e6348. doi: 10.1371/journal.pone.0006348. PubMed PMID: 19633713; PubMed Central PMCID: PMCPMC2711329.

114. Mehta R, Steinkraus KA, Sutphin GL, Ramos FJ, Shamieh LS, Huh A, et al. Proteasomal regulation of the hypoxic response modulates aging in C. elegans. Science. 2009;324(5931):1196-8. doi: 1173507 [pii]
10.1126/science.1173507. PubMed PMID: 19372390; PubMed Central PMCID: PMCPMC2737476.

115. Müller RU, Fabretti F, Zank S, Burst V, Benzing T, Schermer B. The von Hippel Lindau tumor suppressor limits longevity. J Am Soc Nephrol. 2009;20(12):2513-7. doi: ASN.2009050497 [pii]
10.1681/ASN.2009050497. PubMed PMID: 19797165; PubMed Central PMCID: PMCPMC2794223.

116. Denko NC. Hypoxia, HIF1 and glucose metabolism in the solid tumour. Nat Rev Cancer. 2008;8(9):705-13. doi: 10.1038/nrc2468. PubMed PMID: 19143055.

117. Semenza GL. HIF-1: upstream and downstream of cancer metabolism. Curr Opin Genet Dev. 2010;20(1):51-6. doi: 10.1016/j.gde.2009.10.009. PubMed PMID: 19942427; PubMed Central PMCID: PMCPMC2822127.

118. Leiser SF, Miller H, Rossner R, Fletcher M, Leonard A, Primitivo M, et al. Cell nonautonomous activation of flavin-containing monooxygenase promotes longevity and health span. Science. 2015;350(6266):1375-8. doi: 10.1126/science.aac9257. PubMed PMID: 26586189.

119. Van Raamsdonk JM, Hekimi S. Deletion of the mitochondrial superoxide dismutase sod-2 extends lifespan in Caenorhabditis elegans. PLoS Genet. 2009;5(2):e1000361. doi: 10.1371/journal.pgen.1000361. PubMed PMID: 19197346; PubMed Central PMCID: PMCPMC2628729.

120. Pan Y. Mitochondria, reactive oxygen species, and chronological aging: a message from yeast. Exp Gerontol. 2011;46(11):847-52. doi: 10.1016/j.exger.2011.08.007. PubMed PMID: 21884780.

121. Ristow M, Schmeisser S. Extending life span by increasing oxidative stress. Free Radic Biol Med. 2011;51(2):327-36. doi: 10.1016/j.freeradbiomed.2011.05.010. PubMed PMID: 21619928.

122. Ristow M, Zarse K. How increased oxidative stress promotes longevity and metabolic health: The concept of mitochondrial hormesis (mitohormesis). Exp Gerontol. 2010;45(6):410-8. doi: 10.1016/j.exger.2010.03.014. PubMed PMID: 20350594.

123. Schulz TJ, Zarse K, Voigt A, Urban N, Birringer M, Ristow M. Glucose restriction extends Caenorhabditis elegans life span by inducing mitochondrial respiration and increasing oxidative stress. Cell Metab. 2007;6(4):280-93. doi: 10.1016/j.cmet.2007.08.011. PubMed PMID: 17908557.

124. Zarse K, Schmeisser S, Groth M, Priebe S, Beuster G, Kuhlow D, et al. Impaired insulin/IGF1 signaling extends life span by promoting mitochondrial L-proline catabolism to induce a transient ROS signal. Cell Metab. 2012;15(4):451-65. doi: 10.1016/j.cmet.2012.02.013. PubMed PMID: 22482728.

125. Dingley S, Polyak E, Lightfoot R, Ostrovsky J, Rao M, Greco T, et al. Mitochondrial respiratory chain dysfunction variably increases oxidant stress in Caenorhabditis elegans. Mitochondrion. 2010;10(2):125-36. doi: 10.1016/j.mito.2009.11.003. PubMed PMID: 19900588; PubMed Central PMCID: PMCPMC3638869.

126. Rea SL, Ventura N, Johnson TE. Relationship between mitochondrial electron transport chain dysfunction, development, and life extension in Caenorhabditis elegans. PLoS Biol. 2007;5(10):e259. doi: 06-PLBI-RA-2325 [pii] 10.1371/journal.pbio.0050259. PubMed PMID: 17914900; PubMed Central PMCID: PMCPMC1994989.

127. Tullet JM, Hertweck M, An JH, Baker J, Hwang JY, Liu S, et al. Direct inhibition of the longevity-promoting factor SKN-1 by insulin-like signaling in C. elegans. Cell. 2008;132(6):1025-38. doi: 10.1016/j.cell.2008.01.030. PubMed PMID: 18358814; PubMed Central PMCID: PMCPMC2367249.

128. Curtis R, O'Connor G, DiStefano PS. Aging networks in Caenorhabditis elegans: AMP-activated protein kinase (aak-2) links multiple aging and metabolism pathways. Aging Cell. 2006;5(2):119-26. doi: 10.1111/j.1474-9726.2006.00205.x. PubMed PMID: 16626391.

129. De Haes W, Frooninckx L, Van Assche R, Smolders A, Depuydt G, Billen J, et al. Metformin promotes lifespan through mitohormesis via the peroxiredoxin PRDX-2. Proc Natl Acad Sci U S A. 2014;111(24):E2501-9. doi: 10.1073/pnas.1321776111. PubMed PMID: 24889636; PubMed Central PMCID: PMCPMC4066537.

130. Schmeisser S, Priebe S, Groth M, Monajembashi S, Hemmerich P, Guthke R, et al. Neuronal ROS signaling rather than AMPK/sirtuin-mediated energy sensing links dietary restriction to lifespan extension. Mol Metab. 2013;2(2):92-102. doi: 10.1016/j.molmet.2013.02.002. PubMed PMID: 24199155; PubMed Central PMCID: PMCPMC3817383.

131. Inoue H, Hisamoto N, An JH, Oliveira RP, Nishida E, Blackwell TK, et al. The C. elegans p38 MAPK pathway regulates nuclear localization of the transcription factor SKN-1 in

oxidative stress response. Genes Dev. 2005;19(19):2278-83. doi: 10.1101/gad.1324805. PubMed PMID: 16166371; PubMed Central PMCID: PMCPMC1240035.

132. Sykiotis GP, Bohmann D. Keap1/Nrf2 signaling regulates oxidative stress tolerance and lifespan in Drosophila. Dev Cell. 2008;14(1):76-85. doi: 10.1016/j.devcel.2007.12.002. PubMed PMID: 18194654; PubMed Central PMCID: PMCPMC2257869.

133. D'Autréaux B, Toledano MB. ROS as signalling molecules: mechanisms that generate specificity in ROS homeostasis. Nat Rev Mol Cell Biol. 2007;8(10):813-24. doi: 10.1038/nrm2256. PubMed PMID: 17848967.

134. Oláhová M, Taylor SR, Khazaipoul S, Wang J, Morgan BA, Matsumoto K, et al. A redox-sensitive peroxiredoxin that is important for longevity has tissue- and stress-specific roles in stress resistance. Proc Natl Acad Sci U S A. 2008;105(50):19839-44. doi: 10.1073/pnas.0805507105. PubMed PMID: 19064914; PubMed Central PMCID: PMCPMC2604961.

135. Hall A, Karplus PA, Poole LB. Typical 2-Cys peroxiredoxins--structures, mechanisms and functions. FEBS J. 2009;276(9):2469-77. doi: 10.1111/j.1742-4658.2009.06985.x. PubMed PMID: 19476488; PubMed Central PMCID: PMCPMC2747500.

136. Jarvis RM, Hughes SM, Ledgerwood EC. Peroxiredoxin 1 functions as a signal peroxidase to receive, transduce, and transmit peroxide signals in mammalian cells. Free Radic Biol Med. 2012;53(7):1522-30. doi: 10.1016/j.freeradbiomed.2012.08.001. PubMed PMID: 22902630.

137. Ray PD, Huang BW, Tsuji Y. Reactive oxygen species (ROS) homeostasis and redox regulation in cellular signaling. Cell Signal. 2012;24(5):981-90. doi:

10.1016/j.cellsig.2012.01.008. PubMed PMID: 22286106; PubMed Central PMCID: PMCPMC3454471.

138. Saitoh M, Nishitoh H, Fujii M, Takeda K, Tobiume K, Sawada Y, et al. Mammalian thioredoxin is a direct inhibitor of apoptosis signal-regulating kinase (ASK) 1. EMBO J. 1998;17(9):2596-606. doi: 10.1093/emboj/17.9.2596. PubMed PMID: 9564042; PubMed Central PMCID: PMCPMC1170601.

139. Ichijo H, Nishida E, Irie K, ten Dijke P, Saitoh M, Moriguchi T, et al. Induction of apoptosis by ASK1, a mammalian MAPKKK that activates SAPK/JNK and p38 signaling pathways. Science. 1997;275(5296):90-4. PubMed PMID: 8974401.

140. Tobiume K, Matsuzawa A, Takahashi T, Nishitoh H, Morita K, Takeda K, et al. ASK1 is required for sustained activations of JNK/p38 MAP kinases and apoptosis. EMBO Rep. 2001;2(3):222-8. doi: 10.1093/embo-reports/kve046. PubMed PMID: 11266364; PubMed Central PMCID: PMCPMC1083842.

141. Picard M, Zhang J, Hancock S, Derbeneva O, Golhar R, Golik P, et al. Progressive increase in mtDNA 3243A>G heteroplasmy causes abrupt transcriptional reprogramming. Proc Natl Acad Sci U S A. 2014;111(38):E4033-42. doi: 10.1073/pnas.1414028111. PubMed PMID: 25192935; PubMed Central PMCID: PMCPMC4183335.

142. Durieux J, Wolff S, Dillin A. The cell-non-autonomous nature of electron transport chain-mediated longevity. Cell. 2011;144(1):79-91. doi: S0092-8674(10)01434-0 [pii] 10.1016/j.cell.2010.12.016. PubMed PMID: 21215371; PubMed Central PMCID: PMCPMC3062502.

143. Houtkooper RH, Mouchiroud L, Ryu D, Moullan N, Katsyuba E, Knott G, et al. Mitonuclear protein imbalance as a conserved longevity mechanism. Nature.

2013;497(7450):451-7. doi: 10.1038/nature12188. PubMed PMID: 23698443; PubMed Central PMCID: PMCPMC3663447.

144. Arnold I, Langer T. Membrane protein degradation by AAA proteases in mitochondria. Biochim Biophys Acta. 2002;1592(1):89-96. PubMed PMID: 12191771.

145. Merkwirth C, Dargazanli S, Tatsuta T, Geimer S, Löwer B, Wunderlich FT, et al. Prohibitins control cell proliferation and apoptosis by regulating OPA1-dependent cristae morphogenesis in mitochondria. Genes Dev. 2008;22(4):476-88. doi: 10.1101/gad.460708. PubMed PMID: 18281461; PubMed Central PMCID: PMCPMC2238669.

146. Nijtmans LG, Artal SM, Grivell LA, Coates PJ. The mitochondrial PHB complex: roles in mitochondrial respiratory complex assembly, ageing and degenerative disease. Cell Mol Life Sci. 2002;59(1):143-55. PubMed PMID: 11852914.

147. Tatsuta T, Model K, Langer T. Formation of membrane-bound ring complexes by prohibitins in mitochondria. Mol Biol Cell. 2005;16(1):248-59. doi: 10.1091/mbc.E04-09-0807. PubMed PMID: 15525670; PubMed Central PMCID: PMCPMC539169.

148. Artal-Sanz M, Tavernarakis N. Prohibitin couples diapause signalling to mitochondrial metabolism during ageing in C. elegans. Nature. 2009;461(7265):793-7. doi: 10.1038/nature08466. PubMed PMID: 19812672.

149. Coates PJ, Jamieson DJ, Smart K, Prescott AR, Hall PA. The prohibitin family of mitochondrial proteins regulate replicative lifespan. Curr Biol. 1997;7(8):607-10. PubMed PMID: 9259555.

150. Piper PW, Bringloe D. Loss of prohibitins, though it shortens the replicative life span of yeast cells undergoing division, does not shorten the chronological life span of G0-arrested cells. Mech Ageing Dev. 2002;123(4):287-95. PubMed PMID: 11744041.

151. Piper PW, Jones GW, Bringloe D, Harris N, MacLean M, Mollapour M. The shortened replicative life span of prohibitin mutants of yeast appears to be due to defective mitochondrial segregation in old mother cells. Aging Cell. 2002;1(2):149-57. PubMed PMID: 12882345.

152. Schleit J, Johnson SC, Bennett CF, Simko M, Trongtham N, Castanza A, et al. Molecular mechanisms underlying genotype-dependent responses to dietary restriction. Aging Cell. 2013;12(6):1050-61. doi: 10.1111/acel.12130. PubMed PMID: 23837470; PubMed Central PMCID: PMCPMC3838465.

153. Ishii N, Fujii M, Hartman PS, Tsuda M, Yasuda K, Senoo-Matsuda N, et al. A mutation in succinate dehydrogenase cytochrome b causes oxidative stress and ageing in nematodes. Nature. 1998;394(6694):694-7. doi: 10.1038/29331. PubMed PMID: 9716135.

154. Kayser EB, Sedensky MM, Morgan PG. The effects of complex I function and oxidative damage on lifespan and anesthetic sensitivity in Caenorhabditis elegans. Mech Ageing Dev. 2004;125(6):455-64. doi: S0047637404000740 [pii]
10.1016/j.mad.2004.04.002. PubMed PMID: 15178135.

155. Ventura N, Rea SL. Caenorhabditis elegans mitochondrial mutants as an investigative tool to study human neurodegenerative diseases associated with mitochondrial dysfunction. Biotechnol J. 2007;2(5):584-95. doi: 10.1002/biot.200600248. PubMed PMID: 17443764.

156. Mishra SK, Ammon T, Popowicz GM, Krajewski M, Nagel RJ, Ares M, et al. Role of the ubiquitin-like protein Hub1 in splice-site usage and alternative splicing. Nature. 2011;474(7350):173-8. doi: 10.1038/nature10143. PubMed PMID: 21614000; PubMed Central PMCID: PMCPMC3587138.

157. Merkwirth C, Jovaisaite V, Durieux J, Matilainen O, Jordan SD, Quiros PM, et al. Two Conserved Histone Demethylases Regulate Mitochondrial Stress-Induced Longevity. Cell.

2016;165(5):1209-23. doi: 10.1016/j.cell.2016.04.012. PubMed PMID: 27133168; PubMed Central PMCID: PMCPMC4889222.

158. Tian Y, Garcia G, Bian Q, Steffen KK, Joe L, Wolff S, et al. Mitochondrial Stress Induces Chromatin Reorganization to Promote Longevity and UPR(mt). Cell. 2016;165(5):1197-208. doi: 10.1016/j.cell.2016.04.011. PubMed PMID: 27133166; PubMed Central PMCID: PMCPMC4889216.

159. Baqri RM, Pietron AV, Gokhale RH, Turner BA, Kaguni LS, Shingleton AW, et al. Mitochondrial chaperone TRAP1 activates the mitochondrial UPR and extends healthspan in Drosophila. Mech Ageing Dev. 2014;141-142:35-45. doi: 10.1016/j.mad.2014.09.002. PubMed PMID: 25265088; PubMed Central PMCID: PMCPMC4310785.

160. Pulliam DA, Deepa SS, Liu Y, Hill S, Lin AL, Bhattacharya A, et al. Complex IV-deficient Surf1(-/-) mice initiate mitochondrial stress responses. Biochem J. 2014;462(2):359-71. doi: 10.1042/BJ20140291. PubMed PMID: 24911525; PubMed Central PMCID: PMCPMC4145821.

161. Pharaoh G, Pulliam D, Hill S, Sataranatarajan K, Van Remmen H. Ablation of the mitochondrial complex IV assembly protein Surf1 leads to increased expression of the UPR(MT) and increased resistance to oxidative stress in primary cultures of fibroblasts. Redox Biol. 2016;8:430-8. doi: 10.1016/j.redox.2016.05.001. PubMed PMID: 27208630; PubMed Central PMCID: PMCPMC4878459.

162. Munkácsy E, Khan MH, Lane RK, Borror MB, Park JH, Bokov AF, et al. DLK-1, SEK-3 and PMK-3 Are Required for the Life Extension Induced by Mitochondrial Bioenergetic Disruption in C. elegans. PLoS Genet. 2016;12(7):e1006133. doi: 10.1371/journal.pgen.1006133. PubMed PMID: 27420916.

163. Bennett CF, Choi H, Kaeberlein M. Searching for the elusive mitochondrial longevity signal in C. elegans. Worm. 2014;3(3):e959404. doi: 10.4161/21624046.2014.959404. PubMed PMID: 26430544; PubMed Central PMCID: PMCPMC4588544.

164. Ren Y, Chen S, Ma M, Yao X, Sun D, Li B, et al. The activation of protein homeostasis protective mechanisms perhaps is not responsible for lifespan extension caused by deficiencies of mitochondrial proteins in C. elegans. Exp Gerontol. 2015;65:53-7. doi: 10.1016/j.exger.2015.03.005. PubMed PMID: 25769692.

165. Yee C, Yang W, Hekimi S. The intrinsic apoptosis pathway mediates the pro-longevity response to mitochondrial ROS in C. elegans. Cell. 2014;157(4):897-909. doi: 10.1016/j.cell.2014.02.055. PubMed PMID: 24813612; PubMed Central PMCID: PMCPMC4454526.

166. Butler JA, Mishur RJ, Bhaskaran S, Rea SL. A metabolic signature for long life in the Caenorhabditis elegans Mit mutants. Aging Cell. 2013;12(1):130-8. doi: 10.1111/acel.12029. PubMed PMID: 23173729; PubMed Central PMCID: PMCPMC3552119.

167. Lu H, Dalgard CL, Mohyeldin A, McFate T, Tait AS, Verma A. Reversible inactivation of HIF-1 prolyl hydroxylases allows cell metabolism to control basal HIF-1. J Biol Chem. 2005;280(51):41928-39. doi: 10.1074/jbc.M508718200. PubMed PMID: 16223732.

168. Chin RM, Fu X, Pai MY, Vergnes L, Hwang H, Deng G, et al. The metabolite α-ketoglutarate extends lifespan by inhibiting ATP synthase and TOR. Nature. 2014;510(7505):397-401. doi: 10.1038/nature13264. PubMed PMID: 24828042; PubMed Central PMCID: PMCPMC4263271.

169. Wallace DC. A mitochondrial paradigm for degenerative diseases and ageing. Novartis Found Symp. 2001;235:247-63; discussion 63-6. PubMed PMID: 11280029.

170. Bratic A, Larsson NG. The role of mitochondria in aging. J Clin Invest. 2013;123(3):951-7. doi: 10.1172/JCI64125. PubMed PMID: 23454757; PubMed Central PMCID: PMCPMC3582127.

171. Harman D. Aging: a theory based on free radical and radiation chemistry. J Gerontol. 1956;11(3):298-300. PubMed PMID: 13332224.

172. Yanos ME, Bennett CF, Kaeberlein M. Genome-Wide RNAi Longevity Screens in Caenorhabditis elegans. Curr Genomics. 2012;13(7):508-18. doi: 10.2174/138920212803251391. PubMed PMID: 23633911; PubMed Central PMCID: PMCPMC3468884.

173. Hwang AB, Jeong DE, Lee SJ. Mitochondria and organismal longevity. Curr Genomics. 2012;13(7):519-32. doi: 10.2174/138920212803251427. PubMed PMID: 23633912; PubMed Central PMCID: PMCPMC3468885.

174. Smith ED, Kaeberlein TL, Lydum BT, Sager J, Welton KL, Kennedy BK, et al. Age- and calorie-independent life span extension from dietary restriction by bacterial deprivation in Caenorhabditis elegans. BMC Dev Biol. 2008;8:49. doi: 10.1186/1471-213X-8-49. PubMed PMID: 18457595; PubMed Central PMCID: PMCPMC2408926.

175. Dillin A, Crawford DK, Kenyon C. Timing requirements for insulin/IGF-1 signaling in C. elegans. Science. 2002;298(5594):830-4. doi: 10.1126/science.1074240. PubMed PMID: 12399591.

176. Leiser SF, Begun A, Kaeberlein M. HIF-1 modulates longevity and healthspan in a temperature-dependent manner. Aging Cell. 2011;10(2):318-26. doi: 10.1111/j.1474-9726.2011.00672.x. PubMed PMID: 21241450.

177. Walter L, Baruah A, Chang HW, Pace HM, Lee SS. The homeobox protein CEH-23 mediates prolonged longevity in response to impaired mitochondrial electron transport chain in C. elegans. PLoS Biol. 2011;9(6):e1001084. doi: 10.1371/journal.pbio.1001084. PubMed PMID: 21713031; PubMed Central PMCID: PMCPMC3119657.

178. Khan MH, Ligon M, Hussey LR, Hufnal B, Farber R, Munkácsy E, et al. TAF-4 is required for the life extension of isp-1, clk-1 and tpk-1 Mit mutants. Aging (Albany NY). 2013;5(10):741-58. doi: 10.18632/aging.100604. PubMed PMID: 24107417; PubMed Central PMCID: PMCPMC3838777.

179. Ventura N, Rea SL, Schiavi A, Torgovnick A, Testi R, Johnson TE. p53/CEP-1 increases or decreases lifespan, depending on level of mitochondrial bioenergetic stress. Aging Cell. 2009;8(4):380-93. doi: 10.1111/j.1474-9726.2009.00482.x. PubMed PMID: 19416129; PubMed Central PMCID: PMCPMC2730656.

180. Ryan MT, Hoogenraad NJ. Mitochondrial-nuclear communications. Annu Rev Biochem. 2007;76:701-22. doi: 10.1146/annurev.biochem.76.052305.091720. PubMed PMID: 17227225.

181. Tsang WY, Lemire BD. Mitochondrial genome content is regulated during nematode development. Biochem Biophys Res Commun. 2002;291(1):8-16. doi: 10.1006/bbrc.2002.6394. PubMed PMID: 11829454.

182. Curran SP, Ruvkun G. Lifespan regulation by evolutionarily conserved genes essential for viability. PLoS Genet. 2007;3(4):e56. doi: 10.1371/journal.pgen.0030056. PubMed PMID: 17411345; PubMed Central PMCID: PMCPMC1847696.

183. Mokranjac D, Neupert W. The many faces of the mitochondrial TIM23 complex. Biochim Biophys Acta. 2010;1797(6-7):1045-54. doi: 10.1016/j.bbabio.2010.01.026. PubMed PMID: 20116361.

184. Rauthan M, Ranji P, Aguilera Pradenas N, Pitot C, Pilon M. The mitochondrial unfolded protein response activator ATFS-1 protects cells from inhibition of the mevalonate pathway. Proc Natl Acad Sci U S A. 2013;110(15):5981-6. doi: 10.1073/pnas.1218778110. PubMed PMID: 23530189; PubMed Central PMCID: PMCPMC3625262.

185. Rezzi S, Martin FP, Shanmuganayagam D, Colman RJ, Nicholson JK, Weindruch R. Metabolic shifts due to long-term caloric restriction revealed in nonhuman primates. Exp Gerontol. 2009;44(5):356-62. doi: 10.1016/j.exger.2009.02.008. PubMed PMID: 19264119; PubMed Central PMCID: PMCPMC2822382.

186. Perl A, Qian Y, Chohan KR, Shirley CR, Amidon W, Banerjee S, et al. Transaldolase is essential for maintenance of the mitochondrial transmembrane potential and fertility of spermatozoa. Proc Natl Acad Sci U S A. 2006;103(40):14813-8. doi: 10.1073/pnas.0602678103. PubMed PMID: 17003133; PubMed Central PMCID: PMCPMC1595434.

187. Rual JF, Ceron J, Koreth J, Hao T, Nicot AS, Hirozane-Kishikawa T, et al. Toward improving Caenorhabditis elegans phenome mapping with an ORFeome-based RNAi library. Genome Res. 2004;14(10B):2162-8. doi: 10.1101/gr.2505604. PubMed PMID: 15489339; PubMed Central PMCID: PMCPMC528933.

188. Sutphin GL, Kaeberlein M. Measuring Caenorhabditis elegans life span on solid media. J Vis Exp. 2009;(27). doi: 10.3791/1152. PubMed PMID: 19488025; PubMed Central PMCID: PMCPMC2794294.

189. Harman D. The biologic clock: the mitochondria? J Am Geriatr Soc. 1972;20(4):145-7. PubMed PMID: 5016631.

190. Barja G. The mitochondrial free radical theory of aging. Prog Mol Biol Transl Sci. 2014;127:1-27. doi: 10.1016/B978-0-12-394625-6.00001-5. PubMed PMID: 25149212.

191. Wang Y, Hekimi S. Mitochondrial dysfunction and longevity in animals: Untangling the knot. Science. 2015;350(6265):1204-7. doi: 10.1126/science.aac4357. PubMed PMID: 26785479.

192. Mouchiroud L, Houtkooper RH, Moullan N, Katsyuba E, Ryu D, Cantó C, et al. The NAD(+)/Sirtuin Pathway Modulates Longevity through Activation of Mitochondrial UPR and FOXO Signaling. Cell. 2013;154(2):430-41. doi: 10.1016/j.cell.2013.06.016. PubMed PMID: 23870130; PubMed Central PMCID: PMCPMC3753670.

193. Schiavi A, Torgovnick A, Kell A, Megalou E, Castelein N, Guccini I, et al. Autophagy induction extends lifespan and reduces lipid content in response to frataxin silencing in C. elegans. Exp Gerontol. 2013;48(2):191-201. doi: 10.1016/j.exger.2012.12.002. PubMed PMID: 23247094; PubMed Central PMCID: PMCPMC3572394.

194. Dancy BM, Kayser E-B, Sedensky MM, Morgan PG. Live worm respiration in 24-well format. The Worm Breeder's Gazette2013. p. 11-2.

195. Suthammarak W, Yang YY, Morgan PG, Sedensky MM. Complex I function is defective in complex IV-deficient Caenorhabditis elegans. J Biol Chem. 2009;284(10):6425-35. doi: 10.1074/jbc.M805733200. PubMed PMID: 19074434; PubMed Central PMCID: PMCPMC2649102.

196. Back P, De Vos WH, Depuydt GG, Matthijssens F, Vanfleteren JR, Braeckman BP. Exploring real-time in vivo redox biology of developing and aging Caenorhabditis elegans. Free Radic Biol Med. 2012;52(5):850-9. doi: 10.1016/j.freeradbiomed.2011.11.037. PubMed PMID: 22226831.

197. Qian Y, Banerjee S, Grossman CE, Amidon W, Nagy G, Barcza M, et al. Transaldolase deficiency influences the pentose phosphate pathway, mitochondrial homoeostasis and apoptosis

signal processing. Biochem J. 2008;415(1):123-34. doi: 10.1042/BJ20080722. PubMed PMID: 18498245.

198. Hanczko R, Fernandez DR, Doherty E, Qian Y, Vas G, Niland B, et al. Prevention of hepatocarcinogenesis and increased susceptibility to acetaminophen-induced liver failure in transaldolase-deficient mice by N-acetylcysteine. J Clin Invest. 2009;119(6):1546-57. doi: 10.1172/JCI35722. PubMed PMID: 19436114; PubMed Central PMCID: PMCPMC2689120.

199. Matsuzawa A, Ichijo H. Redox control of cell fate by MAP kinase: physiological roles of ASK1-MAP kinase pathway in stress signaling. Biochim Biophys Acta. 2008;1780(11):1325-36. doi: 10.1016/j.bbagen.2007.12.011. PubMed PMID: 18206122.

200. Uno M, Honjoh S, Matsuda M, Hoshikawa H, Kishimoto S, Yamamoto T, et al. A fasting-responsive signaling pathway that extends life span in C. elegans. Cell Rep. 2013;3(1):79-91. doi: 10.1016/j.celrep.2012.12.018. PubMed PMID: 23352664.

201. Inoue A, Sawatari E, Hisamoto N, Kitazono T, Teramoto T, Fujiwara M, et al. Forgetting in C. elegans is accelerated by neuronal communication via the TIR-1/JNK-1 pathway. Cell Rep. 2013;3(3):808-19. doi: 10.1016/j.celrep.2013.02.019. PubMed PMID: 23523351.

202. Hoeven R, McCallum KC, Cruz MR, Garsin DA. Ce-Duox1/BLI-3 generated reactive oxygen species trigger protective SKN-1 activity via p38 MAPK signaling during infection in C. elegans. PLoS Pathog. 2011;7(12):e1002453. doi: 10.1371/journal.ppat.1002453. PubMed PMID: 22216003; PubMed Central PMCID: PMCPMC3245310.

203. Pagano DJ, Kingston ER, Kim DH. Tissue expression pattern of PMK-2 p38 MAPK is established by the miR-58 family in C. elegans. PLoS Genet. 2015;11(2):e1004997. doi: 10.1371/journal.pgen.1004997. PubMed PMID: 25671546; PubMed Central PMCID: PMCPMC4335502.

204. Andrusiak MG, Jin Y. Context Specificity of Stress-activated Mitogen-activated Protein (MAP) Kinase Signaling: The Story as Told by Caenorhabditis elegans. J Biol Chem. 2016;291(15):7796-804. doi: 10.1074/jbc.R115.711101. PubMed PMID: 26907690; PubMed Central PMCID: PMCPMC4824986.

205. Kim DH, Feinbaum R, Alloing G, Emerson FE, Garsin DA, Inoue H, et al. A conserved p38 MAP kinase pathway in Caenorhabditis elegans innate immunity. Science. 2002;297(5581):623-6. doi: 10.1126/science.1073759. PubMed PMID: 12142542.

206. Perez CL, Van Gilst MR. A 13C isotope labeling strategy reveals the influence of insulin signaling on lipogenesis in C. elegans. Cell Metab. 2008;8(3):266-74. doi: 10.1016/j.cmet.2008.08.007. PubMed PMID: 18762027.

207. Van Gilst MR, Hadjivassiliou H, Yamamoto KR. A Caenorhabditis elegans nutrient response system partially dependent on nuclear receptor NHR-49. Proc Natl Acad Sci U S A. 2005;102(38):13496-501. doi: 10.1073/pnas.0506234102. PubMed PMID: 16157872; PubMed Central PMCID: PMCPMC1201344.

208. Lee JH, Kong J, Jang JY, Han JS, Ji Y, Lee J, et al. Lipid droplet protein LID-1 mediates ATGL-1-dependent lipolysis during fasting in Caenorhabditis elegans. Mol Cell Biol. 2014;34(22):4165-76. doi: 10.1128/MCB.00722-14. PubMed PMID: 25202121; PubMed Central PMCID: PMCPMC4248714.

209. Van Gilst MR, Hadjivassiliou H, Jolly A, Yamamoto KR. Nuclear hormone receptor NHR-49 controls fat consumption and fatty acid composition in C. elegans. PLoS Biol. 2005;3(2):e53. doi: 10.1371/journal.pbio.0030053. PubMed PMID: 15719061; PubMed Central PMCID: PMCPMC547972.

210. Lapierre LR, De Magalhaes Filho CD, McQuary PR, Chu CC, Visvikis O, Chang JT, et al. The TFEB orthologue HLH-30 regulates autophagy and modulates longevity in Caenorhabditis elegans. Nat Commun. 2013;4:2267. doi: 10.1038/ncomms3267. PubMed PMID: 23925298; PubMed Central PMCID: PMCPMC3866206.

211. O'Rourke EJ, Ruvkun G. MXL-3 and HLH-30 transcriptionally link lipolysis and autophagy to nutrient availability. Nat Cell Biol. 2013;15(6):668-76. doi: 10.1038/ncb2741. PubMed PMID: 23604316; PubMed Central PMCID: PMCPMC3723461.

212. Visvikis O, Ihuegbu N, Labed SA, Luhachack LG, Alves AM, Wollenberg AC, et al. Innate host defense requires TFEB-mediated transcription of cytoprotective and antimicrobial genes. Immunity. 2014;40(6):896-909. doi: 10.1016/j.immuni.2014.05.002. PubMed PMID: 24882217; PubMed Central PMCID: PMCPMC4104614.

213. Zuryn S, Kuang J, Tuck A, Ebert PR. Mitochondrial dysfunction in Caenorhabditis elegans causes metabolic restructuring, but this is not linked to longevity. Mech Ageing Dev. 2010;131(9):554-61. doi: 10.1016/j.mad.2010.07.004. PubMed PMID: 20688098.

214. Settembre C, Di Malta C, Polito VA, Garcia Arencibia M, Vetrini F, Erdin S, et al. TFEB links autophagy to lysosomal biogenesis. Science. 2011;332(6036):1429-33. doi: 10.1126/science.1204592. PubMed PMID: 21617040; PubMed Central PMCID: PMCPMC3638014.

215. Chapin HC, Okada M, Merz AJ, Miller DL. Tissue-specific autophagy responses to aging and stress in C. elegans. Aging (Albany NY). 2015;7(6):419-34. doi: 10.18632/aging.100765. PubMed PMID: 26142908; PubMed Central PMCID: PMCPMC4505168.

216. Jafari G, Wasko BM, Tonge A, Schurman N, Dong C, Li Z, et al. Tether mutations that restore function and suppress pleiotropic phenotypes of the C. elegans isp-1(qm150) Rieske iron-

sulfur protein. Proc Natl Acad Sci U S A. 2015;112(45):E6148-57. doi: 10.1073/pnas.1509416112. PubMed PMID: 26504246; PubMed Central PMCID: PMCPMC4653183.

217. Peña-Llopis S, Vega-Rubin-de-Celis S, Schwartz JC, Wolff NC, Tran TA, Zou L, et al. Regulation of TFEB and V-ATPases by mTORC1. EMBO J. 2011;30(16):3242-58. doi: 10.1038/emboj.2011.257. PubMed PMID: 21804531; PubMed Central PMCID: PMCPMC3160667.

218. Settembre C, Zoncu R, Medina DL, Vetrini F, Erdin S, Huynh T, et al. A lysosome-to-nucleus signalling mechanism senses and regulates the lysosome via mTOR and TFEB. EMBO J. 2012;31(5):1095-108. doi: 10.1038/emboj.2012.32. PubMed PMID: 22343943; PubMed Central PMCID: PMCPMC3298007.

219. Martina JA, Chen Y, Gucek M, Puertollano R. MTORC1 functions as a transcriptional regulator of autophagy by preventing nuclear transport of TFEB. Autophagy. 2012;8(6):903-14. doi: 10.4161/auto.19653. PubMed PMID: 22576015; PubMed Central PMCID: PMCPMC3427256.

220. Roczniak-Ferguson A, Petit CS, Froehlich F, Qian S, Ky J, Angarola B, et al. The transcription factor TFEB links mTORC1 signaling to transcriptional control of lysosome homeostasis. Sci Signal. 2012;5(228):ra42. doi: 10.1126/scisignal.2002790. PubMed PMID: 22692423; PubMed Central PMCID: PMCPMC3437338.

221. Osman C, Voelker DR, Langer T. Making heads or tails of phospholipids in mitochondria. J Cell Biol. 2011;192(1):7-16. doi: 10.1083/jcb.201006159. PubMed PMID: 21220505; PubMed Central PMCID: PMCPMC3019561.

222. Brock TJ, Browse J, Watts JL. Fatty acid desaturation and the regulation of adiposity in Caenorhabditis elegans. Genetics. 2007;176(2):865-75. doi: 10.1534/genetics.107.071860. PubMed PMID: 17435249; PubMed Central PMCID: PMCPMC1894614.

223. Erkut C, Gade VR, Laxman S, Kurzchalia TV. The glyoxylate shunt is essential for desiccation tolerance in C. elegans and budding yeast. Elife. 2016;5. doi: 10.7554/eLife.13614. PubMed PMID: 27090086; PubMed Central PMCID: PMCPMC4880444.

224. Song JJ, Rhee JG, Suntharalingam M, Walsh SA, Spitz DR, Lee YJ. Role of glutaredoxin in metabolic oxidative stress. Glutaredoxin as a sensor of oxidative stress mediated by H2O2. J Biol Chem. 2002;277(48):46566-75. doi: 10.1074/jbc.M206826200. PubMed PMID: 12244106.

225. Song JJ, Lee YJ. Differential role of glutaredoxin and thioredoxin in metabolic oxidative stress-induced activation of apoptosis signal-regulating kinase 1. Biochem J. 2003;373(Pt 3):845-53. doi: 10.1042/BJ20030275. PubMed PMID: 12723971; PubMed Central PMCID: PMCPMC1223534.

226. Kim SY, Kim TJ, Lee KY. A novel function of peroxiredoxin 1 (Prx-1) in apoptosis signal-regulating kinase 1 (ASK1)-mediated signaling pathway. FEBS Lett. 2008;582(13):1913-8. doi: 10.1016/j.febslet.2008.05.015. PubMed PMID: 18501712.

227. Suh JK, Robertus JD. Yeast flavin-containing monooxygenase is induced by the unfolded protein response. Proc Natl Acad Sci U S A. 2000;97(1):121-6. PubMed PMID: 10618381; PubMed Central PMCID: PMCPMC26626.

228. Suh JK, Poulsen LL, Ziegler DM, Robertus JD. Yeast flavin-containing monooxygenase generates oxidizing equivalents that control protein folding in the endoplasmic reticulum. Proc Natl Acad Sci U S A. 1999;96(6):2687-91. PubMed PMID: 10077572; PubMed Central PMCID: PMCPMC15830.

229. Suh JK, Poulsen LL, Ziegler DM, Robertus JD. Redox regulation of yeast flavin-containing monooxygenase. Arch Biochem Biophys. 2000;381(2):317-22. doi: 10.1006/abbi.2000.1965. PubMed PMID: 11032421.

230. Kaeberlein TL, Smith ED, Tsuchiya M, Welton KL, Thomas JH, Fields S, et al. Lifespan extension in Caenorhabditis elegans by complete removal of food. Aging Cell. 2006;5(6):487-94. doi: 10.1111/j.1474-9726.2006.00238.x. PubMed PMID: 17081160.

231. Lee GD, Wilson MA, Zhu M, Wolkow CA, de Cabo R, Ingram DK, et al. Dietary deprivation extends lifespan in Caenorhabditis elegans. Aging Cell. 2006;5(6):515-24. doi: 10.1111/j.1474-9726.2006.00241.x. PubMed PMID: 17096674; PubMed Central PMCID: PMCPMC2546582.

232. Cuervo AM. Autophagy and aging: keeping that old broom working. Trends Genet. 2008;24(12):604-12. doi: 10.1016/j.tig.2008.10.002. PubMed PMID: 18992957; PubMed Central PMCID: PMCPMC2745226.

233. Swindell WR. Genes and gene expression modules associated with caloric restriction and aging in the laboratory mouse. BMC Genomics. 2009;10:585. doi: 10.1186/1471-2164-10-585. PubMed PMID: 19968875; PubMed Central PMCID: PMCPMC2795771.

234. Steinbaugh MJ, Sun LY, Bartke A, Miller RA. Activation of genes involved in xenobiotic metabolism is a shared signature of mouse models with extended lifespan. Am J Physiol Endocrinol Metab. 2012;303(4):E488-95. doi: 10.1152/ajpendo.00110.2012. PubMed PMID: 22693205; PubMed Central PMCID: PMCPMC3423099.

235. Frøkjær-Jensen C, Davis MW, Ailion M, Jorgensen EM. Improved Mos1-mediated transgenesis in C. elegans. Nat Methods. 2012;9(2):117-8. doi: nmeth.1865 [pii] 10.1038/nmeth.1865. PubMed PMID: 22290181.

236. Leiser SF, Jafari G, Primitivo M, Sutphin GL, Dong J, Leonard A, et al. Age-associated vulval integrity is an important marker of nematode healthspan. Age (Dordr). 2016. doi: 10.1007/s11357-016-9936-8. PubMed PMID: 27566309.

237. Kayser EB, Morgan PG, Hoppel CL, Sedensky MM. Mitochondrial expression and function of GAS-1 in Caenorhabditis elegans. J Biol Chem. 2001;276(23):20551-8. doi: 10.1074/jbc.M011066200. PubMed PMID: 11278828.

238. Yen K, Le TT, Bansal A, Narasimhan SD, Cheng JX, Tissenbaum HA. A comparative study of fat storage quantitation in nematode Caenorhabditis elegans using label and label-free methods. PLoS One. 2010;5(9). doi: 10.1371/journal.pone.0012810. PubMed PMID: 20862331; PubMed Central PMCID: PMCPMC2940797.

239. Bogoyevitch MA, Kobe B. Uses for JNK: the many and varied substrates of the c-Jun N-terminal kinases. Microbiol Mol Biol Rev. 2006;70(4):1061-95. doi: 10.1128/MMBR.00025-06. PubMed PMID: 17158707; PubMed Central PMCID: PMCPMC1698509.

240. Zhang D, Li J, Costa M, Gao J, Huang C. JNK1 mediates degradation HIF-1alpha by a VHL-independent mechanism that involves the chaperones Hsp90/Hsp70. Cancer Res. 2010;70(2):813-23. doi: 10.1158/0008-5472.CAN-09-0448. PubMed PMID: 20068160; PubMed Central PMCID: PMCPMC2939838.

241. Marcotte EM, Xenarios I, van Der Bliek AM, Eisenberg D. Localizing proteins in the cell from their phylogenetic profiles. Proc Natl Acad Sci U S A. 2000;97(22):12115-20. doi: 10.1073/pnas.220399497. PubMed PMID: 11035803; PubMed Central PMCID: PMCPMC17303.

242. Zhang Y, Cheng YT, Bi D, Palma K, Li X. MOS2, a protein containing G-patch and KOW motifs, is essential for innate immunity in Arabidopsis thaliana. Curr Biol. 2005;15(21):1936-42. doi: 10.1016/j.cub.2005.09.038. PubMed PMID: 16271871.

CURRICULUM VITAE

Christopher F. Bennett

Phone: 760-519-5471
Email: cfb2@uw.edu

Education

University:
University of Washington **2010-2016**
Molecular Cellular Biology Graduate Program Seattle, Washington

McGill University **2006-2010**
(Major: Honors Biochemistry) Montreal, Quebec

High School:
The Bishops School **2002-2006**
La Jolla, California

Honors, Awards, and Scholarships

Environmental Pathology/Toxicology Training Grant, University of Washington (2014-2016)

Cell and Molecular Biology Training Grant, University of Washington (2012-2013)

NSF Honorable Mention 2012

Distinction (McGill University)

First Class Honours (McGill University)

Dean Honours List - Winter 2009 (McGill University)

Robert H.P. Olney Foundation Scholar (while at CSHL)

Research Experience

University of Washington **Summer 2011-November 2016**
Matt Kaeberlein Lab Seattle, WA
Graduate Student

- Studying the regulation of the mitochondrial unfolded protein response in *C. elegans* and the function of this pathway in mitochondrial protein quality control and aging
- Exploring the function of the pentose phosphate pathway in regulating cellular redox homeostasis, mitochondrial function, and lifespan in *C. elegans*

- Acquired expertise in design and implementation of large-scale RNAi fluorescent microscopy screens, fluorescent and confocal microscopy, flow cytometry, Western blotting, qRT-PCR, mitochondrial isolation and Clarke electrode assays, Seahorse XF Analyzer assays, micromanipulation of *C. elegans*, and lifespan and healthspan assays in *C. elegans*

Fred Hutchinson Cancer Research Center **March 2011-June 2011**
Daniel Gottschling Lab Seattle, WA
Rotating Graduate Student
- Created yeast strains integrated with overexpression constructs to study the effect of genes on aging
- Learned techniques in fluorescent microscopy to study changes in mitochondrial morphology and function with lifespan

Fred Hutchinson Cancer Research Center **January 2011-March 2011**
David Hockenbery Lab Seattle, WA
Rotating Graduate Student
- Studied the metabolic differences between triple negative and non-triple negative breast cancer cells
- Learned to analyze real-time metabolic changes of cells with the Seahorse XF Analyzer

Fred Hutchinson Cancer Research Center **September 2010-December 2010**
Muneesh Tewari Lab Seattle, WA
Rotating Graduate Student
- Developed a cell culture model for studying extracellular miRNAs
- Analyzed miRNA expression in samples by qRT-PCR and miRNA arrays

McGill University **September 2009-July 2010**
Nahum Sonenberg Lab Montreal, Quebec
Undergraduate Researcher
- Created plasmid constructs with mutations to study effect on protein binding interaction
- Perfected techniques of PCR mutagenesis, transformations, mammalian cell culture, and plasmid transfection techniques
- Learned skills involved in protein study and analysis including protein isolation, co-immunoprecipitation, SDS-PAGE, and western blotting

Cold Spring Harbor Laboratories **June 2009-August 2009**
Adrian Krainer Lab Cold Spring Harbor, NY
Undergraduate Researcher
- Created minigenes carrying serial deletions to study effect of the deletion on pre-mRNA splicing
- Acquired skills for preparing constructs, learned mammalian cell culture and plasmid transfection techniques, and methods to analyze pre-mRNA splicing

Isis Pharmaceuticals **June 2006-August 2006 & June 2005–August 2005**
Student Intern Carlsbad, California

- Aided in the manufacturing and purification of chemically modified oligonucleotides
- Facilitated development of an *in-vitro* assay measuring oligonucleotide metabolism in rodents
- Developed skills in the synthesis of oligonucleotides, column chromatography, TLC, HPLC, CGE, spectrophotometry techniques

Publications

Bennett CF, Kwon J, Chen C, Acosta K, Vander Wende H, Simko M, Pineda V, Rossner R, Wasko BM, Choi H, Chen S, Park S, Jafari G, Sands B, Perez Olsen C, Mendenhall A, Morgan PG, Kaeberlein M. Transaldolase inhibition impairs mitochondrial respiration and induces a starvation-like longevity response in *C. elegans* (2016), manuscript in review.

McCormick MA, Delaney JR, Tsuchiya M, Tsuchiyama S, Shemorry A, Sim S, Chou AC-Z, Ahmed U, Carr D, Murakami CJ, Schleit J, Sutphin GL, Wasko BM, **Bennett CF**, Wang AM, Olsen B, Beyer RP, Bammler TK, Prunkard D, Johnson SC, Pennypacker JK, An E, Anies A, Castanza AS, Choi E, Dang N, Enerio S, Fletcher M, Fox L, Goswami S, Higgins SA, Holmberg MA, Hu D, Hui J, Jelic M, Jeong K-S, Johnston E, Kerr EO, Kim J, Kim D, Kirkland K, Klum S, Kotireddy S, Liao E, Lim M, Lin MS, Lo WC, Lockshon D, Miller HA, Moller RM, Muller B, Oakes J, Pak DN, Peng ZJ, Pham KM, Pollard TG, Pradeep P, Pruett D, Rai D, Robison B, Rodriguez AA, Ros B, Sage M, Singh MK, Smith ED, Snead K, Solanky A, Spector BL, Steffen KK, Tchao BN, Ting MK, Vander Wende H, Wang D, Welton KL, Westman EA, Brem RB, Liu X-G, Suh Y, Zhou Z, Kaeberlein M, Kennedy BK. A Comprehensive Analysis of Replicative Lifespan in 4,698 Single-Gene Deletion Strains Uncovers Conserved Mechanisms of Aging. (2015) *Cell Metabolism* **22**: 895–906.

Bitto A, Wang AM, **Bennett CF**, Kaeberlein M. Biochemical Genetic Pathways that Modulate Aging in Multiple Species. (2015) *Cold Spring Harbor Perspectives in Medicine*. **5**: a025114.

Bennett CF, Choi H, Kaeberlein M. Searching for the elusive mitochondrial longevity signal in *C. elegans*. (2014) *Worm* **3**: e959404.

Bennett CF, Vander Wende H, Simko M, Klum S, Barfield S, Choi H, Pineda V, Kaeberlein M. Activation of the mitochondrial unfolded protein response does not predict longevity in *Caenorhabditis elegans*. (2014) *Nature Communications* **5**: 1–10.

Bennett CF, Kaeberlein M. The mitochondrial unfolded protein response and increased longevity: cause, consequence, or correlation? (2014) *Experimental Gerontology* **56**: 142–146.

Schleit J*, Johnson SC*, **Bennett CF**, Simko M, Trongtham N, Castanza A, Hsieh EJ, Moller RM, Wasko BM, Delaney JR, Sutphin GL, Carr D, Murakami CJ, Tocchi A, Xian B, Chen W, Yu T, Goswami S, Higgins S, Holmberg M, Jeong K-S, Kim JR, Klum S, Liao E, Lin MS, Lo W, Miller H, Olsen B, Peng ZJ, Pollard T, Pradeep P, Pruett D, Rai D, Ros V, Singh M, Spector BL, Vander Wende H, An EH, Fletcher M, Jelic M, Rabinovitch PS, MacCoss MJ, Han J-DJ,

Kennedy BK, Kaeberlein M. Molecular mechanisms underlying genotype-dependent responses to dietary restriction. (2013) *Aging Cell* **12**:1050–1061.

Yanos ME*, **Bennett CF***, Kaeberlein M. Genome-Wide RNAi Longevity Screens in *Caenorhabditis elegans*. (2012) *Current Genomics* **13**: 508–518.

Morita M, Ler LW, Fabian MR, Siddiqui N, Mullin M, Henderson V, Alain T, Fonseca BD, Karashchuk G, **Bennett CF**, Kabuta T, Higashi S, Larsson O, Topisirovic I, Smith R, Gingras AC, Sonenberg N. A Novel 4EHP-GIGYF2 Translational Repressor Complex Is Essential for Mammalian Development. (2012) *Molecular and Cellular Biology* **32**: 3585–3593.

Fonseca BD, Alain T, Finestone LK, Huang BPH, Rolfe M, Jiang T, Yao Z, Hernandez G, **Bennett CF**, and Proud CG. Pharmacological and genetic evaluation of proposed roles of mitogen-activated protein kinase/extracellular signal-regulated kinase kinase (MEK), extracellular signal-regulated kinase (ERK), and p90(RSK) in the control of mTORC1 protein signaling by phorbol esters. (2011) *Journal Biological Chemistry* **286**: 27111–27122.

Arroyo JD, Chevillet JR, Kroh EM, Ruf IK, Pritchard CC, Gibson DF, Mitchell PS, **Bennett CF**, Pogosova-Agadjanyan EL, Stirewalt DL, Tait JF, Tewari M. Argonaute2 complexes carry a population of circulating microRNAs independent of vesicles in human plasma. (2011) *Proceedings of the National Academy of Sciences* **108**: 5003–5008.

Conferences/Presentations

Inhibition of the pentose phosphate pathway causes a pro-longevity mitochondrial starvation response in *C. elegans*. American Aging Association Annual Meeting, Seattle, WA (2016). Poster.

Genome-Wide RNAi Screen for positive regulators of the mitochondrial unfolded protein response (UPR^{mt}). EP/T Training Grant Retreat, Seattle, WA (2015). Poster.

A screen for genes that regulate the mitochondrial unfolded protein response and pesticide resistance. EP/T Training Grant Retreat, Seattle, WA (2014). Talk.

The mitochondrial unfolded protein response does not predict longevity in *Caenorhabditis elegans*, UW Medicine Pathology Retreat, Seattle, WA (2014). Poster.

The mitochondrial unfolded protein response does not predict longevity in *Caenorhabditis elegans*, American Aging Association Annual Meeting, San Antonio, TX (2014). Poster.

Genome-wide RNAi screen for inducers of the mitochondrial unfolded protein response (UPR^{mt}) and their role in aging, CMB Training Grant Retreat, Seattle, WA (2013). Poster.

Genome-wide RNAi screen for inducers of the mitochondrial unfolded protein response (UPR^{mt}) and their role in aging, Northwest Worm Meeting, Seattle, WA (2013). Poster.

Volunteer/Teaching Experience

NWABR Life Sciences Research Weekend **November 9th, 2014 & November 7th, 2015**
Volunteer Seattle, WA

- Emphasized to the general public, including children and their parents, the importance of aging research and the ideas we are exploring to alleviate age-associated diseases
- Demonstrated skills in teaching science to the public

Native Youth Enrichment Program **October 15th & August 20th, 2015**
Instructor Seattle, WA

- Introduced elementary, middle school, and high school students from Seattle area schools to scientific research and *C. elegans* as a model system
- Helped teach students micromanipulation of *C. elegans* and fluorescent microscopy to expose them to basic science and aging research

Summer Medical Dental Education Program **Jun. 30th & July 13th, 2015**
Instructor Seattle, WA

- Aided in the organization and mentoring of a program for students from underrepresented minorities interested in careers in medicine, science, and dentistry
- Facilitated a three hour course in *C. elegans* biology, fluorescent microscopy, and flow cytometry to expose undergraduate students to biomedical research

Molecular Biology of Aging Course at Marine Biological Laboratory **Summer 2014**
Teaching Assistant Woods Hole, MA

- Helped design and lead the laboratory component for the Woods Hole aging course
- Instructed post-docs and graduate students in *C. elegans* aging biology and genetics, leading them through genetic screens using EMS mutagenesis, lifespan and healthspan analyses, in addition to their own independent research projects

NWABR Student BioExpo **Spring 2011, Spring 2013**
Judge Seattle, WA

- Discussed BioExpo projects with students to gauge their enthusiasm and understanding of their research topic
- Collaborated with judges to rank student projects according to student presentation performance and research project

Science Education Partnership (SEP) **Summer 2012**
Teaching Assistant Seattle, WA

- Aided in curriculum development for high school students and mentored a high school teacher in my graduate laboratory
- Performed science community outreach to enhance public understanding of science

NWABR Student BioExpo **December 2011–Spring 2012**
Mentor Seattle, WA

- Aiding two students with their BioExpo projects by explaining scientific concepts, brainstorming ideas, providing them access to scientific literature, and correcting research projects

NWABR Life Sciences Research Weekend **November 5th, 2011**
Volunteer Seattle, WA
- Helped young children and adults to extract DNA from strawberries, to teach them about genetic information and biology in general

University of Washington BIOC440 **September 2011-December 2011**
Teaching Assistant Seattle, WA
- Led two quiz sections per week, where I facilitated student understanding of biochemistry through lecturing and problem solving exercises
- Strengthened teaching skills and created a friendly academic environment

McGill Students Offering Support **October 2009-April 2010**
Organic Chemistry I/II Tutor Montreal, Quebec
- Facilitated students learn introductory level organic chemistry reactions and theory behind them
- Displayed effective teaching skills in conveying concepts to large group of students